

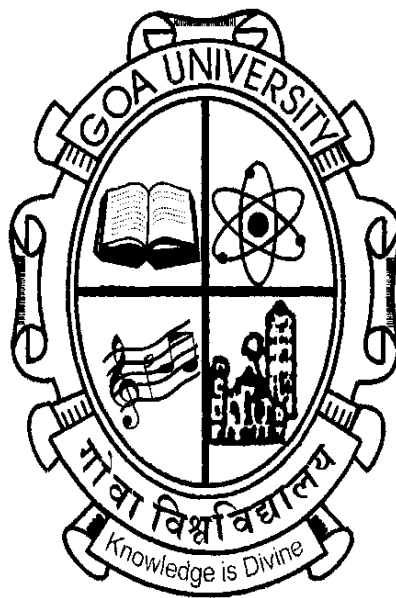
**SEISMIC ANALYSIS OF BUNDS
CONSIDERING COCONUT ROOT
REINFORCEMENT**

A THESIS SUBMITTED IN PARTIAL FULFILMENT TO FOR THE DEGREE OF

DOCTOR OF PHILOSOPHY

CIVIL ENGINEERING

GOA UNIVERSITY



By

Leonardo Roque Do Carmo Souza

**GOA COLLEGE OF ENGINEERING FARMAGUDI
GOA UNIVERSITY
GOA**

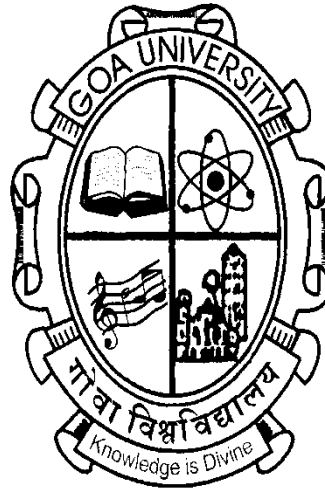
SEISMIC ANALYSIS OF BUNDS CONSIDERING COCONUT ROOT REINFORCEMENT

A THESIS SUBMITTED IN PARTIAL FULFILMENT TO FOR THE DEGREE OF

DOCTOR OF PHILOSOPHY

CIVIL ENGINEERING

GOA UNIVERSITY



By

Leonardo Roque Do Carmo Souza

(Roll No: 1731100004, P R No 201507375)

Under the supervision of

Prof. Purnanand Pundalik Savoikar

GOA COLLEGE OF ENGINEERING FARMAGUDI

GOA UNIVERSITY

GOA

JANUARY 2023

DECLARATION

I, **Leonardo Roque Do Carmo Souza**, hereby declare that this thesis represents work which has been carried out by me and that it has not been submitted, either in part or full, to any other University or Institution for the award of my research degree.

Place: Taleigao

Leonardo Roque Do Carmo Souza

Date:

CERTIFICATE

I, hereby certify that the above Declaration of the candidate, Leonardo Roque Do Carmo Souza, is true and the work was carried out under my supervision.

Dr. Purnanand P. Savoikar

Professor in Civil Engineering

Goa College of Engineering, Farmagudi – Goa

Goa University, Goa

Acknowledgements

First and foremost, I thank Almighty God for blessing me in the completion of this research.

I owe my deep gratitude to my esteemed Guide, Prof. Purnanand P. Savoikar to the Department of Civil Engineering, Goa Engineering College, Farmagudi. His invaluable guidance, visionary ideas, incisive comments, and unflinching motivation have helped and profoundly inspired me in this entire endeavour. I offer my sincere thanks to my Guide for constantly activating and nourishing my intellectual aptitude and encouraging me with intelligent and novel ideas. He has thus assisted me in broadening my perspectives in life.

I express my profound thanks to the members of Departmental Research Committee (DRC) Prof. Ganesh Hegde and Prof. R. Shivashankar for their constant and valuable feedback which helped me to improve my work. I humbly grab this opportunity to acknowledge reverentially, the Director of Technical Education, Dr Vivek B. Kamat for his tremendous boost to me on many occasions. I acknowledge the support rendered by Principal, Goa College of Engineering, Prof. Krupashankara M. S. in assorted ways. Sincere thanks goes to Prof. K. G. Guptha, Head, Department of Civil Engineering, for his whole-hearted extended support. I must thank the staff especially Laboratory Assistants of Civil Engineering at Goa College of Engineering, also particularly staff-members and my students at Agnel Polytechnic. They were very supportive and instrumental in giving an incredible helping hand to me and acted as a catalyst for timely completion of this research work.

I express deep sense of gratitude to my wife and children, for their patience and understanding. I shall forever remain indebted to them for the long hours and holidays that I owed to them which I had spent for this thesis.

A special appreciation goes to everyone associating with me tirelessly in most of the data collection. I would also like to thank the local people of Goa, for their immense support and voluntary participation during the data collection. I am forever indebted to my colleagues in this Doctoral Research under my guide for their invaluable contribution and fellowship.

Date: January 2023

Leonardo Roque Do Carmo Souza

Place: Goa University, Taleigao

DEDICATION

// Paramesvara Kula Mitraih Prati //

// Aasiirvaada Prema – Sneha Tatha Hi Bhaavita //

// AgnyaanaTimiraandhasya //

// Gnyaana Anjana Shalaakayaa //

// Chakshuhu Unmeelitam Yenam //

// Tasmai Sri Guravenamaha. //

It is the fundamental duty of every citizen of the country to protect and preserve (by words and deeds) the rich heritage and composite culture (Built, Natural and Cultural) of our country

Article 51 A (f)

THESIS APPROVAL SHEET

Thesis entitled **Seismic Analysis of Bunds Considering Coconut Root Reinforcement** by **Leonardo Roque Do Carmo Souza**, is approved for the degree of **DOCTOR OF PHILOSOPHY**.

Examiners

Supervisor

Chairman

Date:

Place: Goa University, Taleigao

CONTENTS

1	Introduction	1-17
1.1	Introduction	1
1.2	Historical Geotechnical Structures	2
1.3	TGSB -Ancient Indian Infrastructure Geotechnics	3
1.4	Relevance, Applicability and Civil Engineering Uses of TGSB	6
1.5	Biomimicry and Biomechanics of TGSB Design	9
1.6	Sustainability of TGSB	10
1.7	Coconut tree damping and soil strengthening	13
1.8	Seismicity and Goa	14
1.9	Area of work	15
1.10	Objectives of the Study	16
1.11	Scope of the work	17
2	Literature Survey	18-28
2.1	Introduction	18
2.2	Literature Survey for Computer Aided Seismic Analysis of Bunds considering Coconut Root Reinforcement	18
2.2.1	Traditional Goan Saraswat Bunds as a Sustainable Infrastructure	19
2.2.2	Soil Characterization and Stabilization	20
2.2.3	Coconut Tree Root Geo Reinforcement	21
2.2.4	Seismic Parameters	23
2.2.5	Numerical and computerized analysis	23
2.2.6	Codes and Standards	26
2.3	Critical Appraisal of Literature	26
2.4	Gaps in research and Research Avenues Available.....	27
2.5	Research Area Identified	27
2.6	Difference from Previous Works	28
2.7	Summary	28
3	Methodology	29-86
3.1	Methodology of Study Adopted for Seismic Analysis of TGSB	29
3.2	Study of Traditional Goan Saraswat Bunds	29

3.3	Study of Soils Required for TGSB and their stabilization	40
3.4	Study and Modelling of Coconut Root Soil Reinforcement	56
3.5	Study of Seismic Parameters for TGSB	79
3.6	Summary	85
4	Seismic Analysis of TGSB	87-156
4.1	Use of computers for analysis of TGSB	87
4.2	Spreadsheet Based Computerized Seismic Slope Stability Analysis	91
4.3	Liquefaction Safety of TGSB	118
4.4	Tsunami Safety of TGSB	137
4.5	GeoStudio2019 Analysis TGSB	145
4.6	Midas Analysis of TGSB	151
4.7	Summary	155
5	Results and Discussions	157-195
5.1	Results of Computerized Analysis of TGSB	157
5.2	Results of Spreadsheet Based Analysis of TGSB	157
5.3	Results of Software Analysis of TGSB	167
5.4	Discussions on Results of Computerized Analysis	175
5.5	Comparison of FoS by various methods for Computerized analysis of TGSB	192
5.6	Summary	194
6	Conclusions	196-202
6.1	Introduction	196
6.2	Work Progression and Summary of Thesis Contributions	196
6.3	Major contributions from the present study	197
6.4	Conclusions based on work	199
6.5	Limitations of Present Study	200
6.6	Scope for Future Work	201
6.7	Closing Remarks	202
	Annexure.....	
	References.....	
	List of Publications	

List of figures

1.1	Road and Coconut trees on Traditional Goan Saraswat Bunds in Goa	1
1.2	Bunds of Goa and reclaimed Khazan land.	2
1.3	Typical Traditional Goan Saraswat Bunds (TGSB) in Curtorim, Agasaim, Caranzalem in Goa	4
1.4	Route to Goa and Ancient Saraswat Settlements in Goa	4
1.5	Ancient Saraswat / Indus-Valley Seals showing the sacred animal Cow.....	5
1.6	Ancient Saraswat / Indus-Valley Seals showing the boats used in the ancient Saraswat Civilizations transporting men and animals	5
1.7	Similarity in design of Bunds from Saraswat civilization and Goa.....	6
1.8	Transportation Infrastructure: Road on TGSB.....	7
1.9	Irrigation and Rain water harvesting by TGSB.....	7
1.10	Tidal Control: Traditional Sluice gates and water control mechanism.....	8
1.11	Possible makeover for Sonsodo, (Margao-Goa) MSW dump and actual dump ...	8
1.12	Windbreak and Tsunami protection,	8
1.13	TGSB along Galgibaga river in Canacona	10
1.14	Recent Cyclones Kyarr (2019) and Tauktae (2021) to hit Goa.....	11
1.15	TGSB flood control system at Curtorim-Goa... ..	12
1.16	Fibrous Coconut roots strengthen soil and dampen vibrations.	13
1.17	Earthquake hazard Map showing earthquakes near Goa	15
2.1	Sluice gate on Khazan	19
2.2	Mechanism of root reinforcement of soil	21
2.3	Software analysis of grass reinforced slope with tree at bottom	22
3.1	Standard zigzag pattern of coconut trees 10m c/c in longitudinal direction	31
3.2	Standard dimensions of TGSB.	32
3.3	Failure mechanisms for bunds	33
3.4	Additional Factor of Safety used for TGSBs	34
3.5	TGBS for Embankment and Stabilization	35
3.6	Compaction of TGSB by tamping and bullock chain.....	36
3.7	Construction of TGSB	38
3.8	Map of Goa showing the location of case studies.	39
3.9	Triangular Classification of Lateritic Soils and TGSB soils.....	41
3.10	Envelope of Particle Size Distribution for TGSB soil in red	42

3.11	Comparative Yield Criteria on Deviatoric Plane	44
3.12	Comparison of 3D yield criteria plots	44
3.13	Mohr-Coulomb failure criterion	47
3.14	Sample Location in pit for testing Anisotropy in Lateritic soils in Goa	50
3.15	Coconut Leaf Ash (CLA) Raw Materials, Local Production Technique.	52
3.16	Coconut Leaf Ash (CLA) – 500 X, 1000 X Magnification.....	52
3.17	Coconut Leaf Ash and Burnt Shell Lime used	53
3.18	Fly-Ash and zip-locked packets of soils for testing	53
3.19	Strength Variation of cylinders of lime with ash (A) and fly-ash(FA.....	54
3.20	Cylinders and briquettes cast of stabilized-soil	54
3.21	Shrinkage cracks in LCS left and LFS right briquettes	55
3.22	Unconfined Compressive Strength for CLA (A) and FA with soil	55
3.23	Random internet photo show structures nearer palm trees -s damage	57
3.24	Comparisons of tap and coconut tree roots found on TGSBs.	58
3.25	Coconut Tree Roots - cross section and distribution.....	58
3.26	Root spread of Vetiver Grass and Coconut Tree	60
3.27	Applicability of coconut and Vetiver root systems in TGSB.....	60
3.28	Measuring Coconut Tree Root Branching and Diameter.....	61
3.29	Bending of root that causes increase in shear strength and RAR.....	62
3.30	Increase in cohesion with root tensile strength.....	63
3.31	Coconut Tree Roots Weight For Density.	64
3.32	Root Tension Test Apparatus	64
3.33	PWP measuring instruments.	66
3.34	Soil Water Characteristic Curve (SWCC)	66
3.35	Soil–Plant–Atmosphere System for Coconut -cause of root suction pressure	68
3.36	Change in cohesion with matric suction	68
3.37	Schematic showing series of Roots in Series and Parallel... ..	69
3.38	Airflow around Streamlined Coconut tree and their forces during winds	70
3.39	Front tree canopy flex maximum thus protect the rear trees in cyclones.....	71
3.40	Forces acting on an aerofoil / Coconut canopy.....	71
3.41	Test Apparatus for pull-out of roots.....	73
3.42	Force (N) required for pull-out of roots.....	73
3.43	Variation of root adhesion with soil shear strength.....	74

3.44	Coconut Tree Roots act as combination of micro-pile and geo-textile.....	75
3.45	Comparison of Geo-synthetic and TGSB reinforced normal soils.....	76
3.46	Comparison of Geo-synthetic TGSB reinforced weak soils.....	76
3.47	Soil Cracks and their damage in Tap and Fibrous Roots... ..	77
3.48	Stoppage of soil piping Fibrous roots of coconut tree	77
3.49	Macro-seismic map for the Past earthquakes near Goa.....	80
3.50	Distance and Shake map of Koyna Earthquake to Goa.	81
3.51	Simplified-tectonic-map-of-India.	83
3.52	Faults near Goa	84
3.53	Earthquake from rupture of faults	84
4.1	TGSB (a) Typical section (b) Change in section with height showing benching .	88
4.2	Schematic diagram showing forces acting on a TGSB	92
4.3	Wave pressure and mean wave heights on TGSB.....	94
4.4	Pressures due to water on TGSB.....	95
4.5	Static and Dynamic Pressure on TGSB	98
4.6	Increase in cohesion with suction.....	101
4.7	Method of slices.....	104
4.8	Pseudo-static forces on a soil wedge.....	106
4.9	Division of Spectral Acceleration in 10 parts considering the max as 1.....	110
4.10	Four steps to create an artificial seismograph from sonic velocity and spectrum	111
4.11	Forces acting on active and passive wedge in TGSB for Pseudo-dynamic earthquake analysis	113
4.12	Variation of active and passive wedge weights for TGSBs	113
4.13	Stress Drop for earthquakes in Japan	116
4.14	Loose Sandy in water Soil Before-During-After liquefaction of soil.....	118
4.15	Effects of liquefaction of soil.....	119
4.16	Possible Failure Modes of TGSB after liquefaction of soil.....	119
4.17	Probable Failure Modes of TGSB after liquefaction of soil.....	119
4.18	Ranges of Soils That Liquefy.....	112
4.19	Cyclic triaxial test results for behaviour under earthquake loading.....	113
4.20	Cyclic strength curves on uniform stress cycles for liquefaction.....	121
4.21	Zone of Liquefaction for Calculations.....	122
4.22	Magnification Scaling Factor (MSF) for earthquakes.	123

4.23	Initial Static Shear Factor.....	124
4.24	Stress Normalization Factor.....	124
4.25	Magnitude Scaling Factor (MSF) used in this thesis.....	125
4.26	Relationship between Moment Mw and Other Magnitude Scales.....	126
4.27	Liquefaction from SPT.....	127
4.28	Sand Equivalence Correction.....	128
4.29	Liquefaction from CPT.....	129
4.30	Liquefaction from Vs.....	130
4.31	Plots of SPT, CPT, Vs and CSR7.5 showing the liquefaction potential based on Cyclic Shear Stress.....	131
4.32	Map of Goa showing locations of boreholes for LPI	132
4.33	Types of failure post liquefaction settlement ...	134
4.34	Scaling factor for CSR	135
4.35	Volumetric Strain from CSR	136
4.36.	World Earthquakes for possible Tsunami near Goa.....	137
4.37	Water Levels in Tsunami and Tsunami Surge.....	138
4.38	C/s of Goa showing possible wave levels and water depth during Tsunami	138
4.39	Goa-Flood risk areas, continental shelf, cyclone Tracks	140
4.40	Protective Action of Coastal Mangroves	141
4.41	Protective Action of Coastal TGSBs.....	142
4.42	Combined Protective Action of Coastal Mangroves & Coastal TGSBs	142
4.43	Forces, velocities and heights of water in a Hydraulic Jump	143
4.44	Model studies of Hydraulic Jump with TGSB and normal embankment	144
4.45	GeoStudio2019 model of TGSB.	146
4.46	FoS of 3 m TGSB with components: tree, wall, and root-pile	147
4.47	Drawing the Boundary Conditions for seepage analysis in GeoStudio	148
4.48	Results from GEOSTUDIO 2019 SEEP/W for TGSB	149
4.49	Defining earthquakes in GEOSTUDIO 2019 QUAKE/W	150
4.50	Results for ground acceleration in TGSB in GEOSTUDIO 2019 QUAKE/W	150
4.51	Flow-chart for Midas Analysis... ..	151
4.52	Modelling of roots as horizontal soil-mat with enhanced shear parameters	152
4.53	Different models prepared for Midas analysis.....	153
4.54	Meshed model for 9m TGSB in Midas analysis	154

4.55	Stresses due to static forces in Midas analysis for 9m, 6m and 3m TGSB	154
4.56	Shear in Midas analysis due to earthquakes for 9m TGSB	155
4.57	Acceleration and displacement in Midas analysis due to earthquakes for 9m TGSB	155
5.1	Plot of Liquefaction settlement strains in Goa.....	165
5.2	Horizontal acceleration and deformation of TGSB caused by earthquake	170
5.3	Accelerograms of selected earthquakes	171
5.4	Factor of safety for sliding and overturning for water retaining TGSB for static load	176
5.5	Factor of safety for sliding and overturning for normal TGSB embankment for static load	176
5.6	Factor of safety for sliding and overturning for dynamic load	177
5.7	Factor of safety for sliding and overturning for earthquake load	177
5.8	Factor of safety for sliding and overturning for wind load.....	177
5.9	Factor of safety for sliding and overturning for cyclonic load.....	178
5.10	Factor of safety for pseudo-static approach as per IS code.....	180
5.11	Factor of safety for spectral acceleration based approach	181
5.12	Factor of safety for simplified pseudo-dynamic approach	182
5.13	Liquefaction Potential Index of TGSB.....	183
5.14	Liquefaction Settlement of TGSB in millimeters.....	184
5.15	Incoming wave height and outgoing wave parameters for Tsunami.....	185
5.16	Increase in FoS due to TGSB Components	186
5.17	FoS Trend in static stability of TGSB.....	187
5.18	FoS by different methods in static stability of TGSB.....	188
5.19	Seepage in TGSB.....	188
5.20	Dynamic factor of safety at top and at toe of TGSB.....	189
5.21	Variation of Factor of safety with height.....	190
5.22	Horizontal and Vertical displacements by Midas analysis	191
5.23	Major Principal Stress by Midas analysis.....	191
5.24	Plots of static and dynamic factor of safety obtained for TGSB considering root reinforcement by different approaches for 3, 6 and 9 m TGSB	193
5.25	Trend of Factor of safety obtained for TGSB.....	193

List of Tables

3.1	TGSB Design parameters	30
3.2	Failure mechanisms for TGSBs.....	33
3.3	Factor of Safety used for TGSBs.....	34
3.4	Additional Contributors for increase in factor of safety of TGSBs	35
3.5	Estimated Constituents of Traditional Goan Saraswat Bund.....	37
3.6	Typical soil properties for TGSB soils.....	42
3.7	Typical soil values used in software for evaluation of TGSB	43
3.8	Comparison of common yield criteria	45
3.9	Anisotropy in soil at same level in Salcete Lateritic formation in Goa	49
3.10	Coefficient for root spread for different types of soil	61
3.11	Increase in UCS v/s RAR of coconut tree roots	62
3.12	Properties of coconut tree roots	65
3.13	Parameters a and b for matric root suction.....	67
3.14	Combined factor of safety for geosynthetic action	79
3.15	Seismicity parameters for Goa in India.....	82
4.1	General properties of soil used for static and dynamic design of TGSB.....	87
4.2.	Values for wave coefficient α_2	93
4.3	Value of Wind lift and drag Coefficients for Coconut Tree	97
4.4	Factor of Safety for Soil-Nail Action of Coconut Roots	100
4.5	Matric root suction for coconut tree roots at varying depth from top.....	101
4.6	Combination of loads and moments for overall factor of safety.....	102
4.7	Comparative Pseudo-Static Coefficients.....	107
4.8	Magnitude Scaling Factor (MSF)	125
4.9	Correction factors for SPT-N.....	127
4.10	CRR for Liquefaction from SPT.....	128
4.11	CRR for Liquefaction from CPT.....	129
4.12	CRR for Liquefaction from V_s	129
4.13	LPI based Occurrence Potential classification.....	130
4.14	Co-relationships between SPT CPT and V_s for Goa region.....	133
4.15	Tsunami Velocity and Wave Height....	139
4.16	Tsunami Wave Dimensions depending on seabed depth of Earthquake.....	139
4.17	Time for Tsunami to travel to Goa in Hours from Nicobar.....	141

4.18	Tsunami Hydraulic Jump Velocity and Wave Height for 3m TGSB.....	145
5.1	Summary of forces for various heights of bunds.....	158
5.2	Static Factor of Safety for various heights of bunds.....	160
5.3	Dynamic Factor of Safety for various heights of bunds if all loads act simultaneously	161
5.4	Dynamic Factor of Safety for various heights of bunds if maximum earthquake only acts	161
5.5	Dynamic Factor of Safety for various heights of bunds if normal wind only acts	161
5.6	Dynamic Factor of Safety for various heights of bunds if Cyclonic wind only acts	162
5.7	Pseudo static Factor of Safety of TGSB as per IS Code.....	162
5.8	Simplified Spectral Force Based Factor of Safety... ..	163
5.9	Factor of Safety from Simplified Pseudo-Dynamic Analysis.....	164
5.10	Liquefaction Potential Index of soil profile at Goa.....	164
5.11	Liquefaction Settlement mm of soil profile at Goa.....	165
5.12	Tsunami Velocity and Quantity change by using TGSB	166
5.13	Experimental and calculated Tsunami Wave Height for 3m TGSB without trees	167
5.14	Factor of Safety using different components of 3 m TGSB.....	167
5.15	Factor of Safety for TGSB compared with and without roots	168
5.16	FoS from Different soil models	169
5.17	Results of seepage from SWEEP/W.....	169
5.18	Results of QUAKE/W analysis.....	171
5.19	Dynamic Factor of safety of TGSB	171
5.20	Comparison for QUAKE/W for earthquakes at 9m-TGSB Top.	172
5.21	Comparison for QUAKE/W for earthquakes at 9m-TGSB Toe	173
5.22	Static Factor of Safety of Slope	174
5.23	Horizontal and vertical displacements.	174
5.24	Major and Minor Principal Stress	175
5.25	Equations for factor of safety of TGSB	179
5.26	Comparison of Static and Dynamic Factor of Safety Obtained for TGSB Considering Root Reinforcement by Different Approaches	192
5.27	Trend of Factor of safety obtained for TGSB	194

LIST OF ANNEXURES

1	Annexure-I-Additional Information On TGSB	xxii
2	Annexure-II-Soil and Rock Properties	xxvi
3	Annexure-III-Soil Stabilization Studies	xxxvi
4	Annexure-IV-Coconut Root Properties	xxxviii
5	Annexure-V-Earthquake Magnitude Studies	xli
6	Annexure-VI-Borehole Logs for Liquefaction Studies	xlii
7	Annexure-VII-Liquefaction Potential Index of Soil In Goa	xlvi
8	Annexure-VIII-Liquefaction Settlement for Soil In Goa	lvi
9	Annexure-IX-Tsunami Protection for Goa	lvii
10	Annexure-X-Recent Natural Disasters to Strike Goa	lix
11	Annexure-XI-General Earthquake Data	lxiii
12	Annexure-XII-Spectral Force	lxxviii
13	Annexure-XIII-Artificial Seismograph From SPT/CPT	lxxx
14	Annexure-XIV-Computational Modelling For TGSB.....	lxxxvii
15	Annexure-XV-Case Studies of TGSB.....	xcii
16	Annexure-XVI- Additional Photographs of TGSB	ciii
17	Annexure-XVII-Destruction of TGSB	cvii

List of standard symbols and their units

Symbol	Description	Unit
γ	Unit weight or Bulk Unit Weight	kN/m^3
γ_d	Dry Unit weight	kN/m^3
γ_{sat}	Saturated Unit weight	kN/m^3
γ_{sub}	Submerged Unit weight	kN/m^3
ε	Soil strain	ratio
ν	Poisson's ratio.....	ratio
σ	Soil stress	kN/m^2
τ	Soil Shear Stress	kN/m^2
ϕ	Shear-Friction angle	$^\circ$
c	Shear-cohesion	kN/m^2
C_d	drag coefficient	ratio
C_l	lift coefficient	ratio
CRR	Cyclic resistance ratio	ratio
CSR	Cyclic stress ratio	ratio
c_u or q_u	maximum unit axial compressive stress	
	undrained shear cohesion	kN/m^2
Dr	Relative density.....	%
d_r	root diameter.....	m
E	Young's Modulus.....	GPa
e	Void ratio.....	%
e_0	Initial Void ratio.....	%
FoS	Factor of safety.....	ratio
Fw	wind force	N
f_{yr}	root tensile strength	kN/m^2
Gs	Specific Gravity	ratio
k_h	Seismic acceleration coefficient-horizontal	g
k_v	Seismic acceleration coefficient-vertical	g
k_x	permeability of soil – horizontal	m/day
k_y	permeability of soil – vertical	m/day
l_r	root spacing	m
MDD	Maximum dry density	kN/m^3
M_L	local Earthquake magnitude-Richter	

M_o	Earthquake moment magnitude	
M_w	Earthquake moment	
N	Standard penetration test blow number	
OMC	Optimum moisture content	%
RAR	Root Area Ratio	ratio
S_u	Matric soil suction.....	kPa
$s_v = s_h$	root spacing	m
TGSB	Traditional Goan Saraswat Bund	
UCS	Unconfined compressive strength	kN/m ²
V_p	Primary wave velocity	m/s
V_s	Shear wave velocity	m/s
w or w_n	Moisture content	%
w_L	Liquid limit	%
w_P	Plastic limit	%
z	Depth of soil strata	m

ABSTRACT

This thesis focuses on exploring the seismic stability of Traditional Goan Saraswat Bunds (TGSB) and the contribution of coconut roots in strengthening it. TGSB is the only embankment in the world that carries a double row of coconut trees planted along the two sides and have functioned for centuries. The TGSB has survived storms of over 150 kmph and other forces that have wrecked destruction for similar incidents in other parts of India and the world. Because of scarcity of land and spurt of construction activities it is extremely important to carry out research towards sustainable ancient structures for use in today's world. Hence these ancient geotechnical embankment structure called variously as '*Traditional Goan Saraswat Bunds*' or just '*Bunds*' and locally as '*Baand*', that has lasted for millennia deserved to be studied. This present work aims to discover the explanation for this longevity and sustainability using computer-based analysis.

In the literature review, extensive reassessment of available literature on TGSB and soils, soil stabilization, roots and earthquakes was researched. No much research was carried out in past on this topic, hence the data available for similar structures was studied for optimized computerized analysis. A critical analysis of the literature searched showed that there was no previous research carried out in this area. There was consequently sufficient gaps and scope for this research. The problem of no previous research meant that extensive parallel research had to be done and reviewed. It was seen that there is scope for finding the seismic slope stability of TGSB by different methods. At the same time, a very-brief analysis of liquefaction and tsunami safety was needed as it is a vital part of seismic stability analysis.

In the methodology, first the TGSB is studied for its geometric and geotechnical properties. The soils used and the soil stabilization used traditionally in TGSBs was studied to reaffirm the proportions traditionally used. The reason that the TGSB have lasted for thousands of years through storms and earthquakes and cannon-fire is the coconut tree roots that act as a bio reinforcement. Coconut tree roots were tested for their mechanical properties. The thesis then investigates the improvement in soil properties by coconut roots in TGSBs. Lastly the section describes the most likely earthquake parameters that can impact TGSBs. For verification of this, spreadsheet calculations using faults within 400 km of Goa Local moment magnitude calculated by excel sheet.

Once the required data was found out the analysis was carried out. Computer based seismic analysis of TGSB in this thesis has been carried out in limit equilibrium spread sheet and limit equilibrium and FEM software analysis. In the analysis section the thesis initially describes the static and dynamic stability using spreadsheets and GEOSTUDIO and MIDAS-GTS-NX software. Two software with different approaches (Limit Equilibrium and FEM) were used as this is the first study in this area and hence needed self-validation.

The results obtained in the thesis give the fair understanding of the geotechnical reasons for the long lasting sustainable historic geotechnical infrastructure. From the results we can determine the increase in the safety due to the presence of coconut tree roots. We can also see how the seismic stability increases with the presence of coconut tree roots.

The factor of safety was found out for sliding and overturning at toe using Microsoft excel for existing 3, 6, 9 m TGSB and additional 12m TGSB.

A whole range of methods was used to evaluate the safety of TGSB. The final conclusion can be thus only be decided by comparing all the methods with each other to get an overall idea of the factor of safety of TGSB and the trend of the results.

The results arrived at this thesis show that the Factor of safety increases greatly by the action of Coconut tree roots and this explains the sustainability of TGSB. Based on the work conducted in this thesis along with the experimental results, it is possible to draw the conclusion that, Existing TGSBs are statically and seismically safe.

TGSB technology can be extended for higher bunds than those in existence with suitable modification in sizes. From this one can safely deduce that such carbon-negative, sustainable low-height embankment infrastructures must be replicated in similar situations all over the world. The present research fills the research-gap by study of the coconut tree root as a natural geo-reinforcement in embankments.

Keywords: *Seismic Stability, Traditional Goan Saraswat Bunds, Bunds, Coconut Root Soil*

CHAPTER 1

INTRODUCTION

1.1 Introduction

This thesis performs the Computer Based Seismic Analysis of Traditional Goan Saraswat Bund (TGSB) considering coconut-root reinforcement. This is the first thesis in this area of research in Geotechnical Engineering, which necessitates a vast but brief review and assessment of various technical aspects of TGSB which will be dealt as briefly as possible in the thesis as it is necessary to support the main hypothesis.

The main hypothesis of this thesis is that: the TGSBs are the best reliable option for low-rise embankments and revetments as their coconut root reinforcement and traditional soil stabilization makes these seismically better which can be demonstrated by simple computer-based assessment.



Figure 1.1 Road and Coconut trees on Traditional Goan Saraswat Bunds in Goa

TGSBs (Figure 1.1) are coconut tree topped earth-embankments with rubble facing. They were used for centuries in Goa-India for various purposes, initially for land reclamation called ‘khazans’ (Keni1998), (Keni2019), (Kamat 2004), (Sonak et al 2006), (Iyer 2014), (De Sousa 2007). They also serve multiple other functions like transportation, rain-water management, river training, flood mitigation, hill-side stabilization etc. (Figure 1.2).



Figure 1.2 Bunds of Goa and reclaimed Khazan land.

It is extremely important to carry out research towards the avenues of evaluation of ancient structures especially geotechnical structures that have successfully withstood earthquakes and floods. This is because there is an increase in construction activities in many earthquake and flood prone zones all over the world which subsequently frequently fail. This present work aims to geotechnically determine the explanation for the longevity and sustainability of TGSB using computer aided analysis.

1.2 Historical Geotechnical Structures

Today a significantly growing population segment has realized the importance of conserving our past. Currently, the concept of bio-mimicry, bioengineering and sustainable

construction practices is gaining growing recognition hence these ancient geotechnical embankment structure called variously as '*Traditional Goan Saraswat Bunds*' or just '*Bunds*' and locally as '*Baand*', that has lasted for millennia deserved to be studied. Forensic geotechnical examination of ancient geo-structures is necessary in such studies. Sustainability, minimizing Carbon footprint and longevity of structures is the hallmark of ancient engineering technologies. Soil was extensively used by our ancestors for various activities like from buildings, infrastructure-construction, flood control and irrigation. Geotechnical infrastructure includes footings, foundations especially seismic resistant foundations. The earth structures of ancient Egypt, Europe, China, Mesopotamia and Saraswat (also called Harappa or Indus-Valley Civilization) are testament to the longevity and sustainability of ancient geo-structures. TGSB is in this category as it predates written history. Most ancient structures are Geo-structures i.e., structures made of mud, mud products and rock bonded by stabilized-mud. Many ancient structures in India and abroad, like TGSB are worthy of a systematic geotechnical study. Preserving ancient fast disappearing structures and substructures with their technologies is an important modern engineering challenge.

In this thesis whatever available historical documents are technically analysed and all case related information is collectively studied. Based on garnered information, the monitoring and in-situ investigations of the historical TGSB structure and subsoil are carried out. Advanced analysis methodologies available today are applied, once all data have been collected and detailed geotechnical modelling and analysis of the historical structures and substructures is done.

1.3 TGSB -Ancient Indian Infrastructure Geotechnics

Saraswat or Indus civilization is the oldest known civilization to build megacities from 3000 to 1500 BC (Marshall 1931), (Jansen 1985), (Possel 1990), (Dani and Thappar 1992), (Kundu 2013). It predated Mesopotamian, Sumerian, Chinese and Egyptian civilizations which existed from 2500 to 500 BC. These ancient people extensively used mud embankments for river training, transportation, and defensive purposes. Cities were enclosed by massive mud-brick walls with narrow gates only wide enough for entry and

exit of a single ox cart. They built ancient geo-structures which varied from forts, religious structures, ports, residences, pyramids, embankments, dams, tunnels, piers, storage facilities and tombs. Ancient mud structures found around the world give extensive Geo-engineering knowledge when properly investigated. Reinforced Stabilized Mud Technology was developed by them over Millennia.



Figure 1.3 Typical Traditional Goan Saraswat Bunds (TGSB) in Curtorim, Agasaim, Caranzalem in Goa

TGSBs were developed from these structures (Figure 1.3) when these Saraswats settled in Goa (Keni 1998), (Keni 2019), (Wikipedia 2021) after the sudden and mysterious destruction of their cities.

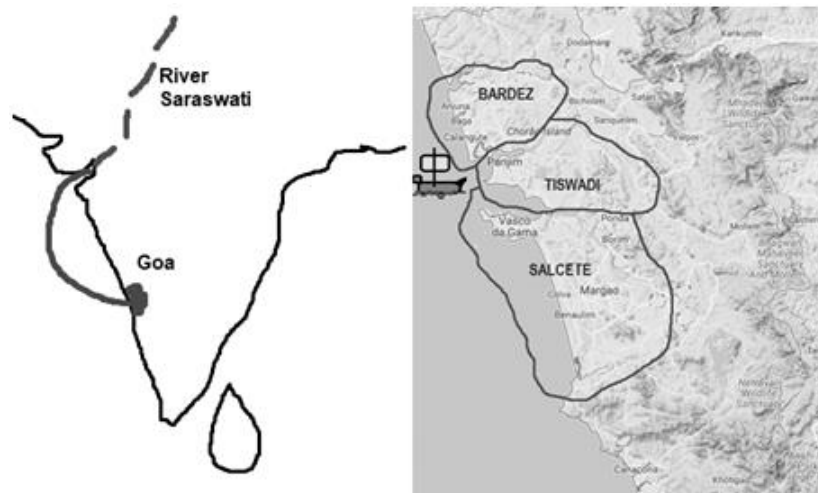


Figure 1.4 Route to Goa and Ancient Saraswat Settlements in Goa

As per local folklore, when the mythical River Sarawati disappeared, due to the destruction of the bunds protecting them and the subsequent shifting of the river from the present Thar desert in Rajasthan to the present River Indus, many survivors under the leadership of the twelve (Bara – Zonn = council of Twelve Ones / leaders) boarded boats and set forth south to a promised land (Figure 1.4).

They settled in this Promised Land then named it as Gowa after the principal Saraswat/Harappan animal- Cow and the newly reclaimed territories were named after the settlers: twelve republics (bara-desh = Bardez), thirty colonies (tis-waadi = Tiswadi), and sixty-six serfdoms (shashasti = xasti = Salcete) (Figure 1.5 and 1.6).



Figure 1.5 Ancient Saraswat / Indus-Valley Seals showing the sacred animal Cow= Gowa (Harappa.com).



Figure 1.6 Ancient Saraswat / Indus-Valley Seals showing the boats used in the ancient Saraswat Civilizations transporting men and animals (Harappa.com) and old Goa boat

As TGSB is a Unique Historical Sustainable Geotechnology from Goa used to reclaim saline land called khazans (GCCCI 2007), (D'Silva and Barreto2012), (Sonak et al 2006,2014), (Iyer 2014), (Souza et al 2016), (Nayak 2017). The origins and utility of this

fragile traditional technology needs additional research to give an insight into the significance and modern-day utility of these bunds.



Figure 1.7 Similarity in design of Bunds from Saraswat civilization and Goa

In India in ancient times the Engineers (Rishis or Enlightened/Learned ones) of Saraswat Civilization (normally called Harappa Civilization or Indus-Valley Civilization) had integrated many key geotechnical procedures in embankment building in the lost cities of Harappa and Mohenjo-Daro civilization. These are still observed in the Bunds (TGSBs) seen in Goa (Figure 1.7) (Souza and Savoikar 2019b).

1.4 Relevance, Applicability and Civil Engineering Uses of TGSB

A constant debate exists about the relevance and applicability of ancient structures like TGSB to modern Civilization which is settled by the continual performance and utility and new areas of applicability of TGSB. Their ease of construction and low-cost construction methodology increases their importance. TGSB technology simultaneously encompasses different branches of civil-engineering: - Construction, Soil-Mechanics, Geotechnical-Engineering, Irrigation, Transportation, Environmental-Engineering, etc. The different traditional applications and civil engineering use of TGSB are: Land Reclamation, Slope Stabilization, Habitation, Transportation, River Training Works, Irrigation, Rain Water Harvesting, Ground Water Recharge. The different additional possible modern applications and civil engineering use of TGSB include: Solid Waste Retention System, Seismic and Liquefaction Stability, Coastal Storm Shield (Wind Break), Tidal Control, Tsunami

Protection, Tourism Infrastructure, Environmental Up-Gradation, Carbon-Footprint Reduction in infrastructure, etc. (Figures 1.8 to 1.12)



Figure 1.8 Transportation Infrastructure: Road on TGSB

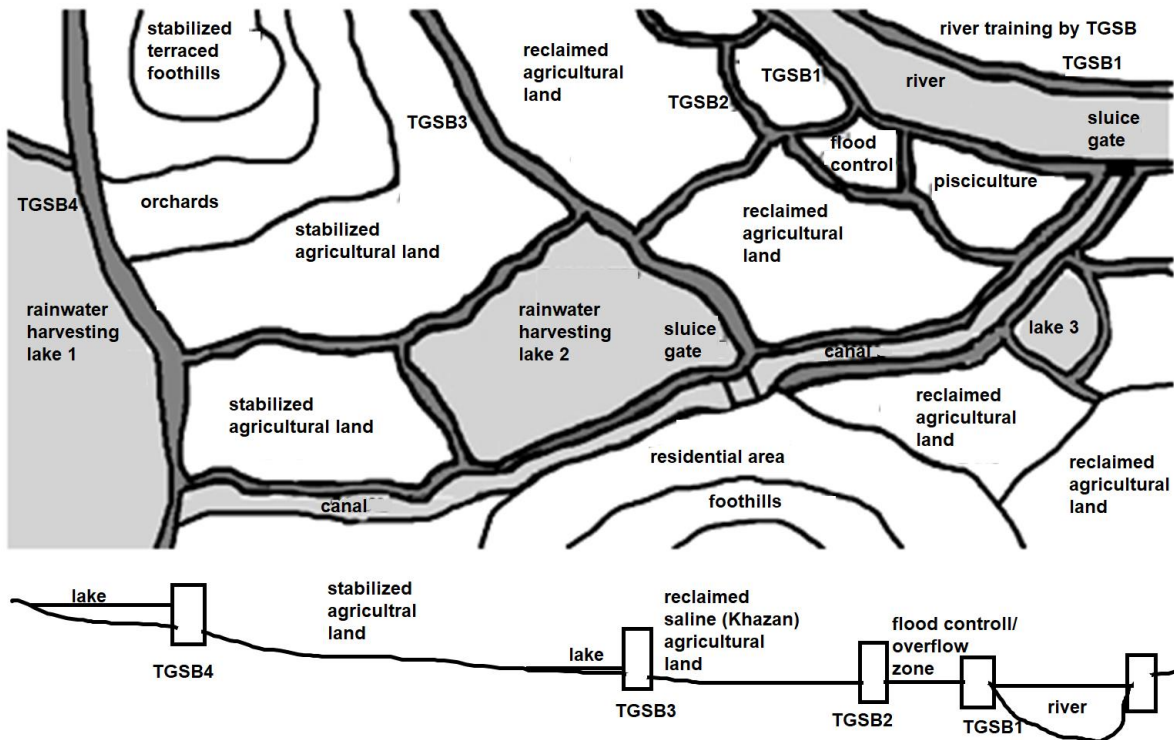


Figure1.9 Irrigation and Rain water harvesting by TGSB

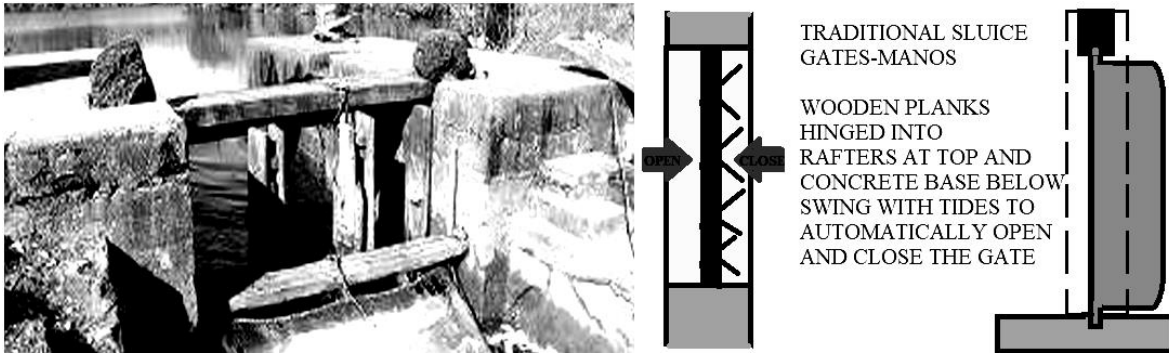


Figure1.10 Tidal Control: Traditional Sluice gates and water control mechanism in plan and section.

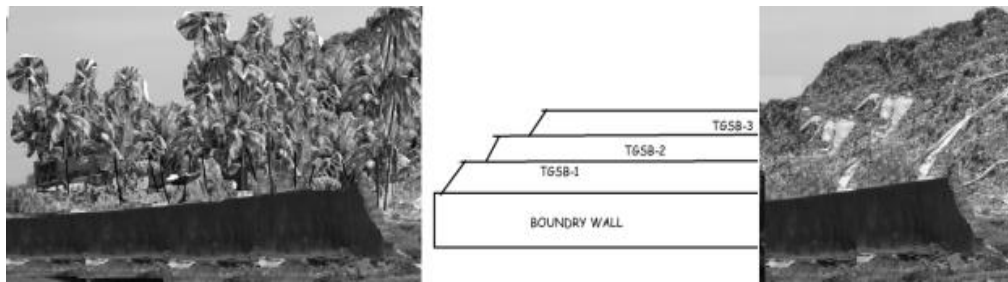


Figure1.11 Possible makeover for (Sonsodo, Margao-Goa) MSW dump and actual dump



Figure 1.12 Windbreak and Tsunami protection, (Coconut trees standing straight on Riverside Bund even as Cyclonic Gusty Winds lash at over 100 Kmph at Carona Goa- note the aerodynamic shape of each leaf-frond and tree canopy as a whole)

In addition to this the maintenance and repair of TGSBs is a good source of income for civil-engineers and their associated trades (masons, helpers, suppliers). The coconut trees on TGSB further increase their utility and economic value. Coconut stems are used as rafters in traditional homes and their leaves serve as roof thatching and as walls for temporary sheds. Coconut stems are used as traditional fender piles in shore protection. They are also used to demarcate sand bars in rivers. Today coco-wood a new product made from desiccated coconut husk and stem sawdust is gaining wide popularity as a construction and furniture material. The world faces a resource crunch so sustainability takes a centre stage making a green-structure like TGSB that has lasted millennia truly relevant.

1.5 Biomimicry and Biomechanics of TGSB Design

Biomechanics and Biomimicry was the art and science used in developing the TGSB technology by ancient Saraswat Rishis.

Biomechanics which is used today for natural soil strengthening (Chou2007), (Cazzuffiet al 2014), (Capilleria et al 2016), (Wu 2013), (Wu et al 1979), (Zanetti et al 2011, 2014), was first used in ancient times by historic technologies like TGSB. Roots and their gummy secretions increased the shear strength of soil biomechanically. Penetrating fibrous roots biomechanically compacted the soil by slowly reorienting the particles and filling in loose pockets.

Biomimicry, the expertise of doing nature-similar structures is also growing in importance in modern geo-technology (Badarnah et al., 2010), (Maglic, 2012), (Heil and Belkadi, 2017), (Turner and Soar, 2008), (Zari, 2007) as we push towards sustainability. Ancient Rishis observed how coastal coconut trees strengthened surrounding soil. They observed how soil into which lime from burnt shells and ash from burnt coconut leaves was dumped resisted erosion and was stronger. They adapted these secrets of nature into their engineering. A double row of coconut trees was planted in a zigzag pattern 10m apart centre to centre, along the length, on the top of the TGSB 1m from the face to strengthen them by their roots (Figure 1.13).



Figure 1.13 TGSB along Galgibaga river in Canacona

Intermediate Breams were introduced when the embankment was higher than 3m for every 2.5 to 3m step, which carried additional single line of coconut trees. These trees were replaced every 100 years during periodic maintenance. The sides were protected by lateritic rubble stone pitching 0.5m thick that projected 0.3 to 0.5m above the embankment as they observed how stone rows on a hill-terrace prevented erosion thus avoiding overtopping failure. No other tree was allowed on top however in rains some vegetable creepers (pumpkin / gherkins / cucumber / gourds / beans / peas) were permitted. Grasses were allowed but trimmed. No vegetation was permitted on the sides. They observed the deleterious effect of tall tap root trees on the TGSB and forbade them. The TGSB design evolved from Nature using the bio-inspired geo-mechanics and mimicking the successful designs from nature.

1.6 Sustainability of TGSB

Sustainability can be divided into three components: Lowering Carbon Footprint (Cordero 2013), (Wandana et al 2021), Waste Re-Utilization (Izverciana and Ivascua 2015), (Menikpura et al 2013) and Longevity (Becker 2014). TGSB as explained below has all three components.

Today extreme climate events triggered by climate change are putting a focus on reducing Carbon-footprint. Construction and infrastructure industry is a major culprit as it depletes

natural resources and cuts down trees. TGSB on the other hand uses locally available materials which are easily replenished by natural processes (Souza and Savoikar 2019b) and the top coconut trees which generate oxygen from carbon-dioxide making this truly a carbon negative structure.

Significantly modern studies on sustainability deal with reutilization of by-products. Three waste products are traditionally used in TGSB: – 1 –burnt and powdered lime from waste shells of locally consumed shellfish and, 2 –molasses from sugar, and 3 –ash (pozzolan) of cooking fires from coconut leaf (Souza and Savoikar2017). Thus, waste reutilization is significant to TGSB design.

Longevity of TGSB can be gauged from extreme-climate events they have withstood. Today embankments are failing the world over due to rainstorms, cloudbursts and cyclones.

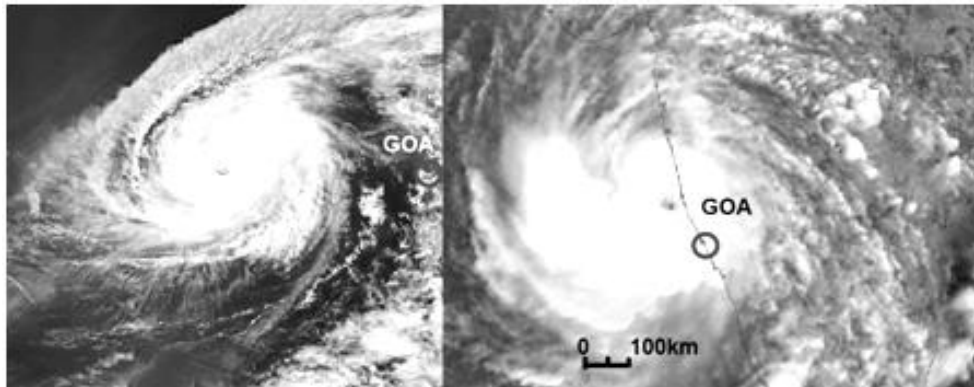


Figure. 1.14. Cyclones Kyarr (2019) and Tauktae (2021) which struck Goa recently (USGS)

The TGSB meanwhile have survived and functioned in Goa in spite of two mega cyclones with maximum wind speeds 150 to 210 kmph, namely (Figure. 1.14) Kyarr-2019 and Tauktae-2012 (IMD-Goa 2021), (IMD-India 2021) with minimum flooding. The unique TGSB rain water harvesting consisting of a series of holding reservoirs and channelling system (Figure 1.15) systematically take care of the runoff while the series of TGSB limit and dissipate the flood impact.

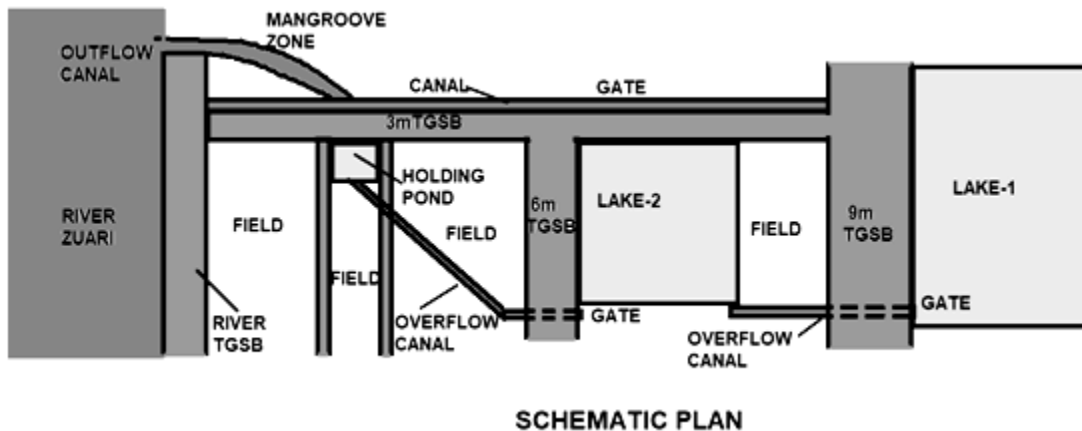


Figure 1.15 TGSB flood control system at Curtorim-Goa

In comparison the famous Hurricane Katrina in USA with wind speed of just 130 kmph left behind a trail of destruction with death toll of close to two thousand. Thousands of fertile acres of farmland were degenerated to swamps. The main cause was the collapse of modern American levees leading to inflow of saline water (Sastry 2007). In the year 2021 exactly sixteen years after Katrina Hurricane Ida (New York Times 2021) struck Louisiana just to the side of the previous hurricane. It made similar damages to infrastructure and land but there were fortunately less human losses. Levees failure caused floods in Louisiana-USA with weeks of power-cuts. In Goa electric power loss was restricted to limited locations for a couple of days and flood waters receded in two to three days.

It is noteworthy that Global warming has caused sea water rise due to melting of Glaciers and Polar caps. Recently released data showed that the water levels in the world will rise in all coastal cities (IPCC 2021), (NASA 2021) with Goa showing a coastal rise of up to 90 cm. TGSBs with a 1.5 m freeboard will act as levees to absorb and limit any such melt damage. Though most coastlines in the world show climate driven vulnerability, the unique TGSB network allows Goa to be more resilient to such climatic-variation while these ancient geo-structures last without ‘renovation’.

The secret to the sustainability of TGSB was the serial repairs carried out by the Saraswats through their ‘Gaokari System’ (Keni 1998), (Keni 2019) (Kamat 2004), (Sonak 2006), (D’Silva and Barretto 2012). Serial repair meant that all of the bunds were in repaired in circulation, and work was equitably divided in the village. Yearly maintenance consisted of

replenishing of washed-out soil to original level, weeding, removal of tap root trees from the top, replacing damaged facing and checking burrowing animal damage. It included repairs of damaged parts and replanting of coconut trees every 75 to 100 years. They allowed 15 years for growth then cut the older trees which were then used for lumber. Sadly, due to socio-economic reasons such-maintenance is virtually non-existent today.

The TGSB has lasted thousands of years, they have faced floods and earthquakes without damage, and they have absorbed the dynamic loading of bombardment by cannon from different forces both local (Muslims, Marathas and Indian Army during annexation) and foreign (Arabs in 1400, Portuguese conquest of 1500 and Dutch blockade of 1600). Throughout this period, they performed their intended functions flawlessly (Souza et al 2016), thus making the sustainable TGSB a structure worthy for engineering technical research.

1.7 Coconut tree damping and soil strengthening

Seismic contribution of the coconut tree consists of two parts: the damping of vibration by the coconut tree as an inverted pendulum and the damping of the vibration by the root mass in the soil. Due to this TGSBs have lasted for over 5000 years ever since the Saraswat migration (Keni 2019) through storms and earthquakes and repeated dynamic loads of bombardments by cannon. Coconut tree roots are self-repairable natural geo-reinforcement for embankment soils that are fibrous in nature which act as a combination of geo-fabrics, geo-drains and elastic springs thus increasing the shear strength hence seismic resistance of bund soil in multiple fashions.



Figure 1.16 Fibrous Coconut roots strengthen soil and dampen vibrations.

Soil is retained by coconut tree roots even in sandy beaches of Goa despite dynamic wave impact. This is due to the dynamic Soil Root Interaction of the fibrous roots of coconut tree and soil (Figure 1.16). There is a scope to study this damping phenomenon and arrive at its technical understanding in this thesis. We need to model the coconut tree roots and study the possible role of roots in damping of the dynamic waves (Tobin et al 2007a, b), (Dupuy et al 2010), (Wolf 1985). Coconut roots can grow post-facto under structures after the structure is built, thus act as a seismic-retrofit. Unlike geo-textiles they don't have to be put in first and unlike micro-piles they can extend at any angle even horizontally under the structure. Their roots suck soil water and strengthen the soil (Indraratna et al 2006, 2014, 2015) and increase its cohesion (Estabragh and Javadi 2012). Today, as the concept of bioengineering and sustainable construction practices gains growing recognition, a natural-geosynthetic reinforced structure that has lasted for millennia and the role of coconut tree root reinforcement deserved to be studied.

1.8 Seismicity and Goa

Currently earthquakes and seismic activity are a major growing concern. There is a paucity of studies done on the seismicity of Goa considering the soil and sub-soil profile. As construction industry is grows at an exponential pace sustainability of geo-structures built in these zones is a major concern in today's world. A green-sustainable seismically stable structure Like TGSB is needed in such areas. The greatest threat during earthquake is ground failure. Ground can fail by liquefaction and slope failure. Natural and manmade slopes which are stable and safe under static conditions could become unstable during earthquakes. Ground shaking induced by earthquakes adds a destabilizing force to the slope, reducing the factor of safety against failure. TGSB with their coconut tree root damping is a good solution to consider in areas with these concerns. There is needed to be study protection by TGSB from Tsunamis triggered by earthquakes in Coastal areas. Goa is relatively free of dangerous earthquakes (USGS2021), (BMTPC2021), (NCS-MoES2021).

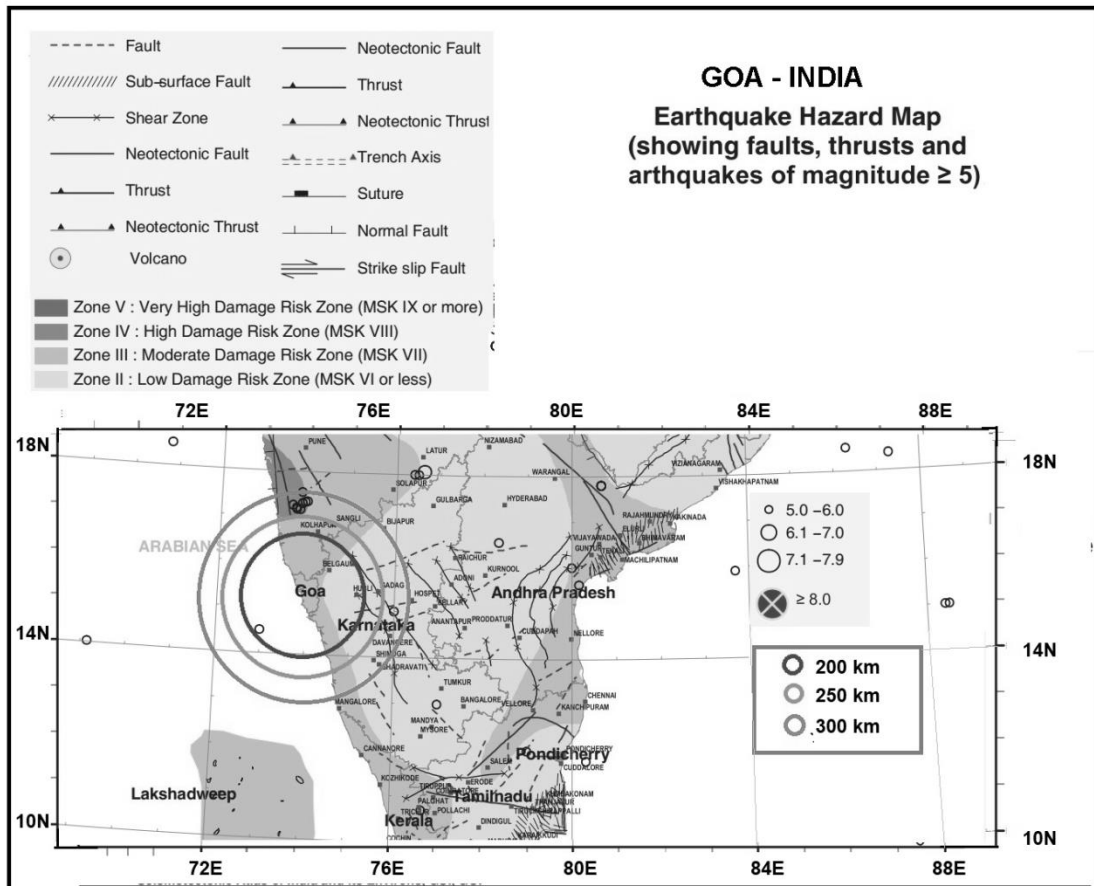


Figure 1.17 Earthquake hazard Map showing earthquakes near Goa (BMTPC).

It is also relatively far from any potential fault zones (Figure 1.17). It is seen from the map given above that there was only one earthquake of magnitude 5 within 200 km radial distance from centre of Goa. There were no earthquakes of magnitude greater than 5 from till 250 km radial distance from centre of Goa. There were 12 earthquakes of magnitude greater than 5 from 300 to 350 km radial distance from centre of Goa. There is limited number of studies done on the seismicity of Goa considering the lateritic profile. This gives a scope for more research in this area.

1.9 Area of work

The general area of work primarily identified was therefore the study of TGSBs of Goa and their seismic stability.

In order to do this in an inclusive and extensive manner, the following tasks were identified:

1. Detailed literature survey and the specific area of study to be identified.
2. Further studies in Parallel areas of research may have to be done and correlated to this area as there is no research in this section of geotechnical studies.
3. Brief study of TGSB, including construction methods, and techniques needs to be done.
4. Testing of lateritic soil for properties needed for input in software needs to be done.
5. Testing of coconut roots and soil for properties needed for input in software needs to be done.
6. Generating of Earthquake of parameters using Software and Excel for input in software.
7. Computer based static and seismic analysis of bunds can be carried out after this.
8. Finally, necessary conclusions may be drawn and scope for further post-doctoral work can be identified.

1.10 Objectives of the Study

This work thus seeks to discover the explanation for the longevity and sustainability of TGSB using computer-based analysis. This thesis is organized into the initial chapter which introduces TGSB and a literature review chapter followed by four chapters. The next chapter deals with methodology of study and includes research and laboratory experiments needed for this thesis. The subsequent chapter deals with the analysis done both static and seismic of TGSB. The consequent chapter deals with the results and discussions on the results. The last chapter deals with the conclusions drawn. Additional information including brief case-studies will be provided in the annexure given at the end in the thesis. The objectives of the present research were as follows:

1. To review extensively the available literature in the area of coconut tree lined embankments/bunds.
2. To perform laboratory studies to evaluate geotechnical properties of soils used in the embankments/bunds in Goa

3. To test the coconut tree roots, root reinforced soil and their geosynthetic reinforcing actions in bunds.
4. To study the seismic ground motion parameters affecting the seismic behaviour of bunds.
5. To perform static and seismic analysis of bunds considering coconut tree root reinforcements.

1.11 Scope of the work

In the present thesis, introduction about the TGSB is given in Chapter 1.

Chapter 2 deals with the literature review available in this area and the critical appraisal of the literature.

Chapter 3 describes the methodology used analysis of soil properties, root properties and static and seismic analysis.

Chapter 4 deals with static and seismic analysis of the TGSB while the detailed results and discussions are presented in Chapter 5. Conclusions drawn from the present study are presented in Chapter 6.

Additional and supplementary data is presented in 17 annexures.

CHAPTER 2

LITERATURE SURVEY

2.1 Introduction

When researching a historic technology there are scant if any records available. Most of the literature has to be gleaned from parallel sources dealing with similar technologies and similar topics. A structured method was employed to identify the area of research. An extensive Literature survey was carried out. A critical appraisal of it followed. The study conducted and what can be applied to the present area was identified using the multi pass strategy: Glance, Store, Note and Journaling. Research avenues available were identified and the appropriate research area was chosen while ensuring difference with previous research. Literature was studied for the carrying out of the thesis work and for covering the topics adequately.

As this is the first of its kind study in this area there is no research available on the various aspects and topics for review. Wherever possible nearest possible parallel research was studied in similar areas of expertise so these could be extended and incorporated in the present study.

2.2 Literature Survey for Computer Aided Seismic Analysis of Bunds considering Coconut Root Reinforcement

In order to give adequate coverage to all areas concerning the research the literature was broadly divided into following broad categories:

- Available literature on History, information and origins of bunds in Goa.
- Available literature on for geotechnical properties of soils, roots and material used and their testing and soil stabilization.
- Available literature on seismicity and seismic parameters and any other relevant information.

- Available literature on computerized analysis of bunds as embankment and levees with respect to their static and seismic stability and other effects of earthquakes.

The above four broad were then further subdivided for better understanding of the bunds, root reinforcement and seismic analysis using computer. During the course of this review the following areas were studied by reviewing literature about them: TGSB, sustainability, Soil Characterization, Soil Stabilization, Coconut Tree Root Geo Reinforcement, Seismic Parameters, Numerical and computerized analysis Liquefaction Potential, Tsunami dynamics, Computational Methods and Codes and Standards.

2.2.1 Traditional Goan Saraswat Bunds as a Sustainable Infrastructure

This area has been mainly studied socio-environmental purposes. As this research area is not geo-technically studied yet, secondary tertiary and parallel sources had to be referred. This review was performed to establish the historicity, extent and sustainability of bunds in Goa.

Wikipedia (2021), Keni (1998 & 2019), Souza et al (2016), describes how the Saraswats arrived in Goa after the disappearance of the River Saraswati and constructed Bunds to reclaim and stabilize land for usage with the help of locals.



Figure 2.1 Sluice gate on Khazan (Sonak 2014)

Most of the other authors like Kamat (2004, 2013), Sonak et al (2006&2014), Iyer(2014),GCCCI (2007), D'Silva and Barreto (2012), Nayak (2017), mainly concentrate on the land reclamation called 'khazans', and the socio economic and ecological benefits that Goa derived from them, bunds are studied as an appendage to the Khazans (Figure 2.1). They also mention their maintenance and repairs.

The antiquity and life and location of the Saraswats or Harrapan civilization is described by Marshal (1931), Jansen (1985), Possel (1990), Dani and Thappar (1992), Kundu (2013). They demonstrate the mastery of earthen structures of these early engineers. More data and pictures of the civilization can be found at www.harappa.com. As TGSB have survived through centuries; while absorbing carbon from air and utilizing waste products; its sustainability characteristic needs investigation. Review was also done on the three aspects of Sustainability wherein; Lowering Carbon Footprint aspect was deliberated by Cordero (2013), Wandana (et al 2021), Waste Re-Utilization aspect was studied by Izverciana and Ivascua(2015), Menikpura et al (2013) and Longevity aspect was discussed by Becker (2014). The extent of cyclones affecting Goa, Kyarr-2019 and Tauktae-2012 was obtained from IMD-Goa (2021), IMD-India(2021) and USGS (2019, 2021), was studied to demonstrate sustainability in face of disaster. The impact of failure of modern American levees in similar storms was studied from Sastry (2007) and news reports from New York Times (2021). The effect of global warming caused sea water rise which may affect TGSB is studied from IPCC (2021), NASA (2021).

2.2.2 Soil Characterization and Stabilization

This review studies the soil properties and their stabilization in bunds in Goa.

Constitutive models, their equation and yield criterion for soil are given by several researchers like Coulomb (1770, 1776), Mohr (1900), Taylor (1948), Tresca (1857), von-Mises (1913), Drucker and Prager (1952), Lade-Duncan (1975). Each is valid for different conditions and different soils. The Mohr - Coulomb is best suited for the soils used in TGSB.

Horslev (1937, 1960) gave relationship for anisotropy in soil depending on shear property. Anisotropy in lateritic soils has been studied by Liu et al (1997), Ling et al (2002), Zhang et al (2018), and Liu et al (2020).

Souza and Savoikar (2017) explained how lime, molasses, and coconut leaf ash were used as pozzolan and stabilizers for TGSB soil in traditional methods. Supplementary Cementitious Material, are by-products that have been used by several researchers such as Karthik et al (2014), Bin-Shafique et al (2003), Sadeeq et al (2015), Fay et al (2012), Padalkar et al (2013), Goswami (2004), James and Saraswathy (2020), Amadi (2010), Al-Chaar et al (2013), Amiralian et al (2012), Isah (2014), Okafor and Okonkwo (2009), Olugbenga and Akinwale (2010) for soil stabilization in addition to cement and lime. Different products have different stabilization effects but no research has been done using coconut leaf ash.

2.2.3 Coconut Tree Root Geo Reinforcement

This review studies the properties and effects of coconut tree roots and their geo-reinforcement effect in bunds in Goa. As this borders on Geotechnical and biological sciences a lot of review was needed in this area.

Ali et al (2012), Burrall et al (2020) Preti and Giadrossich (2009) have studied how different types of roots reinforce soil in various ways. The biomechanics of roots are used for soil strengthening by TGSB. Chou (2007), Cazzuffi et al (2014), Capilleria et al (2016), Wu (2013), Wu et al (1979), Zanetti et al (2011, 2014), have discussed how Biomechanics especially roots of plants helps in natural soil strengthening (Figure 2.2). DeJong et al (2009, 2010) and Chou (2007) researched the bio-mediated soil improvement and the ability of trees to improve the soil strength and other properties by tenfold or more.

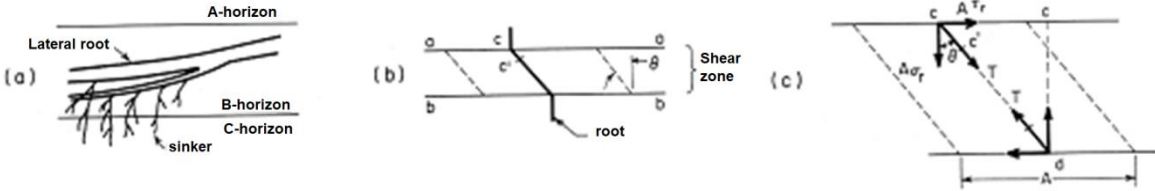


Figure 2.2 Mechanism of root reinforcement of soil (Wu et al 1979)

The main type of fibrous roots are grass roots have been examined by several researchers Anaswara and Shivashankar (2015), Nasrin (2013), Gobinath et al (2015), Hengchaovanich (2003), Truong (2013), Teerawattanasuk et al (2014). Grass is taken as a root mat due to difficulty in modelling fibrous roots (Figure 2.3).

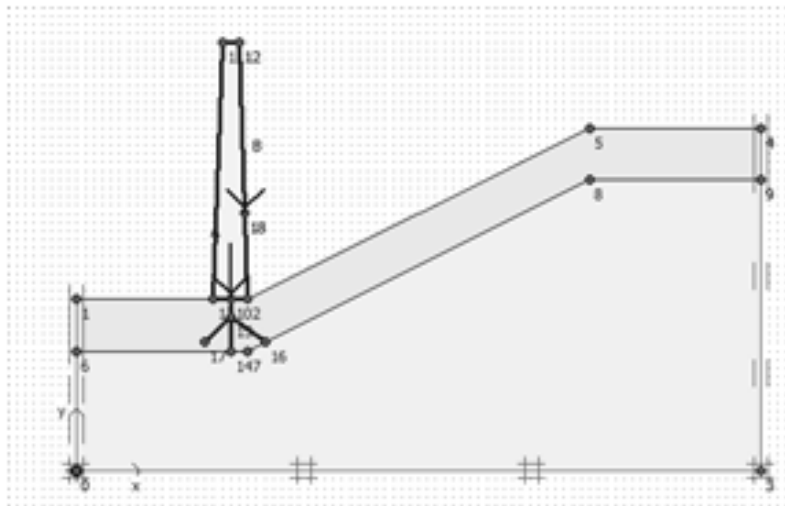


Figure 2.3 Software analysis of grass reinforced slope with tree at bottom (considering fibrous roots as a mat and tap roots as beams) (Anaswara and Shivashankar 2015)

TGSB evolved from observing and adapting natural processes and techniques. Significance of Biomimicry in modern geo-technology is discussed by Badarnah et al (2010), Maglic(2012), Heil and Belkadi (2017), Turner and Soar (2008), Zari (2007).

Damping of vibrations contributes to seismic stability. The seismic damping and properties of tree root for possible role in damping of the dynamic waves of tree roots was studied from Tobin et al (2007a,b), Dupuy et al (2010), Wolf (1985).

Negative pore pressure developed by the roots also called as matric root suction strengthens the soil. Indraratna et al (2006, 2014, 2015) and Fatahi et al (2007 a, 2007b and 2008) showed that roots suck soil water and strengthen the soil and gave a method to find it for tap-root trees in Australia. Some pore pressure measuring instruments can be studied at Wikipedia 2021. These can be used for in-situ measurement. Estabragh and Javadi (2012) demonstrated that roots increase cohesion thus strengthen the soil and gave a graph-plot to

find it. Fredlund et al 1978, 1996 gave a Soil Water Characteristic Curve which is today the basis for measuring soil suction.

Coconut tree roots act as geo-textiles and thus improve soil properties. Geo-textile which are usually synthetic in nature and their uses and properties are described by Zornberg (2011), Boyle (2013), Palmeira et al (2008), Moldovan (2010) and Handbook for Geosynthetics (2013). Many natural geotextiles used are especially jute and coir. Satyanarayana et al (1982), Gray and Ohashi (1983), Ali (2010), Fathi (2014), Das et al (2016), Anggraini (2016), Kalita et al (2016). There exists insufficient technical literature on coconut tree roots.

2.2.4 Seismic Parameters

This review studies the seismic parameters meant to be used for the seismic analysis of TGSB in Goa.

According to maps and literature given by USGS (2021), BMTPC (2021), NCS-MoES (2021), Goa is relatively free of dangerous earthquakes. There were no earthquakes of magnitude greater than 5 from till 250 km radial distance from centre of Goa. However due to its strategic importance as a defence point and major harbour it is given a higher seismic zone in the Indian code.

Himalayan earthquakes are described by Saikia et al (2016), seismic maps can be found at website of Earthquake Track (2020).

Liu and Tsai (2005), Iyengar and Raghukant (2004), Raghukant and Iyengar (2007) Rao et al. (1998) Sharma et al (2007) and NDMA (2008) have given attenuation relationships for different regions some of which are applicable to Goa. Valdiya (2010) and IIT Madras have produced fault maps which can be used to generate earthquake magnitudes from above information.

2.2.5 Numerical and computerized analysis

This review studies the different computer based analysis for all seismic effect including stability, liquefaction and tsunami-dynamics for bunds in Goa and the computational methods available.

The factor of safety for the TGSB for both static and seismic condition needs to be investigated. Static and dynamic analysis of slopes and embankment structure similar to TGSB have been carried out by several researchers like Clough and Penzien (1993), Getachew (2018), Taylor (1948), Kramer (1996), Meheroff and Adams (1968), Morgenstern and Price (1965), Pelecanos (2013).

The computerized analysis can be carried out using readymade software and also the flexible and adaptable ability of spreadsheets. Using programming languages even a problem specific code can be written. Christy (2000), Lipjac (2013), Srbulov (1999) and many others used Microsoft Excel software in solving problems in civil engineering especially geotechnical engineering.

In stability analysis while doing specific spread sheet analysis the different forces need to be considered. Dynamic forces due to waves are obtained from Goda's (1985) equation also used by Wiebe et al (2014). Previous 100 year records of waves are available at Metrological Department of India or IMD (2021), as studied by Aboobacker (2010) and Wilson et al (2015). IMD also gives wind records. Tidal fluctuation in riverside bunds occurring in Goa has been studied by Mehra et al (2009), Mörner (2016), Subeesh et al (2013), Sundar and Shetye (2005). Hydrodynamic pressure is calculated using Westergaard's wet block formula as given by Westergaard (1938) and used by Fellenius (1936 and 2006). Earth pressure can be found out using Rankine's formula due to its simplicity. Seismic force can be calculated from the Mononobe and Matsuo (1929) modification of the Okabe method (1926) called as Mononobe-Okabe method.

The first pseudo-static approach to seismic slope stability analysis has been given by Terzaghi (1950) Terzagi et al (1950). pseudo-static coefficients have been compiled by Melo and Sharma (2004). Simplified pseudo dynamic analysis based on response spectrum method is carried out for different structures by researchers like Jain (2013), Elia and Rouainia (2013), Iai (2001), Løkke and Chopra (2013), Bretas et al (2014, 2015), Ghobrial and Karray (2015). Another approach is by using site specific seismograph which can then be inputted in software to obtain Site Specific Response is dealt with by several researchers Boore and Atkinson (2008, 2006), Boore and Joyner (1997), Cho et al (2012), Kanamori et al (1993a,b), Raghunandan and Juneja (2009).

Dynamic analysis is very complex but simplified procedure for Pseudo Dynamic approach can be used based on the work of many researchers like Choudhury et al (2006), Nimbalkar et al (2006), Presti et al (2010), Choudhury and Savoikar (2009), Savoikar and Choudhury (2009, 2010a, 2010b, 2012), Bray et al (2018), Bray and Travararou (2007, 2009), Bray and Machedo (2017a, 2017b, 2019), Clough and Penzien (, 1993), Boore (2003), Mitogawa and Nishimura (2020) Abrahamson et al (2014)

Soil liquefaction is a major effect of earthquakes and needs to be studied for seismic analysis of any structure. Youd et al (2001), Marcuson (1978), Ishihara (1985, 1996), Dobry et al (2015), Encyclopedia Britannica (2012) Sasaki et al (1992, 2004), Seed et al (1985, 2003), Seed and Idriss (1971, 1982) have given procedures and methods to calculate the liquefaction vulnerability of soils. Liquefaction Potential Index is given by Iwasaki et al (1978, 1982), Toprak and Holzer (2003), Holzer et al (2006), Maurer et al (2014). Sonic velocity from the SPT test result (N) is developed by Castanga et al (1985), Mavko (1990), Shahien (2007), Wadhwa et al (2010), Madun et al (2015). Liquefaction settlement can be found using the procedures outlined by Seed et al (2001) Tokimatsu and Seed (1987).

A very little studied aspect of seismic event is Tsunamis. As TGSB lie on coast tsunami danger needs investigation. Tsunami Dynamics has been studied by researchers such as Dias and Dutykh (2007), Bryant (2008), Chock et al (2013), Chock (2016), Yang et al (2017), flooding Pasha and Tanaka (2020), Ko et al (2015)), Foster et al (2017). Wave data can be obtained from IMD and Institute of Seismological Research 2019 and NOAA

GEOSTUDIO is widely used suite of software in Geotechnical Analysis of embankments and structures by many researchers including Maula and Zhang (2011), Gustafsson and Lindstrom (2014), Chakraborty and Dey (2016a, b, c), Getachew (2018). For this analysis three of the analyses components of GEOSTUDIO can be are used: SLOPE/W for slope stability, SEEP/W for seepage analysis and QUAKE/W for dynamic and seismic analysis.

Midas-GTX-NX has also been used for FEM analysis by different researchers like Lv(2013), Doshi et al (2015), Le and Dao (2015), Raji et al (2016), El-Kadi (2016), Andreea (2016), Pilecka et al (2016), Baoliang et al (2017), Koda et al (2017), Su et al (2018), Souza and Savoikar (2019a), Yanina et al (2019), Saini and Goyal (2019), Gao (2020), Gao et al (2020), Lv (2020). It can be used to do 3D analysis of the TGSB.

From this review it was observed that it will be necessary to also perform a brief static analysis as none was conducted before in order to compare the safety decrease with seismic effect.

2.2.6 Codes and Standards

This review studies the codes and standards available for the study of seismic analysis and other input properties including testing for bunds in Goa. Engineering standards are important documents that specify technical characteristics and details that must be followed in any investigation. An important use of standards is to ensure unbiased, direct and explicit experimental data to publish in a thesis. Indian and International standards are required to examine the geo-mechanical properties of soil and tree-roots needed for seismic analysis of TGSBs.

Indian codes for earthen embankments and embankment dams and soil testing were used where applicable to standardize the research like SP 36, EM 1100, ENCE 36, ASTM d24871 and IS 1498. International codes for earthen embankments and embankment dams and soil testing were used where applicable as the research must also have international validity IS 7894. Although growing taproot trees on embankment damage them (FEMA-1263 2005), (FEMA-534-2005) there are no standards on fibrous roots on embankment.

2.3 Critical Appraisal of Literature

On doing critical appraisal of literature it was found that studies on TGSBs are mostly of historical and socio-economical nature of the reclaimed land (*Khazan*). No Geotechnical studies on TGSBs prior were conducted to this. Extensive and exhaustive studies on use of Geo-synthetics, coconut coir and jute geo-fabrics in and on new embankments have been carried out in India and abroad. Extensive studies exist of pine and tropical taproot trees and grass root reinforcement in soils, but no studies on use of natural Geo-synthetics or coconut root reinforcement in TGSBs are done. Exhaustive Wide-ranging studies on testing for Geotechnical properties of lateritic soils have already been done, especially in Nigeria but no studies exist on soil from TGSBS in Goa or their stabilization. Widespread studies on finding the seismic parameters in soil including extensive and exhaustive studies on

static and dynamic analysis for embankments and Dams have been carried out but no studies on seismic response of TGSBs exist. Extensive studies with other software like FLAC, OPTUM G2, PLAXIS and GEOSTUDIO, MATHLAB on embankments and earth dams and few studies use MIDAS GTS-NX, but none study TGSBs. Software has no root element so it needs to be modelled as beam or pile element or as a separate (root-mat) layer. Liquefaction is a widely researched topic but no previous research on liquefaction analysis of TGSB is done. Tsunami dynamics is an emerging research area but no previous research on Tsunami dynamics of TGSB is done. There is no study on TGSB in python programming language. There are no codes for TGSBs in India.

2.4 Gaps in previous research and Research Avenues Available

As there was no previous research done in TGSB there were many gaps in the research. It was possible to analyse the embankment using any and every method available and developed for analysis of rooted embankments.

It was seen that the following research avenues were available: Geotechnical Science behind the ancient methods of construction of Traditional-Goan-Saraswat-Bund (TGSB), Sustainability of the TGSB, Better and more modern alternatives for construction of TGSB and their sustainability, Geotechnical Comparison between TGSB and the modern method of MSEW (Mechanically Stabilized Earth Retaining Walls), Possibility of using TGSB technology internationally in hurricane affected areas, Possibility of using TGSB technology in small height earthen dams, Geotechnical Applicability of TGSB in Infrastructure Engineering, Computerized studies of TGSB for stability, seepage, etc. using various software, Development of TGSB design software using Python, Seismic stability of TGSB with Coconut root reinforcement, Comparison of seismic stability of TGSB to MSEW.

2.5 Research Area Identified

The following research area was identified: Testing of Coconut Tree Root Reinforcement (CTRR) for additional soil reinforcement as a bio-geo-textile and its contribution to the seismic stability of the Traditional Goan Saraswat Bund (TGSB).

2.6 Difference from Previous Works

There was sufficient difference found from previous research on embankments. No previous research has been done on coconut trees and its roots to be used as soil reinforcement. No previous research carried out on larger diameter fibrous roots as soil reinforcement (tremendous previous research on mostly concentrates on Vetiver Grass and tap root trees as soil reinforcement). Tall trees planted at bottom of slope recommended not on top as in TGSBs. No previous research on seismic stability using CTRR as soil reinforcement is done. No previous research on liquefaction analysis of TGSB is done. No previous research on Tsunami dynamics of TGSB is done. No previous research on Python programming for TGSB is done. Hence it is seen that there is a vast scope to carry out this research and its applicability and potential is yet to be explored.

2.7 Summary

For the purpose of literature survey the study was divided into subsections: TGSBs, CTTR, Seismic Studies, stability analysis, liquefaction analysis, Tsunami dynamics, computational methods and relevant codes. Subsequently the critical appraisal of the literature was conducted to identify the thesis topic. It was examined if sufficient differences existed with previous works to proceed with the research. Finally the topic chosen was '**Computer Based Seismic Analysis of Bunds Considering Coconut Root Reinforcement**'. Sufficient difference from previous work exists to justify the selection.

CHAPTER 3

METHODOLOGY

3.1 Methodology of Study Adopted for Seismic Analysis of TGSB

As there are no prior technical studies on both coconut roots and TGSB many practical studies needed to be conducted. In order to perform a proper Seismic Analysis of TGSB it is necessary divide it into definite components. The methodology of study adopted for TGSB is to divide the preliminary investigations into following four main study sections with subsections:

1. TGSB Study – design methodology, construction methodology, constituents, case studies
2. Soils Study of TGSB – soils characterization, choice of soil model, soil stabilization
3. Coconut root reinforcement Study of TGSB – root morphology, root strength properties, contribution of roots as natural geo-synthetics, damping coefficient of roots
4. Seismic parameters Study of TGSB – seismicity of Goa, acceleration coefficients.

The values obtained from these studies will then be incorporated in the Analysis, Results and Discussion. Factors of safety will be obtained for static and seismic stability of TGSB and then the conclusions will be drawn. Since there is no technical data available for coconut tree reinforced embankment, a series of tests are needed to be performed. Also, as seismic microzonation and seismic studies in Goa are in nascent stage parametric studies needed to be carried out. Their results are incorporated in the methodology of study and Annexure.

3.2 Study of Traditional Goan Saraswat Bunds

Unlike modern structures that tend to deteriorate in 100 years, TGSBs lasted millennia. Throughout this time these earthen, rubble lined, coconut tree topped embankments have

lined, sheltered and shaped the agronomic lands, seasonal-lakes and waterways of Goa. TGSBs were built by traditional principals using traditional methods and tools and local materials. The knowledge passed down by mentor-apprentice principle has been paraphrased here. In order to gather information about the sizes, design and construction of TGSB, a number of surveys were conducted in different villages of Goa (Annexure I). Old villagers and traditional workmen were interviewed for past knowledge and practices which are briefly paraphrased in this section. Some of these methods were tested by case study and experimented to find out the values needed. Suitable limited surveys were also conducted and some photographs clicked (Annexure XVI). Some case studies were conducted to validate the findings and test some technologies outlined here (Annexure XV). Sadly the new generation of people has abandoned traditional methods in favour of more profitable modern ones leading to many recent failures of these traditional structures (Annexure XVII).

3.2.1 Design parameters for TGSBs

From the study of existing TGSBs the design parameters can be used for maintaining old and constructing new TGSBs have been postulated (Table 3.1).

Table 3.1 TGSB Design Parameters

	Parameters	Sizes
1	Height per lift /berm	H=3m (berm after every 3m) (*in some cases, Lifts of 2 to 3m was noticed)
2	Number of lifts/berms	$N = H / 3 - 1$ (rounded to higher)
3	Crest Width	$C = 5 + 1.5N$
4	Bottom width	$B = C + 2 + 5N$
5	slope	longitudinal 1 – 2 %
	chamber	2 – 4 %
	Side slope	1H: 3V
6	Free board	River side 2-3 m (depend on tidal fluctuations 3m at mouth 1m at rear)
		Lake side 1.5 m
7	Earthwork	In lifts of 0.5m, compacted by hand and bullock train to MDD
8	Side protection	Pitching 0.3 to 0.5 m thick dry-lateritic-rubble coursed masonry built along with earthwork courses

		Curb	0.5 m high lateritic-rubble coursed masonry wall at edge as overflow (topping failure) protection
9	Bream		0.5m waterside (for water retaining bunds only), 1.5 m landward
10	Vegetation	Main	2 rows of coconut trees 10 m c/c diagonally Replanted every 100 years Pattern- zigzag /diamond pattern Edge spacing-1m from edge
		Supplementary	Annual Grasses and herbs in between coconut trees No other perennial vegetation
		Prohibited	No vegetation on sides No taproot trees on top
11	Abutment flaring		3m radius
12	Foundation		Depends on sub-soil conditions and function of TGSB. Usually engineered-soil using boulders, crushed-rubble and tree branches.

3.2.1.1 Standard Dimensions and Traditional Measurement Techniques used in TGSBs

There were two types of TGSB the land reclamation type and the slope stabilization type. The first type again was divided into water-retaining (Primary) and land-side (Secondary) types.

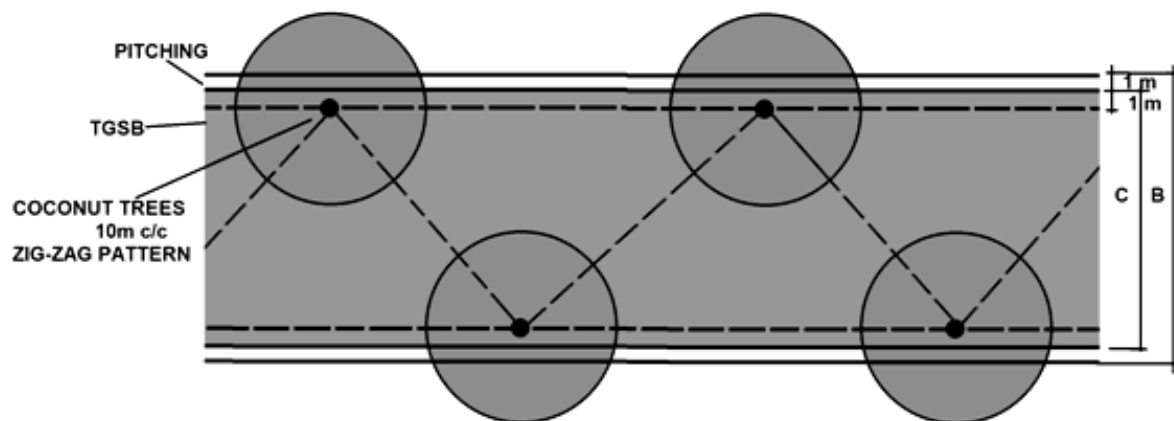


Figure 3.1 Standard zigzag pattern of coconut trees 10m c/c in longitudinal direction.

The top was generally 3 to 5 m wide and the side slope was 1H: 3V (Table 3.1, Figure 3.1, 3.2). The height per stage was 0.5m till 3m height. For slope stabilization TGSB there was

a berm of 1.5 to 2.5 m for every 1 to 2 m terracing. The water-facing side of TGSB had a berm of 1.5 m on land-side and 0.5m on water-side for the next 2.5 to 3m rise. The land facing side of TGSB had a berm of 1.5 m on both sides for the next 2.5 to 3m rise. Coconut trees in a row 9.5m c/c was planted for every berm/rise. As a result, the top had two rows 10 m c/c diagonally. A free-board of 1.5m was provided for tidal fluctuations and rain floods. The standard measurement was one hand (hatt) 0.5m from elbow to fingertip (Figure 3.2).

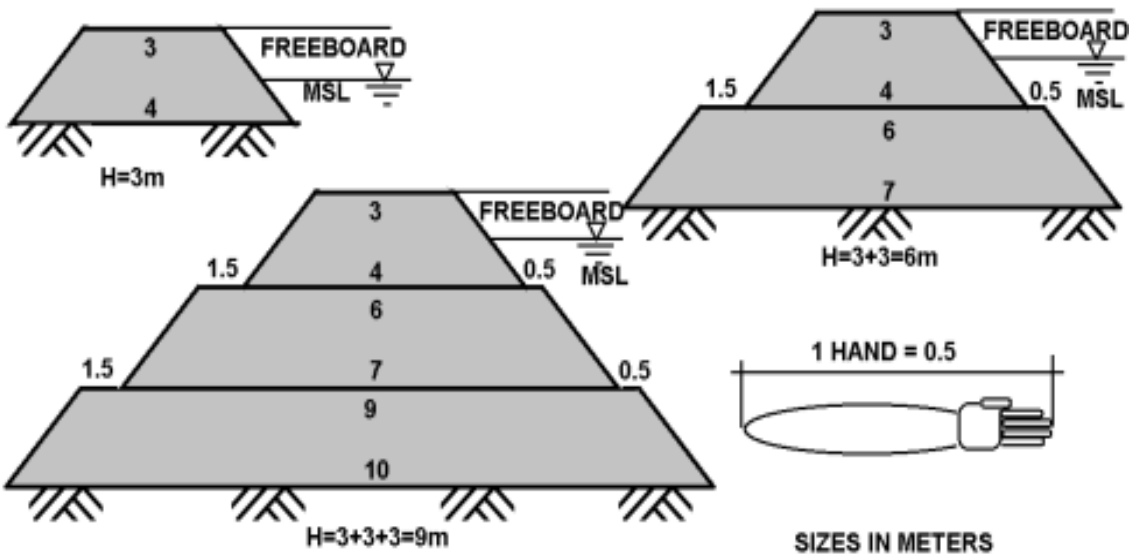


Figure 3.2 Standard dimensions of TGSB in meters

3.2.1.2 Failure mechanisms and Factor of safety for TGSB

For proper analysis of TGSB different possible failure mechanisms of embankments need to be considered (Figure 3.3).

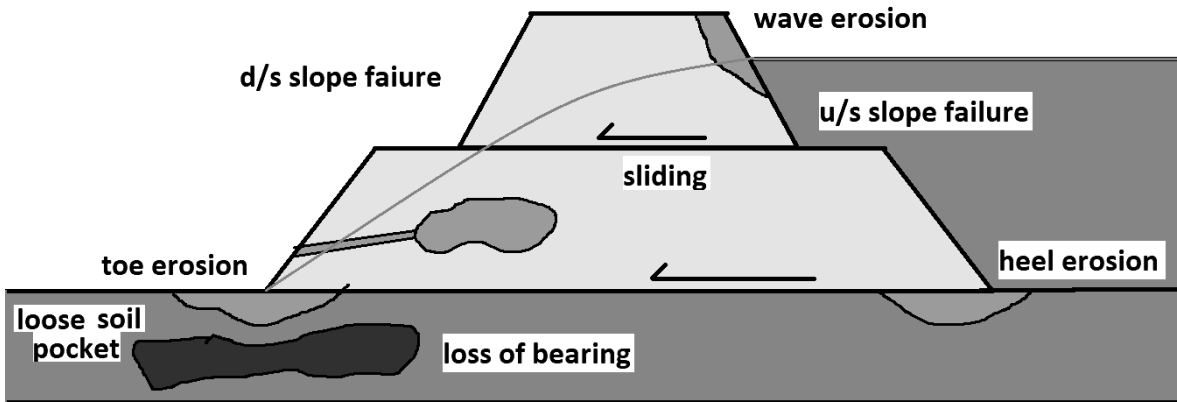


Figure 3.3 Failure mechanisms for bunds

Some potential failure mechanisms are resolved in the traditional design itself, while the values of static, pseudo-static and pseudo-dynamic factor of safety considering sliding, overturning, and general stability must be calculated (Table 3.2).

Table 3.2 Failure mechanisms for TGSBs

Failure mechanism	Protection measures provided
Wave erosion	Rubble facing
Toe erosion	Rubble facing + root suction
Heel erosion	Rubble facing+ root suction
Loose soil pocket	Soil-compaction+ root-mat
Animal burrowing	Pest-control measures + root-mat
Tree overturning	Avoid taproot trees > 2 m high
Inter layer sliding	Tree-root anchorage
Failure mechanism	Safety
Loss of bearing	Needs to be calculated
Sliding	Needs to be calculated
Global U/S Slope Failure	Needs to be calculated
Global D/S Slope Failure	Needs to be calculated
Pseudo static factor of safety	Needs to be calculated
Pseudo dynamic factor of safety	Needs to be calculated
Liquefaction	Needs to be calculated
Tsunami	Needs to be calculated

The factor of safety (FoS) can also be found out in cumulative manner by using the product of various factors of safety for different failure mechanisms (Figure 3.4 and Table 3.3)

$$FoS = \prod FoS_i = FoS_1 FoS_2 FoS_3 \dots \quad (3.1)$$

Table 3.3 Factor of Safety used for TGSBs

Loading condition stages	Shear parameters	Pore-water conditions	Factor of safety
End of construction	Effective	Excess pore water	1.3
Steady state seepage	Effective	Steady state in active pool	1.5
Operational condition	Un-drained	Steady state at max reservoir	1.2
Sliding friction	Effective	Steady state at max reservoir	1.5
Settlement	Effective	Steady state at max reservoir	1.5
Bearing capacity	Effective	Steady state at max reservoir	1.5
Earthquake static	Effective	Steady state at max reservoir	1.0
Earthquake dynamic	Effective	Steady state at max reservoir	1.2
Earthquake liquefaction	Effective	Steady state at max reservoir	1.0
Tsunami	Effective	Steady state at max reservoir	1.0
Other	Effective or un-drained	Drawdown max at outlet	1.2

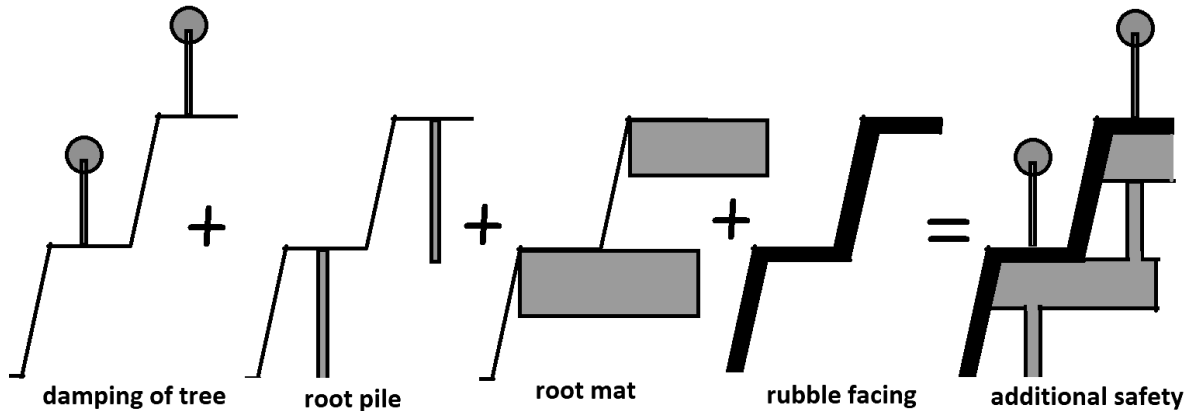


Figure 3.4 Additional Factor of Safety used for TGSBs

TGSBs are safer than other embankments due to contributions from a combination of additional factors like tree damping, root-mat reinforcement, root-pile reinforcement, root suction, rubble facing, increased shear resistance by soil stabilization etc. (Table 3.4).

Table 3.4 Additional Contributors for increase in factor of safety of TGSBs

Contributors	Type
Weight of soil	Static, dynamic
Shear frictional resistance of soil	Static, dynamic
Weight of coconut tree	Static, dynamic
Increase in root shear by root suction	Static, dynamic
Damping of coconut tree	Dynamic
Damping of coconut tree roots as mat	Dynamic
Additional Reinforcement by root pile	Static, dynamic
Additional Reinforcement by root mat	Static, dynamic
Additional resistance by rubble facing	Static, dynamic
Soil stabilization	Static, dynamic

3.2.2 Traditional Construction Methods and Practices

Ancient engineers (*Rishis*) through the scientific process of trial and error arrived at certain construction and maintenance methodologies that were then enshrined in some religious rituals, festivals and traditions to transfer technology theoretically. These were also passed down through the ‘*Guru-Shishya Parampara*’ (Mentor-Apprentice Tradition/Education).

Extensive interviews and interaction with older generation who worked on these structures during pre-liberation times was carried out to gather this data. First the route the bund will take was marked out with bamboo stakes (*kondo*) and coconut coir string (*suttli*). Then along the bund route a layer of lateritic rubble was dumped which acted as the base. Pitching/armour of rubble was next laid on either edge. Then followed alternate layers of 50-30 cm sandy soil filter and rice paddy straw on top (functioning as separator cum initial geo-textile till coconut roots grew). The bund would be raised and compacted course by course along with the outer pitching till desired dimensions were achieved (Figure 3.5).

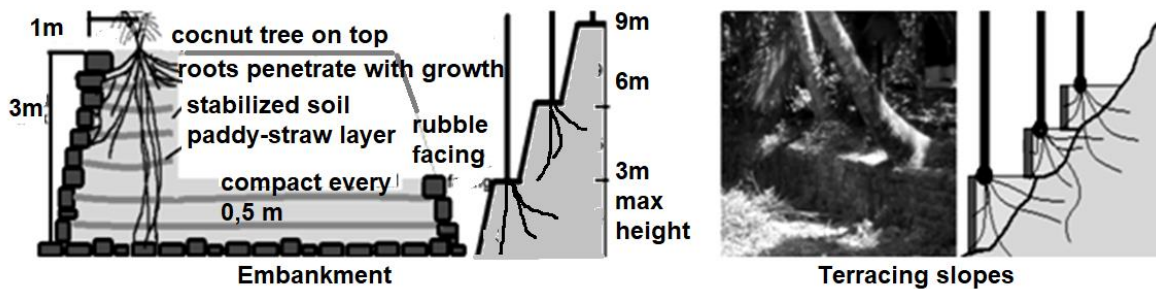


Figure 3.5 TGSBs for Embankment and Slope Stabilization

Mud was obtained from the adjacent riverbed. Two rows zigzag diamond pattern Coconut tree were then planted on top. Every 100 years the trees were replaced and replanted. Line, batter and slope were maintained by coir string tied to bamboo poles trimmed to dimension. Coconut roots penetrated the soil also anchoring to side rubble pitching thus giving more reinforcement by tying up the bund soil. Repair was carried out in similar manner to the construction. By strict adherence to this technology, the TGSB performed their functions for the past 5000 years until the annexation/liberation of Goa by India in 1961.

3.2.2.1 Traditional Equipment used in TGSBs

As per old local practitioners (workers, masons, land-owners etc) of TGSB construction, traditional and hand-held instruments were utilized for construction of these bunds. Tools like bamboo wicker baskets, sledge-hammers, crowbars, pickaxes and shovels were used for soil and stone work. Initial compacting was done using coconut stump tamper and final compaction was done by 10 passes per layer using a chain of 4 to 6 to 8 bullocks (giving an equivalent compaction of 2-ton to 3-ton sheep-foot-rollers). Bullock cart was used for transportation (Figure 3.6).



Figure 3.6 Compaction of TGSB by tamping and bullock chain

3.2.3 Traditional Materials used in TGSBs

Materials used for the TGSB are important for the stability and longevity of the structure. TGSB was constructed using dredged sandy loamy soil from borrow pits on river bed

during low-tide periods. The mixed stabilized soil was called as ‘Kaloi’ in local language Konkani (Kamat 2004, 2013), (Souza et al 2016), (Souza and Savoikar 2019b). Rice straw layers were used as initial geo-fabric till the fibrous coconut root system developed. It was conditioned using 2% Lime, 6% Coconut leaf Ash, 0.5% Jaggery and 0.5% Cow-dung (Table 3.5).

Table 3.5 Estimated Constituents of TGSB

Sr.No	Material	Utility	Quantity
1	River (Silt) Sand	Primary Constituent	90 %
2	Burnt Shell Lime	Stabilizer	2-2.5%
3	Coconut Leaf Ash	Stabilizer / Fines / Weight Reduction	5.5 -6%
4	Coconut Jaggery Molasses	Plasticizer /Workability	0.5%
5	Cow-dung	Fines / Weight Reduction	0.5%
6	Rice Straw	Primary Geo-textile	1%
7	Coconut Tree Root System	Final Geo-textile	--

3.2.3.1 Traditional Soil Improvement used in TGSBs

Earthen jars (*bhann*) plastered with cow-dung were used to ferment Coconut Jaggery Molasses. It acted as an insecticide and fungicide while improving the workability. Cow-dung was mixed with coconut leaf ash and burnt shell lime produced from locally sourced clams (*khube-tisreo-shinaneo*). This addressed the deficiency of fines in soil and its pozzolanic effect fortified the soil. Traditional soil stabilizers provided anti-bacterial effect, soil stabilization and strengthening. Rice straw was used as an initial geo-textile effect, to aid in compaction and for initial soil retention. The following mechanisms gave soil strength enhancing effect and stability to TGSB:

- (a) Puzzolanic action from Burnt Shell Lime and Coconut Leaf Ash mixed with soil,
- (b) The preliminary geo-fabric provided by paddy straw,
- (c) The ultimate geo-fabric strengthening effect of coconut roots,
- (d) The additional strength of Lateritic Rubble Facing (Figure 3.7).

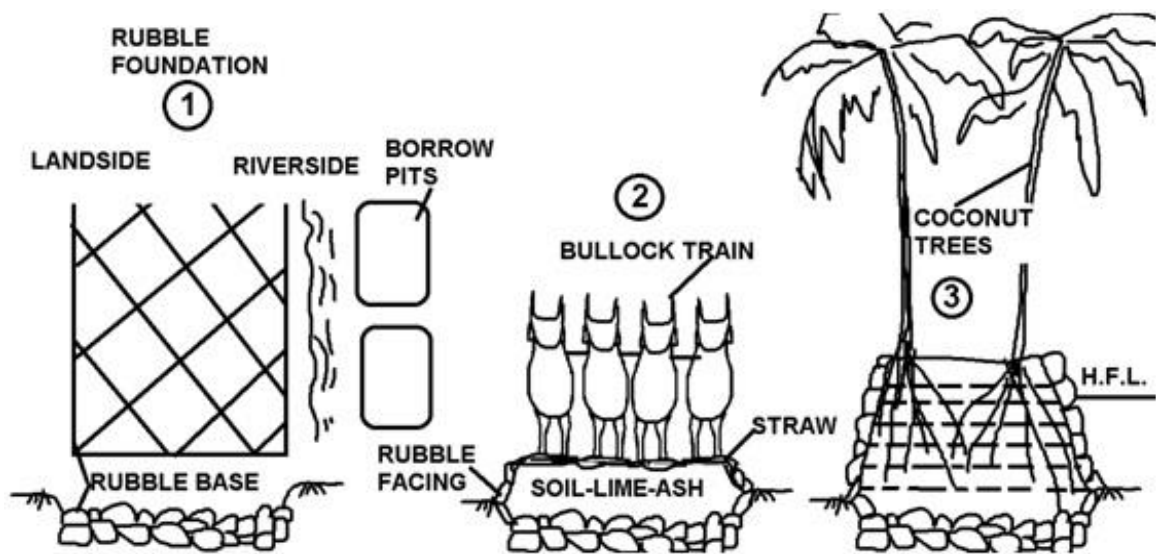


Figure. 3.7 Construction of TGSB
1-layout, 2 bullock train compaction, 3 layers and coconut root reinforcement

3.2.4 Case studies of TGSB

To illustrate and validate the findings case studies were conducted to encompass the past, present and future. The case studies were limited for illustrative purpose only. Further details of the case-studies have been given in Annexure XV. More studies are definitely needed but are beyond the primary, temporal and budgetary scope of the present thesis. For purpose of these studies, seven sites, Aggasaim, (Diwar) Dewadi, Loutolim, Galgibaga, Curtorim 1, Curtorim 2 and Gurim were chosen. The most ancient existing TGSB which also gave Goa its name was studied at Agasaim. The damaged condition of TGSBs and the proposed modern sheet-pile structure to convert the existing bund to a docking site for mining barges is studied at the site in Dewadi. The damage to TGSBs caused by modern day alleged repairs by Government departments while converting it to a road to facilitate travel of mining trucks was studied at the site in Loutolim. The damaged TGSBs, effects of damage and modern solutions like retaining walls and gabion walls were studied at a site at Galgibaga River in Canacona taluka of South Goa. The ancient TGSB based system of rain water harvesting used in Goa and the biodiversity impact was studied at the sites on Curtorim 1 village in Salcete Taluka of South Goa. The novel modern application of

ancient TGSB technologies stabilized earth and coconut root reinforcement was studied at the site in Curtorim 2 and Gurim in north Goa (Figure 3.8).

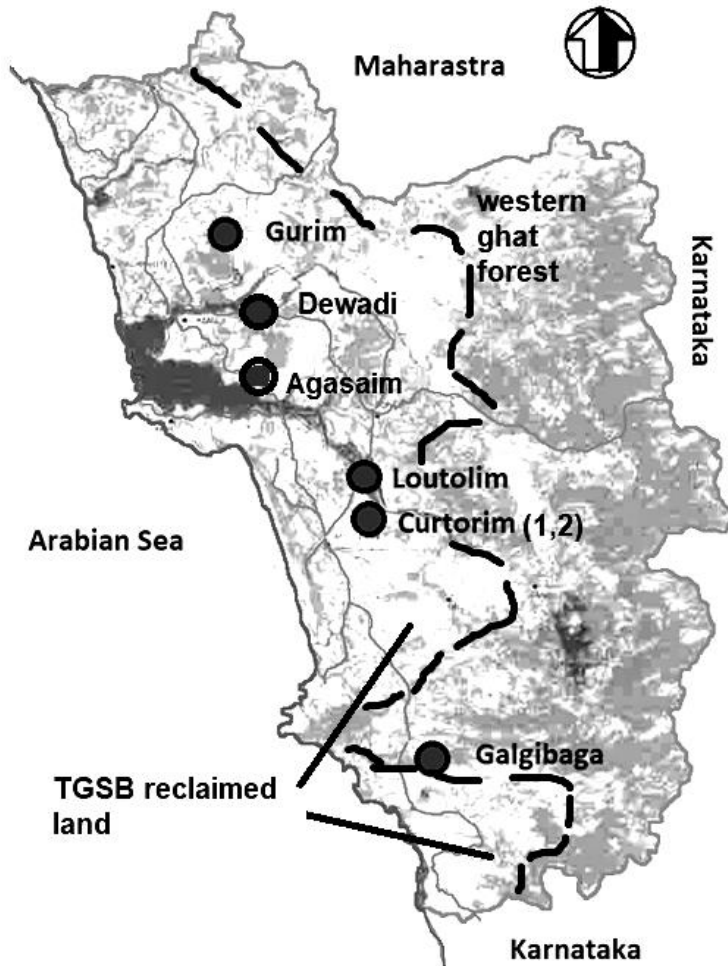


Figure 3.8 Map of Goa showing the location of case studies.

The following conclusions were drawn from the case studies given in Annexure XV:

1. Past success of TGSB technology in land reclamation, flood control, rainwater harvesting and hill-stabilization was studied at the case studies in Galgibaga and Curtorim (Biodiversity Management Committee Curtotim 2018).
2. Mismanagement by government departments when repairing and maintaining the bunds using steel and concrete which fail in the highly saline conditions of Goa Rivers

leading to further degradation of bunds is evident from case-studies at Dewadi, Loutolim and Galgibaga.

3. There is an invasion of mangroves falsely grown inland and not for coastal protection from ocean-flood surges – their original purpose which then narrows down rivers, silt up river-beds, and suffocate waterways and damage bunds by their destabilizing roots and borrowing animals that inhabit them causing increased flooding in monsoon as the runoff is prevented from entering the rivers and the river can't carry it away is evident from the case-studies at Dewadi, Loutolim, and Galgibaga.

4. There are also many other taproot trees other than coconut grown on the bunds that severely impact the stability of bunds and because wide spread damage is evident from the case studies at Dewadi, Loutolim, Curtorim and Galgibaga

5. The applicability of TGSB technology to repair bunds is easily demonstrated at the case study in Curtorim. The retaining wall of the house of a villager was repaired successfully using this technology and has lasted for the past 3 Years. It was previously built of ashlar masonry and frequently collapsed every monsoon.

6. The natural root reinforcement complement supplement the artificial reinforcement in reinforced panel retaining walls as demonstrated at the case study in Guirim where the coconut tree roots have been giving additional reinforcement to a MSEW wall of an over pass in a national highway.

3.3 Study of Soils Required for TGSB and their stabilization

Soil characterization and stabilization for TGSB has been carried out (Souza and Savoikar 2019c). Characterization of Soil is important for determining the constants used in seismic geotechnical analysis. Traditionally, lime-ash-stabilized riverside silty-sand was used in bund construction, but due to excessive demand for river-sand in construction today, deep hill cutting is taking place leading to placement of different types of lateritic soils in TGSBs. So lateritic soils also have been studied (Widdowson 2009), (Dessai 2018), (Mascarenhas and Kalavampara 2009), (Aginam et al 2014), (Raychaudhuri 1980). Additional information and tables of test-results are available in Annexure II.

3.3.1 General Soil Parameters for TGSB

Visual inspection showed the soil had a brownish red to brownish yellow colour. It had significant light weight organic content. Wet soil was very soft and showed expansive nature. It exhibited shrinkage and cracking on drying. As TGSB fill was from eroded riverbed sediment it demonstrated uniformity in values in most samples. The TGSB soil may be classified as Sandy Loam in the triangular textural classification chart of US Bureau of soils (Figure 3.9).

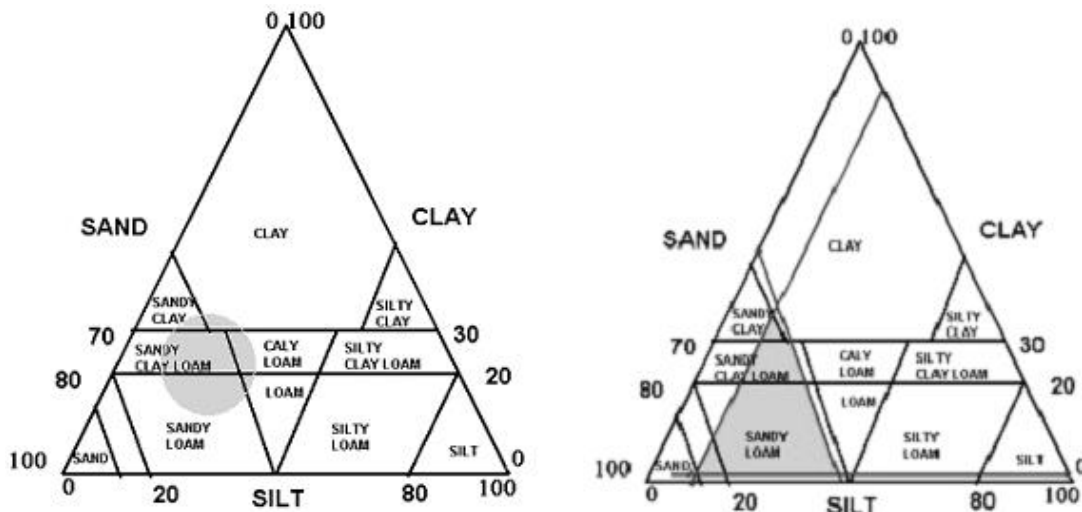


Figure 3.9 Triangular Classification of Lateritic Soils and TGSB soils

Four soil samples (A, B, C, D) from different bunds were tested for properties. Their grain size distribution Clay(C), silt (M), fine sand (FS), medium sand (MS), coarse sand (CS), fine gravel (FG), coarse gravel (CG) and cobble (Cob) content was found out along with their consistency limits (liquid- w_L and plastic- w_P) and specific gravity (Gs). Soil is coarse grained soil with fines or Sand with organic fines Organic fines vary from 1-2%. From Atterberg limits they also fall in CL and ML classification (Table 3.6).

Table 3.6 Typical TGSB Soil Properties

Soil properties	Grain Size								consistency		
	C	M	FS	MS	CS	FG	CG	Cob	w _L	w _p	G _s
A	7	15	20	26	29	2	1	0	25	15	2.53
B	4	20	22	35	15	2	1	1	28	17	2.54
C	10	16	28	18	20	5	2	1	26	17	2.51
D	12	20	26	25	14	1	2	0	24	16	2.50

Soils A, B and C were plotted on semi-log graph. All soils were classified as SC to SM as per USCS-ASTMd2478-11 and IS1498-1970 (Figure 3.10). They lie within an envelope and thus the soils needed for these embankments can be determined for use in other areas.

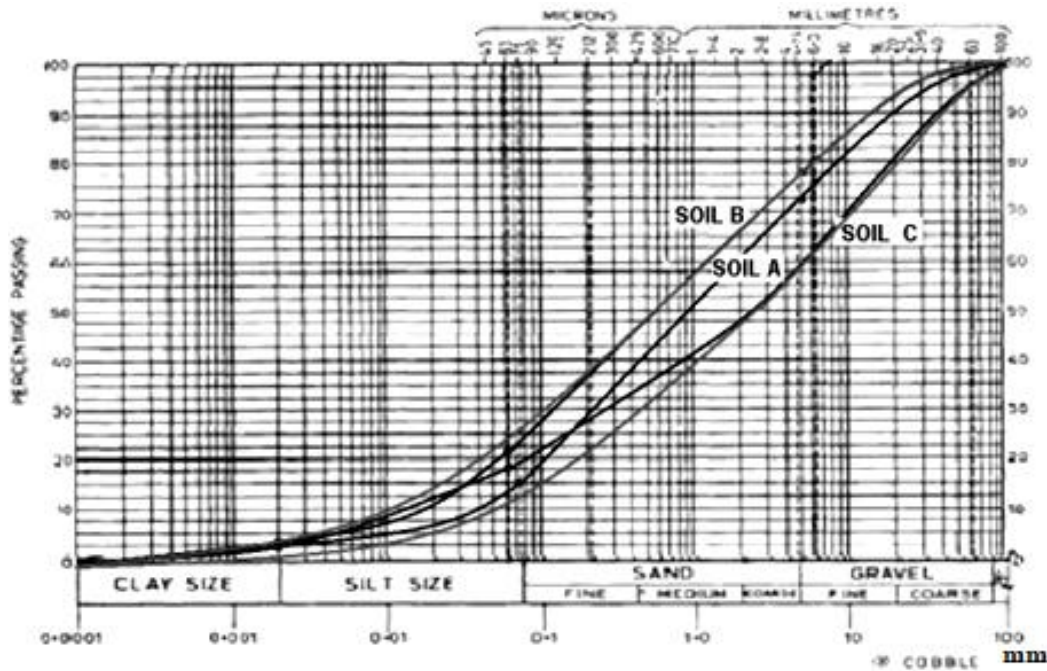


Figure 3.10 Envelope of Particle Size Distribution for TGSB soil.

The other components (Soil of embankment without and with roots, soil below the embankment, and the rubble facing) of the TGSB were tested for properties (young's modulus E , porosity v , dry density γ_d , saturated density γ_{sat} , cohesion c , friction ϕ and permeability k_x, k_y) needed to be inputted in software for evaluation (Table 3.7).

Table 3.7 Typical soil values used in software for evaluation of TGSB

Soil properties	E	v	γ_d	γ_{sat}	c	ϕ	$k_x=k_y$
units	MPa		kN/mm³	kN/mm³	kPa	°	m/day
Bund	5	0.33	16.1	18.3	20	30	2.0e-5
Root-soil	10	0.30	15.3	17.1	30	40	0.2e-5
Bottom soil	2	0.25	18.2	20.0	15	30	0.3e-5
Rubble facing	100	0.30	24.4	25.3	200	45	2.0e-5

The coefficient of earth pressure at rest (K_0) and the unloading Modulus for subgrade (E_{ur}) can be estimated from the equations

$$K_0 = 1 - \sin \phi \quad (3.2)$$

$$E_{ur} = 3 E \quad (3.3)$$

3.3.2 Constitutive Soil Model

Soil and rock receive normal stress but produce both vertical and horizontal resistance. Soil exerts active and passive earth pressures on retaining structures. Soil and rock can also fail in bearing. Soil and rock are strong in compression and weak in extension. A common set of parameters was needed for their study. These are given by Yield-Criteria and their Constitutive-Soil-Model. A constitutive model is essential to describe the stress-strain action in soil

3.3.2.1 Comparison of common yield criteria used for soils

Each soil behaves differently and has a different set of propositions (yield criterion) that represent different soil modulus. They depend on the relationships between principal direct stress (σ_{xx} , σ_{yy} , σ_{zz} or σ_1 , σ_2 , σ_3) on 3 principal planes and three shear stress (τ_{xy} , τ_{yz} , τ_{zx}) on three orthogonal surfaces. The Mohr-Coulomb yield surface (Coulomb 1776) (Mohr 1900) comparative yield criteria on deviatoric plane is shown in Figure 3.11.

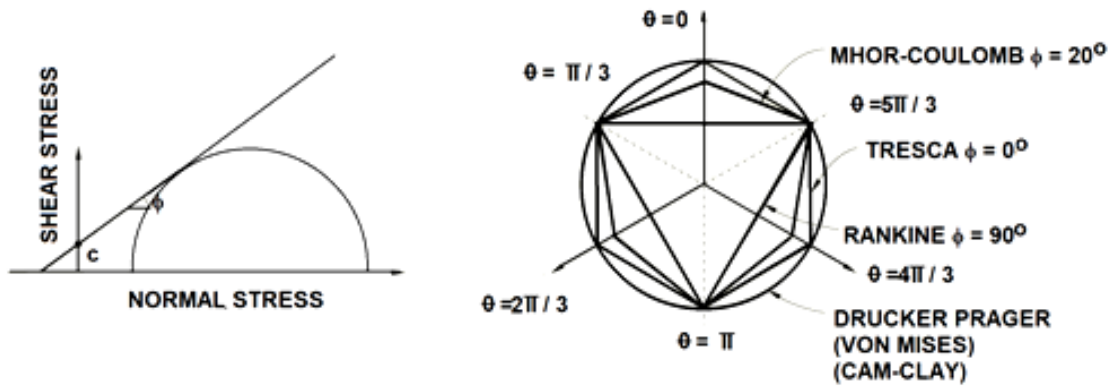


Figure 3.11 Comparative Yield Criteria on Deviatoric Plane

They have different failure criteria and are treated differently to arrive at the yield-criteria. They need different tests for their shear properties. The equation of the failure surface is described by the yield criteria. The various yield criteria have been developed as research progressed and it was discovered that soil is dependent on a multitude of factors hence needed different soil models- Mohr, Mohr-Coulomb, Extended Tresca, Cam-Clay, Drucker-Prager, Extended Von Mises, etc. Some are better for rocks some are better for soils. Some are better for cohesionless, some are better for cohesive. Each has a different set of factors, different equations and different shape of envelope. Each is chosen as per the merits of the case. They are plotted on the principal axis $\sigma_1 = \sigma_2 = \sigma_3$. Some are capped, some are uncapped (Figure 3.12).

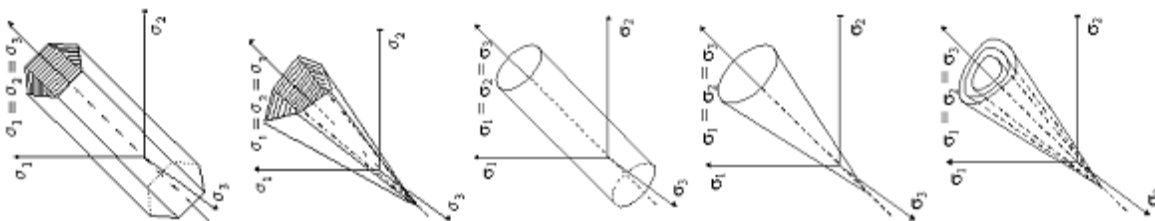


Figure 3.12 Comparison of Tresca (uncapped), Mohr-coulomb, von Mises (capped), Drucker-Prager (capped), Lade-Duncan (uncapped) 3D yield criteria plots

The suitability and salient features of different yield criteria for lateritic soils as discussed in Table 3.8 depends on the failure criteria and the type of soil. The yield criteria are defined by equations given by Stress = σ , angle of soil friction = ϕ and shear stress = τ .

Table 3.8 Comparison of common yield criteria

Criterion	Mohr – Coulomb (1900)(1776)
Test	Triaxial compression test.
Failure criteria	By impending sliding along plane of maximum principal stress obliquity.
Soil treated as	Rigid frictional media.
Best suited for	Long term, over consolidated, dense sands, homogeneous and non-homogeneous soils
Equations	$\sin \phi = (\sigma_1 - \sigma_3) / (\sigma_1 + \sigma_3)$ $\tan^2(45 - \phi/2)_{cs} = ((1 - \sin \phi) + (1 + \sin \phi))_{cs}$ $\tan^2(45 - \phi/2)_{p} = ((1 - \sin \phi) + (1 + \sin \phi))_{p}$ $\sigma_{np} = \sigma_{ncs} = (\sigma_1 + \sigma_3) / 2 - (\sigma_1 - \sigma_3) \sin \phi_p / 2$ $\tau_{cs} = \tau_p = (\sigma_1 - \sigma_3) \cos \phi_p / 2$
Advantages	It is Simple. Its validity is well established for different soils. Used for mixed soils with high sand content.
Limitations	Has Corners. It neglects the effect of intermediate principal stress. There is Excessive plastic dilatancy at yielding.
Soils	Best suited for all lateritic soils
Criterion	Taylor (1948)
Test	Direct shear test.
Failure criteria	By sliding and interlocking of particles.
Soil treated as	Deformed frictional media.
Best suited for	Short and long term. Homogeneous soils.
Equations	$\tau_p = \sigma_p (\tan \phi_{cs} + \tan \alpha_p)$ $\tau_{cs} = \sigma'_{nf} \tan \phi_{cs}$
Soils	Best suited for Beach area Lateritic sandy soils
Criterion	Coulomb (1770,1776)
Test	Direct shear test
Failure criteria	By impending friction along sliding plane
Soil treated as	Rigid frictional media
Best suited for	Layered, fissured, over consolidated, where preferred plane of failure exists
Equations	$\tau_p = \sigma_{nf} \tan (\phi_{cs} + \alpha_p) = \sigma_{nf} \tan \phi_p$ $\tau_{cs} = \tau_f = \sigma'_{nf} \tan \phi_{cs}$
Soils	For fractured Lateritic soils with clear separate layers
Criterion	Tresca (1857)
Test	triaxial compression test

Failure criteria	When $\frac{1}{2}$ major principal shear stress is achieved
Soil treated as	Homogeneous media
Best suited for	Short term, undrained, fine grained
Equations	$\sigma_{np} = (\sigma_1 - \sigma_3)_p / 2$ $\sigma_{ncs} = (\sigma_1 - \sigma_3)_{cs} / 2$
Advantages	Simple. All types of soil.
Limitations	Only for undrained saturated soils. Corners
Soils	Not suited for Goa as less clayey soils

Criterion	von-Mises (1913)
Test	Direct shear test, total stress
Advantages	It is Simple and Smooth
Limitations	It is only for undrained saturated soils. It can overestimate strength.
Soils	Clayey soils, Not suited for Goa

Criterion	Drucker-Prager (1952)
Test	Triaxial test
Advantages	It is Simple and Smooth. It matches Mohr-Coulomb if proper constants are chosen. Good for limit analysis techniques.
Limitations	It gives a circular deviatoric trace contradicting experimental values. Excessive plastic dilatancy is shown at yielding
Soils	Clayey soils, Not suited for Goa

Criterion	Lade-Duncan (1975)
Test	Triaxial test
Advantages	It is Simple and Smooth. Effect of intermediate principal stress is considered. It has a Curved meridian. It can be used for a wider range of pressure than other criteria.
Limitations	It is only suitable for purely cohesionless soils
Soils	purely Sandy soils, Not suited for Goa

For a totally heterogeneous, anisotropic soil like lateritic soils a general model like Mohr-Coulomb is the preferred yield criteria.

3.3.2.2 Spatial variation in properties

As lateritic soil is non homogeneous material its parameters usually strength or elasticity vary spatially, they may be considered constant for small footings. Actually, they may vary with depth and width. However, for ease of calculations it is often taken as constant. Linear elasticity is assumed in Mohr-Coulomb materials. Two parameters: cohesion and friction angle define their yield function. However, this apparent minimalism of the Mohr-

Coulomb model with its limitations makes it the proper model for realistic geotechnical analysis of highly heterogeneous sandy-clayey-loam Lateritic soil of Goa. The soil behaviour models should include: multi-phase nature, anisotropy, irrecoverable (plastic) strains, non-linear soil response load history, time-dependent behaviour etc. Nevertheless, for simplicity's sake most of these factors are ignored. For soil in TGSB considering the complex nature of Lateritic soils Mohr-Coulomb model is selected.

3.3.2.3 The Mohr-Coulomb criteria

The Mohr-Coulomb curve is used commonly for a large number of routine soil design calculations in geotechnical research. The Mohr-Coulomb criterion presupposes failure to be restricted by the maximum shear stress. The shear stress at failure is proportional to the normal stress, represented by the Mohr's circle (Figure 3.13) for maximum and minimum principal stresses.

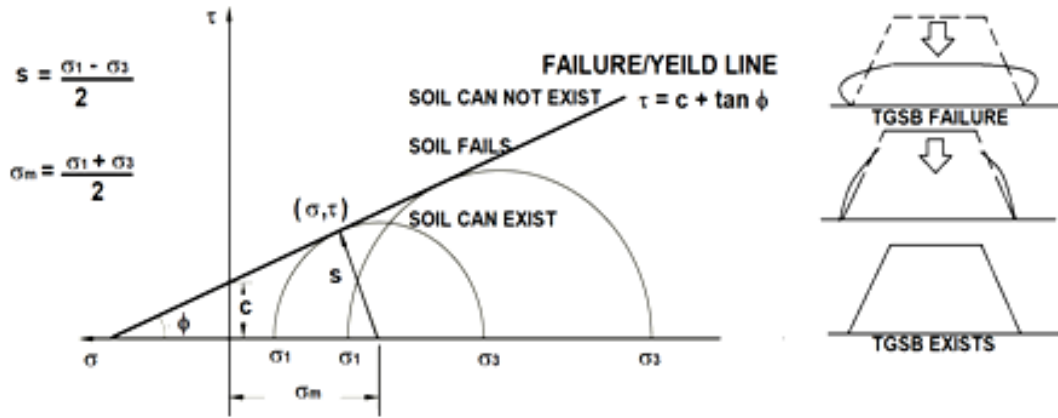


Figure 3.13 Mohr-Coulomb failure criterion.

The Mohr-Coulomb failure curve is the best fit straight line touching the plotted circles. The Mohr-Coulomb failure criterion is given by

$$\tau = c - \sigma \tan \phi \quad (3.4)$$

Where τ is the shear stress, σ is the normal stress (negative in compression), c is the cohesion of the material, and ϕ is the material angle of friction.

From Mohr's circle one can obtain the following equations,

$$\tau = s \cdot \tan\phi \quad (3.5)$$

$$\sigma = \sigma_m + s \cdot \sin\phi \quad (3.6)$$

Where, s is half of the difference between the maximum and minimum principal stresses.

Therefore, the maximum shear stress given by

$$s = \frac{1}{2}(\sigma_1 - \sigma_3) \quad (3.7)$$

and σ_m the average of the maximum and minimum principal stresses (the normal stress) given by

$$\sigma_m = \frac{1}{2}(\sigma_1 + \sigma_3) \quad (3.8)$$

Substituting τ and σ in the Mohr-Coulomb equation one can obtain

$$s + \sigma_m \sin\phi - c \cos\phi = 0 \quad (3.9)$$

One can see that the Mohr-Coulomb criterion presumes failure to be independent of intermediate principal stress although for most geotechnical materials failure generally has a bare minimum dependence on the intermediate principal stress. However, Mohr-Coulomb model normally gives sufficiently precise values. The behavior of soil is considered as elastic, linear and isotropic.

The friction angle of soil, ϕ , controls the yield surface in the deviatoric plane. The range of values for friction angle is $0^\circ \leq \phi \leq 90^\circ$. When $\phi = 0^\circ$, then the Mohr-Coulomb model reduces to the pressure-independent Tresca model with a perfectly hexagonal deviatoric section. When $\phi = 90^\circ$ the Mohr-Coulomb model reduces to the tension cut-off Rankine model with a triangular deviatoric section. The Lade-Duncan, Von Mises, and Drucker-Prager model use the intermediate stress are not used here.

3.3.2.4 Anisotropic Elasticity

Due to their formation, Lateritic soils exhibit anisotropy. Their elastic parameters differ in the horizontal and vertical directions. It can be shown that the Poisson's ratio must be limited to

$$-1 \leq \alpha_{xy} \leq 1/2 \quad (3.10)$$

The anisotropy parameter α , is related to the Young's moduli in each direction as well as the respective shear moduli by:

$$\alpha = \sqrt{\frac{E_{xx}}{E_{yy}}} = \frac{G_{xx}}{G_{yy}} \quad (3.11)$$

3.3.2.5 Interface Strength Parameters

The interaction between the wall, footing, tree roots etc. and the surrounding soil material in box shear test gave similar stress-displacement behaviour to the interface behaviour between soils. There is a variation and loss of strength at interface that is often ignored for small projects like TGSB but must be considered for larger projects.

3.3.2.6 Unconfined compressive test.

The unconfined compressive strength (UCS), c_u or q_u is given by maximum unit axial failure compressive stress or stress at 15 % strain. In this study only α_{UCS} (anisotropy in UCS) was studied as it was not used in software analysis.

Table 3.9 Anisotropy in soil at same level in Salcete Lateritic formation in Goa

Location	Direction	unconfined compressive strength kg/cm ²				Average	α_{UCS}	ϕ
Lateritic	Z	4.8	5.5	4.8	4.9	5.000		
Lowland (Konkan Railway Site)	X	3.3	3.8	3.4	3.6	3.525	0.7025	25
	Y	3.6	3.7	3.3	3.4	3.500		
Lateritic Plateau (Curtorim site)	Z	8.1	7.9	7.8	8.2	8.000		
	X	6.7	6.3	6.5	6.0	6.375	0.8000	38
	Y	6.5	6.2	6.6	6.4	6.425		

The undrained shear strength, s_u , is understood to be equal to half the value of unconfined compressive strength (ENCE 361 -2001). Anisotropy exists in lateritic soils (Liu et al 1997) (Ling et al 2002) (Zhang et al 2018) (Liu et al 2020). An easy test to find out anisotropy in UCS in soils and was used for two cases. 50mm core samples were taken for field and hillside soils at depths 1.50 m (Figure 3.14) Tests were carried out in Vertical (y) and Horizontal (x and z) directions to find out the anisotropy α_{UCS} in UCS values (Table 3.9). Studies for finding out true anisotropy in Young's modulus and shear modulus are beyond the scope of the present study.

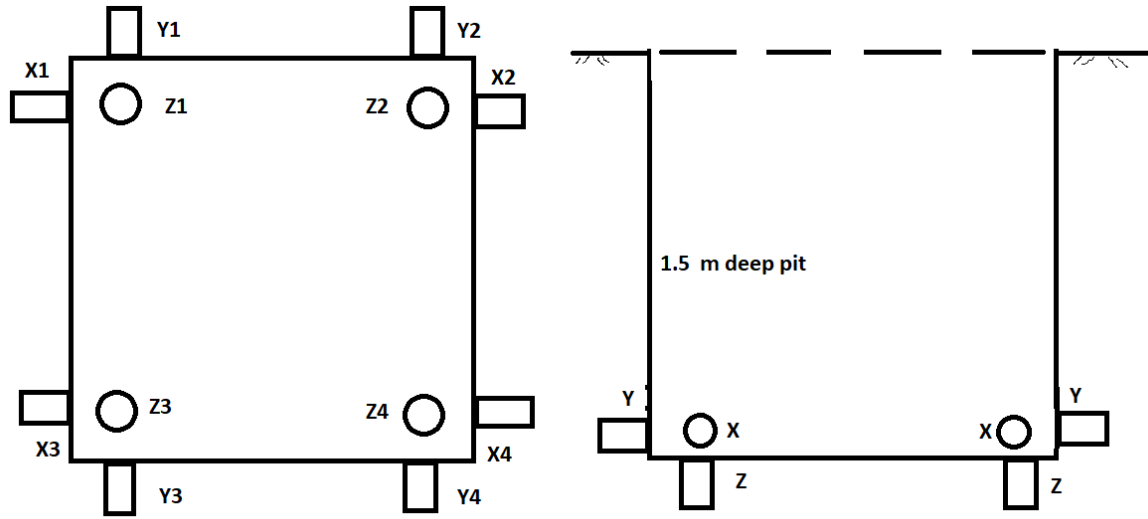


Figure 3.14 Sample Location in pit for testing Anisotropy in Lateritic soils in Goa

On examination of results, it was found that there exists an anisotropy in UCS in Lateritic formations in Goa. The extensive property can be derived based on friction angle and Horslev's formula and Horslev equivalent parameters (Horslev 1937).

$$\tau_{ff} = c'_e + \sigma'_{ff} \tan \phi'_e \quad (3.12)$$

To fully utilize the Mohr-Coulomb failure criteria one need to do extension and compression tests in triaxial testing machine to find the values of $(\sigma_1 + \sigma_3)$ and $(\sigma_1 - \sigma_3)$. However due to some limitation in many labs it is possible to obtain the compressive stress but not the extension stress, in such cases the values suggested by Horslev (1937, 1960) may be used (Table 3.13). He postulated that compression to extension ratio is independent of cohesion

$$\frac{\text{compression}}{\text{extension}} = \left(\frac{1 - \frac{1}{3} \sin \phi}{1 + \frac{1}{3} \sin \phi} \right) \quad (3.13)$$

The soil behaviour models should include: multi-phase nature, anisotropy, irrecoverable (plastic) strains, non-linear soil response load history, time-dependent behaviour etc. However, for simplicity's sake most of these factors are ignored. As TGSB is not deposited but engineered soil the anisotropy does not come into play so it is ignored for calculation. For soil in TGSB considering the complex nature of Lateritic soils isotropic Mohr-Coulomb model is selected.

3.3.3 Soil Stabilization Studies

Different types of ash in combination with lime is commonly used to stabilize soils by puzolanic action. Coconut leaf ash was traditionally used for ground improvement and soil-stabilization in Goa for embankments, mud-houses, revetments, etc. (Souza et al 2016). Ancients Saraswat Civilization who settled in Goa (Wikipedia 2021) used soil mixed with River-Shell-Lime and Coconut-Leaf-Ash (CLA) in TGSBs to stabilize the sandy loamy locally sourced soil called Lime-Cocoash-Soil mix (LCS). The proportions used were from rough estimates obtained from experience by original builders and are now unavailable hence needing new studies to estimate the proper proportions. For purpose of comparison limited study was also carried out on lime-fly-ash-Soil (LFS) mix which is a recent practice used for geotechnical stabilization of soils. Fly Ash (FA) a very easily available by-product from coal combustion, is today's most frequently utilized Supplementary Cementitious Material, although many other by products have also been used by different researchers (Karthikey al 2014), (Bin-Shafique et al 2003), (Sadeeq et al 2015), (Fay et al 2012), (Padalkar et al 2013), (Goswami 2004), (James and Saraswathy 2020), (Amadi 2010) (Al-Chaar et al 2013), (Amiralian et al 2012), (Isah 2014), (Okafor and Okonkwo 2009), (Olugbenga and Akinwole 2010). FA-Lime stabilization is better than Lime alone. This section attempts to estimate the optimum percentage of lime and coconut ash necessary for proper stabilization of lateritic soils. Further details and tabulation of test results are available in Annexure III.

3.3.3.1 Improvement in soil properties

CLA is produced locally for cooking and heating water then stored in a dump before usage (Figure 3.15). It is flaky in nature even in high magnification (Figure 3.16).



Figure 3.15 Coconut Leaf Ash (CLA) Raw Materials, Local Production Technique

This reduces the flow ability and saturation-liquefaction of the soil and makes it stable even at high water content. In contrast fly ash is spheroidal hence flows freely. This property of CLA enables TGSB to have a near vertical profile.

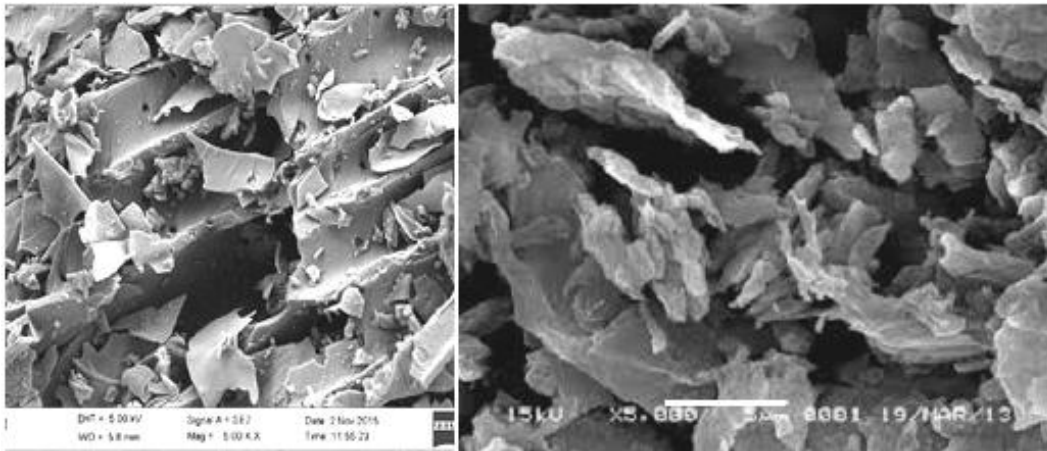


Figure 3.16 Coconut Leaf Ash (CLA) – 500 X, 1000 X Magnification showing flaky structure

First only Lime:FA and Lime:CLA proportions were finalized. Commercial grade lime used in painting was used instead of Burnt Shell Lime (Figure 3.17).



Figure 3.17 Coconut Leaf Ash and Burnt Shell Lime in bags

They were mixed in different proportion in dry state. The samples were kept in zip-locked bags with paper label identification to recognize the mix proportion (Figure 3.18).



Figure 3.18 Fly-Ash and zip-locked bags of soils for testing.

4 cm diameter cylinders were cast to 8 cm height using various proportions of Lime and CLA to obtain the optimum proportion for soil stabilization. Similar Lime and Lime-FA mix cylinders were also cast. These were cured for three, seven and fourteen days so that pozzolanic reaction is completed. Then their unconfined compression tests were done. From resultant graph (Figure 3.19) it was seen that best ratio was 4:10 or 2:5 Lime: CLA and 2:10 or 1:5 Lime: FA for most advantageous strength.

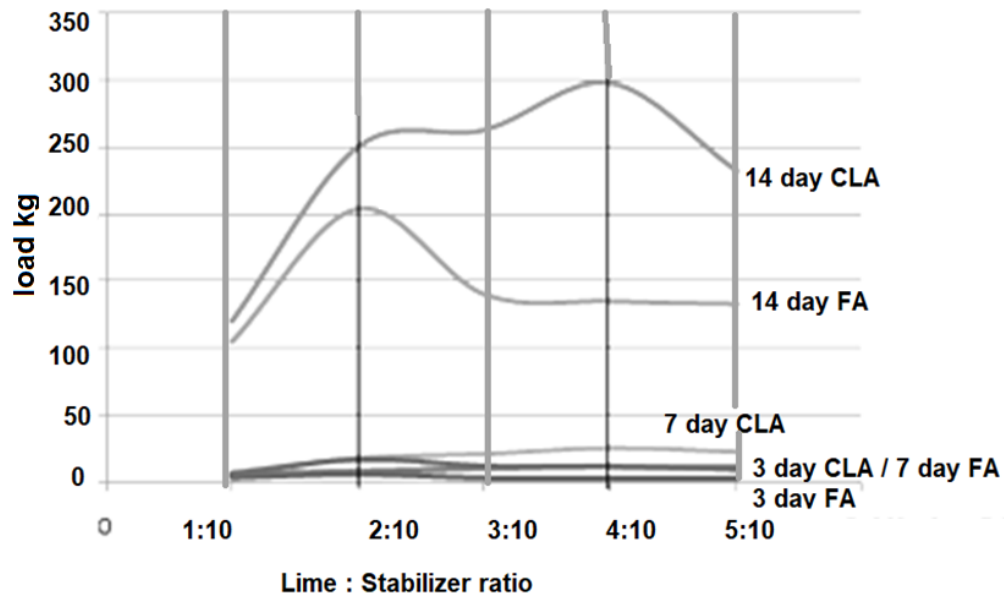


Figure 3.19 Failure Load variation of cylinders of lime with coconut leaf ash (CLA) and fly-ash(FA) - no soil added.

Using results from the graph, a mix of two parts Lime and five parts CLA was readied and mixed with soil in proportions of 2, 4, 6, 8, 10 and 15 %. Briquettes and Cylinders were cast in sets from this mix for Box Shear Strength and Unconfined Compressive Strength tests (Figure 3.20).

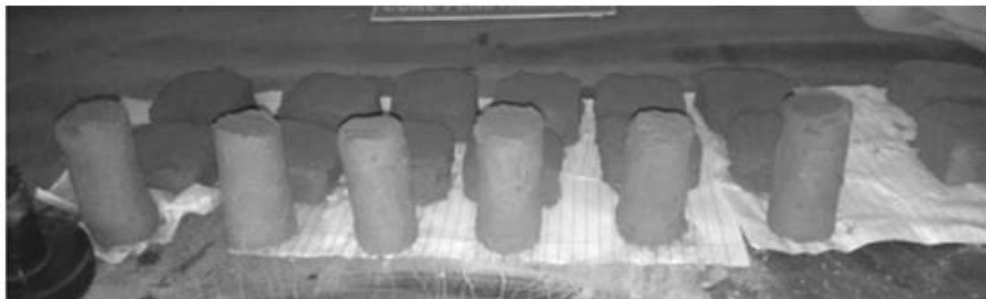


Figure 3.20 Cylinders and briquettes cast of stabilized-soil

Tests were conducted to find out the variation in soil properties thus attain the final percentage for use in TGSB.

It was seen that after drying LFS sample shrunk and cracked more than the LCS sample (Figure 3.21).

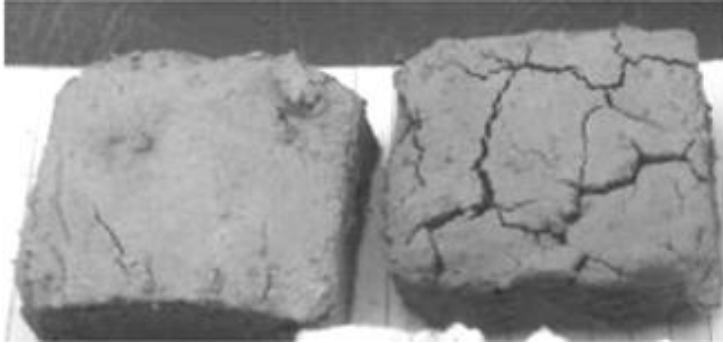


Figure 3.21 Shrinkage cracks in LCS (left) and LFS (right) briquettes

Unconfined Compressive Strength tests demonstrated strain hardening on attaining 50% strength. It was greater for LCS than LFS (Figure 3.22). There is a significant strength rise after 10% stabilizer use which is due to excess lime but it is uneconomical to consider for TGSB.

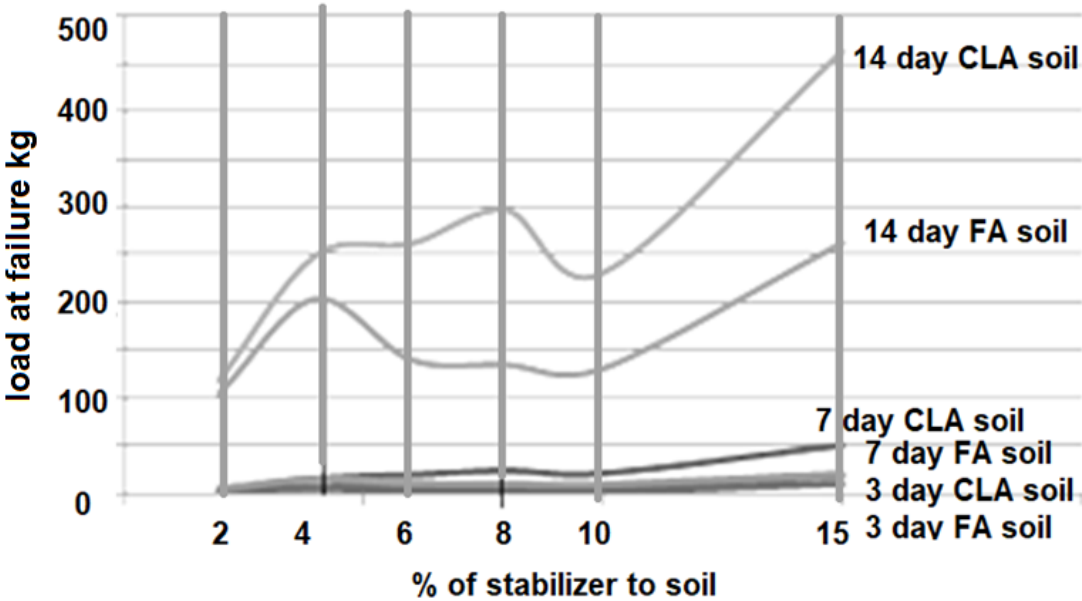


Figure 3.22 Failure Load for Unconfined Compressive Strength for CLA (A) and FA stabilized soil

The strength tripled at 8% stabilizer use, doubled at 10% stabilizer use and quadrupled at 15 % stabilizer used probably due to free lime-ash. As the free lime ash would get washed away 8 % is optimum dosage. On average one can assume a triple increase in strength on CLA stabilization.

3.3.3.2 Correct proportions for TGSBs

From the analysis of the data generated, a ratio of 4:10 or 2:5 Lime: CLA and a ratio of 2:10 or 1:5 Lime: FA gave best strength. The samples of LFS sample shrunk and cracked more than the LCS hence LFS will weaken faster and are more susceptible as embankment material than LCS. LFS flows more easily with slight enhancement in water due to globular nature of FA as compared to the flaky nature of CLA and hence, LCS is better option in monsoon. The shear strength of LCS was higher than that of the LFS. Also, as LCS is less dense, the load of the embankment on foundation is less, leading to lower settlement and consolidation. A mix of 1.7 – 2.5 % Lime and 4.3 - 5.8 % Coconut Leaf Ash with balance % soil showed optimum results for soil stabilization. Further studies for 28-day, 90 day and 3-year strength are needed for final strength of the mix, but were not carried out as the purpose of the study was limited to finding the correct proportions of LCS mixture. Studies with actual burnt shell lime are also needed.

3.4 Study and Modelling of Coconut Root Soil Reinforcement

The reason that the TGSB have lasted for thousands of years through storms and earthquakes and cannon-fire is the coconut tree roots that act as a bio reinforcement. Coconut tree has fibrous roots which are self-repairable natural geo-fabric for embankment soils. Many studies show that roots reinforce soil (Ali et al 2012), (Burrall et al 2020) (Preti and Giadrossich 2009), (Gentile et al 2016).



Figure 3.23 Random internet photos show structures nearer palm trees suffering less damage while structures away show more damage.

Available photographic evidence (Figure 3.23) of recent earthquakes show Structures near coconut and palm trees are less damaged than other structures. Coconut tree roots act as soil spring anchors so they have a significant contribution in seismic and dynamic strength of the TGSBs. Study of seismic stability of TGSB needs study of the coconut-roots. Today TGSBs are getting destroyed because people are unwittingly growing weaker tall taproot trees on them, (FEMA-1263 2005), (FEMA-534-2005)

This thesis attempts to model the coconut tree roots, spatially and study their possible role in damping of the earthquake waves and give a brief idea about the improvement in slope stability by coconut tree roots. A number of tests were carried out for this purpose. Additional information and tables of test results are available in Annexure IV.

3.4.1 Coconut Tree Roots

Studies across trees (Bessonov and Volpert 2000, 2006) (Fourcaud et al 2003, 2008) (Pages 2014) have shown that contrary to common misconception – that tree roots follow the hemispherical tree canopy – it is in reality more of a tee-shape. The horizontal root mat extends to canopy in width and 1 to 2 m deep for coconut tree roots and up to 5m for tap roots. The vertical root pile extends up to variation of max and minimum water table in summer for all roots (Figure 3.24).

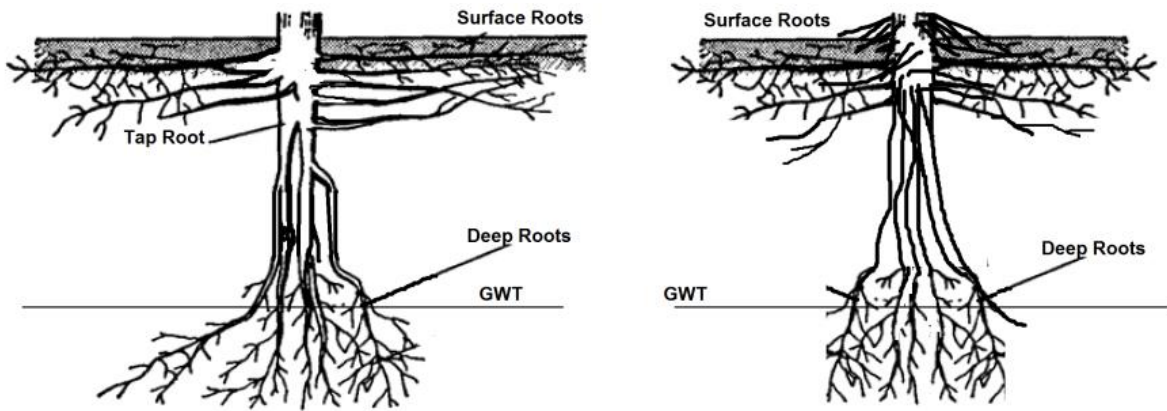


Figure 3.24 Comparisons of tap and coconut tree roots found on TGSBs

Trees provide resistances to wind which is transferred to their horizontal roots. Coconut tree roots are self-repairable natural Geo-reinforcement for embankment soils that are fibrous in nature (TNAU 2014) (Kuriakose et al 2009). Coconut tree roots that act as flexible soil anchors, prefabricated vertical drains and geo-nets all in one. They increase the shear strength of soil by matric suction and reinforcement and also decrease the pore-water of the soil. Coconut trees suck 35 to 50 liters of water for a height of 10 to 15m per day. The roots of the coconut tree are spread mostly in the top 1-2 m of the soil with a root diameter of 5 to 10 mm and a root density of 100-400 roots per square meter (Figure 3.25).

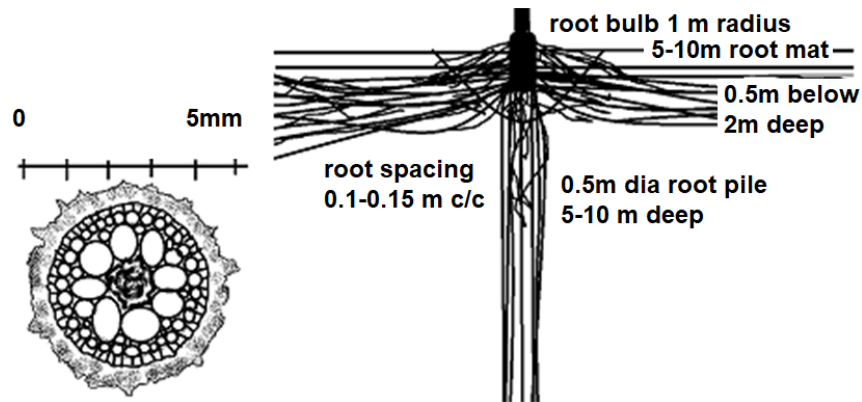


Figure 3.25 Coconut Tree Roots - cross section and distribution

Coconut Tree roots grow as annual rings just like the stem. The number of root rings depends on the age of the tree. At inception there are 4 to 5 roots. The number of roots per ring increases every year as the tree grows. Each ring contains about 200 to 250 roots at stem in a mature tree. The lateral root group of a coconut tree may be considered as an interwoven mat about 2 to 3 meters thick radiating outwards from the tree. Their lateral spread varies from 3 meters in normal soil to 10 meters in sandy area. A root pile of roughly 50 to 60 cm diameter penetrates vertically into the ground up to the water table but not exceeding the height of the tree. Therefore, the roots need to be modelled in two groups the lateral group and the vertical group. The bio-mediated soil improvement needs study of the various components and their interplay. One need to study the trees ability to amend in-situ soil strength and associated properties (DeJong et al 2009, 2010), (Chou 2007), (Chok 2008). The properties of soil (permeability, stiffness, compressibility, shear strength, volumetric behaviour etc.) can appreciate tenfold or sometimes even more with bio-mediation. Repaired roots also obtain supplementary tensile strength from strain hardening on the growth of scar tissue.

3.4.2 Fibrous Root Reinforced soil

The main natural root-based slope reinforcement used nowadays is Vetiver grass. While Vetiver grass roots is ideally suited for on slope vegetation (Anaswara and Shivashankar 2015), (Nasrin 2013), coconut tree roots is best suited for on-top vegetation in embankments. The enhancement of soil properties by grass roots has been studied at length (Gobinath et al., 2015), (Hengchaovanich, 2003), (Wu TH 1976), (Truong 2013), (Teerawattanasuk et al 2014). Fibrous roots can penetrate soils containing stone, shingle and even passing layers of asphalt or hard pan. Vetiver-roots which are approximately 0.5 m diameter and 2-3 m deep perform as flexible vertical pile group. These roots travel vertically downwards which is why, they also don't extend as rapidly like normal grass. Coconut tree roots use double action: a geo-mat about 2 m in depth and 5 to 10 m in spread and vertical pile more or less 0.5 to 1 m diameter and 5 to 10 m deep depending on soil type and tree age. One need to compare the mechanical properties of both fibrous root systems (Annexure IV) to see which is better suited for reinforcing TGSB (Figure 3.26).

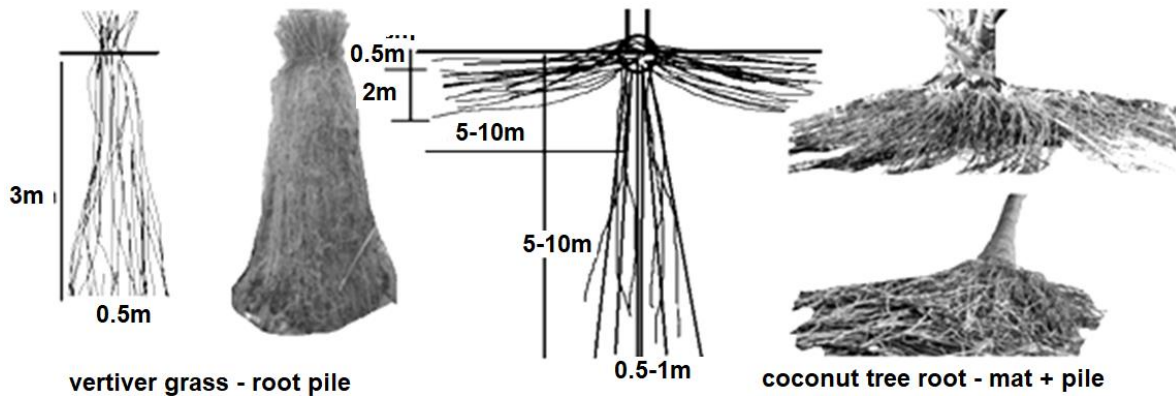


Figure 3.26 Root spread of Vetiver Grass and Coconut Tree

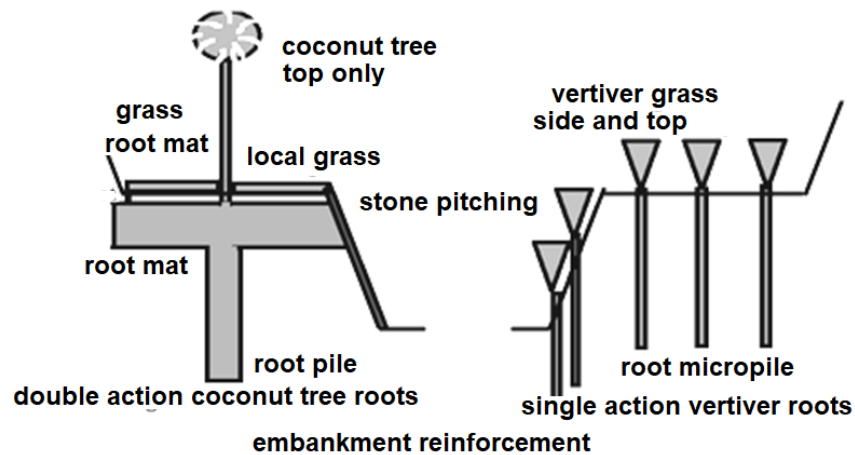


Figure 3.27 Applicability of coconut and Vetiver root systems in TGSB.

Coconut tree roots have double action of root pile and root mat while Vetiver grass roots only acts as root pile so coconut roots are better suited for reinforcing TGSB (Figure 3.27).

3.4.3 Properties of coconut tree roots found on TGSB

Coconut tree roots spread by bifurcation after 0.5 to 1 m. The diameter of the parent and daughter roots were measured at 200 bifurcation points. These were made about 5 cm away from the point of bifurcation, to avoid the root swelling at branching point. Measurement was done using Digital Vernier Callipers to accuracy of 0.01 mm (Figure 3.28). In a coconut tree the vertical root group can be considered as a micro-piles-group 50 cm in

overall diameter and 3 to 10 m deep. The horizontal root group can be considered as a root mat 5 to 10 m in overall diameter and 2 m deep.



Figure 3.28 Measuring Coconut Tree Root Branching and Diameter using Digital Vernier Calliper

$$d_{pr} = \beta d_{ar} \quad (3.14)$$

Number of roots in the horizontal root mat

$$n_{x\theta} = \alpha_r \int_{\theta=0}^{360} \int_{x=1}^{10} \int_{z=0}^2 (100 - 0.6x - 0.9x^2) (2 - 0.8x)(x \tan \theta) dz dx d\theta \quad (3.15)$$

Where x is distance from tree-stump and θ is the polar angle for a total of 360° . The values of coefficient for root branching (β) and coefficient for root spread for different types of soil (α_r) has been experimentally determined (Table 3.10). Coefficient for root branching varies from 0.9 to 0.7 (Annexure IV).

Table 3.10 Coefficient for root spread for different types of soil

Soil	Sand	Silt	Clay	TGSB	Laterite	Crushed Rock	Fractured Rock
α	2	1.5	0.8	1.1	1.0	0.6	0.4

Number of roots in the vertical root pile is

$$n_{xz} = 30\alpha_r \quad (3.16)$$

Depth of root pile is

$$Z_{x\theta} = 5\alpha_r \quad (3.17)$$

Depending on the roots in the soil there is an increase in cohesion and increase in friction angle or increase in shear strength as a whole. This is caused by the bending without breaking of roots (Figure 3.29). Increase in unconfined compressive strength (Table 3.11) and shear strength of soil sample depends on Root area Ratio (RAR).

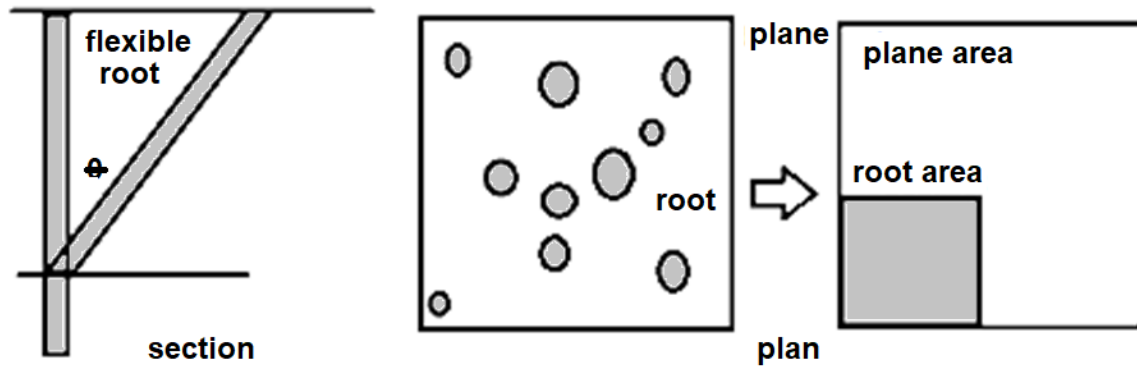


Figure 3.29 Bending of root causes increase in RAR and shear strength

RAR or Root Area Ratio gives the relation of total of root area to the plane area in the cutting plane.

$$RAR = \frac{A_{root--plane}}{A_{plane}} \quad (3.18)$$

Table 3.11 Increase in UCS v/s RAR of coconut tree roots

RAR	0	0.05	0.1	0.15	0.2	0.3	0.4	0.5	0.6	0.7
UCS	700	710	720	745	770	790	810	825	850	800
Change	0	10	20	45	70	90	110	125	150	100

As root is flexible and 3D mesh, it is generally taken that whole shear strength is increased and not friction angle of soil as is case with geo-synthetics. This is determined by in-situ shear tests. There are multiple methods to account for increase in shear strength. The first method accounts for over all increase in shear strength.

$$\tau = (c + \sigma_v \tan \phi) + \Delta s \quad (3.19)$$

$$\Delta s = B \cdot RAR + C \quad (3.20)$$

Where c is the cohesion of soil, ϕ is the angle of friction, σ_v is the vertical stress and B and C are coefficients based on tree-type and have to be experimentally determined.

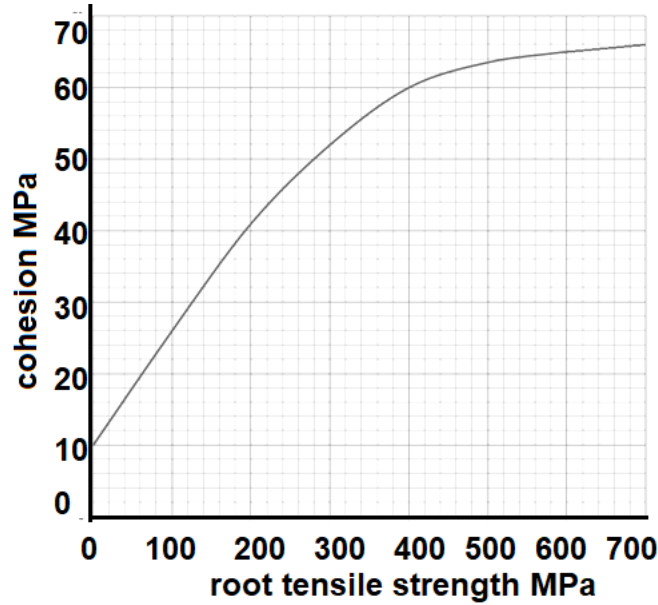


Figure 3.30 Increase in cohesion with root tensile strength.

The second method links the increase as increase in cohesion proportional to tensile strength of roots (Figure 3.30) Root reinforced soil shear strength is then given by:

$$\tau = (c + RAR\Delta\sigma_r) + \sigma'tan\phi \quad (3.21)$$

Where σ_r is the apparent root increase in cohesion, σ' is the effective stress in the soil. The third method links the increase as increase in friction proportional to soil friction. Root reinforced soil shear strength is then given by:

$$\tau = c + \sigma'tan(RAR.\phi^1) \quad (3.22)$$

Where, ϕ^1 is the apparent increased angle of friction of soil due to geosynthetic action of roots.



Figure 3.31 Coconut Tree Roots Weight For Density.

Roots were cut off from the depth of not more than 30cm and were collected in plastic sealable bags. It was kept in plastic bags so that they do not lose their moisture content. Each root was cut to a length of 20cm for its suitability with the apparatus for testing and weighed (Figure 3.31) to determine the density.

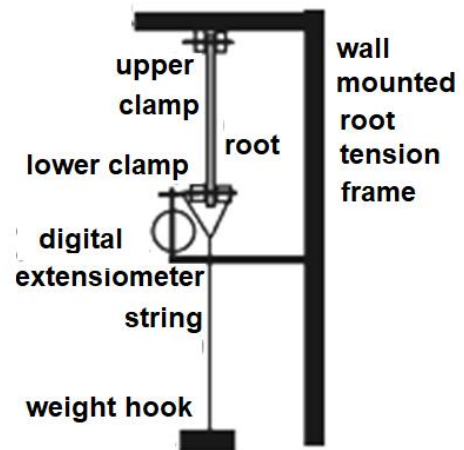
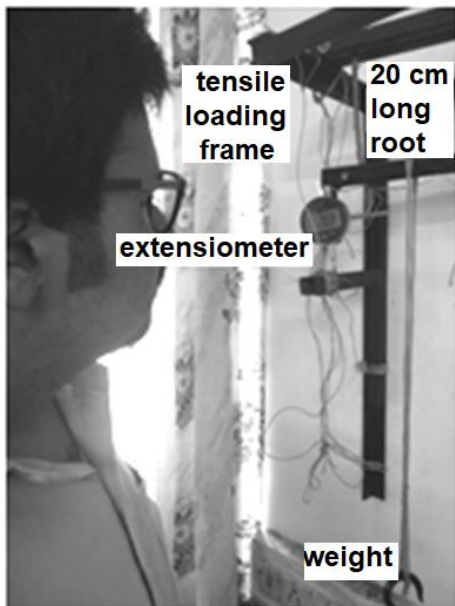


Figure 3.32 Root Tension Test Apparatus

The mechanical properties of roots (Table 3.12) were found out for 5 sets of roots from 5 different trees using specially designed equipment (Figure 3.32) as standard equipment used for steel were unable to do necessary measurements.

Table 3.12 Properties of coconut tree roots

Property		1	2	3	4	5
d_r	mm	8	5	10	7	6
γ	kN/m³	2.0	1.24	1.4	1.15	1.30
E	kN/m²	6000	4800	5000	4500	5300
Max elongation	mm	5.0	3.5	4.0	3.0	4.2
Fibre length	mm	200	125	150	160	185
Tenacity	N in 5 sec	5000	4000	4500	3500	4700
Tensile strength	kN/m²	48	35	42	30	45
Damping factor		0.13	0.11	0.12	0.11	0.12
Water absorption	%	15	20	10	18	17

The fibrous root mat of coconut tree is difficult to model unlike taproot which has fewer and thicker roots. For simplification in finding different FoS for different actions, wherever possible, the average root distribution is assumed as uniformly 10 cm c/c in both directions. When not possible, the root-mat and soil is taken as uniform layer with different properties.

3.4.4 Effect of Matric Root Suction

Matric root suction is caused due to the suction pressure caused by transpiration of the tree leaves. Water from the soil reaches the leaves from the roots through the stem by a special layer just below the surface of the plant. The water travels due to the negative pressure caused by the water leaving the leaves during the day time. This pressure is continuous and so strong that sap may even drip from leaves during the night. It is caused by Osmosis. This natural process helps in reaching the nutrients to the leaves for processing. This process while benefiting the plant also benefits the soil by adding to the strength. Soil Bearing capacity and Strength is amplified with reduction in moisture and simultaneously the pore pressure reduction causes an increase in seismic stability and reduction in liquefaction

potential. In saturated grounds suction is measured with piezometers. In unsaturated conditions suction is measured with tensiometers (Figure 3.33).

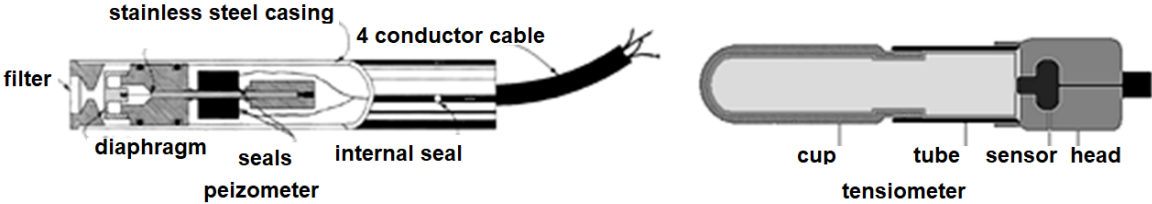


Figure 3.33 PWP measuring instruments (Wikipedia 2021b)

Soil Water Characteristic Curve (SWCC) is a curve that shows the change in volumetric water content with matric suction plotted on a semi-log graph (Fredlund et al 1978, 1996). All SWCC tend to zero at extreme high suction of 1,000,000 kPa. The SWCC curve for TGSB may be assumed as between clay and sand on upper side and between rock and sand on lower side (Figure 3.34).

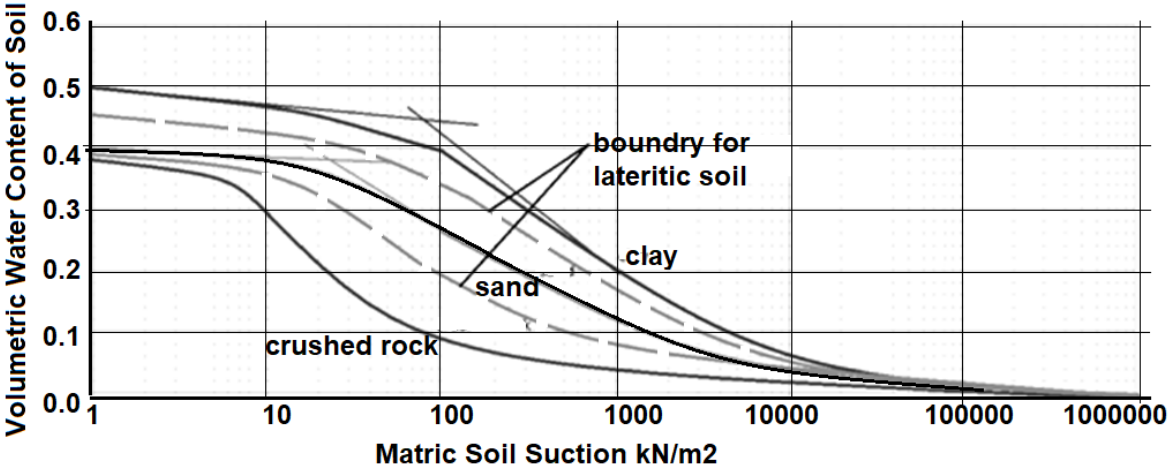


Figure 3.34 Soil Water Characteristic Curve (SWCC) (after Fredlund et al 1978, 1996)

Matric Suction in general S_u (kPa) is calculated experimentally depending on the moisture content of soil.

$$S_u = (wa)^b \tag{3.23}$$

Where w is the natural moisture content of soil in % and a and b are constants (Table 3.13)

Table 3.13 Parameters a and b for matric root suction (adapted from literature)

w	0	2.5	5	7.5	10	12.5	15	17.5	20	>20
a	0	336	598	820	1003	1147	1252	1317	1344	1345
b	1	0.860	0.764	0.682	0.609	0.550	0.504	0.472	0.449	0.444

For TGSB soils the natural water content at any distance from the tree was calculated by

$$w = 10.5(x)^{0.4} = 5.5(y)^{0.8} \quad (3.24)$$

Where x and y are horizontal and vertical distance from tree for root uptake of $0.5\text{m}^3/\text{day}$ and soil permeability of $0.005\text{m}/\text{day}$ poisons ratio 0.3 and fully saturated soil (rainy season). Full experimental study on matric suction by coconut tree root is beyond the scope of this study. There is a decrease in matric suction S_u with overburden pressure σ_v in MPa caused by soil and overlying structures. The effect depends on the depth and overburden pressure. Matric suction increases the shear strength by increasing the friction between the soils by angle δ

$$\delta = 0.67\phi \text{ to } 0.5\phi \quad (3.25)$$

Factor of safety for slope considering matric root suction by method of slices

$$FoS_{Su} = \sum \frac{cl + N \tan \phi + S_u \tan \delta \tan \phi}{T} \quad (3.26)$$

There are many factors affecting matric suction they have been studied in detail by different researchers (Indraratna et al 2006, 2014, and 2015), (Fatahi et al 2007 a, 2007b and 2008). They are mainly dependent on soil water uptake by roots (Figure 3.35).

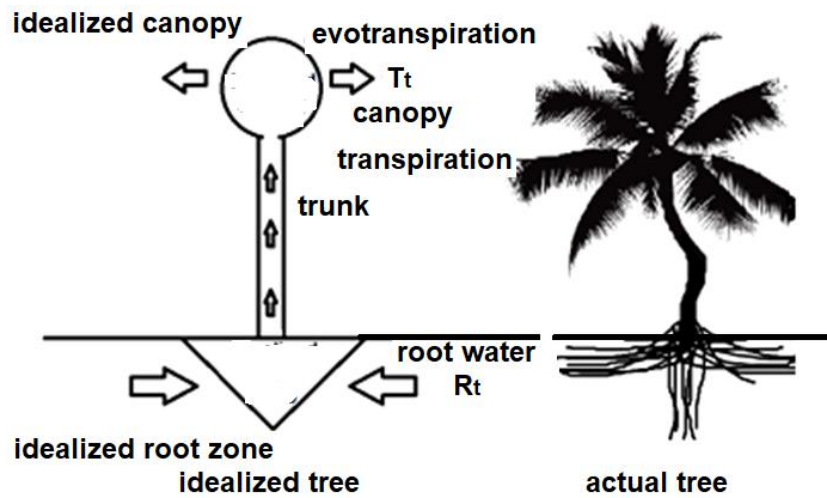


Figure 3.35 Soil–Plant–Atmosphere System for Coconut -cause of root suction pressure

Shear strength increases due to reduction of water content in soil. This increased strength is caused by an apparent rise in the soil cohesion component (Figure 3.36). This increase is proportional to the Matric root suction (Estabragh and Javedi 2012). Suction decreases as distance from tree increases and also hence shear strength varies with distance from the tree. As the TGSB soil is mostly sandy in nature there is minimal settlement.

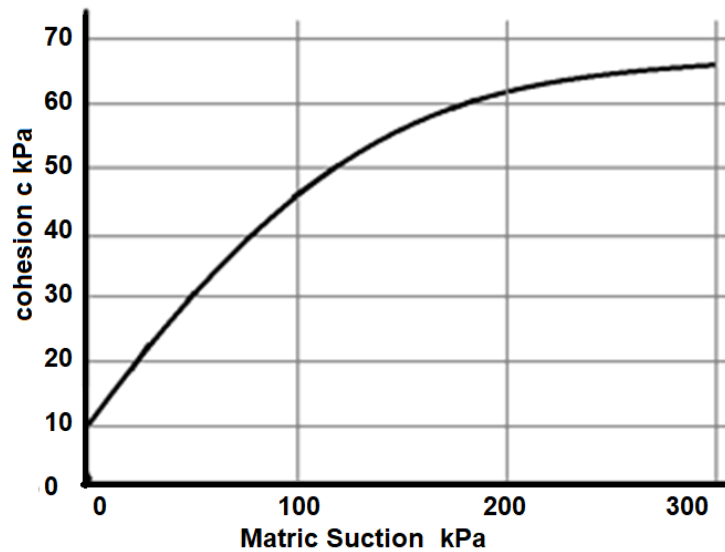


Figure 3.36 Change in cohesion with matric suction (after Estabragh and Javedi 2012)

3.4.5 Spring damping action of Coconut roots

To find the damping of roots they must be evaluated for the overall effect. For this purpose roots are considered set out from the tree as a series (one connected to the next) of parallel (many connected at a point) roots. There are several interconnected roots and they need to be evaluated schematically in parallel and in series (Figure 3.37). They are in parallel before branching. They become in series at points of branching.

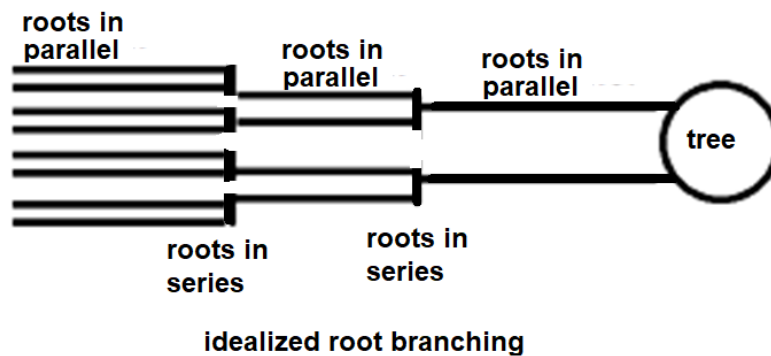


Figure 3.37 Schematic showing series of Roots in Series and Parallel

Spring damping equation is used as the roots act as springs to damp vibration. Root spring damping action of each root

$$K_i = \frac{AE}{L} \quad (3.27)$$

Where A is root area and L is the root length of the section considered and E is the elastic modulus of root. Total root spring parallel action is at a node is

$$K_p = \sum K_i \quad (3.28)$$

Total root spring series action for all nodes is

$$K_s = \frac{1}{\sum \frac{1}{K_p}} \quad (3.29)$$

Considering a bifurcate parallel branching and nodes for every 1 m, the cumulative damping factor provided by each coconut tree is 0.165. The damping factor provided by each double row of coconut tree is $0.165/2 = 0.0825$, The range of damping factor provided by coconut trees on TGSB can be taken as 0.0825 ± 0.0275 i.e. 0.055 to 0.11

3.4.6 Wind damping action of Coconut stem

Due to its aerodynamic shape coconut tree stem and canopy contribute significantly to the stability of TGSB. The pendulum cum spring action of the extremely flexible stem gives it a good additional damping capability. The ability of the coconut tree to alter its canopy shape by sweeping back of leaf-branches in response to a prevailing wind, thence reducing drag upon the tree is streamlining. Streamlining of canopy reduce wind loading by reducing the speed specific drag. There is avoidance of stress on the roots and hence the embankment by shedding the load.

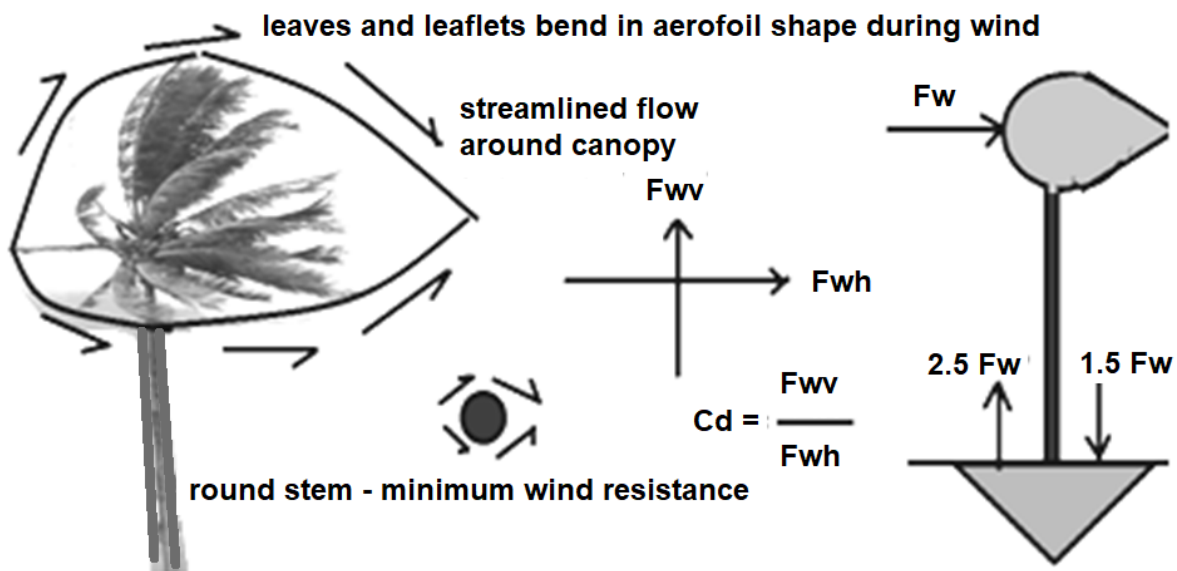


Figure 3.38 Airflow around Streamlined Coconut tree and their forces during winds.

This reduces the drag considerably (Figure 3.38). The canopy pivots around the top so the upwind and downwind reactions are equal. The tree that directly faces the wind wraps more and the tree at rear wraps less these showcases the effect of reduction and wind break provided by coconut trees (Figure 3.39). This ensures that the tree can resist any wind from any direction.

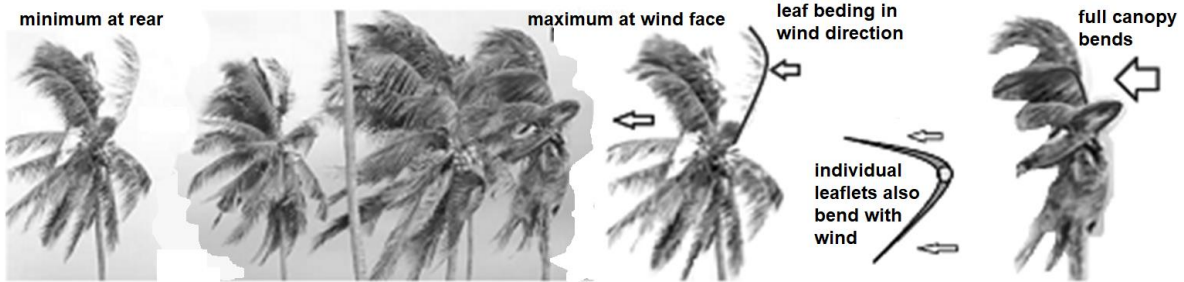


Figure 3.39 Front tree canopy flex maximum thus protect the rear trees in cyclones.

The whole coconut tree canopy acts like an aerofoil to negate the wind force thus increase the safety of the TGSB (Figure 3.40). The respective components of the leaflets and leaf as a whole and the canopy self-adjust as seen in the pictures and the upward and downward forces are self-balanced. Each leaf and leaflet bends and balances as per the force it receives thus achieving stability even in storms of wind speeds exceeding 150 kmph (sustained) and 210 kmph (gusts) as seen in recent cyclones Kyarr-2019 and Tautake-2021.

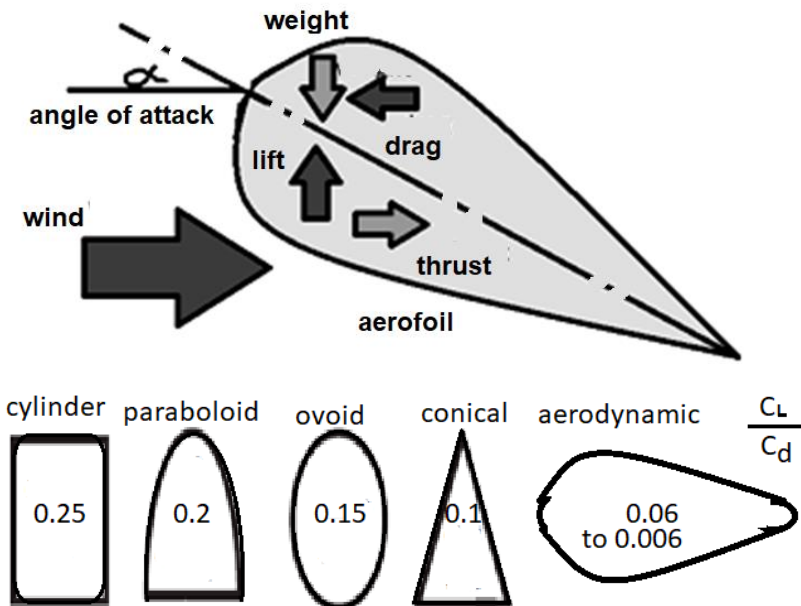


Figure 3.40 Forces acting on an aerofoil / Coconut canopy (adapted from Wikipedia).

Wind force developed on tree top depends on air density (assume 1.185 at 25°C) .

$$F_w = 0.5 C_d \gamma_{air} v_w^2 A f_h \quad (3.30)$$

$$C_d = \frac{F_{wv}}{F_{wh}} = \frac{2F_d}{\rho_{air}v_w^2 A_d} \quad (3.31)$$

$$C_l = \frac{2F_l}{\rho_{air}v_w^2 A_l} \quad (3.32)$$

C_d will vary from 0.02 to 0.04 and C_l will vary from 0.00012 to 0.00024 for coconut tree.

Where f_n is height coefficient

$$f_h = 0.99 + 0.0092h \quad (3.33)$$

The shear contribution of root tensile strength on horizontal roots in increasing the resistance has not been considered (it depends on soil and varies from 11% at 10 m away to 90% at base).

$$F_{wv} = 0.5 \times 0.0012 \times 1.15 \times 30^2 \times 67 \times 1.128 = 46.93 \text{ kN} \quad (3.34)$$

$$F_r = (3.142 \times 0.52 / 4) \times 800 = 157.1 \text{ kN} \quad (3.35)$$

Weight balances the lift, and thrust balances the drag in moving vehicles. In trees weight reduces the lift (vertical) force and root mat balances moment due to drag (horizontal) force. Then

$$W_T = \text{density} \times \text{volume} = 1.2 \times 6.3 = 7.56 \text{ kN} \quad (3.36)$$

$$F_w = W_T - F_{wv} = 46.93 - 7.56 = 39.37 \text{ kN} \quad (3.37)$$

$$FoS_{\text{uplift}} = 157.1 / 39.37 = 3.99 > 2.5 \quad (3.38)$$

This is the reason coconut trees can withstand heavy storms

$$F_w = W_T - F_{wv} = 46.93 - 7.56 = 39.37 \text{ kN} \quad (3.39)$$

Strength of stem against uplift breakage

$$F_s = (3.142 \times 0.352 / 4) \times 500 = 48.11 \text{ kN} \quad (3.40)$$

$$FoS_{\text{stem}} = 48.11 / 39.37 = 1.22 \quad (3.41)$$

During sustained peak storm winds coconut tree canopies shed leaves thus reducing their lift to almost zero and still staying within safety limits. These additional FoS can be multiplied to Static FoS for estimating the overall effect of stem and canopy in cyclonic event.

3.4.7 Pullout test of coconut tree roots in sand.

Pullout resistance plays a major role in geo-synthetic action of roots by preventing slope failure, reinforcing the soil and increasing the soil strength.

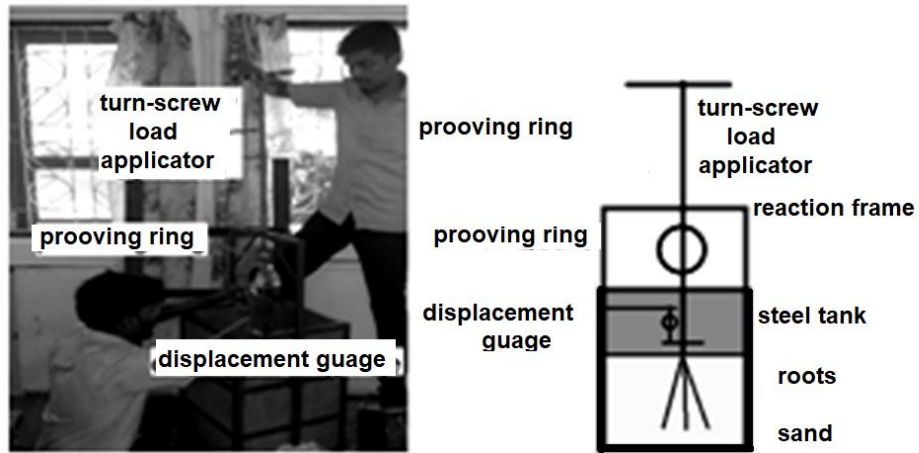


Figure 3.41 Test Apparatus for pull-out of roots

Root pullout test were conducted to find out the pullout capacity (Figure 3.41 & 3.42), and the graph of force verses displacement for different number of roots was found out.

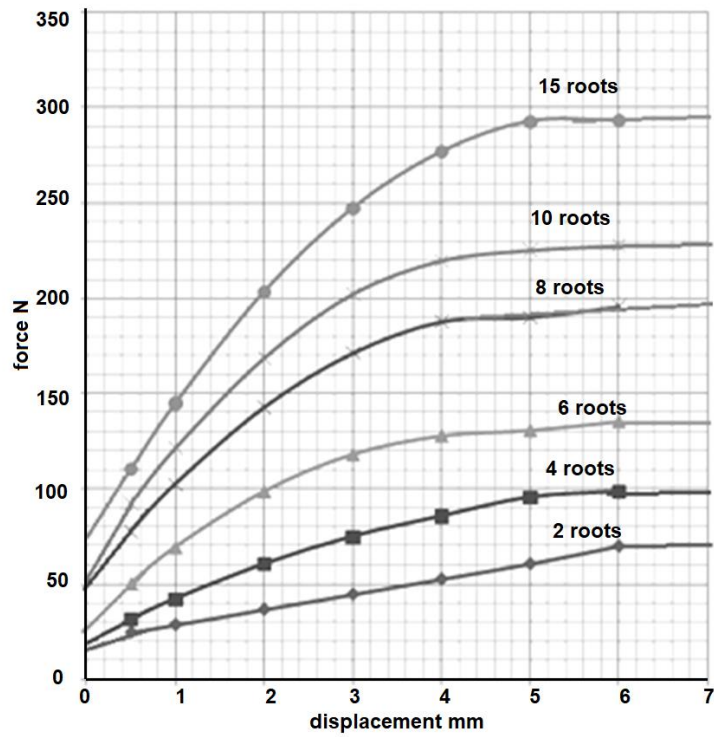


Figure 3.42 Force (N) required for pull-out of roots

The additional friction angle given by the roots was found out. Pullout Force F required for number of roots N can be estimated from the expression

$$F = 38.57N^{-0.25} \quad (3.42)$$

Shear force for sand

$$\tau = \sigma \tan \phi' \quad (3.43)$$

Average overburden pressure is $\sigma = (0 + 18 \times 0.3 / 1000) / 2 = 0.0027 \text{ N/m}$

Average overburden force is $\tau h = 0.0027 \times 0.3 \tan \phi' = 0.00081 \tan \phi' = 19.5$

Apparent friction angle = 89.99

Sand friction angle = 30

Additional friction angle due to roots = 59.99

Pullout can also be related to additional cohesion as apparent root adhesion factor α .

$$\tau = \alpha c + \sigma \tan \phi = F / \text{perimeter} \quad (3.44)$$

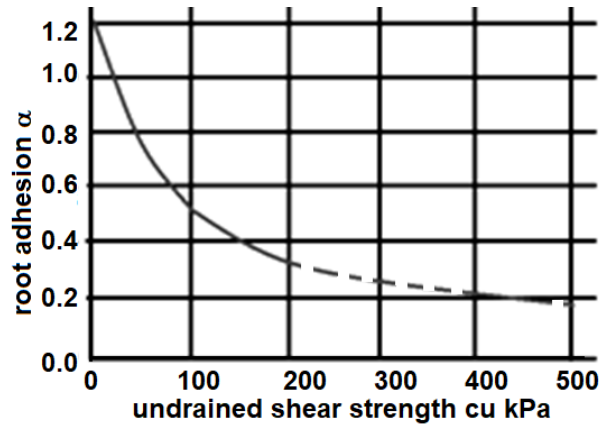


Figure 3.43 Variation of root adhesion with soil shear strength.

The undrained soil shear strength and root adhesion for different soils and stabilized soils is found out and plotted. Root adhesion varies with soil shear strength (Figure 3.43).

3.4.8 Comparison of Coconut Root with Other Geotextiles

Geotextiles (GT) are materials that act as a flexible skin and reinforcement in the soil. Although they have been around and used for millennia the term Geo-textile was recently

used to describe such materials (Zornberg 2011), (Handbook for Geo-synthetics 2013). Unlike other stabilizers they don't alter the soil properties itself but use the soil properties in conjugation with its own properties to get the desired engineering results (Boyle 2013). Henry Vidal, a Frenchman in 1960 first patented this technology. Bio-remediation, bio-stabilization, bio-engineering and sustainable infrastructure are the engines driving modern research (Preti and Giadrossich 2009). In this context it is essential to also study the centuries-old TGSB coconut root technique which is classified today as natural geotextiles. Natural Geotextiles used are especially jute and coir (Satyanarayana et al 1982), (Gray and Ohashi 1983), (Ali 2010), (Fathi 2014), (Das et al 2016), (Anggraini 2016), (Kalita et al 2016). There exists scant scientific literature on coconut tree roots as most literature dwell on other geosynthetics (Palmeira et al 2008), (Moldovan 2010). Today the area of research has gravitated from plastics use to sustainable natural products like jute and coir. Coconut roots (Figure 3.44) like act like Geo-synthetics increase shear strength confining pressure and reduce particle dilation and breakage in sub soil. The vertical roots act like micro-piles strengthening the soil and like PVDs to effectively mitigate the build-up of excess Pore Water Pressure from high cyclic loading during earthquakes.

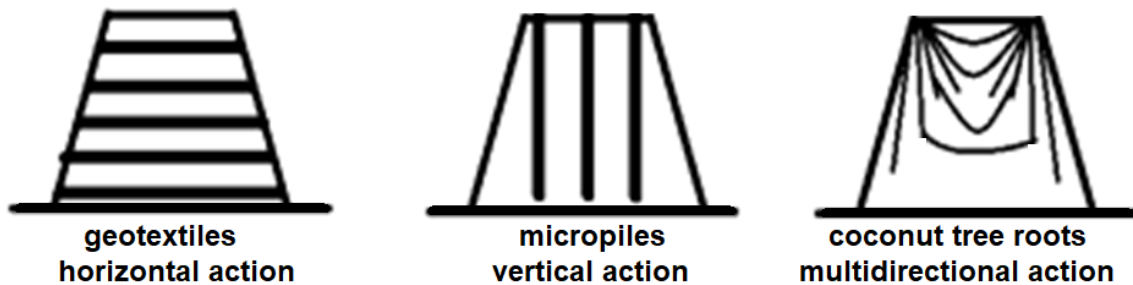


Figure 3.44 Coconut Tree Roots act as combination of micro-pile and geo-textile.

Coconut Roots can grow under structures after the structure is built, thus act as a seismic-retrofit. Unlike geo-textiles they don't have to be put in first and unlike micro-piles they can extend horizontally under the structure. As they have uniform diameter throughout their length, they don't cause upheaval like tap roots and hence don't damage the structure. The Coconut tree root mechanically enhance soil stability by these systems

(a) Strong soil particle binding by root mat in top surface layers, causing an increase in soil shear strength parameters($c-\phi$), aided by local grasses roots which grow round the coconut roots

(b) Root water uptake to increase slope stability by reducing moisture,

(c) soil anchor action of deep root systems.

Geotextiles have wide applicability in transport infrastructure and coconut roots perform similar functions in normal soils (Figure 3.45) and weak soils (Figure 3.46).

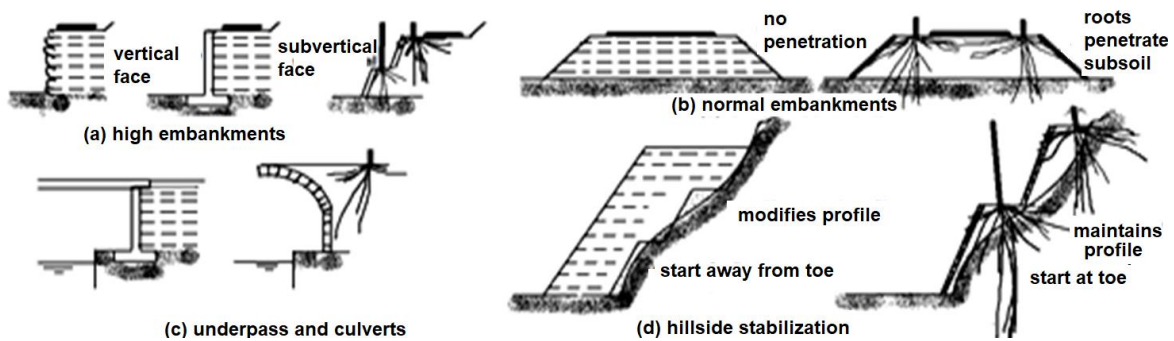


Figure 3.45 Comparison of Geo-synthetic and TGSB Reinforced normal Soil.

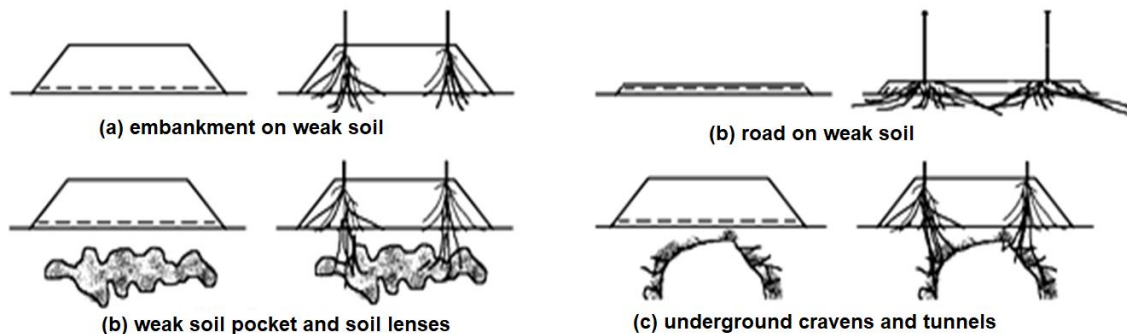


Figure 3.46 Comparison of Geo-synthetic and TGSB Reinforced weak Soil.

There is further 170 % less area required for TGSB construction over geotextile reinforced embankment (except for panel faced walls with vertical face). This results in proportional reduction in construction and material costs. Once a tap root snaps the whole reinforcement loses its utility (strength), not so for coconut roots (Figure 3.47). As only the outer roots are damaged, the loss is minimal.

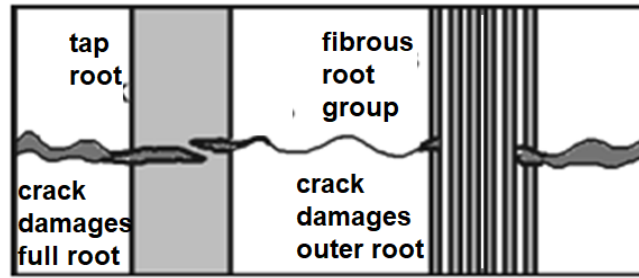


Figure 3.47 Soil Cracks and their damage in Tap and Fibrous Roots

Short and thin taproots (shrub and less) and fibrous roots act as cross-reinforced surface zone trapping soil in matrix and prevent piping although some fines may escape most of the soil remains in place (Figure 3.48). Big tap roots can't do this.

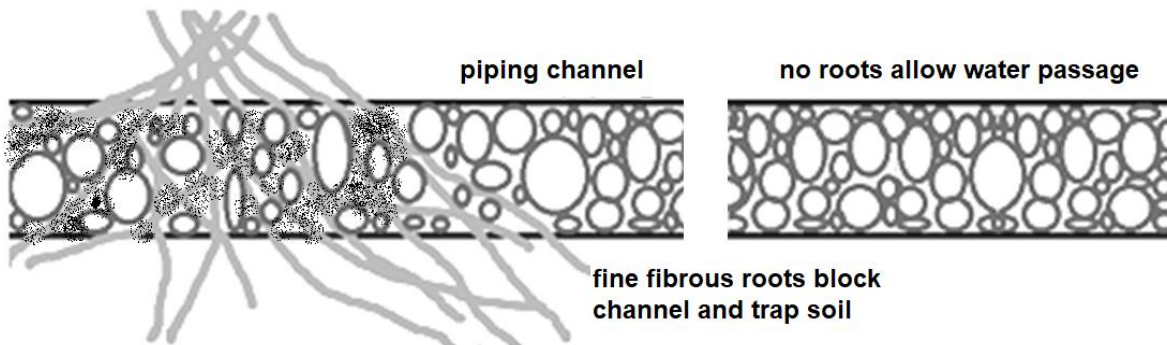


Figure 3.48 Stoppage of soil piping by fibrous roots of coconut tree in a potential piping channel

Due to their porous mat structure the fibrous roots increase water infiltration. They absorb water and soluble salts by matric root suction. Their canopy transpiration promotes and increases matric root suction which in turn increases the soil shear strength and decreases land-slide potential. Coconut trees prevent soil water evaporation by their shade and increase humidity below the canopy thus increase in rainfall potential. Coconut tree roots protect against wind erosion of surface soils. Cementation by biochemical root secretions containing cellulose, protein-gum, polysaccharides, fat and wax adds chemical-

strengthening to the mechanical soil-strengthening properties of coconut tree roots. In a TGSB the coconut tree roots act as geo-synthetics in different ways:

1. Vacuum Drains – sucking up the water and strengthening soil.
2. Soil grouting drains – due to root chemicals strengthening soil.
3. Root mat – damping vibrations.
4. Root pile – reinforcing soil.
5. Root nail – reinforcing soil.
6. Root anchor – reinforcing soil.
7. Mechanically Stabilized Earth wall – in combination with Rubble facing

The effect of each action needs to be considered separately as the concepts behind each is different.

3.4.8.1 Combined factor of safety for Geo-synthetic action

Combined factor of safety for Geo-Synthetic-Action of TGSB has been taken as the average of Factors of safety for each action. This is because each Geo-Synthetic-Action is estimated separately and concurrently. Only soil nail and soil anchor action of root was considered for this thesis.

Soil nail

$$T_{dn} = \pi d_r l_r q_u \quad (3.45)$$

$$q_u = \left(\frac{A_{fyr}}{FoS} \times \frac{1}{\left(\frac{1-\sin\phi}{1+\sin\phi} \right)} \times \frac{1}{s_v s_h} \right) - \gamma Z \quad (3.46)$$

$$T_{eq} = \frac{\sum T_{dn}}{s_h} \quad (3.47)$$

Soil anchor

$$T_{da} = \pi d_r l_r \alpha c_u \quad (3.48)$$

$$T_{eq} = \frac{\sum T_{da}}{s_h} \quad (3.49)$$

$s_v = s_h = 0.1$ = root spacing

$c_u = 250$ = undrained shear cohesion

$d_r = 0.005$ = root diameter

$l_r = 10$ = root length

$\alpha = 0.25$ = adhesion factor

f_{yr} = root tensile strength

A= root tension

h= TGSB height

$$P = 0.5 \left(\frac{1 - \sin \phi}{1 + \sin \phi} \right) \gamma h^2 \quad (3.50)$$

$$FoS_{sliding} = \frac{W \tan \phi + T_{eq}}{P} \quad (3.51)$$

$$FoS_{global} = \frac{cL + N \tan \phi + T_{eq} \tan \phi}{T} \quad (3.52)$$

Table 3.14 Combined factor of safety for geosynthetic action

Action	sliding				global			
	3	6	9	12	3	6	9	12
Height	3	6	9	12	3	6	9	12
Soil Nail	11.3	3.2	2.7	2.8	17.9	10.3	6.8	4.0
Soil Anchor	13.4	3.8	3.4	3.5	24.1	13.4	8.1	5.5
Average value	12.35	3.5	3.05	3.15	21	11.85	7.45	4.75
Plain Soil	5.9	1.5	1.2	1.1	11.2	7.0	3.9	2.3
Increase	6.45	2	1.85	2.05	9.8	4.85	3.55	2.45
% Increase	109	133	154	186	88	69	91	107

There is a 109 to 186 % increase in FoS against sliding and 69 to 107 % increase in global FoS due to geo-synthetic action of Coconut tree roots (Table 3.14). This FoS has to be multiplied to static FoS of TGSB without roots to get combined FoS due to geo-synthetic action of roots.

3.5 Study of Seismic Parameters for TGSB

The Indian subcontinent is seismogenically non-homogeneous.

There is a clear variation in the spatial density of past epicenters and time-period. Certain areas like the North East, the Andaman-Nicobar Islands, and the Himalayas (Saikia et al 2016), (Chandra 1992) are more active than Peninsular India which is more stable and it is where Goa lies. There are no reported earthquakes that are capable of creating severe damage near Goa and the intensity of effect decreases with distance (Figure 3.49). For

finding the earthquake magnitude and seismic study of Goa it is necessary to study the geomorphology of the region and do Seismic Hazard Analysis (SHA) and quantify it in terms of potential maximum magnitude. It is also necessary to find site specific seismograms. A limited number of earthquakes have been studied and their data including accelerograms, absolute and spectral acceleration, displacements and velocities have been given in Annexure XI for further reference and study.

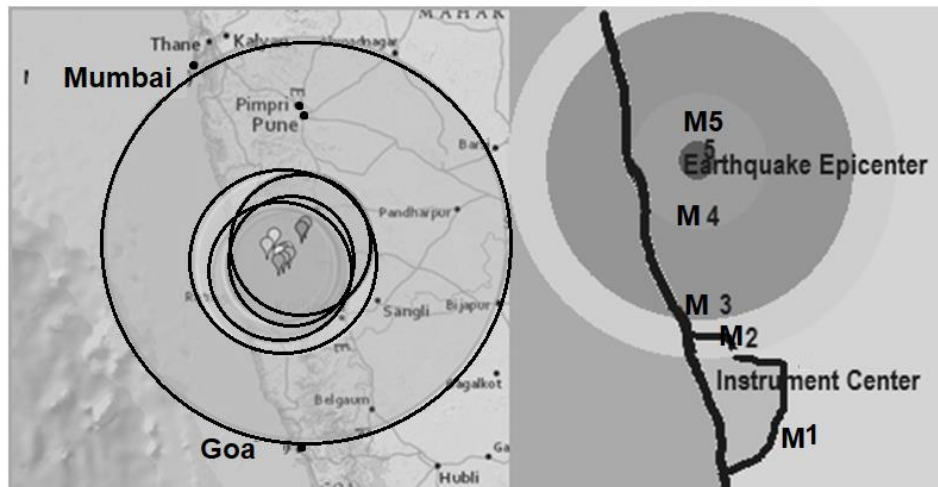


Figure 3.49 Macro-seismic map for the Past earthquakes near Goa and reduction in magnitude as earthquake near Goa (Earthquake Track 2020).

(Largest circle was 51 years old based on unreliable verbal description. Smaller circles are instrumented measurements of impacted regions which are nowhere near Goa)

Earthquake magnitude gives a number relating to its amplitude. In magnitude scales of earthquake every unit rise in magnitude matches to a tenfold rise in amplitude as they are logarithmic. The true earthquake magnitude is measured by estimating its effect. Thus earthquakes can thus have varying magnitude depending on the method used for magnitude estimation and the datasets needed for them.

3.5.1 Earthquakes near Goa

Most local experts depend on data of Koyna earthquake to compute seismic effects on Goa region. The nearest earthquake to strike Goa was the Koyna earthquake of 1967. It occurred

on 11 December in Maharashtra close to town of Koynanagar with a magnitude 6.6 having Mercalli intensity of Severe (VIII) near Koyna dam. Many geologists consider the earthquake to be seismic activity that was reservoir-triggered. Minimum 177 died and over 2,200 got injured and 80% of the houses in Koynanagar Township were damaged. It generated a 10–15 cm (3.9–5.9 in) ground fissure spread over 25 kilometres (16 miles) length. There was no major damage to the dam except minor cracks which were swiftly repaired. Several earthquakes of smaller magnitude have occurred there since 1967.

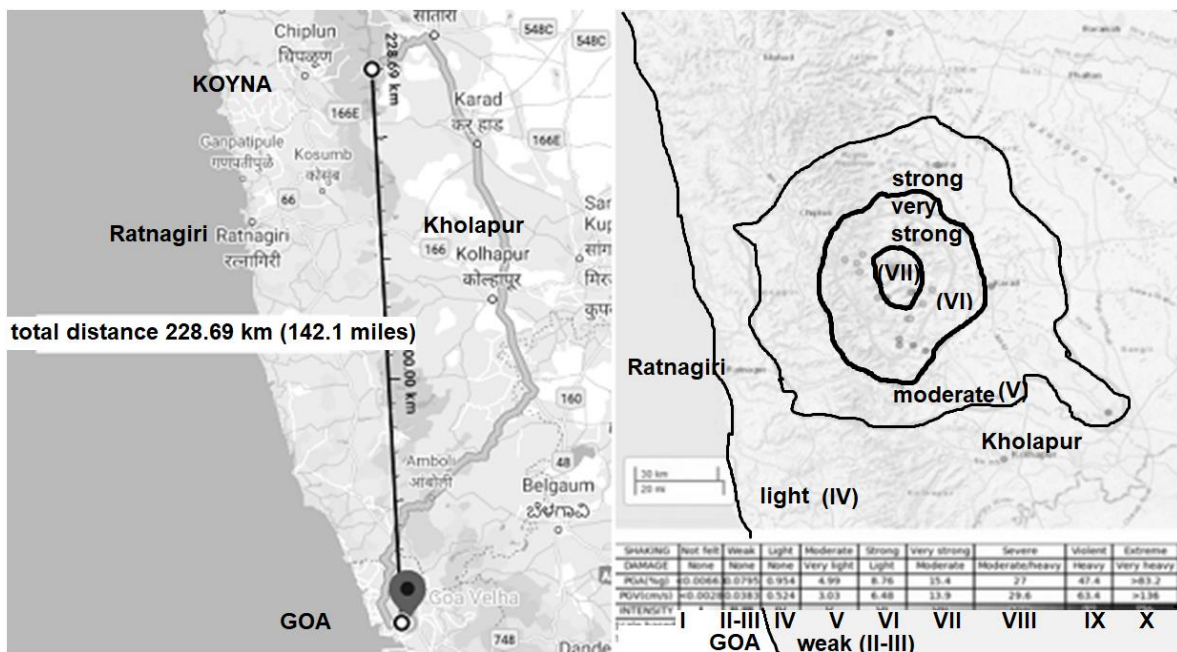


Figure 3.50 Distance and Shake map of Koyna Earthquake to Goa shows the weakness of impact on Goa. (Google maps, USGS)

Goa had minimum effect. This is because the northern tip of Goa is the southernmost tip of the Deccan traps (same basaltic bed rock that underlies Koyna). The distance of Koyna to Goa is 228.69 km as per Google Maps (Figure 3.50). Shake map of Koyna Earthquake from USGS shows that the peak Ground acceleration from that earthquake in Goa is less than 0.0066g and the peak ground velocity is less than 0.0028m/s. there is no damage and no shaking felt. Since damage causing earthquakes are rare in Goa the possible earthquakes magnitudes from potential nearby fault ruptures are studied. Even USGS confirms in its

Probabilistic Statistical Hazard Analysis for 10% reliability and 50-year occurrence that there is no risk in Goa. Further information is given in (Annexure V)

3.5.2 Magnitude calculations for Goa

Though the full seismic microzonation on body magnitude or local magnitude scale is not within the scope of this thesis a partial attempt will be done to evaluate the earthquake threat to its three main cities Panjim, Margao and Mapusa.

Strong seismic ground-motion data is obtained and used to derive attenuation relationships (Liu and Tsai 2005), (Iyengar and Raghukant 2004), (Raghukant and Iyengar 2007). Such a relationship is needed for Goa. An Excel sheet was prepared to calculate the earthquake magnitude in terms of local magnitude M_L that can affect Goa if any of the nearby faults rupture (Annexure V). Amplitude A in micrometers for different earthquakes magnitudes M_L at distances D in Km is calculated using the relationships

$$A = 10(M_L + 1.67 - 2.56 \log (D)) \quad (3.53)$$

Period T of the earthquake is given by

$$T = 10(0.32 M - 0.14) \quad (3.54)$$

Local Moment Magnitude from faults was calculated (Table 3.15).

Table 3.15 Seismicity parameters for Goa in India (IIT Madras)

Zone No.	Zones	b-value	N(4)	Max. Potential Magnitude (M_{max})	No. of earthquakes	a
20	Western Passive Margin	0.76±0.07	0.37	6.8	70	2.75±0.08

The Indian peninsular shield has a complex system of folds and faults in the basement rock, due to the powerful tectonic movement during its evolution.

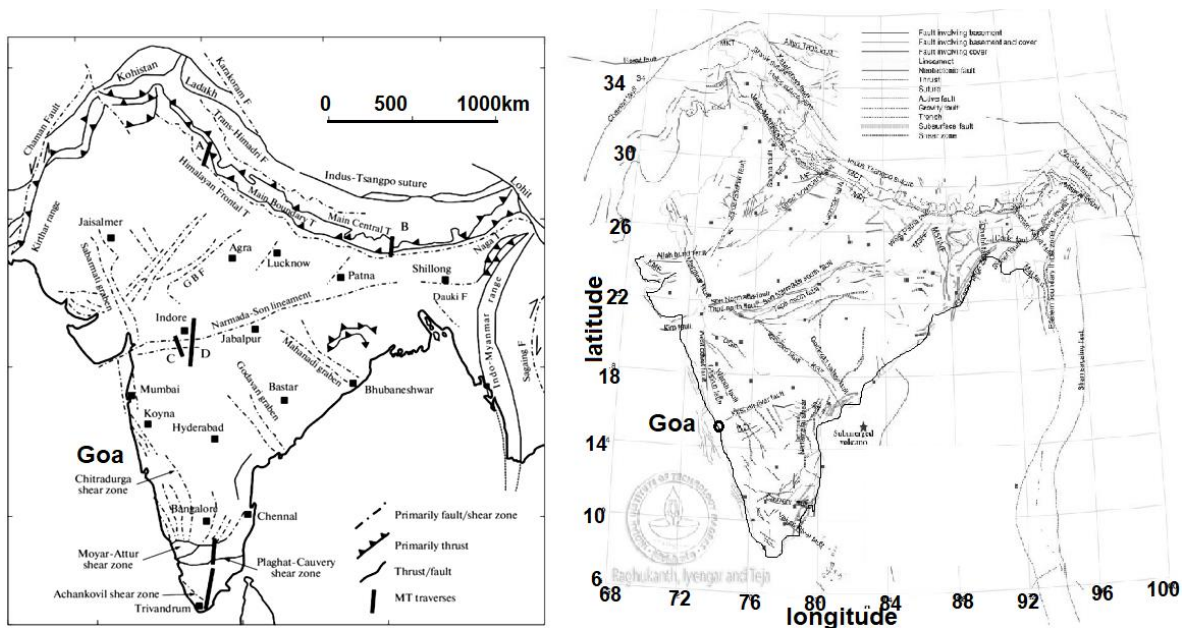


Figure 3.51 Simplified-tectonic-map-of-India. (Valdiya 2010), (IIT Madras)

Peninsular region contains most of the stratigraphical units and rock formations in India. More than half of the Indian shield is occupied by the Dharwar rocks from the oldest Archean era. The seismicity parameters for the west coast of India which affect Goa in particular are given in Table 3.68. After studying the maps produced by Valdiya (Figure 3.51), BMPTC, National Centre for Seismology (Seismo.gov.in), IIT madras, II Geomorphology Navi-Mumbai, IIT Bombay, for this calculation a separate map was drawn considering only the faults within 400 kms of Goa.

From the map produced by IIT madras only 28 faults within 400 km of Goa were considered for these calculations. The distances were measured from three principal cities of Goa i.e. Mapusa to north, Panaji to centre and Margao to the south, as there represent the main cluster of populations and where major damage can take place (Figure 3.52).

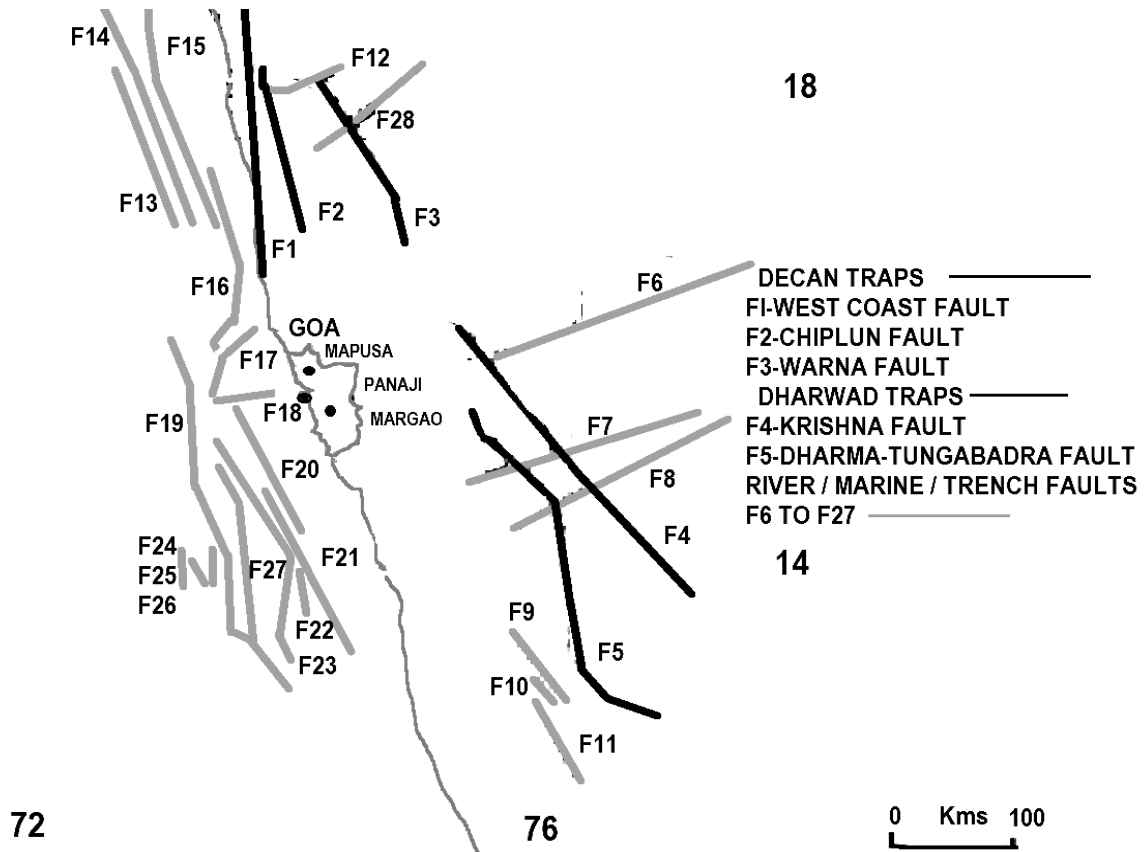


Figure 3.52 Faults near Goa (based on IIT Madras)

It was assumed that nearest 1/3 of the fault ruptured (Figure 3.53). Rupture area ($B * H$) slip-length (L) Distance from local area (D) were considered and used in the calculations.

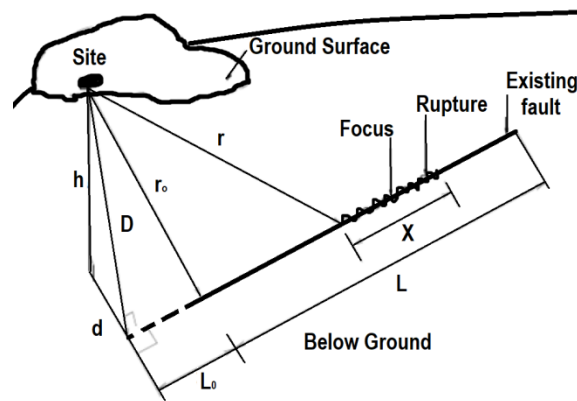


Figure 3.53 Earthquake from rupture of faults.

Seismic moment is given by

$$M_o = 30,000,000,000 * B * H * L \quad (3.55)$$

Distant Moment magnitude is calculated using

$$M_{w1} = 2/3 \log(M_o) - 6.06 \quad (3.56)$$

Local Moment magnitude was calculated by excel sheet (Annexure V) for the three types of faults using the relationships shown below from the relationships developed by Rao et al. (1998) and Sharma et al (2007) for NDMA in 2008.

---Basaltic

F 1,2,3 -- H= 15, L =10

$$M_w = 3.47 + 0.85 \log(M_{w1}) - 0.0011 D - 1.91 \log(D) \quad (3.57)$$

---Granitic

F 4,5 -- H= 25, L =15

$$M_w = 3.22 + 0.85 \log(M_{w1}) - 0.0011 D - 1.91 \log(D) \quad (3.58)$$

---Deep Granitic

F others -- H= 50, L =5

$$M_w = 3.07 + 0.85 \log(M_{w1}) - 0.0011 D - 1.91 \log(D) \quad (3.59)$$

The maximum local magnitude in Goa is 1.013 at Panjim.

However seismic stability needs specific inputs like site specific seismograms. Using STP values and CPT co-relationship with coordination with spectral acceleration diagrams such artificial seismograms can be developed. Six such have been developed for Goa in this thesis for use in software to use in liquefaction analysis and seismic stability analysis (Annexure XIII).

3.6 Summary

In ancient times the Saraswats settling in Goa had constructed unique embankments (TGSBs) with double row of coconut trees on top. TGSB were constructed by traditional specialists using traditional methods and equipment. They have great applicability in modern day from sustainability point of view: Habitation, transportation, irrigation, solid waste retention systems and, seismic and liquefaction stability. However, lack of studies in

TGSB has necessitated some investigations and experimentation that has been listed in this chapter.

The physical dimensions and design parameters including material, dimensions, sizes, shape and necessary properties of the constituents' parts were investigated.

This study researched physical properties of some lateritic soil formations used today for TGSBs in Goa, India. The soils below varied in colour and properties to a depth of 25 to 30 m where granitic or basaltic bed rock is found. Properties also varied both with colour and depth. The particle size distribution generally showed greater percentage of coarse soil at the reddish lateritic layer while the clay size percentage increased at the lower layers. Suitable soil stabilization studies were conducted to find the proportions used for these structures.

The main contributor to sustainability of TGSB is the Coconut tree with fibrous roots which are self-repairable natural geo-reinforcement for embankment soils which are planted on top of them. Root properties were found out. Coconut tree roots also strengthen the soil by matric root suction. Root pull-out tests showed added contributions of roots to Factor of safety. The aerodynamic properties of the tree that help it to withstand the dynamic wind loads were also studied. TGSBs use natural Geosynthetics i.e., coconut tree root reinforcement to strengthen the soil which almost doubles its factor of safety.

Since damage causing earthquakes are rare in Goa the possible earthquakes magnitudes from potential nearby fault ruptures were studied. Even USGS confirms in its Probabilistic Statistical Hazard Analysis for 10% reliability and 50-year occurrence that there is no risk in Goa. However seismic stability needs specific inputs like site specific seismograms. Six such have been developed in this thesis for use in Goa.

The sizes and properties found out in this chapter will be used for computer based static and seismic analysis considering the effect of coconut tree roots in the next chapter.

CHAPTER 4

SEISMIC ANALYSIS OF TGSB

4.1 Use of computers for analysis of TGSB

The computer based seismic analysis of TGSB considering coconut root reinforcement will be primarily carried out using three software: Microsoft Excel (using Limit Equilibrium Approach), GeoStudio2019-Student version (using Limit Equilibrium Approach) and Midas GTX NX 2016 (using Finite Element Method Approach). Static analysis will be also done for comparison or results as no previous study exist in this area of study. The computerized seismic analysis of TGSB done in this thesis will consist of following components: static analysis, pseudo-static analysis, pseudo-dynamic analysis, the liquefaction analysis, and a brief tsunami protection analysis. The data to be inputted was experimentally found out (EM 1110-1-1906, IS 1498-1970, IS SP 36 1988) and has been already studied in chapter 3 (Table 4.1 and Fig 4.1).

Table 4.1 General properties of soil used for static and dynamic design of TGSB

	k_h	γ	γ_{sat}	c	ϕ	ξ
TGSB soil		kN/m^3	kN/m^3	kN/m^2	°	
plain soil	0.11	1.8	1.98	20	30	0.05
rooted soil	0.11	1.5	1.7	30	40	0.5

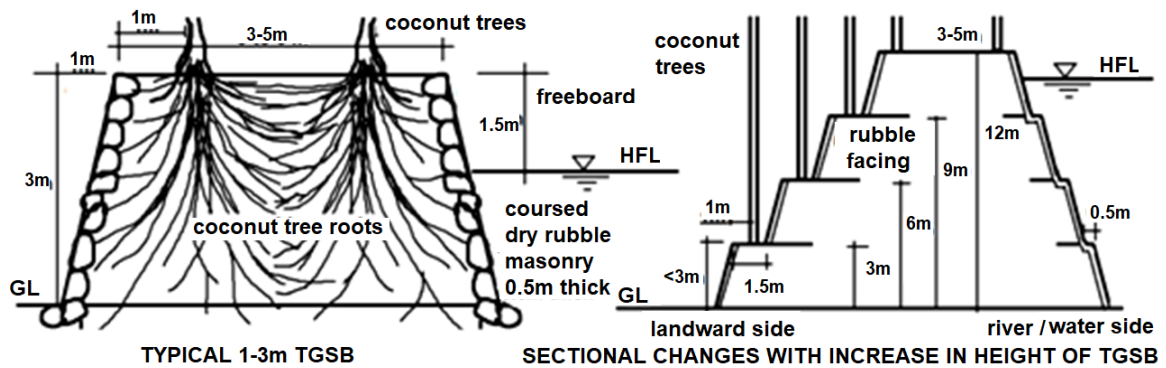


Figure.4.1 TGSB (a) Typical section (b) Change in section with height showing benching

As the soil is not purely sandy or purely clayey, and also due to variation in property due to soil stabilization, standard soil models like Cam-Clay, Tresca, etc. cannot be used. The reinforcement by roots further complicates the model. Furthermore due to the complex nature and variability of lateritic soil the Mohr-Coulomb model is followed for software inputs as necessary (Coulomb 1776, Mohr 1900). Analysis was done incorporating relevant parts of national and international standards (IS 1904 -1986), (IS 8009 Part I -1976), (IS 1893), (ASCE 7-05-2006), (ASCE/SEI 7-10), (EM 1110-2-1902), (EM 1110-2-1913), (EN 1998-1 2004), (Eurocode 8 2004) (FEMA 356 2000), (FEMA 440 2005), (FEMA 450 2003), (FWHA-NHI-05-039 2005), (JSCE 2007).

Various Geotechnical Engineering Software Suites like GeosStudio-2019, Midas-GTX-NX, GeoSlope2019, OptumG2, Plaxis, ANSYS, FLAC, etc. are available. They are normally used to analyse embankment dams. As TGSBs can retain water, this software may be utilized for their scrutiny. Of these two were used in this thesis to validate the results from Microsoft Excel spread-sheet based analysis as Excel is semi-manual in nature.

The GeoStudio suite is well established commercially and academically available software used in geotechnical engineering for analysing slopes, dams and embankment. Three packages of the software-suite GeoStudio2019 were used for analysis of the TGSB viz. SLOPE/W, QUAKE/W and SEEP/W. Analyses were done investigating different aspects and geotechnical properties by: SLOPE/W for various heights of TGSB; QUAKE/W for action of characteristic earthquake in Goa, India and abroad; SEEP/W for the seepage of water in water retaining TGSB structures.

The Midas suite is commercially and academically available established software also used in geotechnical engineering. GTX NX of this is used in analysing embankment and slopes. The software allows for different types of analysis simultaneously including static, pseudo-static and dynamic simultaneously as construction stage sets.

All software has their limitations and advantages. Their results can however be used to compare with Excel results within a range of similitude and equivalence for uniformity of results and this will be done in results and discussions chapter.

4.1.1 Seismic Slope Stability Analysis

The seismic analysis includes finding the factor of safety for seismic slope stability, liquefaction and tsunami damage. Seismic stability Analysis of slopes is intricate compared to static analysis, due to the effects of Dynamic earthquake induced Stresses including the effects on the strength and stress—strain behaviour of the base materials. Various techniques for the analysis of inertial instability of slopes during earthquake are espoused. These methodologies primarily differ in accurateness of earthquake motion and corresponding dynamic response of the slope considered. The main existing methods for evaluating soil structure performance subjected to seismic load are divided in three broad categories depending on the primary method adopted in each technique, including:

1. pseudo static or Force-based methods;
2. sliding block or Displacement-based methods; and
3. Dynamic Analysis or Finite element methods (FEM)

One of the frequent methods for inertial instability analysis is Pseudo-static analysis. Pseudo static analysis estimates the factor of safety for seismic slope collapse analogous to static limit equilibrium analyses. Displacement block analysis use Newman's block analysis considering a sliding block lying on an infinite inclined plane with the action and reaction forces. Dynamic analysis uses the time based input for displacement, velocity, acceleration and hence forces as the earthquake wave varies with time. It requires FEM analysis and is very complicated so it needs to be done on high-speed computers using modern specialized software. The latest practice is pseudo-dynamic analysis which

combines the advantages of pseudo-static method with dynamic method using a horizontal slice technique.

4.1.2 Computer Based Seismic Analysis of TGSB

Computer Based Seismic Analysis of TGSB in this thesis has been carried out in spread sheet based and software based analysis.

The spread sheet based analysis has been further divided into the following categories:

1. Spread Sheet Based Slope Stability Analysis
2. Spread Sheet Based Liquefaction Analysis
3. Spread Sheet Based Tsunami Analysis

The spread sheet based slope stability analysis has been further divided into the following categories:

1. Static Slope Stability Analysis
2. Dynamic Slope Stability Analysis
3. Pseudo Static Slope Stability Analysis
4. Spectral Pseudo Dynamic Analysis
5. Simplified Pseudo Dynamic Analysis

The spread sheet based liquefaction analysis has been further divided into the following categories:

1. Liquefaction potential analysis
2. Liquefaction settlement analysis

The spread sheet based tsunami analysis has been further divided into the following categories:

1. Hydraulic Jump Analysis
2. Experimental Verification Of Analysis

The software based analysis has been further divided into the following categories:

1. Limit equilibrium based - GeoStudio-2019 - Analysis
2. FEM based- Midas GTS-NX- Analysis

The different analysis approaches and the procedures followed in this thesis are outlined hereunder. Their results and subsequent discussions are listed in the next chapter.

4.2 Spreadsheet Based Computerized Seismic Slope Stability Analysis

Many Geotechnical Engineering Software Suites are available; however, the use of computer programs for geotechnical engineering practice should be done judiciously since every software is designed with different operation algorithms. It frequently gets ill used by mostly young and even sometimes experienced engineers, who then cannot ascertain and isolate reasonable results. Their GUI can be daunting and varies from software to software necessitating the need to stick to limited amount of software. Rather than using readymade software, writing your own program on a spreadsheet can be just as effective. They are very useful in minimizing costs and maximizing accuracy because you can input a desired set of identified and specific parameters and easily compare the results on the same screen. Semi-Manual Calculations have been performed for geotechnical evaluations using Microsoft Excel software which is part of Window Office Suite by many researchers in civil engineering and it has vast application in geotechnical engineering (Christy 2000), (Lipjac 2013), (Srbulov 1999). Recent developments in operating systems and computer technology have allowed the development of spreadsheet based programs that greatly simplify the process of data input presentation and computation. We can harness the powerful formulas in Spreadsheets to do complex calculations and the accuracy of the results is dependent on the input. The results can be presented in varied formats. The requisite data and formulas are inputted in cells and the result is automatically generated.

4.2.1 Spreadsheet Based Computerized Static and Dynamic Slope Stability Analysis

TGSB are embankments that are also used to retain water. These can be designed similar to earthen dams however certain additional forces need to be considered due to the coconut trees on the top. There are many static and dynamic forces acting on TGSB embankment structure (Clough and Penzien 1993), (Getachew 2018), (Kramer 1996), (Meheroff and Adams 1968), (Morgenstern and Price 1965), (Pelecanos 2013), (Taylor 1948).

The factor of safety varies with the type of load and the height of the TGSB. The static forces are: self-weight of the bund, weight of trees, hydrostatic pressure and uplift pressure (Figure 4.2).

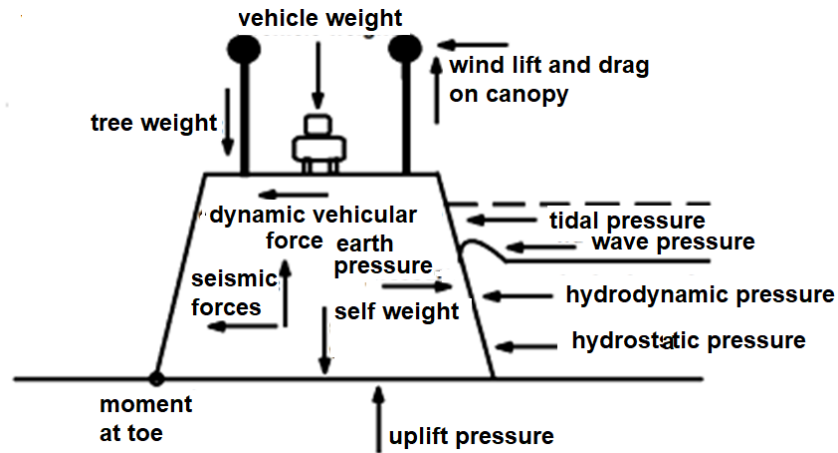


Figure. 4.2 Schematic diagram showing forces acting on a TGSB

The dynamic forces are: tidal pressure, wave pressure, wind pressure, vehicular pressure, seismic pressure and hydrodynamic pressure. In dynamic design we need to consider all the types of forces acting simultaneously in the worst case scenario. The change in factor of safety by soil stabilization is taken care of in the soil properties. The increase in safety due to the rubble facing has been ignored in this calculation for the purpose of simplification. The formulas used in the spreadsheet are discussed below while the results are discussed in the next chapter.

4.2.1.1 Wave pressure

Wave forces affect the top of embankments on water-side. Dynamic force due to waves is generally obtained from the well-known Goda's equation (Goda 1985), (Wiebe et al 2014). There are three intensities of wave pressures acting at three different points in linear variation as per Goda's diagram (Fig 4.3 a).

$$p_{w1} = \frac{1}{2}(1 + \cos\beta)(\alpha_1 + \alpha_2 \cos^2\beta)\rho g H_{wmax} \quad (4.1)$$

$$p_{w2} = \frac{p_{w1}}{\cosh\left(\frac{2\pi h}{L}\right)} \quad (4.2)$$

$$p_{w3} = \alpha_3 p_1 \quad (4.3)$$

Where: - angle between wave pitch and line normal to wall $\beta = 20^\circ$, $\rho g = 9.8 \text{ KN/m}^3$, max wave height $H_{wmax} = (h+1)$, h is height of TGSB, average highest wavelength $L=4\text{m}$, and

$$\alpha_1 = 0.6 + 0.5 \left[\frac{\left(\frac{4\pi h}{L}\right)}{\left(\sinh\left(\frac{4\pi h}{L}\right)\right)} \right] \quad (4.4)$$

$$\alpha_3 = 0.3 \frac{h}{d} \quad (4.5)$$

The coefficient α_2 depends on the properties of the surface on which the wave breaks (table 4.2).

We get $\alpha_2=0.001$.

Table 4.2 Values for wave coefficient α_2

Interface-wall	Rough/rubble	Smooth/steel
α_2	0.001	0

Wave coefficients are taken from available previous 100 year records at Metrological Department of India (Aboobacker 2010), (IMD 2021), (Wilson et al 2015).

Wave depths were compiled from IMD data (Fig. 4.3 b, c).

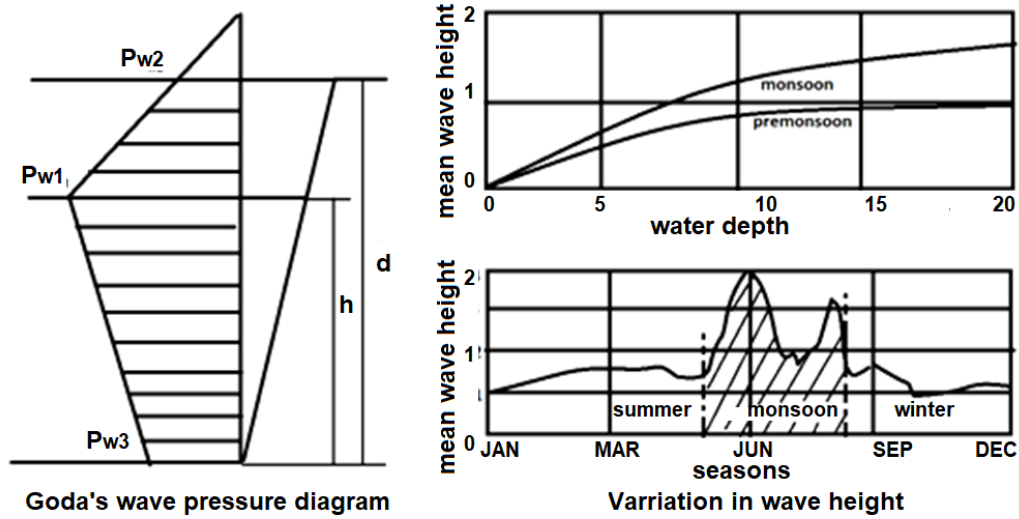


Figure. 4.3 (a) Wave pressure on TGSB (b) Mean wave heights on riverside TGSB (c) Mean wave heights on seaside TGSB

$$P_w = [(p_{w1} + p_{w2}) (d-h) + (p_{w2} + p_{w3}) (h)] / 2 \tag{4.6}$$

$$M_w = (p_{w1} - p_{w2}) ((d-h)^2 / 3) + p_{w2} (d-h)^2 / 2 + (p_{w2} - p_{w3}) (h^2 / 3) + p_{w3} h^2 / 2 \tag{4.7}$$

4.2.1.2 Excess Tidal pore-pressure

Tides fluctuate quarter-daily, lunar-monthly and seasonally. Tides cause drawdown pressure on the water side after the tide passes out. This has to be taken into account. The 100 year average for tidal fluctuation in riverside bunds is taken into account as same as occurring in rest of Goa (Mehra et al 2009), (Mörner 2016), (Subeesh et al 2013), (Sundar and Shetye 2005). Pore pressure depends on various factors including permeability of soil and weight of surcharge and position of the point in the embankment etc. Pore pressure varies from 0.2 to 0.4 for fine to medium sand. Pore water pressure is

$$U = r_u \gamma_w H_T \tag{4.8a}$$

Where U is pore water pressure, r_u is pore water pressure ratio, H_T is tidal fluctuation height. Assume pore water pressure ratio $r_u = 0.25$

$$P_{UT} = U H_T / 2 = 0.25 \gamma_w H_T^2 / 2 \tag{4.8b}$$

Moment due to tidal excess pore pressure

$$M_{UT} = P_{UT}(H_t/3 + h) \quad (4.9)$$

4.2.1.3 Uplift pressure

The water causes uplift by buoyancy under the embankment. Buoyancy varies from 0 at toe to max at heel.

Uplift pressure due to the buoyancy of water acts upwards (Figure 4.4).

$$P_{UB} = \frac{\gamma_w h b}{2} \quad (4.10)$$

Uplift Moment

$$M_{UB} = P_{UB}(2 b/3) \quad (4.11)$$

Moments are evaluated from TGSB toe opposite to water.

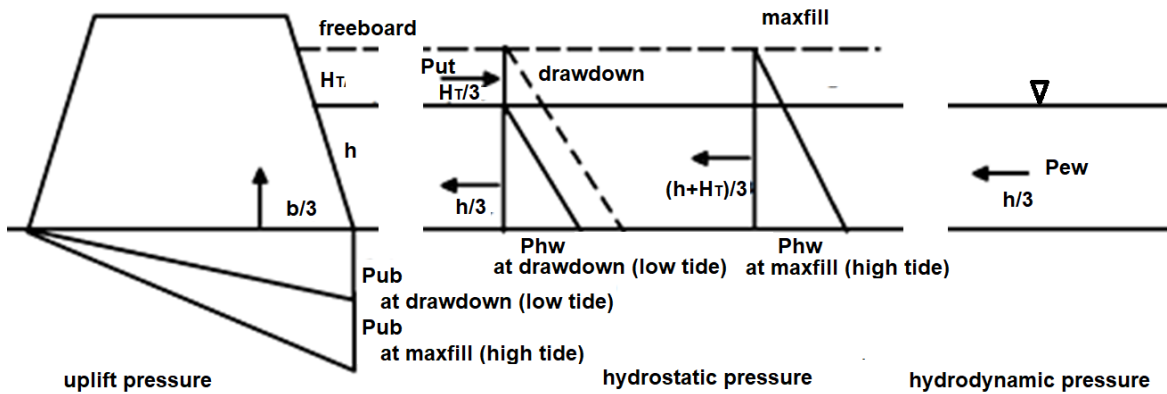


Figure 4.4 Pressures due to water on TGSB

4.2.1.4 Hydrostatic pressure

This is the pressure due to the body of water retained on one side. It is maximum at high tide level. The pressure at the FHL is considered.

$$P_{hw} = \frac{\gamma_w h^2}{2} \quad (4.12)$$

Hydrostatic Moment

$$M_{hw} = P_{hw}(h/3) \quad (4.13)$$

4.2.1.5 Hydrodynamic pressure

Earthquake creates hydrodynamic forces in the water that act on the embankment. Pressure due to the body of water during an earthquake is calculated using Westergaard's wet block formula (Fellenius 2006), (Fellenius 1936), (Westergaard 1938). A modified coefficient of horizontal earth pressure is taken for finding the dynamic force of body of water on the embankment.

Hydrodynamic Force

$$P_{ew} = \frac{7kh\gamma_{sat}h^2}{12} \quad (4.14)$$

Hydrodynamic Moment

$$M_{ew} = P_{ew}(h/3) \quad (4.15)$$

4.2.1.6 Wind pressure

Due to the canopy of the coconut trees there is wind pressure acting on the TGSB. Wind force gets divided into two components Lift (vertical) and Drag (horizontal). Drag and lift act on spherical canopy while drag acts on the long cylindrical stem. These affect the stability of the TGSB. Wind strength varies daily and seasonally (IMD 2021). The maximum wind strengths are seen during monsoon season.

Horizontal Wind Drag force

$$F_{whi} = n_t(0.5C_{d1}\gamma_a V_{wi}^2 A_{tc} + 0.5C_{d2}\gamma_a V_{wi}^2 A_{ts}) \quad (4.16)$$

Vertical Wind Lift force per tree

$$F_{wvi1} = C_L(0.5C_{d1}\gamma_a V_{wi}^2 A_{tc}) \quad (4.17a)$$

Total Vertical Wind Lift force

$$F_{wvi} = n_t F_{wvi1} \quad (4.17b)$$

Mean velocity of wind $V_{wi}=4.4$ m/s,

Density of air $= \gamma_a= 11.84$ N/m³,

Height of tree (H_t) =10 m, number of lifts = n,

Number of trees = $n_t=2.n$.

Height of tree $H_t=10$ m

Exposed area of canopy=15.7

Exposed area of stem=3

Total bench width $b_b= 1\text{m}$

Canopy has lower drag and lift due to aerodynamic shape given by wind coefficients (Table 4.3),

Table 4.3 Value of Wind lift and drag Coefficients for Coconut Tree (adapted from Wikipedia)

Wind Coefficient		Coconut Tree Top	Coconut Tree stem
Drag	C_d	0.4	0.82
Lift	C_L	0.036	

Moment at base of TGSB at opposite to water end due to vertical force

$$M_{wiT} = \sum[F_{wvi1} * (1.5 + b_b)] + \sum[F_{wvi1} * ((b - 3 - b_b))] \quad (4.18)$$

Moment at base of tree due to horizontal force

$$M_{wbT} = F_{whi}H_t \quad (4.19)$$

4.2.1.7 Earth pressure

The soil density influences the static earth pressure. The pressure in this case has been calculated by using Rankine formula (Rankine 1857) for active earth pressure. Static Earth pressure depending on water level is given by

$$P_{a1} = K_a \frac{1}{2} \gamma_{sat} (d - h)^2 \quad (4.20a)$$

$$P_{a2} = K_a \frac{1}{2} \gamma h^2 \quad (4.20b)$$

$$K_a = \frac{1 - \sin\phi}{1 + \sin\phi} \quad (4.21)$$

$$P_a = P_{a1} + P_{a2} \quad (4.22)$$

$$M_a = P_{a1}(h + 0.5) + P_{a1}(h/2) + P_{a2}(h/3) \quad (4.23)$$

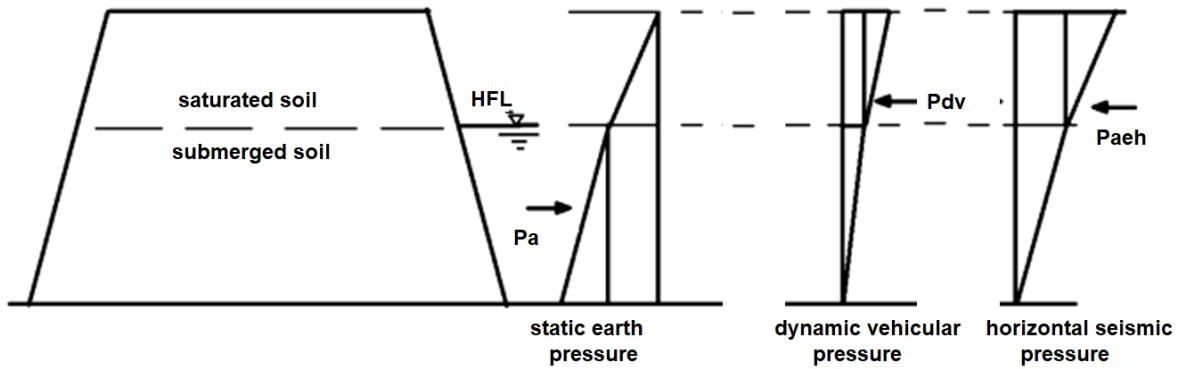


Figure. 4.5 Static and Dynamic Pressure on TGSB

4.2.1.8 Dynamic Vehicular load.

Weight of the vehicle is additional point load on the top centre. The vehicles also cause a dynamic load maximum at the top and zero at the bottom of the embankment.

Extra pressure due to Vehicular force

$$P_{dv} = \frac{1}{2} k_{dv} d^2 \gamma \quad (4.24)$$

Extra moment due to Vehicular force

$$M_{dv} = 2P_{dv} d/3 \quad (4.25)$$

Due to low vehicular traffic (max 5 ton) on bunds assume $k_{dv} = 0.001$.

4.2.1.9 Seismic force

Earthquakes cause horizontal and vertical forces in the embankments.

Seismic force are calculated using Mononobe-Okabe technique (Mononobe and Matsuo 1929, Okabe 1926)

Seismic Horizontal Force

$$P_{aeh} = \frac{1}{2} k_{ae} d^2 \gamma (1 - k_v) \quad (4.26)$$

$$k_{ae} = \frac{\cos^2(\phi - \psi - \theta)}{\cos \psi \cos^2 \theta \cos(\psi + \theta + \delta) \left[1 + \left(\frac{\sin(\theta + \delta) \sin(\phi - \psi - \theta)}{\cos(\phi - \theta) \cos(\psi + \theta + \delta)} \right)^2 \right]^{\frac{1}{2}}} \quad (4.27)$$

$$\psi = \tan^{-1} \left(\frac{k_h}{1 - k_v} \right) \quad (4.28)$$

Seismic Vertical Force

$$P_{aev} = \frac{1}{2}d^2\gamma k_v \quad (4.29)$$

Seismic coefficient $k_h = 2k_v$,

Slope angle $\theta = 0$,

Backfill angle $i = 0$,

$\delta = 2\phi/3$

Seismic Moment

$$M_{ae} = P_{aeh}(2d/3) + P_{aev}(2.5 + 0.2d) \quad (4.30)$$

Force is max at top and 0 at bottom. It acts at $2d/3$ from bottom. (Figure 4)

4.2.1.10 Tree load

Each coconut tree provides a point load (assume $P_{TR} = 10\text{kN}$) at the top of the bund. The moment at toe because of trees is given by

$$M_T = \sum[P_{TR}(1.5 + b_b)] + \sum[P_{TR}((b - 3 - b_b))] \quad (4.31)$$

4.2.1.11 Self-weight

This is due to the weight of the bund itself. The rubble fascia of the TGSB has been ignored and the whole weight is taken as earth itself.

Self-weight

$$P_{sw} = (5 + 0.2d)\gamma_{sat}d \quad (4.32)$$

Self-weight Moment

$$M_{sw} = P_{sw}(b/2) \quad (4.33)$$

4.2.1.12 Root Mat Reinforcement

The embankment safety because of Coconut tree roots is calculated for soil anchor action. Soil is reinforced by the roots as each root acts as a soil anchor.

Root anchorage

$$T_{pa} = (\pi d)l_r\alpha c_u \quad (4.34)$$

l_r is root length, d is root diameter, α is adhesion factor=0.25, c_u is undrained cohesion =250 kPa,

s_h is horizontal spacing of root = s_v is vertical spacing of root = 0.01m

Equivalent Root anchorage

$$T_{eq} = \frac{\sum T_{pa}}{s_h} \quad (4.35)$$

Safe Maximum Tension in longest root

$$T_{max} = \frac{A_r f_{yr}}{FoS_t} = \left(\frac{1-\sin\phi}{1+\sin\phi} \right) (q_u + \gamma z) s_h s_v \quad (4.36)$$

Experimentally maximum tension in root is 0.4,

Assume Factor of safety in tension per root = $FoS_t = 1.8$,

A_r is area of root = $2 \times 10^{-5} \text{ m}^2$,

f_{yr} is tensile strength of root = 2000 kN/m^2

Find q_u from above equation = 65.5

Factor of safety sliding

$$\alpha_r = \frac{q_u L + [(W + T_{eq}) \cos \phi] \tan \phi}{(W + T_{eq}) \sin \phi} \quad (4.37)$$

Table 4.4 Factor of Safety for Soil-Nail Action of Coconut Roots

H	3	6	9	12
$\alpha_r = FoS$	2.72	1.77	1.42	1.21

Root mat increases the shear sliding resisting force. It is suitably incorporated in the total FoS. No change in resisting moment has been considered in the present study. Resisting moment will be the integral of total moment in all roots at interface of TGSB and subsoil.

4.2.1.13 Root suction pressure

The trees take in water from soil by suction through roots. Roots of trees give matric suction (vacuum pressure-negative pressure) that increases the shear properties of soil (Indraratna et al 2006, Fatani et al 2008, Estabragh and Javedi 2012).

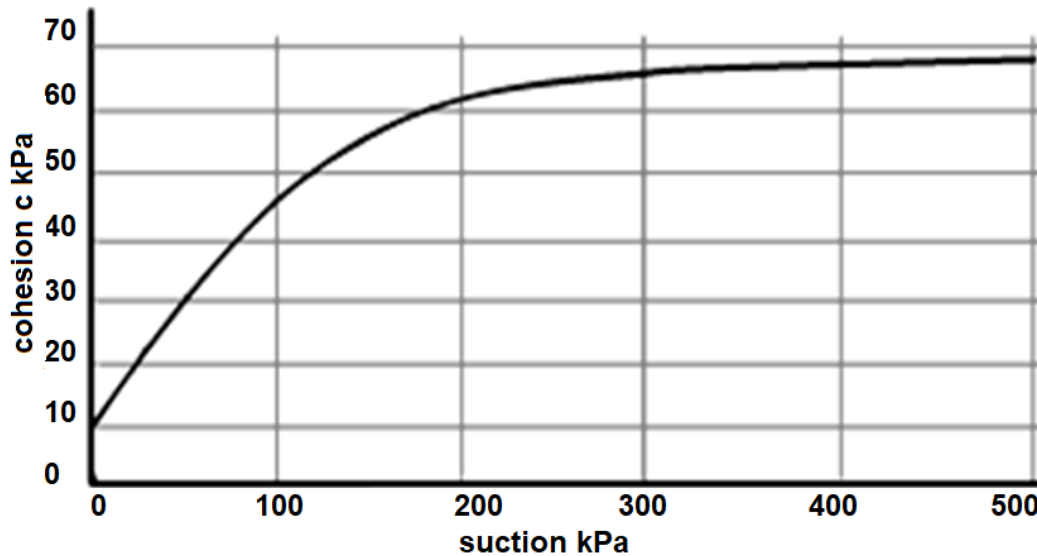


Figure. 4.6 Increase in cohesion with suction (after Estabragh and Javedi 2012)

Table 4.5 Matric root suction for coconut tree roots at varying depth from top

Depth	suction pressure kPa	increase in cohesion at depth kPa	average increase		shear strength $\tau = c + \sigma_v \tan \phi$		
			increase	total	no roots	with roots	increase α_m
0	441	65	increase	total	no roots	with roots	increase α_m
3	357	62	42.33	62.33	23.117	65.447	2.83
6	170	60	20.83	40.83	26.235	47.065	1.79
9	25	12	8.55	28.55	29.352	37.902	1.29
12	1	10	6.25	26.25	32.470	38.720	1.19

The coconut trees need enough suction to pull water up a 10m stem. Matric suction pressure was found out at different depths of soil for different depth bunds.

Without roots cohesion of TGSB soil was, $c = 20\text{kN/m}^2$

$$\text{shear strength, } \tau = c + \sigma_v \tan \phi \quad (4.38)$$

Matric root suction increases soil shear strength, especially the shear cohesion parameter of soil. No change in resisting moment. Increase in cohesion due to matric root suction was then found out from graph (Figure 4.6). The corresponding change in shear gives the change in the total factor of safety α_m .

4.2.1.14 Calculation of Factor of safety

Different combinations of forces are acting for different conditions. Their combination is needed to evaluate the factor of safety. In static condition there is no effect of wave, wind, earthquake and vehicles considered. There are two sub conditions considered: when the TGSB is used to retain water and when it is not used to retain water. In dynamic condition the effect of wave, wind, earthquake and vehicles are simultaneously considered. Two other dynamic conditions considered are when earthquake only acts and when wind forces only act with no water retained. Static earth pressure acts as disrupting force when no water is retained and as stabilizing force (P_s) when water is retained. The different combination of forces taken for the various safety has been given in table 4.6.

Table 4.6 Combination of loads and moments for overall factor of safety

Condition	Force	Load Combination
Static- No Water Retained	Sliding Resistance	Tree-Weight Force + Self-Weight Force
	Sliding Force	Earth Pressure Force
	Overturning Resistance	Self-Weight Moment + Tree Weight Moment
	Overturning Moment	Earth Pressure Moment
Static- Water Retained	Sliding Resistance	Tree-Weight Force + Self Weight Force – Uplift Force + Earth Pressure Force
	Sliding Force	Hydrostatic Force – Tidal Pore Pressure
	Overturning Resistance	Tree Weight Moment + Self Weight Moment + Earth Pressure Moment

	Overturning Moment	Uplift Moment + Hydrostatic Moment – Tidal Pore Moment
Dynamic-Full	Sliding Resistance	Self-Weight Force + Tree-Weight Force + Earth Pressure Force – Seismic Vertical Force – Uplift Force – Wind Pressure Vertical Force + Vehicular Weight
	Sliding Force	Wave Pressure Force – Tidal Pore Pressure + Vehicular Pressure Force+ Hydrostatic Force +Seismic Horizontal Force + Hydrodynamic Force
	Overturning Resistance	Tree Weight Moment + Self Weight Moment + Earth Pressure Moment
	Overturning Moment	Wave Pressure Moment – Tidal Pore Moment + Wind Pressure Moment + Vehicular Pressure Moment + Seismic Moment + Uplift Moment + Hydrostatic Moment + Hydrodynamic Moment + Wind Tree Base Moment
Dynamic-earthquake	Sliding Resistance	Self-Weight Force + Tree-Weight Force– Seismic Vertical Force
	Sliding Force	Earth Pressure Force + Seismic Horizontal Force
	Overturning Resistance	Tree Weight Moment + Self Weight Moment
	Overturning Moment	Earth Pressure Moment + Seismic Moment
Dynamic-wind / cyclone	Sliding Resistance	Self-Weight Force + Tree-Weight Force– Wind Pressure Vertical Force
	Sliding Force	Wind Horizontal Force +Earth Pressure Force
	Overturning Resistance	Tree Weight Moment + Self Weight Moment
	Overturning Moment	Earth Pressure Moment + Wind Tree Base Moment

4.2.1.15 Static factor of safety

Factor of safety against sliding is ratio of static resisting force to static sliding force

$$force_{resistance} = Ps + \sum W \tan\phi \quad (4.39)$$

$$FOS_{SS} = \frac{(\alpha_r)(\alpha_m)\sum force_{resistance}}{\sum force_{sliding}} \quad (4.40a)$$

Factor of safety against overturning is ratio of static resisting moment to static overturning moment

$$FOS_{SO} = \frac{\sum moment_{resistance}}{\sum moment_{overturning}} \quad (4.40b)$$

4.2.1.16 Dynamic factor of safety

Factor of safety against sliding is ratio of dynamic resisting force to dynamic sliding force

$$FOS_{DS} = \frac{(\alpha_r)(\alpha_m)\sum force_{resistance}}{\sum force_{sliding}} \quad (4.41a)$$

Factor of safety against overturning is ratio of dynamic resisting moment to dynamic overturning moment

$$FOS_{DO} = \frac{\sum moment_{resistance}}{\sum moment_{overturning}} \quad (4.41b)$$

4.2.1.17 Static and Dynamic General slope failure

The soil is divided into slices. The centre of rotation is found out using Swedish -Fellenius (1936) method.

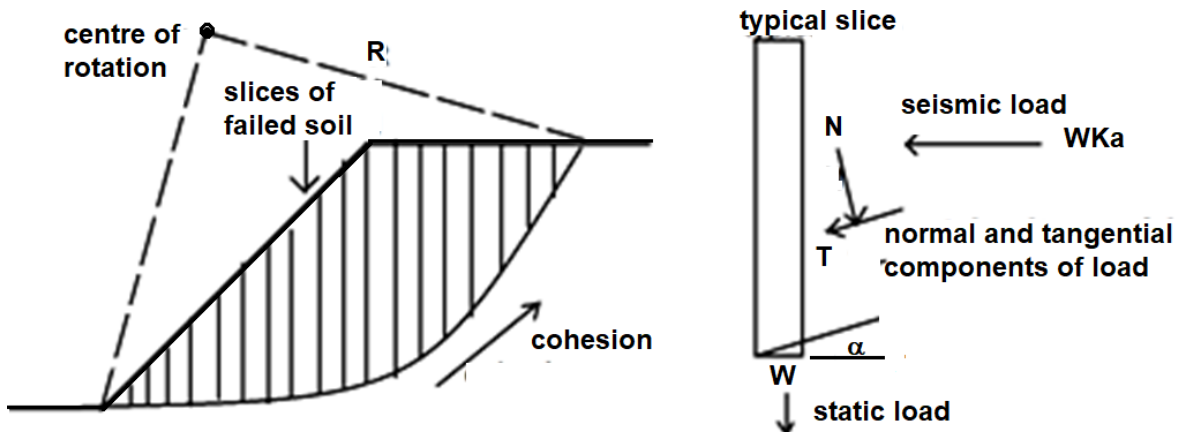


Figure 4.7 Method of slices (after Bishop 1955)

Factor of safety for static general slope failure is found using Bishop's method of slices

$$FOS_{SG} = \frac{cL + \sum N \tan \phi}{\sum T} \quad (4.42)$$

Factor of safety for dynamic general slope failure is found using Bishop's method of slices by considering earthquake acceleration

$$FOS_{DG} = \frac{cL + \sum(N-U) \tan \phi - \sum(Wk_h) \sin \alpha \tan \phi}{\sum T + \sum(Wk_h) \cos \alpha} \quad (4.43)$$

4.2.2 Spreadsheet Based Pseudo Static Safety of TGSB

From the 1920's seismic slope stability analyses used a pseudo-static approach considering slope-stability as simple factor of safety. The consequences of the earthquake are taken care of using a constant horizontal acceleration that producing an inertial force (F) that acts at the centre of portending failure mass in this approach. The horizontal acceleration normalized by gravity is referred to as the seismic yield coefficient (k_y) and is dependent on the soil properties and the slip surface geometry. The seismic yield coefficient is minimum acceleration giving a factor of safety of one, at incipient failure. This is very common and simple method straightforward to practice. The seismic stability of geotechnical structures are analyzed by pseudo static approach where the actions of earthquake are represented by constant accelerations: horizontal and/or vertical. A limiting equilibrium analysis using conventional methods may be performed for seismic loads with inertial forces assumed relative to the load of the impending sliding mass times a horizontal and vertical seismic coefficient given in terms of the gravitational acceleration of the base strata. Each coefficient is assumed as an average value within the sliding mass as the actual coefficient is a function of position and time. A factor of safety analysis may be performed for the sliding mass using a variable horizontal seismic coefficient to identify the critical FoS equal to one. The first clear application of the pseudo-static method for seismic slope stability analysis is developed by Terzaghi (1950) (Terzaghi et al 1950) (Figure. 4.8).

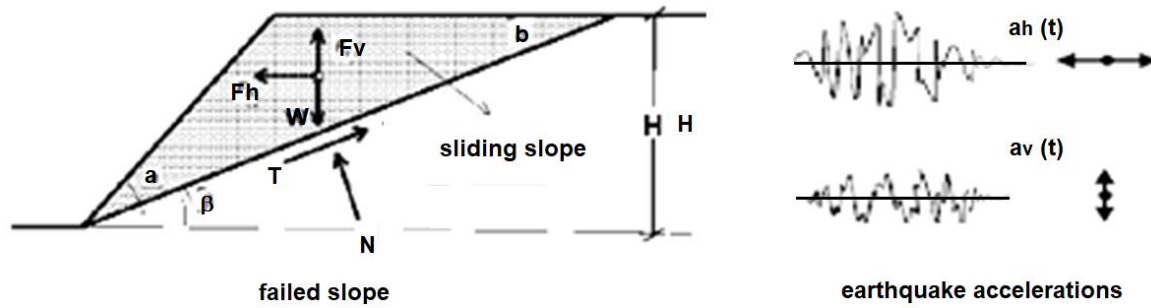


Figure 4.8 Pseudo-static forces on a soil wedge (after Terzaghi1950).

In their most basic form, pseudo-static analyses calculates the earthquake shaking effects using pseudo-static accelerations to generate horizontal and vertical inertia forces, F_h , and F_v passing through the centre of the failed mass.

The pseudo-static forces are:

$$F_h = a_h W / g = k_h W \quad (4.44)$$

$$F_v = a_v W / g = k_v W \quad (4.45)$$

The pseudostatic coefficients are:

$$k_h = a_h / g \quad (4.46)$$

$$k_v = a_v / g \quad (4.47)$$

where: g is gravitational acceleration, W is failure mass weight, F_h is horizontal pseudo-static Force, a_h is horizontal pseudo-static acceleration, k_h is dimensionless horizontal pseudo-static coefficient, F_v is vertical pseudo-static Force, a_v is vertical pseudo-static acceleration, k_v is dimensionless vertical pseudo-static coefficient. The value of the pseudo-static accelerations must be correlated to the severity of the predictable ground motion.

Resolving forces acting on the impending failure mass parallel to the failure surface we get,

$$FOS = \frac{\text{ResistingForce}}{\text{DrivingForce}} \quad (4.48)$$

$$FOS = \frac{(c l_{ab} + [(W - F_v) \cos \beta - F_h \sin \beta] \tan \phi)}{(W - F_v) \sin \beta - F_h \sin \beta} \quad (4.49)$$

Where c and ϕ are Mohr-Coulomb shear strength parameters and l_{ab} is the length of the failure plane. The horizontal pseudo-static force obviously reduces the factor of safety, as it decreases the resistance force while increasing the exciting force. The vertical pseudo-static force normally is less influential on safety since can both reduce or increase: the

resisting and exciting force; depending on its direction, hence vertical accelerations are usually ignored. This method can be utilized to estimate pseudo-static factors of safety for all surfaces. Most commercial geotechnical software for limit equilibrium slope stability analysis can perform pseudo-static analyses.

4.2.2.1 Selection of Pseudo-static Coefficient

The pseudo-static analyses are significantly reliant on the value of horizontal pseudo-static seismic coefficient k_h .

Table 4.7 Comparative Pseudo-Static Coefficients (Melo and Sharma 2004).

Investigator	Recommended Pseudo static coefficients K_h	
Terzaghi 1950	0.1	Severe quake
	0.2	Violent destructive quake
	0.5	Catastrophic quake
Seed 1979	0.1	M6.5 Severe quake
	0.15	M8.25 Catastrophic quake
Marcuson 1981	0.33 PGA/g	Soil
	0.50 PGA/g	Rock
Haynes-Griffith and Franklin 1984	0.50 PGA/g	All
California Division of Mines and Geology 1997	0.15	All
this study	0.11	- Lateritic Alluvial Soil underlain by basalt/granite - for severe quake - extremely unlikely event

Choosing appropriate dimensionless pseudo-static coefficient is the toughest feature of pseudo-static stability analysis. Seismic coefficient gives the pseudo-static force of the failure mass; hence it should be related to the amplitude of inertia force induced in the

unstable mass. Soil slopes are never rigid and the peak acceleration do not exist for big periods so the practically used pseudo-static coefficients usually give to acceleration values well below a_{\max} (Melo and Sharma 2004). The table above gives the pseudo-static coefficients suggested in general by different researchers (Table 4.2). They are to be adopted in case of insufficient data.

4.2.2.2 Pseudo-static (Seismic) Analysis of TGSB as Per IS: 7894 (1975)

The seismic stability analysis of earthen dams from IS 7894 (1975) uses a pseudo-static approach which can be applied to TGSBs as they sometimes also retain water. The critical condition in upstream slope analysis at operating condition is the sudden drawdown combined with earthquake forces. The second is when the reservoir is full. The analysis can be performed by two methods: circular arc method and sliding wedge method. As per IS 7894 (1975), the analysis for earthquake condition by circular arc method, the factor of safety (FoS) for earthquakes can be calculated from the following formula:

$$FoS = \frac{\sum[C+(N-U)\tan\phi]-\sum[W_1\sin\alpha\cos\alpha A_H]}{\sum W\sin\alpha+\sum W_1\cos\alpha A_H} \quad (4.50)$$

Where: C is cohesive resistance of slice, N is force acting normal to slice, U is pore water pressure force, (N-U) is effective normal force on slice failure surface, A_H is horizontal seismic coefficient, W_1 is saturated/moist weight of slice, W is slice weight that is the driving force, ϕ is angle of internal friction, α is angle between slice centre and failure surface radius.

4.2.3 Seismic spectral acceleration and force Based Pseudo-Dynamic-Analysis

Whenever we design a structure in a potential seismic zone we need to know the maximum seismic force that will act on the structure. Various researchers have given various methods of doing so but the use of Spectral acceleration to compute force called spectral force is popular. IS Codes give typical response spectra that help in calculating such spectral force for TGSBs. Spectral displacement, spectral velocity and spectral acceleration are governed by a relationship

$$S_d = \frac{TS_v}{2\pi} = \frac{TS_a^2}{4\pi^2} \quad (4.51)$$

A plot of u_{\max} (max displacement) for certain damping ζ is plotted and the deformation spectrum is drawn from it. From this then the velocity and acceleration spectra are plotted. Response spectrum technique gives a method for calculating equivalent static lateral load analysis (Jain 2013). It is a simple method for calculating design forces for earthquakes. Whenever we design a structure in a potential seismic zone, we need to know the maximum seismic force that will act on the structure (Elia and Rouainia2013), (Iai 2001). For seismic design, not the stress time history but maximum stresses are of important. The equivalence is constrained to single vibration mode. Spectral force hence can be denoted in terms of acceleration due to gravity.

Spectral force

$$F_{sa} = P_a/g \quad (4.52)$$

We can then plot the spectral force for different damping ratios.

Knowing the natural period and damping of the soil the spectral force (F_{sa}) is read from the plots given below, then the horizontal force (F_h) acting on the bund can then be calculated (Table 4.7, 4.8, 4.9 and figure 4.6, 4.7, 4.8) using the seismic acceleration ($k_h = a_{\max}/g$).

$$F_h = F_{sa} \cdot k_h \cdot g \quad (4.53)$$

4.2.3.2 The Simplified Spectral Force Based Pseudo-Dynamic-Analysis

Spectral force gives a simple method to do simplified pseudo dynamic analysis as has been done by many researchers in the past (Løkke and Chopra 2013), (Bretas et al 2014, 2015), (Ghobrial and Karray 2015). It is simple and direct and can be used for fast initial evaluation using spectral damping curves (Annexure XII). From the typical spectrum given in IS codes the local spectral acceleration was found out. This can be used in Microsoft excel type spreadsheets for Pseudo dynamic analysis.

Fundamental Period $T_s = 4H/V_s$

Dynamic force $= F_h = F_{sa} \cdot k_h \cdot g$

Static force $= K_a \gamma_s H^2/2$

Resisting force $= W \tan \phi$

$$FoS = \frac{\text{resisting force}}{\text{sliding force}} \quad (4.54)$$

4.2.4 Development of site specific seismographs for seismic analysis

Shear velocity V_s gives the variation in waves travelling through the soil. First 30 m of soil are vital for the structure above it (Boore and Atkinson 2008, 2006), (Boore and Joyner 1997), (Cho et al 2012). We can use this for plotting seismograph using complex equations and ‘Greens theorem’. Appropriate to the uncertainties of the simulations, the design seismograph and spectra are then shown (Kanamori et al 1993a,b). The Alternative is that we can try a simple method that uses the same data of Shear wave velocity and simple excel spread sheets. This gives a Site Specific Seismograph (SSS) and hence is more appropriate for predictions based on possible future earthquakes. Site Specific Response (Raghunandan and Juneja 2009) is important and can be got from these. And the acceleration multiplication factor is found out by averaging the two intercepts of the spectral curve on the two boundary lines of the velocity/time set (Figure 4.9).

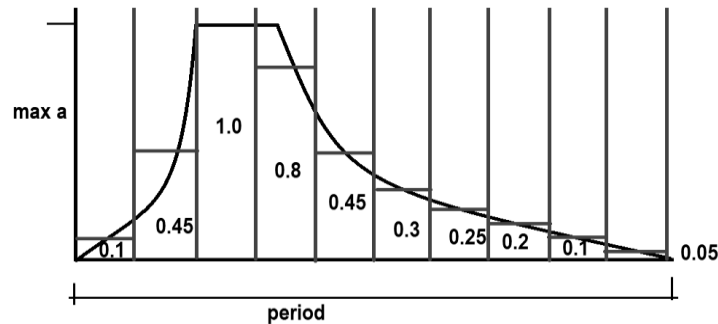


Figure 4.9 Division of Spectral Acceleration in 10 parts considering the max as 1

Shear waves have a close relation to seismographs as has been shown by countless researchers in the past. The plot of sonic velocity in soil closely resembles the seismic waves and this property has been used to simulate the waves in modern software. Their relationship is simple and straight forward,

$$s_{\theta} = R_{\theta} w_{\theta} \quad (4.55)$$

Where: s_{θ} is the seismic function, R_{θ} is the reflectivity operator, w_{θ} is the sonic wavelet function. The equivalent velocity for the top 30 m is used using the correction for depth.

Velocity in shallow layered soils needs to be corrected for 30 m depth or Vs30 models for time-averaged shear-wave velocity and data (USGS).

$$V_{s30} = \frac{\sum V_{si}}{\sum \left(\frac{d_i}{V_{si}}\right)} \tag{4.56}$$

Where: V_{s30} is the sonic velocity normalized for 30 m deposit in V_{si} is the sonic velocity in the i^{th} layer and d_i is the depth of the i^{th} layer

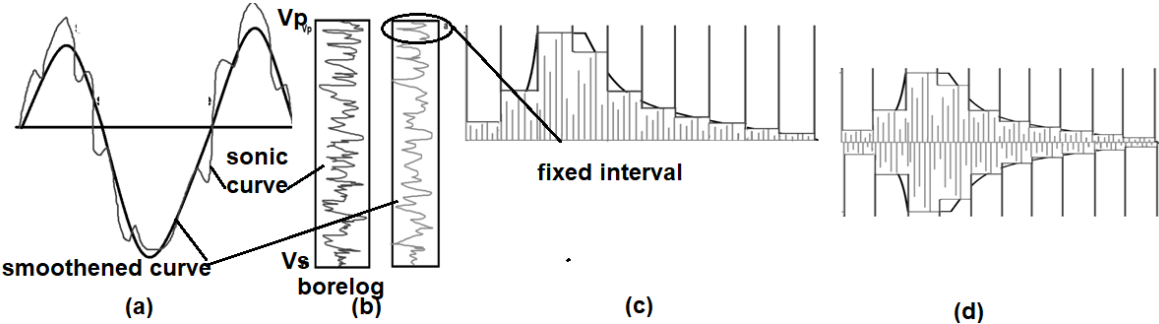


Figure 4.10 Four steps to create an artificial seismograph from sonic velocity and spectrum (a) smoothing of seismic curves (b) sonic and seismograph curves (c) Plot of Factored Shear Velocities for Half and (d) full Seismograph (SSS)

The V_s can be found out from direct Cone Penetration Test or in its absence using Standard Penetration Test and their co-relationship for the given soil to find the shear velocity at each depth. The 30 m V_s is plotted for every 1m which is then plotted to scale in each division of the spectral acceleration. This is then inverted and plotted with 1 interval delay on the other side of the x-axis. The curve joining each point so generated gives a site specific seismograph reflecting the actual strata below. Six such have been generated for future use in software in Annexure XIII: They are developed for Miramar beach-Panaji, Atal Setu Bridge Panaji, TGSB at Santa-Cruz-Panaji, TGSB at Mapusa, TGSB at Vasco and TGSB at Madgao to get site specific response.

4.2.5 Spreadsheet Based Simplified Pseudo-Dynamic-Analysis

Dynamic analysis is very complex and needs specialized software. The Pseudo-Dynamic approach is a specialized emerging aspect of seismic analysis (Choudhury et al 2006),

(Nimbalkar et al 2006), (Presti et al 2010) which can be done using Matlab and similar software. This is an extremely simplified procedure based on the exceptionally detailed parametric-study-based pseudo-dynamic approach. Dr. Savoikar and Dr. Choudhury have developed such a procedure based on the pioneering works developed by Steedman and Zeng (1990) and followed by different researchers calculates seismic stability of geotechnical structures. Bellezza (2014) overcame existing limitations of the pseudo-dynamic approach by assuming visco-elastic soil behavior while considering seismic waves at the zero-stress on ground surface boundary condition. The Savoikar-Choudhury method which originally for meant for MSW land-fills (Choudhury and Savoikar2009), (Savoikar and Choudhury 2009, 2010a, 2010b, 2012) is extended in this work to TGSB. The present method is also an application and extension of the collaborated work by Dr. Bray with Dr. Macedo and Dr. Travararou (Bray et al 2018)(Bray and Travararou2007, 2009)(Bray and Machedo 2017a, 2017b, 2019) which developed simplified procedures for evaluating the seismic slope stability of natural slopes and geotechnical structure. Their method also incorporates the response spectral values S (S_{pv} , S_{pa} and S_{pd}) for earthquake ground motion considered to be a function of different Influence factors (Clough and Penzien, 1993), (Boore 2003). The details of procedures are described in their respective papers. Dr. Bray further gives a simplified slope displacement procedure not used in this work. The Pseudo-Dynamic Factor of Safety depends upon shear velocity (V_s) Richter magnitude (M), source mechanism, focal depth (h), epicentral distance (D), geological conditions, period (T), soil conditions, and damping ratio (ξ). The inter slice friction is also taken into consideration. The Simplified Pseudo-Dynamic Analysis can be used to describe a failure wedge initiated at the top of the embankment of width B making an angle β_{crit} at the soil level (Figure 4.11). The passive wedge starts at the foot of the failure wedge and the active wedge lies in the top portion.

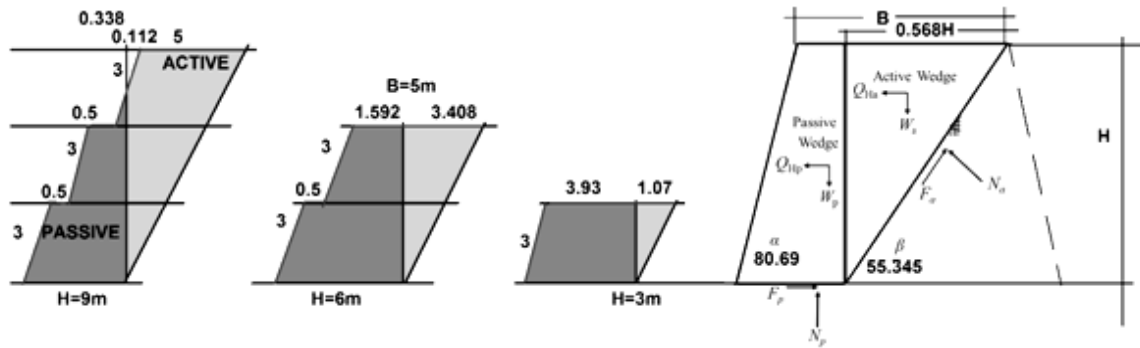


Figure 4.11 Forces acting on active and passive wedge in TGSB for Pseudo-dynamic earthquake analysis

By this analysis as seen in the figure the passive wedge outweighs the active wedge for TGSBs in 3 and 6m heights so it is applicable for heights of greater than 7.25m (Figure 4.12). This can be used in Microsoft excel type spreadsheets for Pseudo dynamic analysis.

From Taylor (1948) Critical wedge angle = $\beta_{crit} = (\alpha + \phi) / 2$

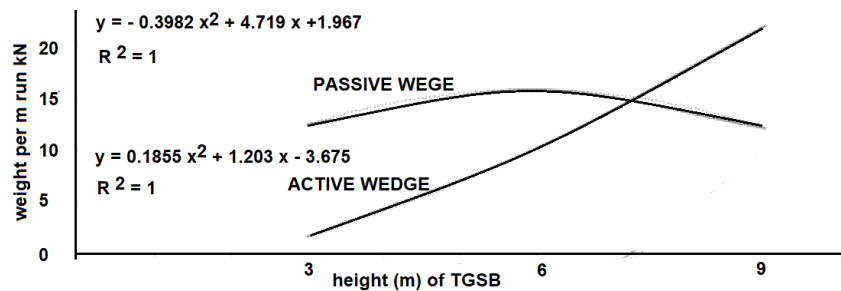


Figure 4.12 Variation of active and passive wedge weights for TGSBs

The active and passive wedge weight of any height TGSB can be obtained from the trend lines with regression coefficient $R^2=1$. The excess line indicates when the active wedge outweighs the passive wedge.

The weight of the active wedge is

$$W_a = \gamma_s (0.1855H^2 + 1.2035H - 3.675) \quad (4.57)$$

The weight of the Passive wedge is

$$W_p = \gamma_s (-0.398H^2 + 4.719H + 1.967) \quad (4.58)$$

For 3 m TGSB the weight of 1 coconut trees (2 kN) is added to the passive wedge and the weight of 1 coconut tree (2 kN) is added to the active wedge. For 6 m TGSB, the weight of 2 coconut trees (4 kN) is added to the passive wedge and the weight of 1 coconut tree (2 kN) is added to the active wedge. For 9 m TGSB the weight of 2 coconut trees (4 kN) is added to the passive wedge and the weight of 2 coconut tree (4kN) is added to the active wedge. The interface between the two wedges also contribute to the stability. While this may not be big for small height embankments its contribution increases with height of TGSB. Interface friction angles $\delta_a = \phi/2$ and $\delta_p = 2\phi/3$

The pseudo-dynamic horizontal and vertical inertia accelerations are

$$a_h(z, t) = a_h \sin \omega \left(t - \frac{H-z}{V_s} \right) \quad (4.59)$$

$$a_v(z, t) = a_v \sin \omega \left(t - \frac{H-z}{V_p} \right) \quad (4.60)$$

Mass of the slice of soil is given by

$$m_z = \frac{\gamma}{g} \left(\frac{H-z}{\tan \alpha} \right) dz \quad (4.61)$$

Where V_p and V_s are the primary and shear wave velocity, ω is circular frequency, a_h and a_v are the horizontal and vertical components of seismic-acceleration and t is the period of the earthquake. By integrating the above we get very large equations for the pseudo-dynamic earthquake induced active and passive forces which can be written in simplified form as

$$Q_{Ha}(t) = \frac{k_h W_a}{\tan \beta} \left[\frac{CI_1 + SI_2}{C^2 + S^2} \cos(\omega t) + \frac{CI_1 - SI_2}{C^2 + S^2} \sin(\omega t) \right] - \frac{k_h W_a}{\tan \alpha} \left[\frac{CI_3 + SI_4}{C^2 + S^2} \cos(\omega t) + \frac{CI_3 - SI_4}{C^2 + S^2} \sin(\omega t) \right] \quad (4.62)$$

$$Q_{Hp}(t) = \frac{k_h W_p}{\tan \alpha} \left[\frac{CI_5 + SI_6}{C^2 + S^2} \cos(\omega t) + \frac{CI_5 - SI_6}{C^2 + S^2} \sin(\omega t) \right] \quad (4.63)$$

Where, $I_1, I_2, I_3, I_4, I_5, I_6, C$ and S are coefficients given below. From simple harmonic damped vibrations where ξ is damping ratio,

$$C = \cos(y_1) \cosh(y_2) \quad (4.64)$$

$$S = \sin(y_1) \sinh(y_2) \quad (4.65)$$

Where

$$y_1 = \frac{\omega H}{V_s} \sqrt{\frac{\sqrt{1+4\xi^2}+1}{2(1+4\xi^2)}} \quad (4.66)$$

$$y_2 = \frac{\omega H}{V_p} \sqrt{\frac{\sqrt{1+4\xi^2}-1}{2(1+4\xi^2)}} \quad (4.67)$$

And the response spectral values are functions expressed in the form of four influence factors $I_1, I_2, I_3, I_4, I_5, I_6$, adapted from Boore2003.

Active pressure influence factors for Source mechanisms

$$I_1 = \left(\frac{H^2}{y_1^2 + y_2^2} \right) (C_s M S_s) \quad (4.68)$$

Active pressure influence factors for Path

$$I_2 = \left(\frac{H^2}{y_1^2 + y_2^2} \right) \left(\frac{R_o}{R} e^{\frac{-\pi f R}{680 f^{0.38}}} \right) \quad (4.69)$$

Active pressure influence factors for Site conditions and geology

$$I_3 = \left(\frac{H^2}{y_1^2 + y_2^2} \right) (A_f D_f) \quad (4.70)$$

Active pressure influence factors for Ground motion

$$I_4 = \left(\frac{H^2}{y_1^2 + y_2^2} \right) (2 \pi / f^2) \quad (4.71)$$

Passive pressure influence factors for Source mechanisms

$$I_5 = \left(\frac{H^2}{y_1^2 + y_2^2} \right) \left(\frac{H^2}{y_1^2 - y_2^2} \right) (C_s M S_s) \quad (4.72)$$

Passive pressure influence factors for Path

$$I_6 = \left(\frac{H^2}{y_1^2 + y_2^2} \right) \left(\frac{H^2}{y_1^2 - y_2^2} \right) \left(\frac{R_o}{R} e^{\frac{-\pi f R}{680 f^{0.38}}} \right) \quad (4.73)$$

Source constant

$$C_s = \frac{0.1125}{\gamma_s V_s^2 R_o} \quad (4.74)$$

Spectral constant

$$S_s = \frac{1}{\sqrt{1 + \left(\frac{f}{f_s} \right)^2}} \quad (4.75)$$

Epicentral distance of earthquake

$$R = \sqrt{D^2 + h_e^2} \quad (4.76)$$

Site amplification

$$A_f = \sqrt{\frac{\gamma_{ss} V_{ss}}{\int_0^z \gamma_{sz} V_{sz}}} \quad (4.77)$$

Site diminution

$$D_f = e^{-0.04\pi f} \quad (4.78)$$

$$f = 4.9V_s \left(\frac{\Delta\sigma}{M_o}\right)^{\frac{1}{3}} \quad (4.79)$$

$$f_s = (0.0173h)^{0.913} \quad (4.80)$$

$$M = \frac{2}{3} \log M_o - 10.7 \quad (4.81)$$

$M = 5.5$, $M_o = 0.178Nm = 0.178 \times 10^7$ dyne-cm, $f_s = 0.5494$, $R = 231.948$, V_s m/s = $V_s/1000$ km/s, R_o is reference distance = 1 km usually, γ_s is soil unit weight (18), $\Delta\sigma$ is stress drop (Figure 4.22) in coulomb stress state due to earthquake ($6kN/m^2$), D is distance of earthquake (230) km and h_e is depth of earthquake (30) km, γ_{ss} is soil unit weight near source (15), γ_{sz} is soil unit weight per layer, V_{ss} is shear velocity near source km/s, V_{sz} is shear velocity per layer. All of these depend on the fundamental frequency (f) of near surface soil deposits. Thus the fundamental frequencies of the site are a valuable tool for developing earthquake disaster mitigation strategies.

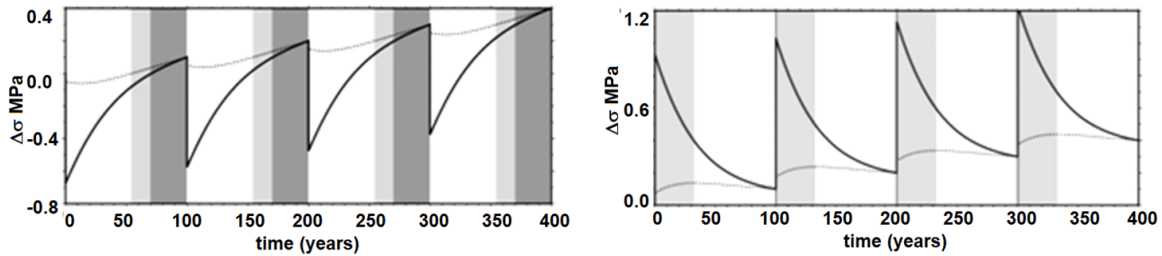


Figure 4.13 ($\Delta\sigma$) Stress Drop for earthquakes in Japan (Mitogawa and Nishimura 2020)

Material damping ratio may be taken for this thesis as

$$\xi = 30(1 - e^{-1.4\gamma_u^{0.36}}) \quad (4.82)$$

where γ_u is the % cyclic strain from Normalized shear modulus

$$\frac{G}{G_{max}} = \frac{1}{1 + 7.85\gamma_u^{0.95}} \quad (4.83)$$

Shear modulus $G_{max} = 8000$ kN/m²

Shear strain

$$G = \frac{\tau}{\gamma} = \frac{\text{shear stress}}{\text{shear strain}} \quad (4.84)$$

Shear stress

$$\tau = k_h \gamma_s z = (0.11) (18) (z) = 1.98 z \quad (4.85)$$

Use Bray-Travasarou seismic coefficient,

$$k_h = \exp\left(\frac{-a+\sqrt{b}}{0.665}\right) \quad (4.86)$$

$$a = 2.83 - 0.566 \ln(S_a) \quad (4.87)$$

$$b = a^2 - 1.33\{\ln(D_a) + 1.1 - 3.04 \ln(S_a) + 0.244[\ln(S_a)]^2 - 1.5T_s - 0.278(M - 7) - \varepsilon\} \quad (4.88)$$

Allowable seismic displacement D_a in centimetres = 5

Use Abrahamson et al (2014)ASK-14model,

Seismic coefficient = S_a =

$$= a_1 + a_5(M - M_1) + a_8(8.5 - M)^2 + [a_1 + a_3(M - M_1)] \ln R + a_{17} R_{rup} \quad (4.89)$$

$$= 0.973 - 0.41(5.5 - 5) - 0.15(8.5 - 5.5)^2 + [0.973 + 0.275(5.5 - 5)] \ln(230) - 0.0089(30)$$

$$= 5.189 = 0.529 g$$

Use Bray-Travasarou fundamental period

$$T_s = 4H/V_s = (4)(3)/(150) = 0.08 \quad (4.90)$$

Use Bray-Travasarou degraded period = $1.5T_s = 1.5 \times 0.08 = 0.12s$

$$\varepsilon = 0, a = 2.793, b = 4.98, k = 0.293$$

For TGSB

$$\alpha = 80.69,$$

$$\phi = 30,$$

$$\beta = \beta_{crit} = 55.345,$$

$$\delta_a = \phi/2 = 15,$$

$$\delta_p = 2\phi/3 = 20,$$

$$\text{Circular frequency} = \omega = 2\pi/0.12 = 52.33 \text{ rad/s}$$

$$\tau = k_h \gamma_s z = (0.11) (18) (z) = 1.98 z$$

Using force equilibrium and simplifying we get

$$FoS = \frac{\text{resisting force}}{\text{sliding force}} \quad (4.91)$$

$$FoS = \frac{W_p \tan \phi + W_a \sin \beta \tan \phi + Q_p \tan \delta_p + cL_a}{Q_a + Q_p + Q_a \tan \delta_a + W_a \cos \beta} \quad (4.92)$$

4.3 Liquefaction Safety of TGSB

Loss of soil shear strength during undrained loading causing the mud to flow like liquid is called Soil liquefaction (Marcuson 1978), (Ishihara 1985, 1996), (Dobry et al 2015). It is a foremost component of earthquake damages. It takes place when soils are saturated. Pore Pressure from water in the soil exerts the pressure on soil particles that dictates how the soil particles are compressed. Before earthquake there is low pore pressure. Shaking by earthquakes, in undrained condition, cause pore pressure to increase, till it touches the ratio of Overburden press to Confining stress and making the Effective stress Zero. Now there is absence of Shear Strength. Particles of soil easily move in the mass at zero shear strength so soil flows like liquid and Liquefaction occurs. The particles get packed even more tightly than before after liquefaction thus avoiding subsequent events (Figure 4.14).

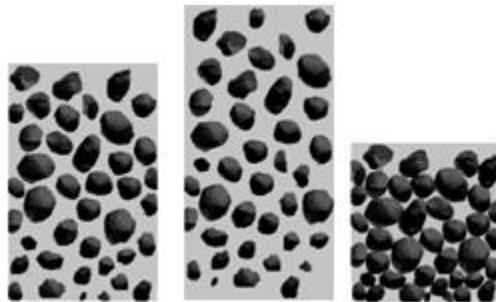
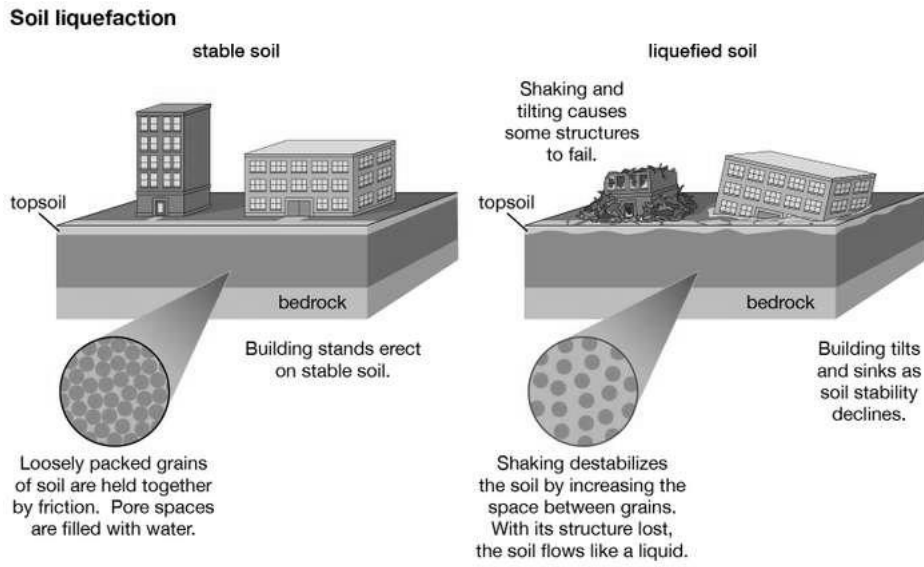


Figure 4.14 Loose Sandy in water Soil Before-During-After liquefaction of soil

In excessive cases the pore-water pressure increases so much that particles of soil lose contact with one another and the soil has so no strength making structures built on top can sink in it just like in water (Figure 4.15)



© 2012 Encyclopædia Britannica, Inc.

Figure 4.15 Effects of liquefaction of soil (Encyclopedia Britannica 2012)

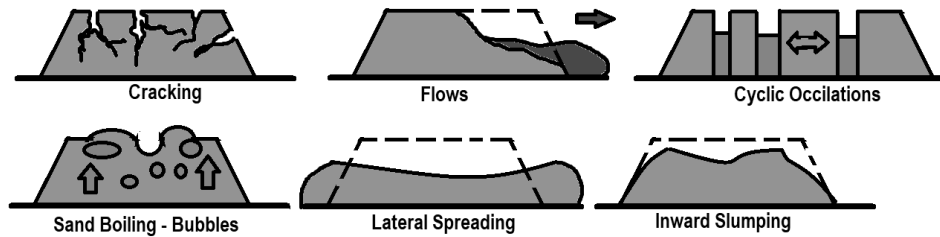


Figure 4.16 Likely Failure Modes of TGSB after liquefaction of soil based on common embankment failure.



Figure 4.17 Probable Failure Modes of TGSB after liquefaction of soil

It is visible in embankments as: Ground Cracks, Ground Oscillations, Sand Boils, subsidence, Slumping of Embankments, Lateral Spreading, Flow Slides (Figure 4.16, 4.17), loss of bearing capacity, tilting retaining walls, uplift of underground utilities like sewers

and manholes. Such events have not so far occurred in TGSB the reason is investigated below.

4.3.1 Liquefiable like soils

Liquefaction usually occurs in sandy soils, however in some cases clays have also known to demonstrate liquefiable behaviour. There is a range of soil that is susceptible for liquefaction (Figure 4.18). Gravels and boulders don't liquefy because they can't flow however extreme earthquakes may cause some gravels to flow. For this reason standard geotechnical classifications can't be applied and Soils with liquefaction potential are basically classified as two types liquefiable-sand-like and liquefiable-clay-like the others are non-liquefiable.

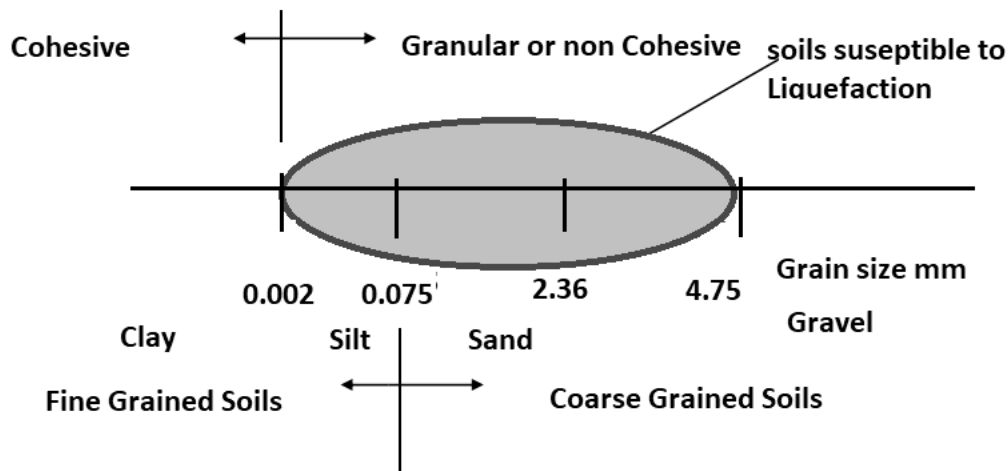


Figure 4.18 Ranges of Soils That Liquefy

During liquefaction loose particles/grains of sand rearrange in a denser packing, this forces the pore-water out, (this is a little more unlikely to occur in over-consolidated, fine grained soils and dense sands). Such action reduces the effective stress. All these thus eventually result in soil behaving like a liquid and undergoing instantaneous deformation due to loss in shear strength. This state is called cyclic mobility and causes great damage especially in dense sands (Figure 4.19) and is determined in triaxial cyclic tests.

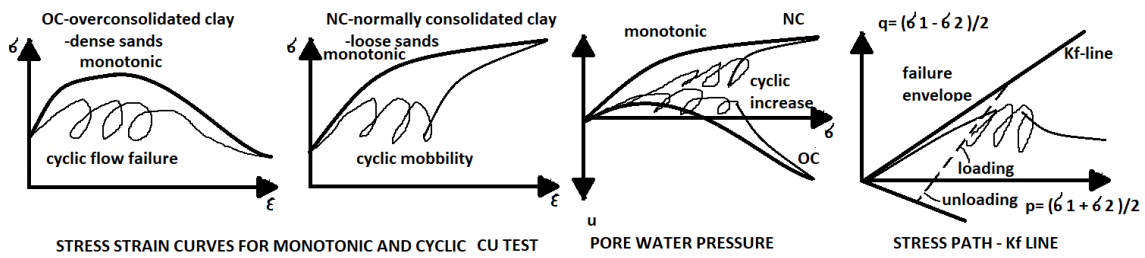


Figure 4.19 Cyclic triaxial test results for behaviour under earthquake loading.

The excess pore pressures under cyclic loading to increases at a faster rate as the amplitude of the cyclic loading increases. There is a relationship between relative soil densities and the number of uniform stress cycles required to induce liquefaction. We can estimate how many cycles it will take to liquefy the soil using curves (Figure 4.20).

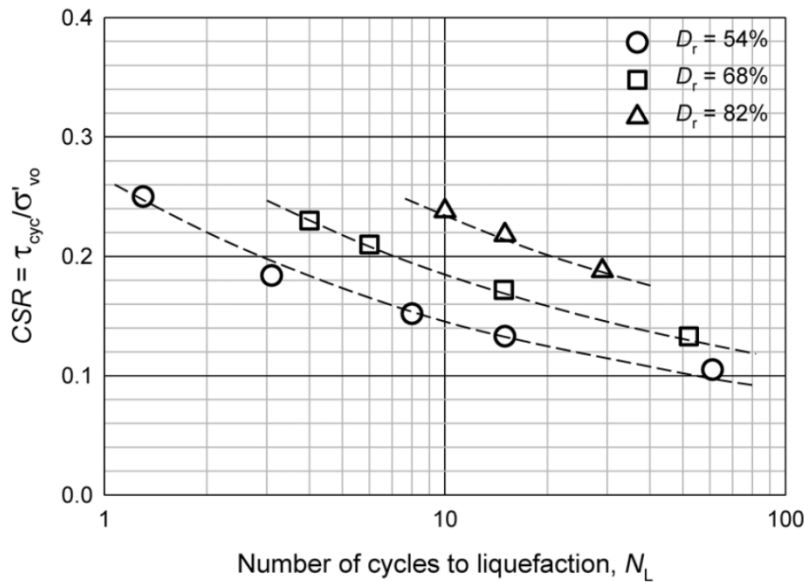


Figure 4.20 Cyclic strength curves on the number of uniform stress cycles required to trigger liquefaction for different relative densities D_r

There is a zone below soil where liquefaction takes place (Figure 4.21). Over the years it has been taken as 5 to 30m depth is the most critical depth. Zones beyond that are not considered for liquefaction.

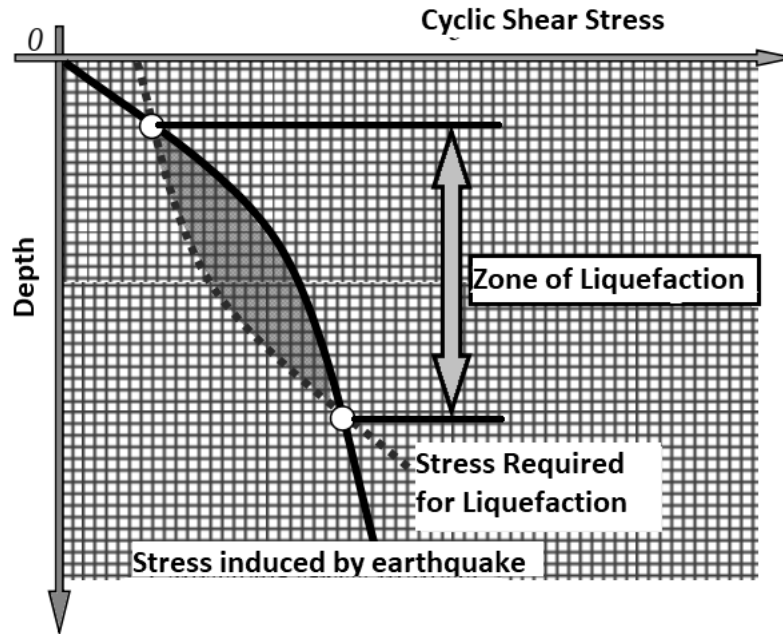


Figure 4.21 Zone of Liquefaction for Calculations

4.3.2 Calculation of Liquefaction

There are many methods to calculate the susceptibility of soils for liquefaction (Sasaki et al. 1992, 2004), (Seed et al 1985, 2003), (Seed and Idriss 1971, 1982). The most common is the cyclic stress criteria by Youd et al (2001) and hence it has been mainly used in this thesis. It was mainly developed for predominantly sandy soils. The critical voids ratio and Atterberg's limits can also be used to find the susceptibility of other soils for liquefaction. The soil stress caused by the earthquake is first found out. For this we need to know the maximum acceleration and the properties of the soil.

$$CSR = \frac{\tau_{av}}{\sigma'_{vo}} = 0.65 \frac{a_{max}}{g} r_d \frac{\sigma_{vo}}{\sigma'_{vo}} \quad (4.93)$$

$$\sigma_{vo} = \sum \gamma z \wedge \sigma'_{vo} = (\sigma_{vo} - p) \text{ where } p = (z - z_w) \quad (4.94)$$

Average force by the earthquake due to variation in acceleration with time

$$\tau_{av} = 0.65 \frac{a_{max}}{g} \quad (4.95)$$

Stress reduction coefficient

$$r_d = 1.0 - 0.00765z \quad \text{for } 0 < z < 9.15 \text{ m}$$

$$r_d = 1.174 - 0.0267z \quad \text{for } 9.15 < z < 23 \text{ m}$$

$$r_d = 0.744 - 0.00865z \quad \text{for } 23.0 < z < 30 \text{ m}$$

$$r_d = 0.5 \quad \text{for } z \geq 30 \text{ m} \quad (4.96)$$

Cyclic Resistance from the Standard Penetration Test (SPT-N), Cone Penetration Test (CPT- q_u) or Shear Wave Velocity (V_s) is found next. The corrected resistance for stress, shear and magnitude is found out next

$$CRR = CRR_{7.5} k_m k_\alpha k_\sigma \quad (4.97)$$

k_m is the magnification scaling factor (MSF) for magnitude other than 7.5 (Figure 4.22)

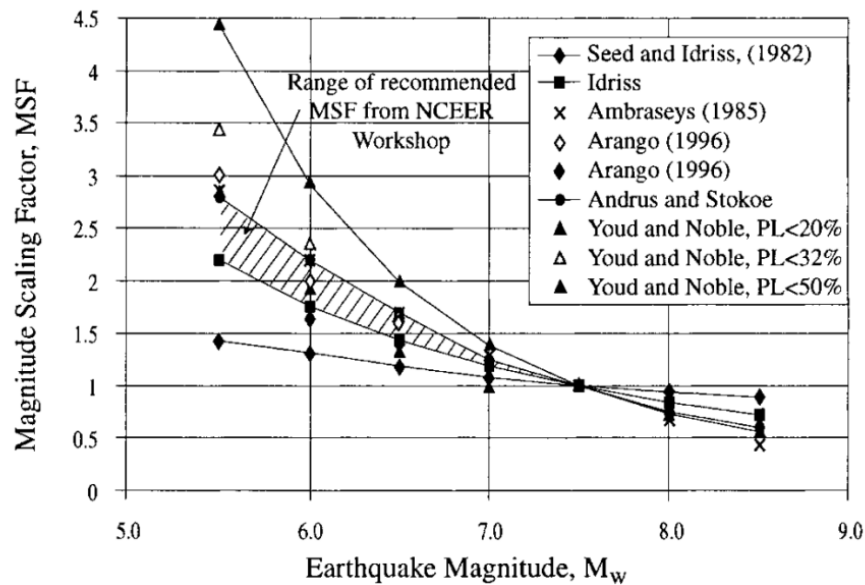


Figure 4.22 Magnification Scaling Factor (MSF) for earthquakes

k_α is the initial static shear factor, where α is the stress ratio (τ_h/τ_v). it depends on relative density of the soil (Figure 4.23).

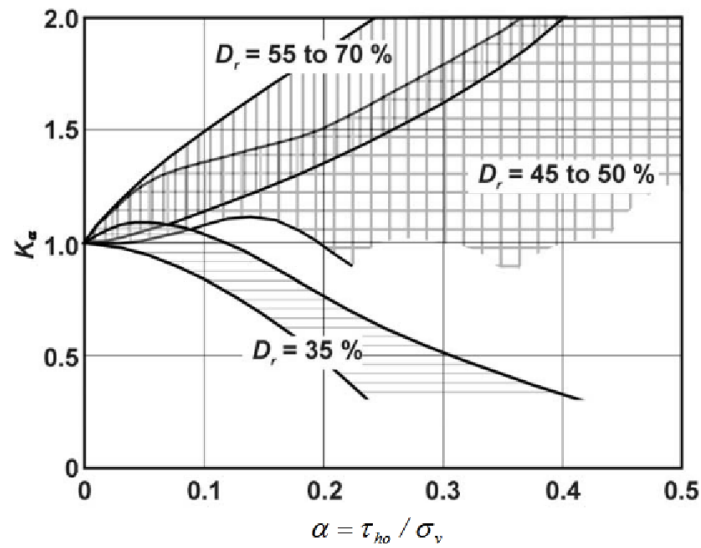


Figure 4.23 Initial Static Shear Factor

k_σ is the stress normalization factor for atmospheric pressure of > 100 kPa. It is found from the relative soil density (Figure 4.24).

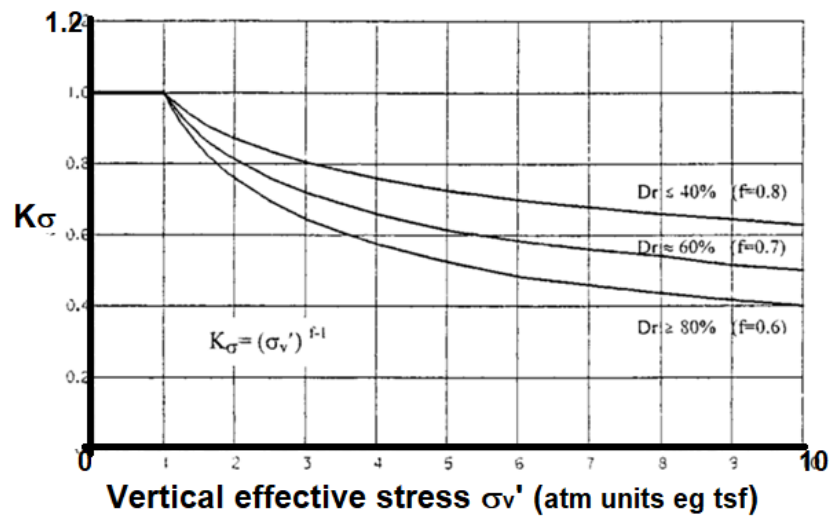


Figure 4.24 Stress Normalization Factor

Factor of safety for liquefaction is found by the ratio of resistance to strength.

$$F_s = \frac{CRR}{CSR} MSF \quad (4.98)$$

Liquefaction occurs when $F_s < 1.0$. For all practical purposes Factor of safety must be ≥ 1.1

As the calculations are meant for a typical earthquake of 7.5 magnitudes, Magnitude Scaling Factor (MSF) is used to normalize values for earthquake other than M7.5. MSF for lateritic soils can be estimated out from the graph or the given bellow (Figure 4.25 or Table 4.8).

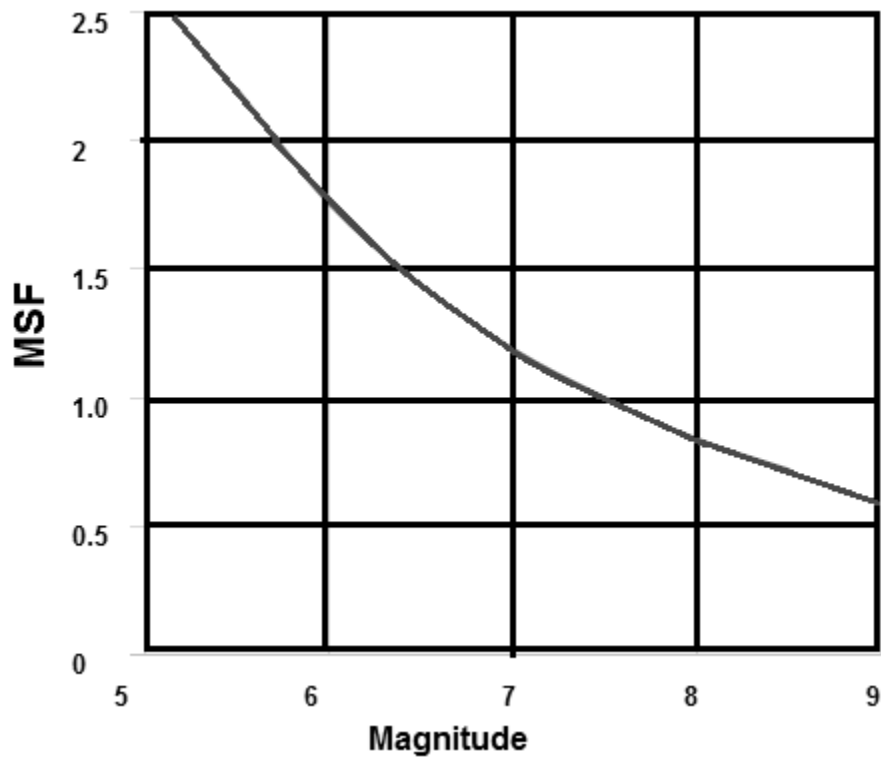


Figure 4.25 Magnitude Scaling Factor (MSF) used in this thesis

MSF for lateritic soils can be estimated out from the table is 4.8 considering an earthquake of 5.5

Table 4.8 Magnitude Scaling Factor (MSF)

Earthquake Magnitude	8.5	8.0	7.5	7.0	6.5	6.0	5.5
MSF	0.72	0.84	1.00	1.19	1.44	1.76	2.20

Magnitude for earthquake on other scales can be converted to M_w scale needed for these calculations by using the curves given below (Figure 4.26).

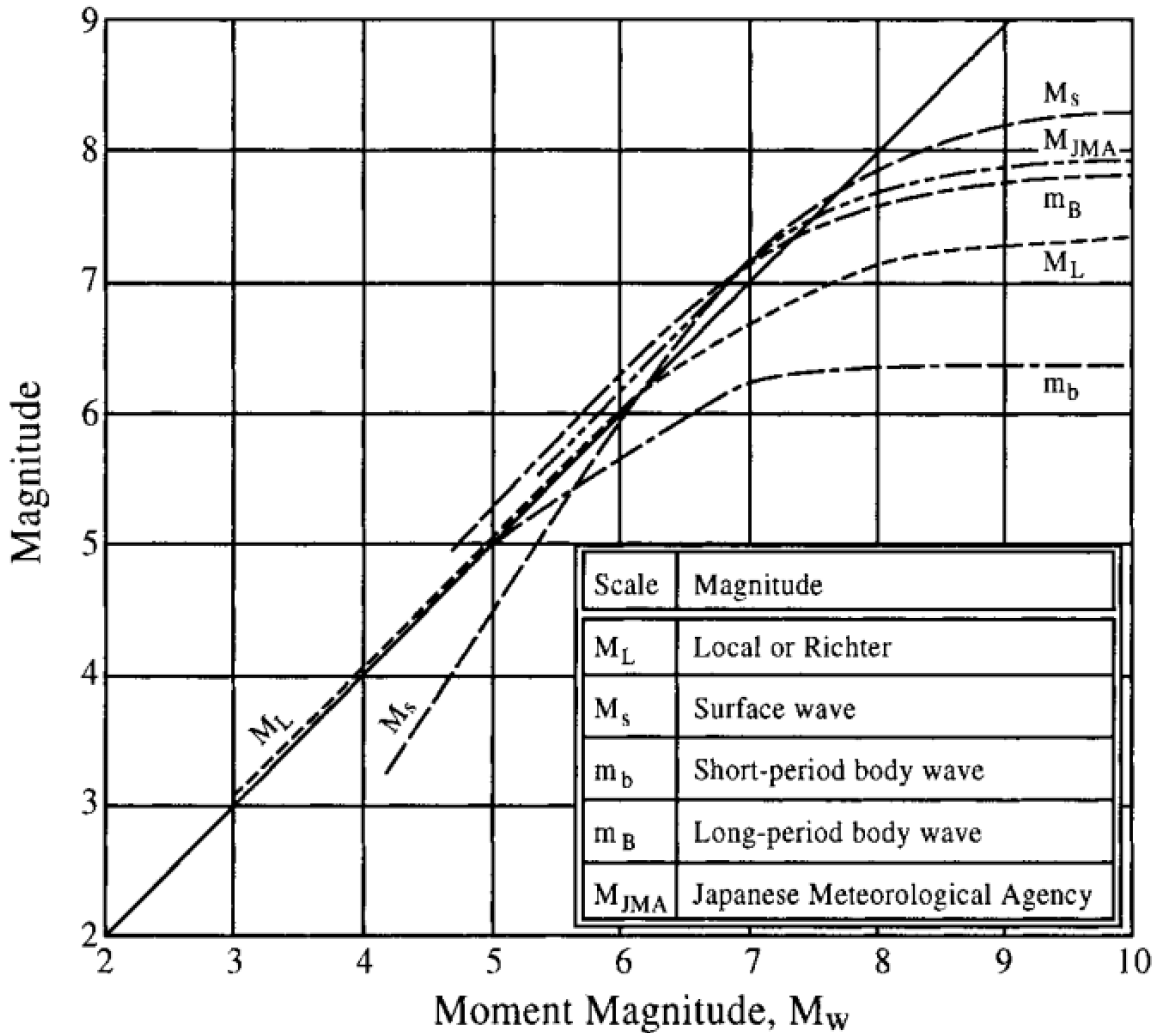


Figure 4.26 Relationship between Moment M_w and Other Magnitude Scales

4.3.3 Liquefaction from SPT (Standard Penetration Test)

Standard penetration test gives Number of blows (N) from which we can find the liquefaction potential of a site. A bore hole is driven and N value is calculated. From this N_{60} value, (N corrected for 60% hammer efficiency) is found out.

$$N_{60} = NC_{60} \quad (4.99)$$

$$C_{60} = C_{HT}C_{HW}C_{SS}C_{RL}C_{BD} \quad (4.100)$$

Table 4.9 Correction factors for SPT-N

Hammer Type	Automatic/chain	Manual/rope
C_{HT}	1.33 –	0.75 –
C_{HW}	Hammer fall height(Hmm)and weight(Wkg) $H W / (762 \times 63.5)$	
C_{SS}	1.1 – Loose Sand	1.2 – Dense Sand
C_{RL}	Rod Length 0.75 – 3m rod	
C_{BD}	1.05 – 150mm bore	1.15 – 200mm bore

Then calculate N corrected (Table 4.9) for overburden of using formula then find the $CRR_{7.5}$ (Table 4.10 and Figure 4.27).

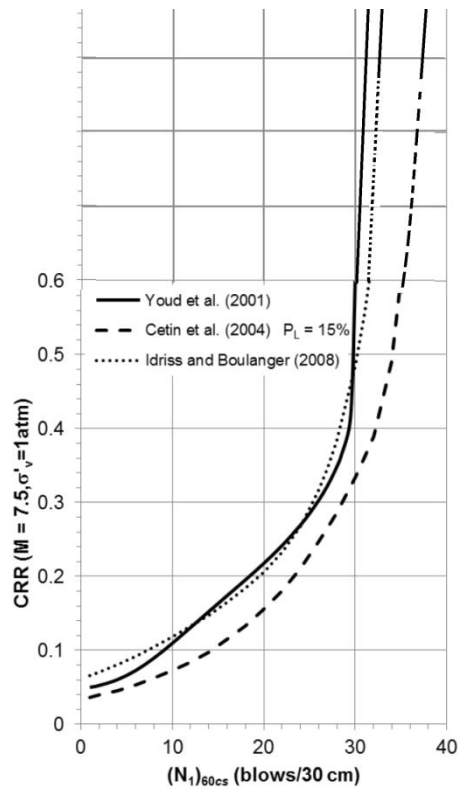


Figure 4.27 Liquefaction from SPT (Standard Penetration Test)

$$C_N = \left(\frac{p_a}{\sigma_v}\right)^{\frac{1}{2}} \leq 2 = \frac{9.7}{\sqrt{\sigma_v}} \quad (4.101)$$

$$N_{60cr} = N_{60} C_N = \frac{9.7 N_{60}}{\sqrt{\sigma_v}} \quad (4.102)$$

Table 4.10 CRR for Liquefaction from SPT (Standard Penetration Test)

N	0	10	20	30	40	50	60
CRR	0.047	0.10356	0.228183	0.502777	1.107818	2.440962	5.378407

4.3.4 Liquefaction from CPT (Cone Penetration Test)

the Cone penetration test jig drives a 60° cone into the ground and the tip resistance is measured. Find CPT value q_u in KN/m^2 . CPT value needs to be normalized for tip resistance and sand equivalence. Calculate corrected value of q_u for atmospheric pressure using formula, then find the $\text{CRR}_{7.5}$ (Table 4.11 and Figure 4.29) from the table or graph.

$$q_{ucr} = K \left(\frac{q_u - \sigma_v}{p_a}\right) \left(\frac{p_a}{\sigma_v}\right)^n \quad (4.103)$$

Where $K = 2.51$ and $n = 0.381$ for lateritic soils of Goa and atmospheric pressure $p_a = 100$.

(K) The Sand Equivalence Correction (Figure 4.28) can be taken from graph shown below depending on sand: silt ratio, (n) is stress exponent that depends on soil it varies from 0.1 to 0.5

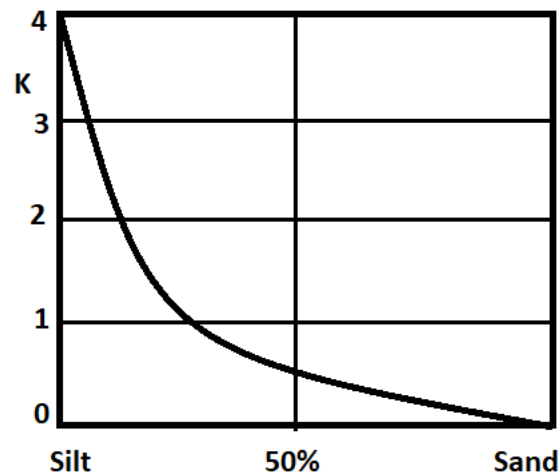


Figure 4.28 Sand Equivalence Correction

Table 4.11 CRR for Liquefaction from CPT (Cone Penetration Test)

q_{ucr}	0	50	100	150	200	250	300
CRR	0.018	0.046543	0.120346	0.31118	0.804621	2.080517	5.379613

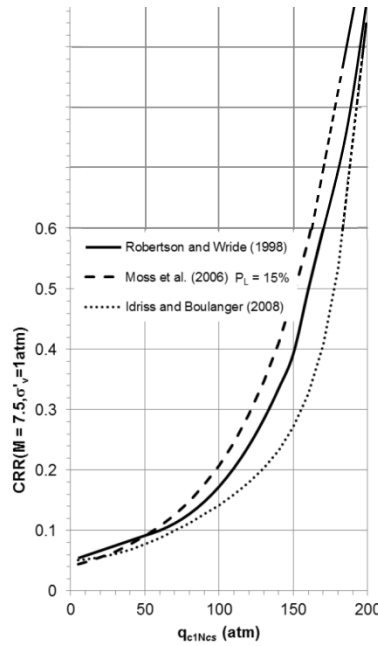


Figure 4.29 Liquefaction from CPT (Cone Penetration Test)

4.3.5 Liquefaction from V_s (Shear wave Velocity)

Find shear wave velocity value V_s in m/s

Calculate corrected value of V_s for atmospheric pressure using formula then find the CRR (Table 4.12 and Figure 4.30) from the table or graph.

$$V_{scr} = V_s \left(\frac{100}{\sigma_v'} \right)^{0.25} \leq 1.3V_s \quad (4.104)$$

Table 4.12 CRR for Liquefaction from V_s (Shear wave Velocity)

V_{scr}	0	50	100	150	200	250	300
CRR	0.034	0.071978	0.152377	0.322583	0.682908	1.445717	3.060582

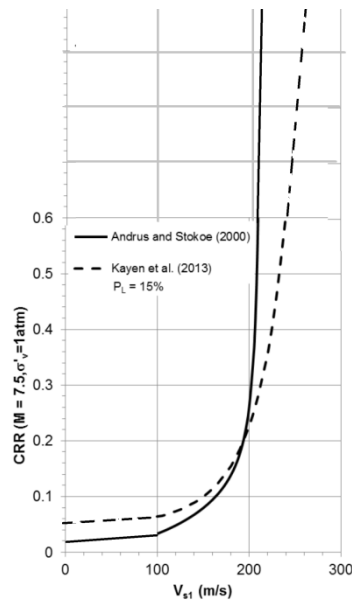


Figure 4.30 Liquefaction from V_s (Shear wave Velocity)

4.3.6 Liquefaction Potential Index (LPI)

The probability for liquefaction can be specified by Liquefaction Potential Index (LPI).

Table 4.13 LPI based Occurrence Potential classification

LPI	Occurrence Potential Classification
< 0	Never
0 – 2	Low
2 – 5	Moderate
5 – 15	High
> 15	Very High

It is calculated from the factor of safety F_s estimated every 10 m (max) with effective layer depth w_z normalized for 10 m. LPI (Iwasaki et al 1978, 1982), (Toprak and Holzer 2003), (Holzer et al 2006), (Maurer et al 2014) is given by

$$LPI = \int_0^z F_L w_z dz \quad (4.105)$$

$$w_z = 10 - \frac{z}{2} \geq 1 \quad (4.106)$$

Layered Factor of safety

$$F_L = 1 - F_s \quad \text{for } F_s \leq 1$$

$$F_L = 0 \quad \text{for } F_s > 1 \quad (4.107)$$

The occurrence potential depends on the LPI (Table 4.13)

4.3.7 Liquefaction Potential for embankment Soils in Goa

Liquefaction potential for soils of Goa needs to be done as the TGSBs are used for multiple purpose and they lie on different soils. Calculations for this thesis has been done on the basis of Youd.et al (2001) as recommended by IS 1893. Sample calculation for certain TGSB soil samples has been done as study of all soils is beyond the scope of this thesis.

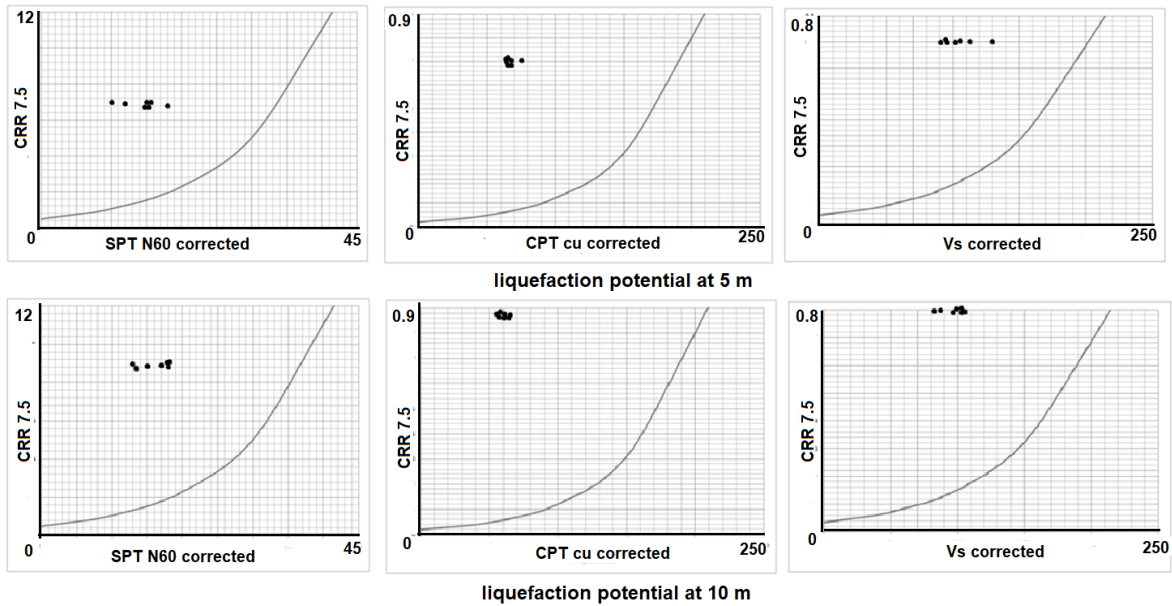


Figure 4.31 Plots of SPT, CPT, Vs and CSR 7.5 showing liquefaction from CSS at 5 and 10 m at sites shown in map below.

Liquefaction of embankments and embankment dams is common during earthquakes. The Dam fails if the displacement is more than the freeboard. As freeboard for TGSB is 1.5m, that is the permissible vertical displacement. However the potential of the soils under the embankment to liquefy must be measured. During Nepal (Kathmandu) earthquake there was massive loss due to liquefaction. Kathmandu lies on a basin less than 30 m thick. Goa

also has bedrock at 20 to 30m depth. A similar loss should not occur in Goa so LPI estimation is necessary. Based on this the LPI was estimated for seven different TGSB Sites in Goa (Figure 4.31, 4.32).



Figure 4.32 Map of Goa showing locations of boreholes for LPI

Bore Hole Data was collected about the SPT N values at 0.45, 5, 10, 15 and 20 meters while CPT shear wave velocity was found by suitable correlations.

CPT SPT correlations are empirical in nature and require a separate set of extensive studies to validate them which is beyond the scope of the present studies but may be taken up as post-doctoral work. Vasco, Ponda and Canacona sites are to study the LPI of plateau areas, Mapusa, Panjim and Margao sites are to study the LPI of lower lying areas, Bicholim site is to study the LPI of higher lying areas. From this research a rough idea of LPI for state of Goa can be estimated. The study showed that the soils lie quite high in non-liquefiable areas of the plots. For the purpose of CPT test and sonic velocity test as it was not available suitable co-relationships were used (Table 4.76) they were derived from the SPT test result N (Castanga et al 1985), (Mavko 1990), (Shahien 2007), (Wadhwa et al 2010), (Madun et al 2015). The regional variation in soil stratification necessitated a variation in the relationships. Further studies and extensive lab and site tests are needed to confirm or reject these but at present they are beyond the scope of this thesis. It will be done as part of post-doctoral work.

Table 4.14 Co-relationships between SPT CPT and Vs for Goa region

Town	qu	V_s
Mapusa	2.40 N ^{0.011}	60 + 3.00 N
Panjim	2.60 N ^{0.011}	60 + 2.85 N
Vasco	2.60 N ^{0.011}	60 + 2.85 N
Margao	2.60 N ^{0.011}	60 + 2.39 N
Ponda	2.89 N ^{0.011}	60 + 3.00 N
Canacona	2.46 N ^{0.011}	60 + 1.80 N
Bicholim	2.51 N ^{0.011}	60 + 2.54 N

Velocity of primary or compression wave can be found out from the velocity of secondary or shear wave by following co-relationships.

For lateritic soils

$$V_P = 1.69V_S \quad (4.108)$$

For lateritic rocks

$$V_p = 1.72V_s \quad (4.109)$$

The LPI for soils of TGSBs in Goa, were calculated on these criteria.

4.3.8 Liquefaction based settlement

Liquefaction settlement can be large scale or small scale (Figure 4.33).

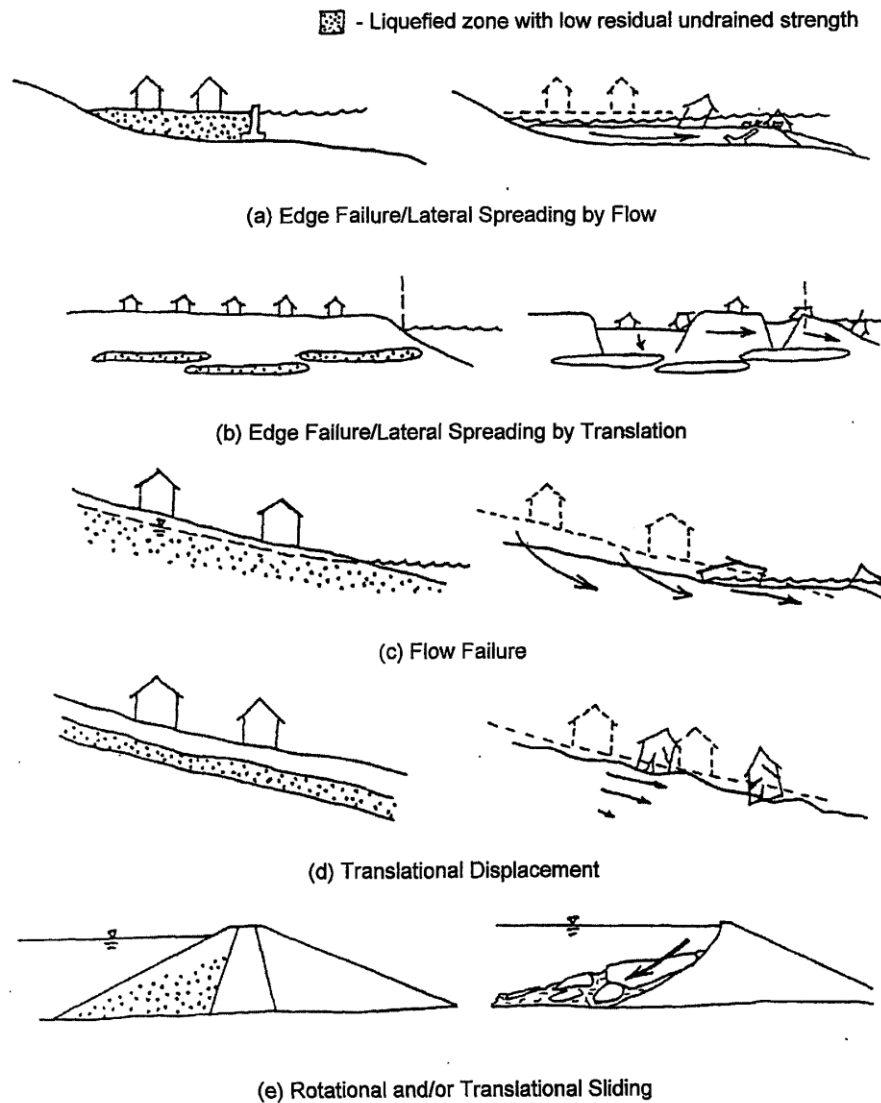


Figure 4.33 Types of failure post liquefaction settlement (Seed et al 2001)

There are three approaches (Seed et al 2001) full non-linear finite element method, statistically derived empirical method, static limit equilibrium analysis. It depends on the liquefied zone and depends on engineer's estimation. Liquefaction causes loose soil particles to permanently deform due to realignment and thus cause irreversible settlement.

4.3.8.1 Estimation of the Earthquake Induced Settlement as per Tokimatsu and Seed 1987

The permanent deformation can be evaluated from procedure given below. For each soil layer for earthquake of magnitude X and Find corrected N value (N_{60}), CSR, CRR. Then calculate factor of safety for each soil layer = CSR/CRR

Consider layers which is vulnerable to liquefaction (ignore all other soil layers have a factor of safety from STP less than 1.25)

Therefore, estimate the settlement contributed by Layer No. ---- only.

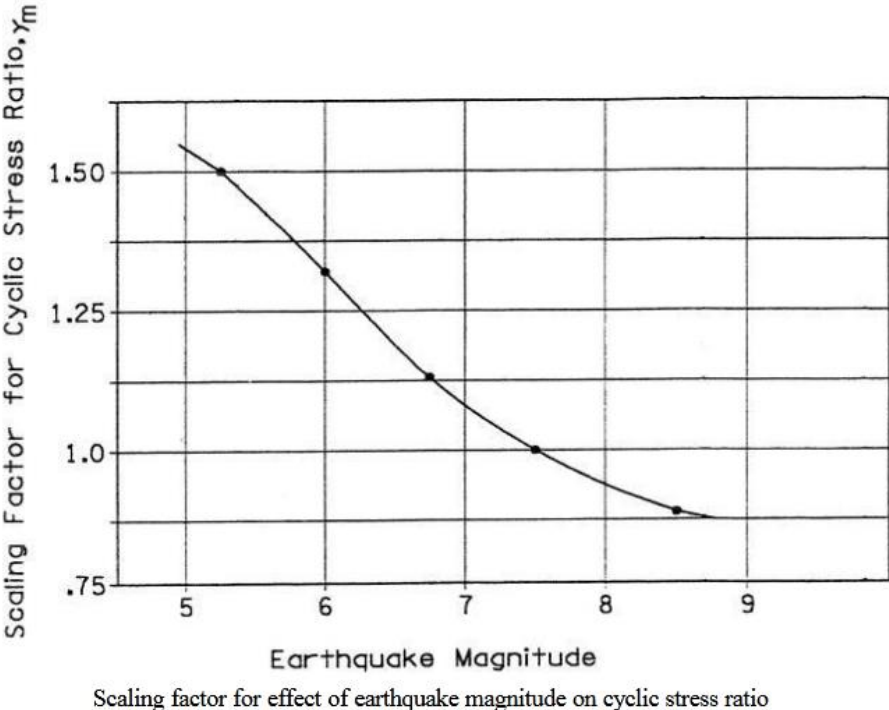
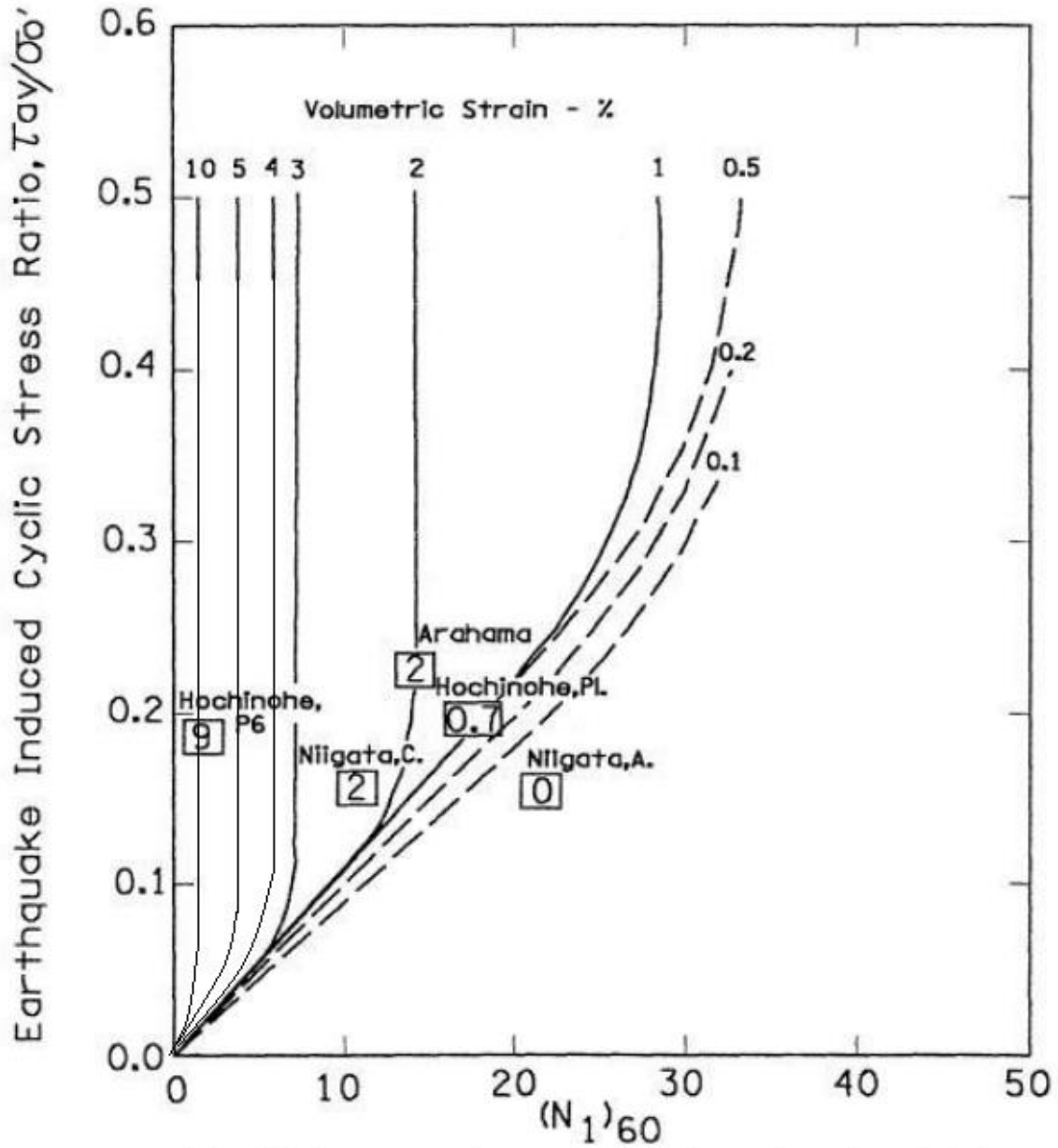


Figure 4.34 Scaling factor for CSR

Correct the calculated earthquake induced stress ratio (Figure 4.87) in Layer No--- to the equivalent stress ratio that would be induced by an M= X event:

From Figure 8.32, $\gamma_m = \underline{\hspace{2cm}}$

Corrected $CSR_{induced\ at\ M=X} = CSR \cdot \gamma_m$



Relationship between cyclic stress ratio, volumetric strain and $(N_1)_{60}$
(Tokimatsu and Seed, 1987)

Figure 4.35 Volumetric Strain from CSR

Find strain (Figure 4.35), say $\epsilon_v = 3.3\%$

Layer --- is 10 m thick,

Therefore Settlement = $(3.3/100)(10)(1000) = 330\text{mm}$.

4.4 Tsunami Safety of TGSB

Tsunamics or Tsunami Dynamics (Dias and Dutykh 2007), (Bryant 2008), (Chock et al 2013), (Chock 2016), (Yang et al 2017) is an emerging branch in Geotechnical engineering that deals with the onshore effect of an offshore dynamic event. Tsunami Dynamics means the science of solving the dynamic forces that effect onshore structures due to tsunamis. Tsunami is derived from Japanese: *tsu* (“harbour”) and *nami* (“waves”). It is a wave sequence produced by an ocean event such as an underwater earthquake or landslide that causes large volume of seawater displacement (BMTPC 2019). They can be very big and catastrophic. Tsunamis are caused by various reasons. The main is earthquake the nearest zone of seismic activity that can cause Tsunami to Goa lies in the Andaman Islands (Figure 4.36).

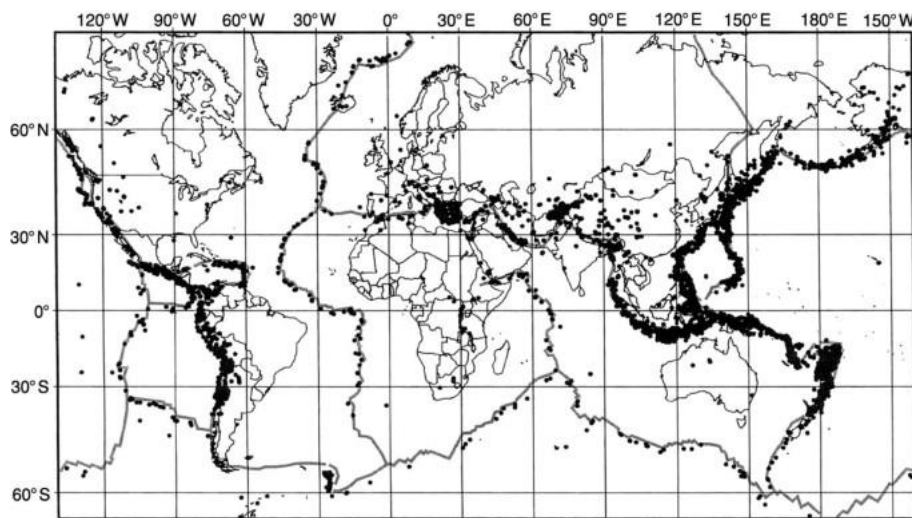


Figure 4.36 All World Earthquakes (USGS) for possible Tsunami near Goa

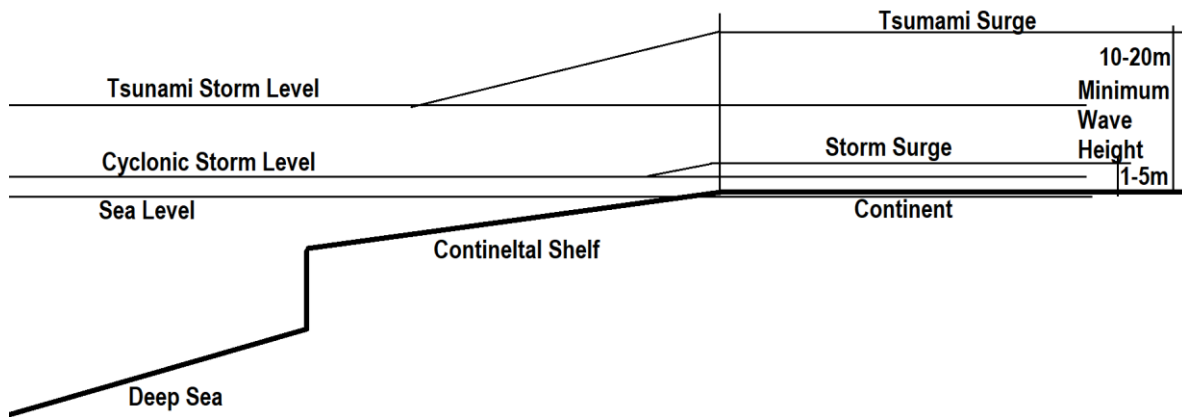


Figure 4.37 Water Levels in Tsunami and Tsunami Surge

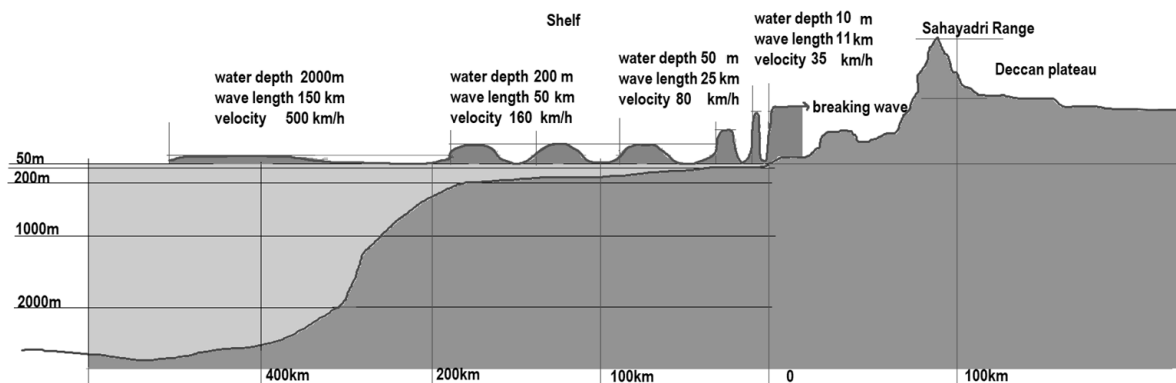


Figure 4.38 C/s of Goa showing possible wave levels and water depth during Tsunami

Cyclones and Tsunamis have an accompanying storm surge as they near the shore (Figure 4.37). The surge is caused by decreasing shore depth and is associated with decreasing wave velocity and increasing wave heights (Figure 4.38), this is because the transfer of energy has to take place as per law of conservation of energy

(Kinetic Energy $mv^2/2 \leq \geq$ Potential Energy mgh).

$$mv^2/2 = mgH$$

$$v^2/2 = gH$$

$$v^2/2g = H \tag{4.110}$$

Table 4.15 Tsunami Velocity and Wave Height

Wave Velocity	Min height	Max Height
300	0.44	0.30
250	0.04	0.03
200	1.17	0.78
150	3.83	2.55
100	8.01	5.34
50	13.73	9.15
20	17.89	11.93
15	18.64	12.43
10	19.40	12.93
5	20.18	13.45

From the loss of kinetic energy and gain in potential energy a simple relationship gives the tremendous increase in heights as the tsunami reaches the shore. When the tsunami enters shallow waters Tsunami wave slows and its height increases (Table 4.15). This causes property destroying and life threatening waves.

Table 4.16 Tsunami Wave Dimensions depending on seabed depth of Earthquake

Sea Depth	Velocity		Wave length	Wave height	Needed depth	Breaking height
	h-m	C- kmph	m/s	W-km	H-m	W/20
7000	943	261.87	282	0.25-0.5	14100	5460
4000	713	198.00	213	0.5-1.0	10650	3120
2000	504	139.96	151	1.0-2.0	7550	1560
200	159	44.15	48	2.0-3.0	2400	156
50	79	21.94	23	5.0-10.0	1150	39
10	36	10.00	10.6	15 – 20	530	7.8

The depth needed for tsunami not to break is 530 m but the depth available is only 10 m. the breaking height is 7.8 m but the wave height is 15 m that is the reason a tsunami breaks and causes destruction on the shore (Table 4.16).

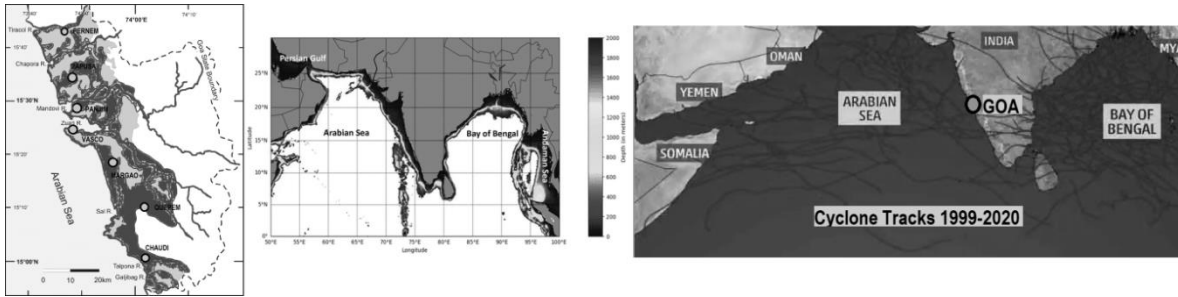


Figure 4.39 Goa-Flood risk areas, continental shelf, cyclone Tracks

The cyclone tracks of the last 30 years (Figure 4.39) show that most cyclones tend to bypass Goa. The Lakasdweep Islands act as a wind deflector and the storms end up in the Gulf of Cambay Gujarat. They pass close to the coast but never make landfall in Goa. This could cause a minor storm surge of max 1 to 2 m. Their speeds are maximum 20 Kmph. However the major risk is because of tsunami exposure. Although the tsunami wave is only 1 m in amplitude its speed is 40 to 100 Kmph. There is a large continental shelf near Goa. This allows for tsunami to build up as they approach the coast and gather much needed water. The earliest estimated time for the first wave to hit Goa is 4 to 5 hours based on Sumatra type earthquake striking Andaman Islands the nearest seismic hotspot to Goa. The mismatch in arrival times (Table 4.17) is due to interference of fresh and reflective waves and ocean current waves. A map from NOAA shows the arrival time of the Tsunami from Nicobar to Goa. (National Centre for Environmental Information-National Oceanic and Atmospheric Administration). The most common measure suggested stopping storm surges are mangrove forests (Figure 4.40).

Table 4.17 Time for Tsunami to travel to Goa in Hours from Nicobar (IRS)

Irs.gujrat.gov.in (Institute of Seismological Research)

Place	Time (hrs)	Amplitude (m)
Lakhpat	2.45	1.2
Kandala	3.30	2.0
Dwarka	2.10	2.0
Mumbai	4.45	2.0
Goa	3.08	1.0
Karwar	3.12	1.0

It acts as a buffer during cyclonic storm surges and can effectively absorb the storm if of sufficient width. There is however a hydraulic jump that occurs during a tsunami which while dissipating dangerous energy does not effectively stop the back-land flooding(Pasha and Tanaka 2020), (Ko et al 2015), (Foster et al 2017).

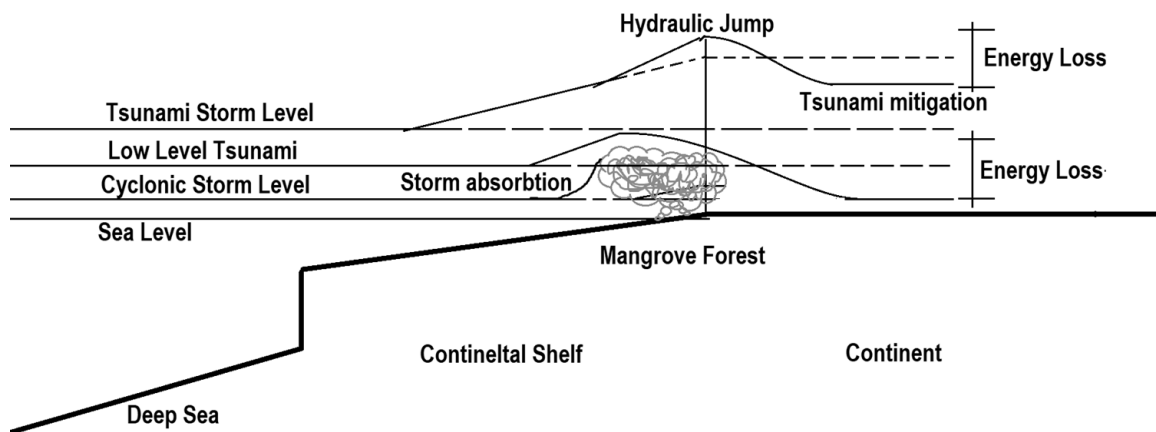


Figure 4.40 Protective Actions of Coastal Mangroves

The most ancient measure existing to stop storm surges are TGSBs (Figure 4.41). They act as a buffer during cyclonic storm surges and can effectively absorb the Tsunamis too when

properly maintained. There are also hydraulic jumps that occur during a tsunami which dissipating dangerous energy in stages to effectively stop the back-land flooding.

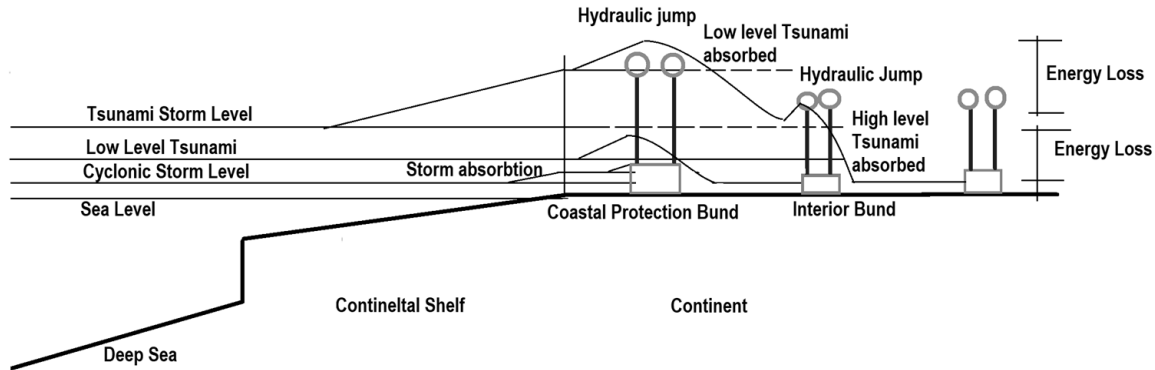


Figure 4.41 Protective Actions of Coastal TGSBs

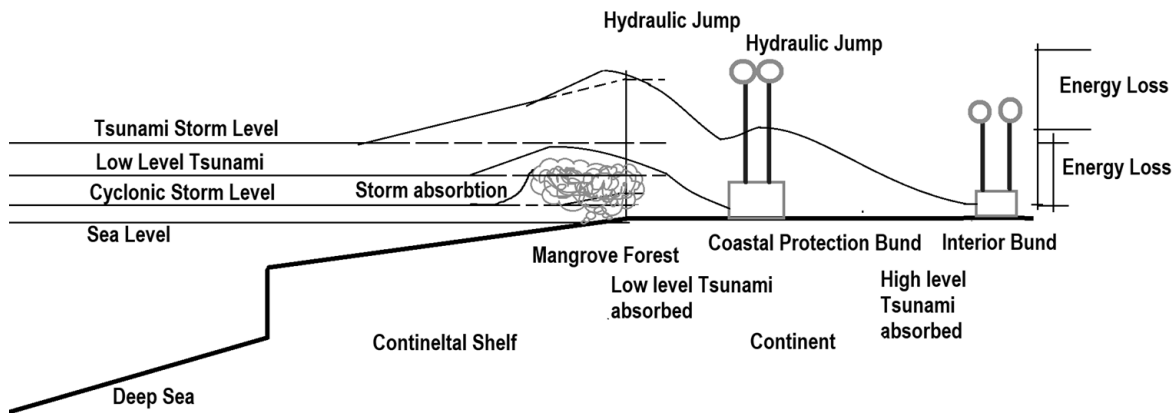


Figure 4.42 Combined Protective Action of Coastal Mangroves & Coastal TGSBs

The best measure existing to stop storm surges are a combination of mangrove forests planted at the coast – (NOT INLAND) and TGSBs (Figure 4.42). They act as a buffer during cyclonic storm surges and very effectively absorb the Tsunamis.

4.4.1 Tsunami Analysis-Hydraulic Jump and Weir action in Coastal Protection works.

Hydraulic Jump is a simple mechanism used to dissipate energy in dams, weirs and important hydraulic structures by using an obstruction in the path of the flow. There are also hydraulic jumps that occur during a tsunami which dissipating dangerous energy in

just two stages to effectively stop the back-land flooding. A hydraulic jump occurs when a subcritical downstream flow with a decreased velocity, v_2 , meets a higher velocity, v_1 , supercritical flow upstream at sufficient water depth. The resultant transition is rapid and involves a large loss of energy caused by turbulence. Initial depth = depth before jump and subsequent depth = depth after jump. The energy equation can't be used as energy is lost in the jump therefore momentum equation is used (Figure 4.43).

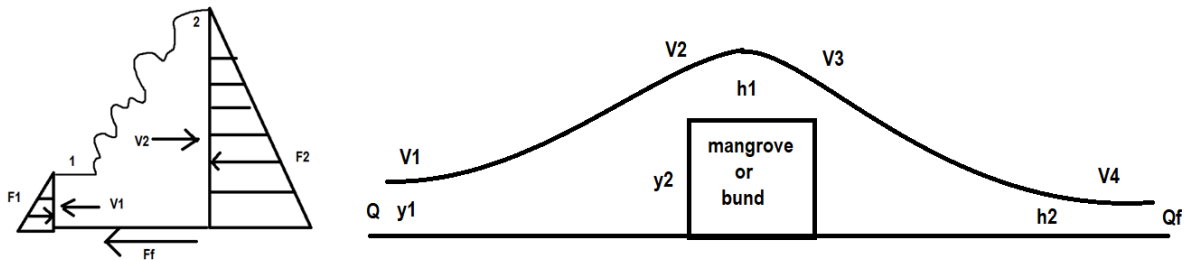


Figure 4.43 Forces, velocities and heights of water in a Hydraulic Jump

The momentum equation states that

$$F = \rho Q(V_1 - V_2). \quad (4.111)$$

Net Force

$$F_1 - F_2 - F_f = M_1 - M_2. \quad (4.112)$$

$$F = \rho g(A\bar{y}). \quad (4.113)$$

$$M = \rho QV. \quad (4.114)$$

Energy Dissipation

$$\Delta H = H_1 - H_2 = \left(y_1 + \frac{V_1^2}{2g}\right) - \left(y_2 + \frac{V_2^2}{2g}\right) \quad (4.115)$$

Length of hydraulic Jump

$$L = 6.1y_2 \quad (4.116)$$

$$y_1 = \frac{Q}{bV_1} \quad (4.117)$$

$$y_2 = \frac{y_1}{2} + \left(\sqrt{\frac{y_1^2}{4} + \frac{2y_1V_1^2}{g}}\right). \quad (4.118)$$

Where

A=area of diagram,

\hat{y} =centroid

y_1 and y_2 are the water depth on each side

H_1 and H_2 are the Hydraulic heads on each side

Discharge over the Mangrove/Bund

$$Q_f = C_d b h_1^{1.5}. \quad (4.119)$$

Velocity over the Mangrove/Bund

$$V_3 = 0.95\sqrt{2gh_1}. \quad (4.120)$$

$$V_4 = C_d\sqrt{2gh_2}. \quad (4.121)$$

Length of Reverse Jump

$$L_2 = 4h_2 \quad (4.122)$$

Where

h_1 , h_2 are the heads over and after the Mangrove/Bund

C_d is coefficient of discharge (2.3-Mangroves, 1.63 Bunds)

4.4.2 Tsunami Analysis – Hydraulic Jump experimental verification.

Hydraulic jumps in a open channel in laboratory can be used to do model studies of effect of tsunami on TGSB.

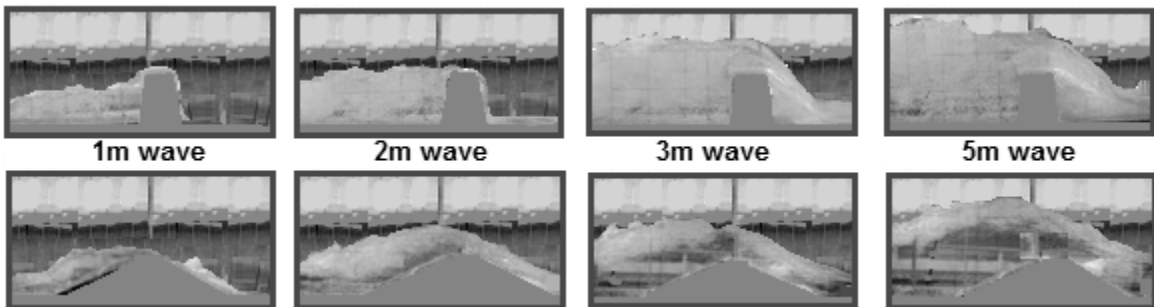


Figure 4.44 Model studies of Hydraulic Jump with TGSB and normal embankment

1:20 scale wooden Model studies of 6m TGSB and 6m normal embankment with 30° slope (Figure 4.44) were conducted in a hydraulic channel to simulate different wave heights (y_1) 1,2,3,5 m at velocity of flow 10m/s. the jump (y_2) and the last height (h_2) were measured. The normal embankment approximately represents a mangrove forest shape. This experiment shows that there is more jump and less discharge from TGSB than normal embankment. There is also greater turbulence in flow for TGSB as compared to normal embankment (Table 4.18).

Table 4.18 Tsunami Hydraulic Jump Velocity and Wave Height for 3m TGSB

TGSB (bund), E (Embankment)

Height of obstruction 6m, $V_1=10$ m/s, $b = 1000$ m, $g=9.81$ m/s²

y_1	m	1	2	3	5
y_{2TGSB}	m	4.5	8.0	10.0	12.5
y_{2E}	m	3.5	7.0	8.5	11.0
h_{2TGSB}	m	0	1	2	2.5
h_{2E}	m	0.75	1.5	1.9	3.1

4.5 GeoStudio2019 Analysis TGSB

GEOSTUDIO is available and widely used suite of software in Geotechnical Analysis (Maula and Zhang 2011), (Gustafsson and Lindstrom 2014), (Chakraborty and Dey2016a, b, c), (Getachew2018). For academic purpose a student’s version is freely available. GEOSTUDIO Student Edition is used in this thesis. It has partial versions of all eight software: SLOPE/W, SEEP/W, QUAKE/W, SIGMA/W, AIR/W, TEMP/W and CTRAN/W. During these analyses only SLOPE/W meant for slope stability, SEEP/W designed for seepage analysis and QUAKE/W intended for dynamic and seismic analysis are used. The limitations of some of them are mentioned below. All of them limit the number of multiple stages to two within a file. They limit the number of regions to 10 and number of elements to 500. Thus, extremely small problems can only be analysed. However, as TGSB uses simple ancient technology the modelling can be simplified to basic

elements that are easily analysed even by student's edition. Within these limited options the data for seismic analyses of TGSBs has to be fitted to match the requirements.

4.5.1 GeoStudio 2019 Modelling

Stability can be analysed taking into consideration the TGSB as an embankment dam. GeoStudio Software analysis being reliable is used in this thesis. For performing analysis of TGSB only three of the software suit is used: SLOPE/W is used for slope stability, SEEP/W is used for seepage analysis and QUAKE/W is used for dynamic and seismic analysis.

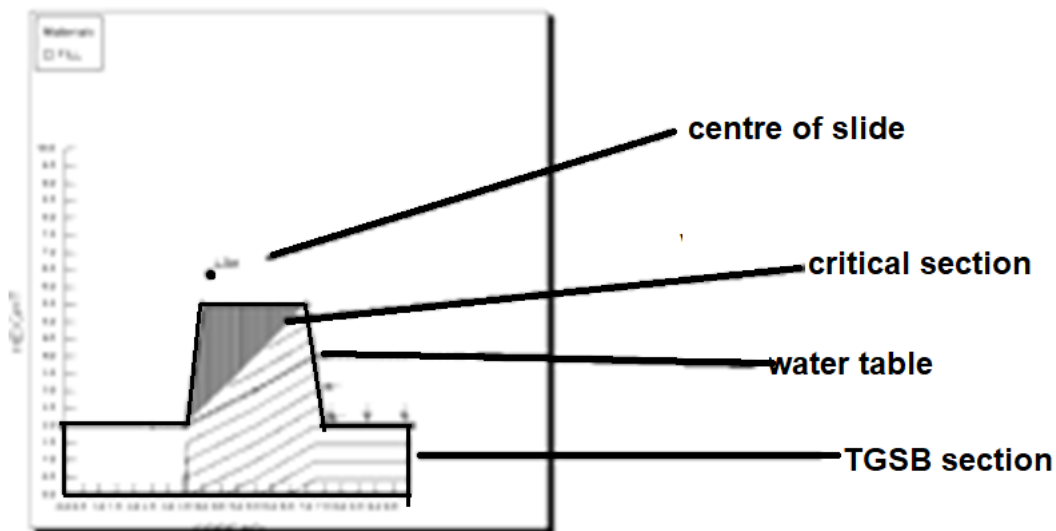


Figure. 4.45 GeoStudio2019 model of 3 m high TGSB.

The slope stability using GeoStudio2019 SLOPE/W was analysed for 3, 6 and 9 m TGSBs only as these were the existing bunds in Goa (Figure 4.45). The first analysis was of increases of strength by each individual component of the TGSB. Next the combined factor of safety of all components was considered. The Mohr-Coulomb soil model was chosen since soil is mixed in nature (fine sand-silt with organic content).

4.5.2 Comparison of FoS for different components

The first study considered how every separate component of the TGSB changes the strength. As the TGSB consists of different components: Plain Soil, Natural Roots reinforcement– addition to FoS, Facing wall retention – addition to FoS, Root pile reinforcement – addition to FoS, Coconut tree on top – subtraction to FoS. All these were studied one at a time. The simplest TGSB a 3 m bund was taken up for the study (Figure 4.46).

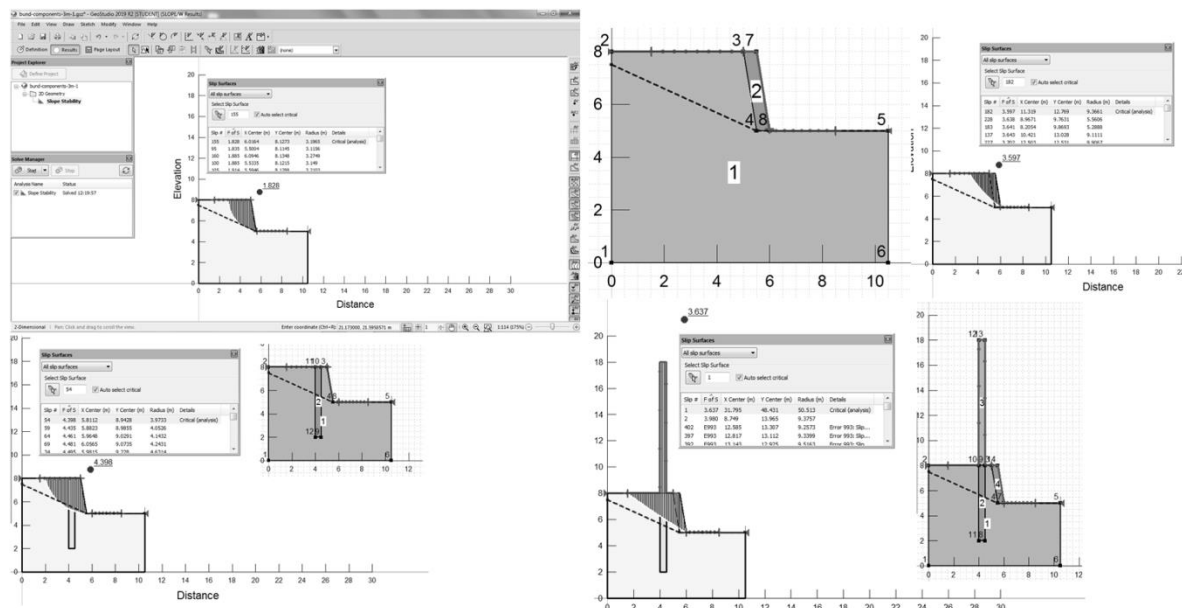


Figure 4.46 FoS of 3 m TGSB with components: tree, wall, and root-pile.

Then the factor of safety of every components acting individually and combined including the coconut tree acting at the top was considered. The next analysis was to see the impact of root reinforced soil. Again only one half of the bund was model. Soil model was a single layer Mohr-Coulomb material. Additional soil shear was considered for root-mat tensile strength. First the 3m high TGSB with plain soil was modelled for finding factor of safety. Next 3m high TGSB with root reinforced soil was modelled for finding factor of safety. This analysis was repeated for TGSB of 6m and 9m heights. The next investigation was to

perceive the effect when water is retained on either bank of the TGSB. Then the total TGSB was modelled. Since Bishop's method was adopted for analysis it was critical to observe if any scope of error would result when other methods are used for TGSB analyses. The plain soil 3m high TGSB was modelled for factor of safety was using the various models offered in GEOSTUDIO 2019 SLOPE/W.

4.5.3 GeoStudio 2019 SEEP/W analysis

Geostudio2019 has separate software SEEP/W to measure seepage. As some TGSBs retain water the seepage amount should be in manageable limits. The material limitation necessitated some adjustments (Figure 4.47). The total pressure head shows the flow net while the flux gives the seepage.

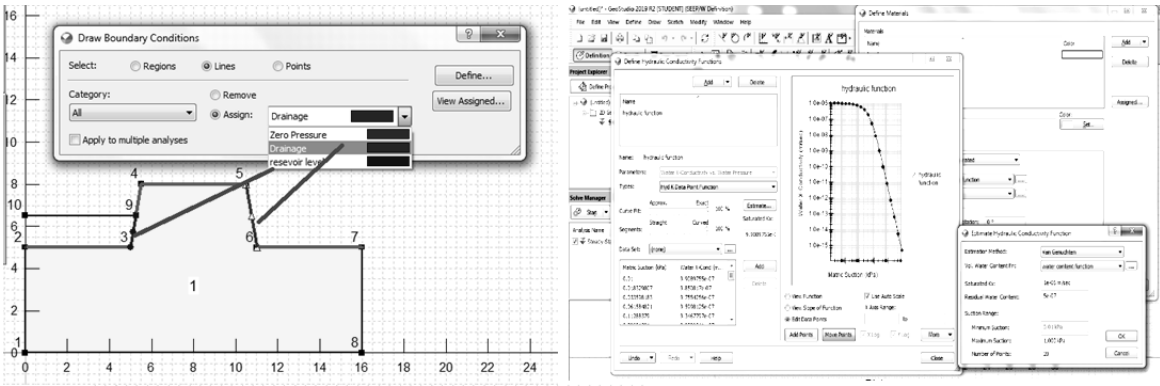


Figure 4.47 Drawing the Boundary Conditions for seepage analysis in GeoStudio.

First a 3m TGSB was analysed and the seepage at the toe was in the range $2e-7$ to $4e-7$ m^3/sec per m^2 of face area which is quite low considering that although the water conductivity was quite high as it was model as a silt-sand backfill. However due to TGSB soil stabilization the actual value will be even lower. The flow net and water pressure head is within the safe zone. Next a 6m TGSB was analysed and the seepage at the toe was in the range $6e-7$ to $8e-7$ m^3/sec per m^2 of face area which is quite low although higher than that of 3 m TGSB. The flow net and water pressure head is within the safe zone. The upstream faces show some high-pressure areas. Subsequently a 9m TGSB was analysed and the

seepage at the toe was in the range $8e-7$ to $10e-7$ m^3/sec per m^2 of face area which is quite low although higher than that of 6 m TGSB (Figure 4.48).

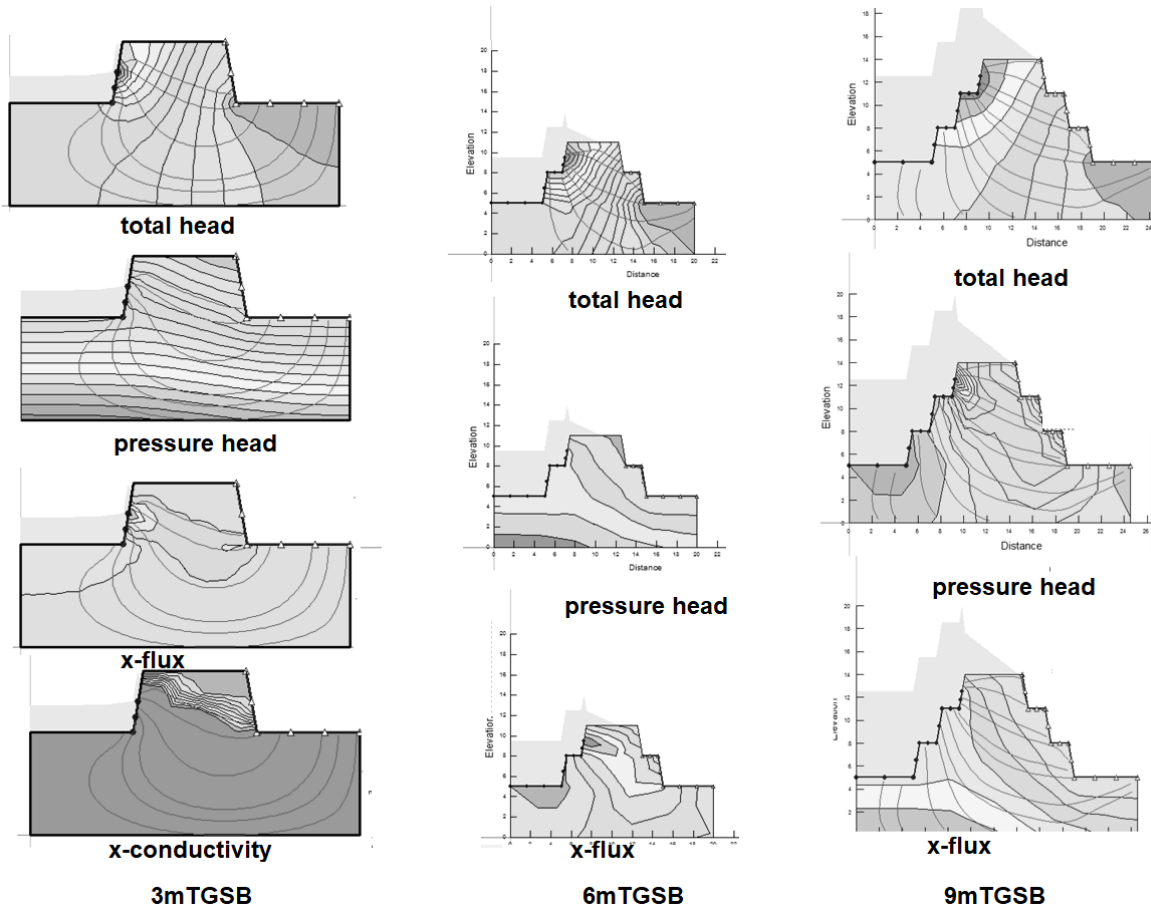


Figure 4.48 Results from GEOSTUDIO 2019 SEEP/W for TGSB.

The water pressure head is within the safe zone. The upstream faces show some high pressure areas in the flow net (Total water head). This is because the bund was analysed as unlined. In reality the TGSB has lateritic rubble facing. This analysis shows why the TGSBs tend to fail when the rubble facing is removed. The high pressure also acts as an additional destabilizing force if a thin concrete wall is built as is the modern practice as discussed in case studies in the appendix. This can cause them to fail if not taken into account.

4.5.4 GeoStudio 2019 QUAKE/W analysis

Geostudio2019 has software QUAKE/W to measure dynamic stability due to the earthquake. Earthquake can be inputted from excel sheets for analysis (Figure 4.49).

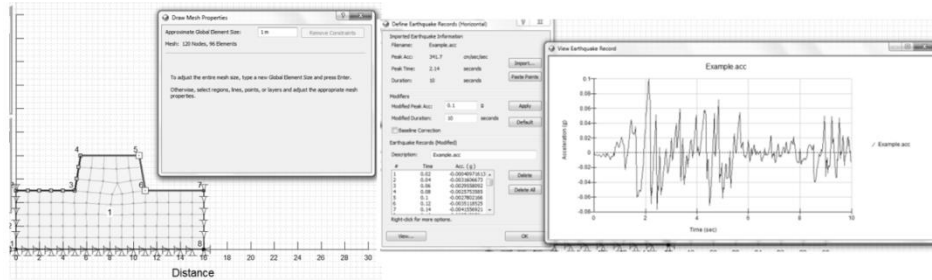


Figure 4.49 Defining earthquakes in GEOSTUDIO 2019 QUAKE/W.

Different sections were modelled and analyzed for seismic forces including one with coconut trees (Figure 4.50)

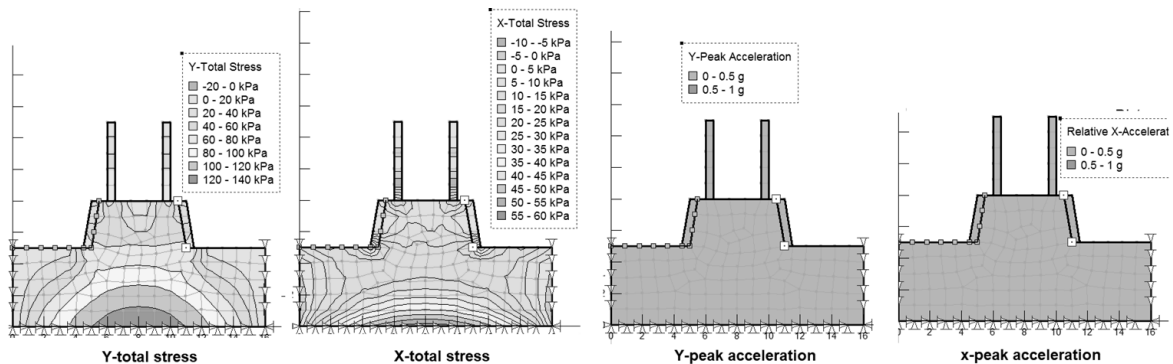


Figure 4.50 Results for ground acceleration in TGSB in GEOSTUDIO 2019 QUAKE/W in 3m TGSB.

First the 3 m TGSB was modelled and the displacements and stresses in both the directions were studied. The original and deformed mesh is seen. The deformation and stresses were measured including the cyclic stress for liquefaction potential. The procedure was repeated for 6 and 9 m TGSB also.

4.6 Midas Analysis of TGSB

Midas-GTX-NX (Geo Technical Solutions-New eXperience) is an Integrated Finite Element Solver Optimized for the next generation 64-bit platform. There are many element types available in Midas for FEM analysis: solid, truss, beam, shell, interface, rigid link etc. GTS NX is used all over the world (Lv 2013), (Doshi et al 2015), (Le and Dao 2015),(Raji et al 2016), (El-Kadi 2016), (Andreea 2016), (Pilecka et al 2016), (Baoliang et al 2017), (Koda et al 2017),(Su et al 2018), (Souza and Savoikar 2019a),(Yanina et al 2019), (Saini and Goyal2019), (Gao et al 2020), (Gao et al 2020), (Lv 2020) for major projects and is fast gaining popularity. It was used to do 3D analysis of the TGSB.

4.6.1 Steps used in this software Midas for analysis of TGSB

The software was used for TGSB analysis using reasonable simplifications as explained below. Midas must be done in a fixed rigid sequence of steps to get accurate results. There are an elaborate set of steps to be followed. Each step must be rigidly followed in particular order. The soil and root-soil-mass were modelled as a Isotropic Mohr-Coulomb material while the roots was modelled as Isotropic Elastic pile material with these properties: Young's Modulus E , poisons ratio ν , density γ , cohesion c , friction angle ϕ , initial void ratio e_0 , and damping factor. It is shown in the following flow chart (Figure 4.51).

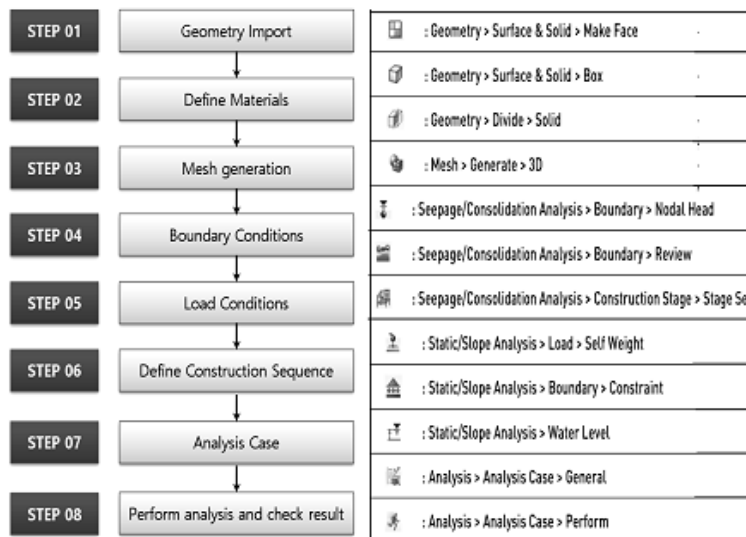


Figure 4.51 Flow-chart for Midas Analysis

4.6.2 Model used for analysis.

Initial attempts at modelling the roots as root piles failed due to the extremely high meshing and limitation of computer RAM. The horizontal root mass was finally model as a horizontal root-soil-mass or root-zone with enhanced soil cohesion and adhesion due to effect of root acting as 3-D tensile reinforcement in the zone (Figure 4.52).

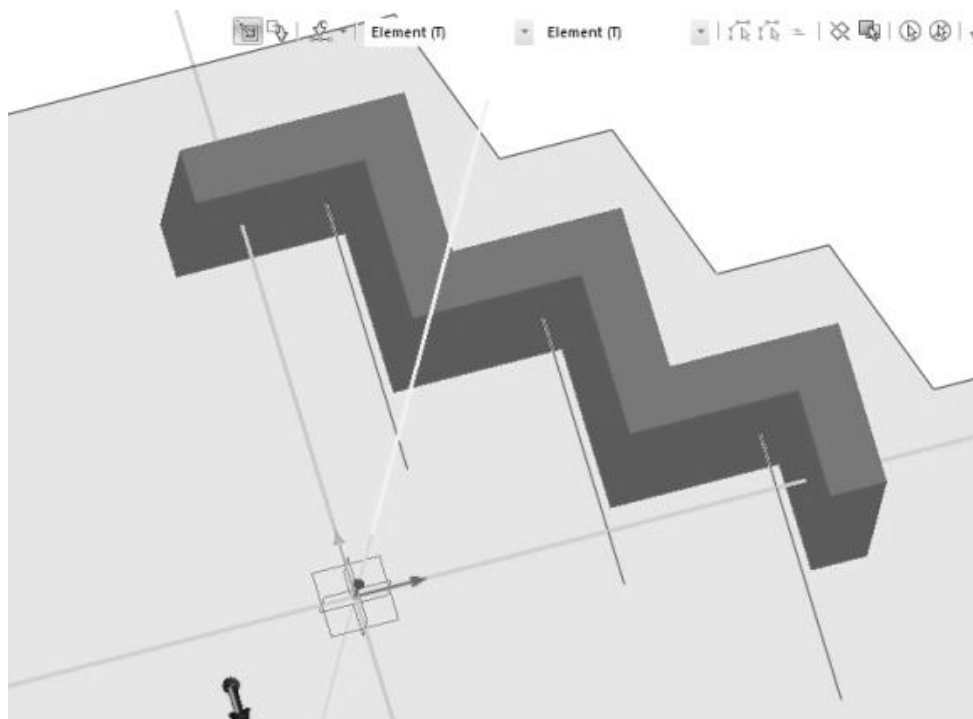


Figure 4.52 Modelling of roots as horizontal soil-mat with enhanced shear parameters

The horizontal root mass was modelled as a continuous layer below the surface 1 meter thick for the full extent of the bund 6 m each side of the tree. The vertical mass of roots was model as a single pile element.

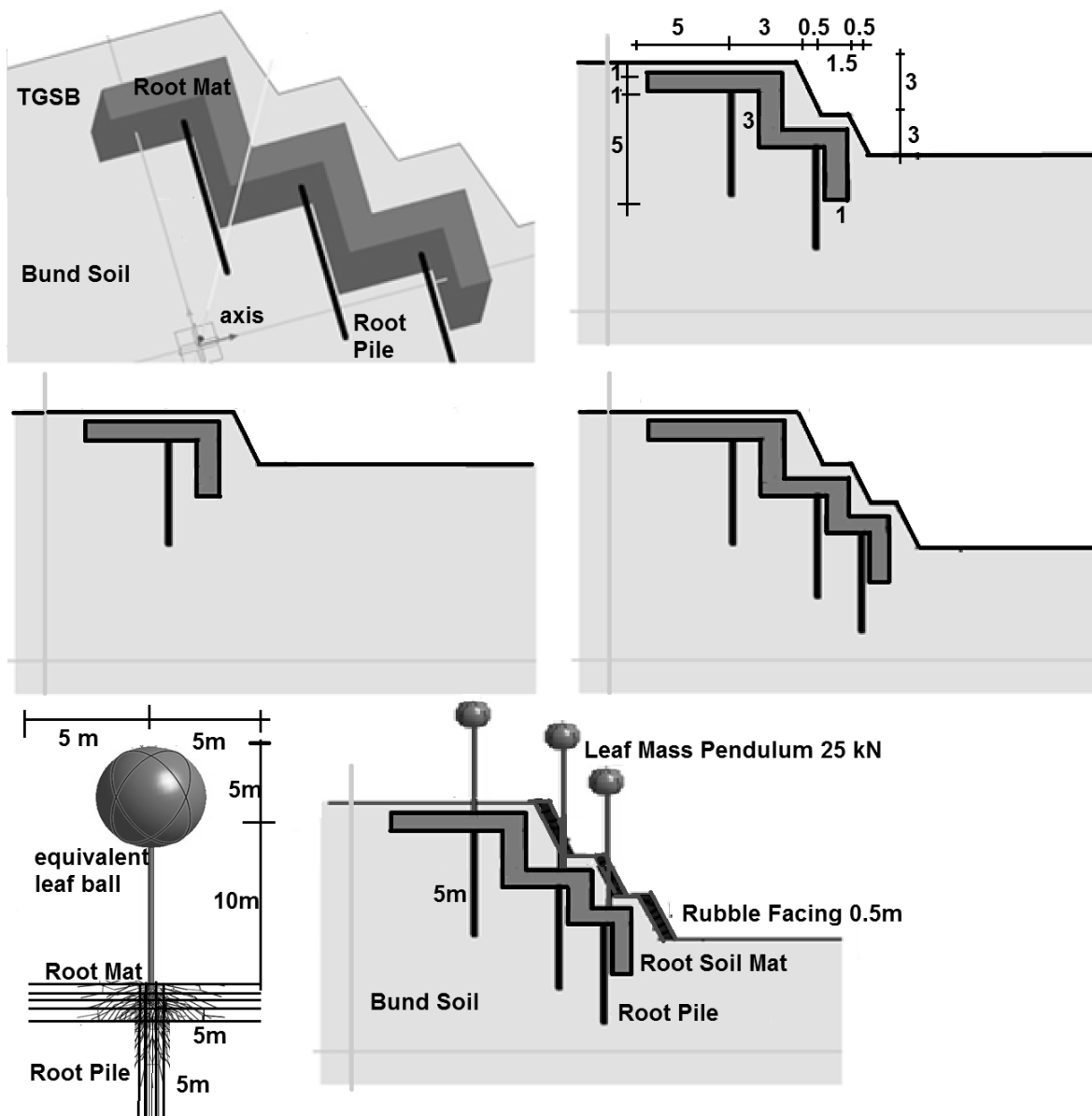


Figure 4.53 Different models prepared for Midas analysis

A total of six computerized models were prepared (Figure 4.53). Three with roots and three without roots for heights of 3, 6 and 9 meters each (only models with root mass are shown).

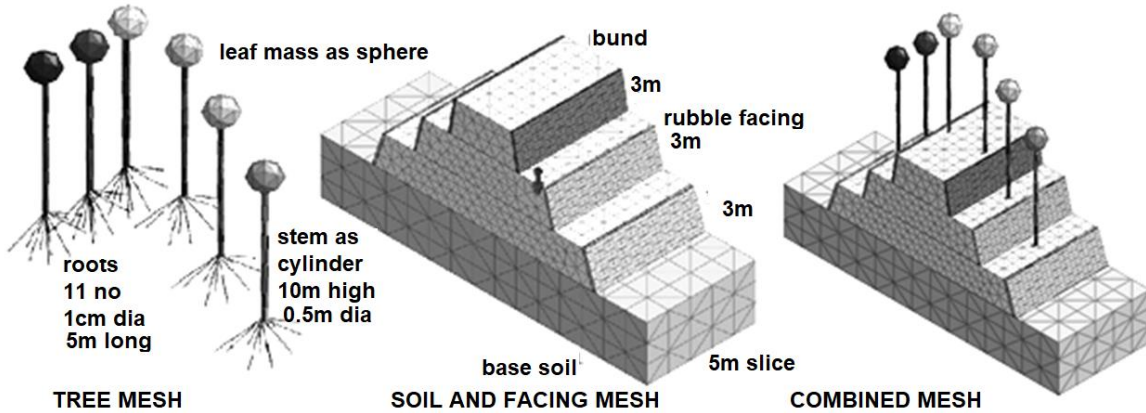


Figure 4.54 Initial Meshed model for 9m TGSB in Midas analysis

Initial modelling was tried with root as micro-piles as shown above (Figure 4.4) but due to computer memory restrictions the root mat model was adopted. The coconut tree was model as a 0.5m diameter cylinder and the leaf mass was model as a sphere 25kN in weight. The leaf mass acted as an inverted pendulum that helped in damping the vibrations caused by dynamic loading by earthquake loads. All layers were assigned properties and meshed (Figure 4.54). The root mass is model below the soil as a continuous root-mat 1 m thick 0.5 m below the surface. As it extends 5 m both sides of the tree it meets the one below.



Figure 4.55 Stresses due to static forces in Midas analysis for 9m, 6m and 3m TGSB

The stresses, deflections and factor of safeties were measured for different height TGSBs for static condition as well as dynamic condition (Figure 5.55).

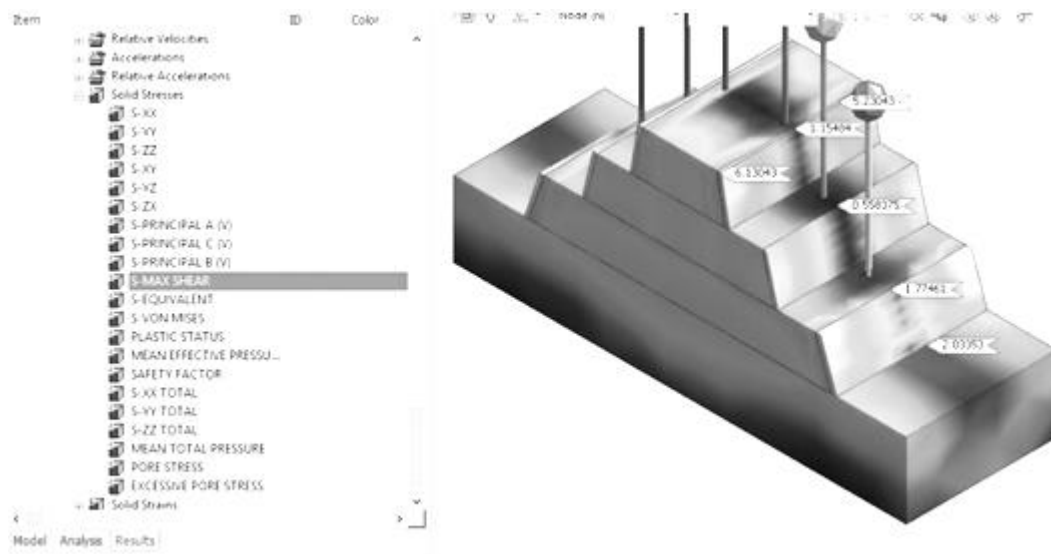


Figure 4.56 Shear in Midas analysis due to earthquakes for 9m TGSB

The results of shear stress in the TGSB for dynamic analysis were measured at top and at toe of each bream for different height TGSBs (Figure 4.56).

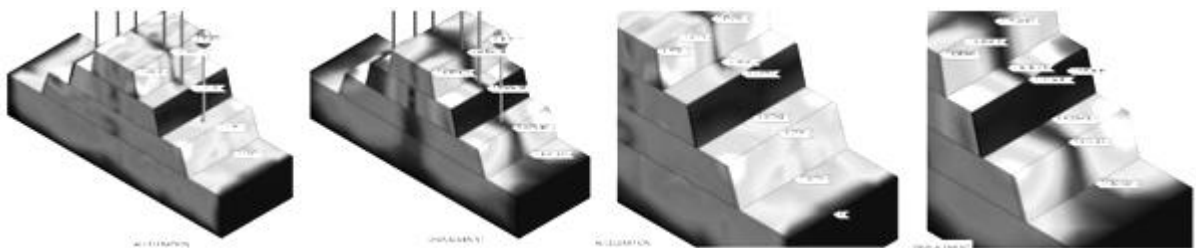


Figure 4.57 Acceleration and displacement in Midas analysis due to earthquakes for 9m TGSB

The acceleration and displacement caused by earthquake as result of dynamic analysis were measured at top and at toe of each bream for different height TGSBs (Figure 4.57).

4.7 Summary

The TGSB were analysed for safety both statically and dynamically using computer software like Microsoft Excel, Geostudio2019 and Midas-GTX-NX. There are many software available in the market but they all have the same shortcoming no software is

available to model the complex root system of coconut tree root mat. This has necessitated certain simplifications which were used in this analysis. The analysis covered liquefaction and tsunami threat also as these often accompany earthquakes along the coast. The spread sheet based analysis was carried out for Spread Sheet Based Slope Stability Analysis, Spread Sheet Based Liquefaction Analysis and Spread Sheet Based Tsunami Analysis. The spreadsheet based slope stability analysis was done for Static Slope Stability Analysis, Dynamic Slope Stability Analysis, Pseudo Static Slope Stability Analysis, Spectral Pseudo Dynamic Analysis and Simplified Pseudo Dynamic Analysis. The spread sheet based liquefaction analysis was done for Liquefaction potential and Liquefaction settlement. The spread sheet based tsunami analysis was carried out for Hydraulic Jump Analysis and Experimental Verification of Analysis. The software based analysis was carried out using the different parts of Geostudio-2019 and Midas. The different approaches and the procedures followed in this thesis are outlined in this chapter. The results of the analysis and their discussions are tabled in the next chapter.

CHAPTER 5

RESULTS AND DISCUSSIONS

5.1 Results of Computerized Analysis of TGSB

The results of the different analysis carried out in the previous chapter has been tabulated and analyzed in this chapter. The results are presented in the same order as the analysis in the previous chapter. The results of spread sheet based slope stability analysis have been further divided into the following categories: Static Slope Stability Analysis, Dynamic Slope Stability Analysis, Pseudo Static Slope Stability Analysis, Spectral Pseudo Dynamic Analysis, and Simplified Pseudo Dynamic Analysis. The results of spread sheet based liquefaction analysis have been further divided into the following categories: Liquefaction potential analysis and Liquefaction settlement analysis. The results of spread sheet based tsunami analysis have been further divided into the following categories: Hydraulic Jump Analysis and Experimental Verification. The results of software based analysis have been further divided into the following categories: Geostudio-2019 Analysis and Midas Analysis. Discussions on the results are presented after the results in the same order. Finally a comparison of the different results has been carried out so that reasonable and logical conclusions can be drawn.

5.2 Results of Spreadsheet Based Analysis

The values of different parameters were inputted in Microsoft excel spreadsheet. Suitable formulae were generated in the respective cells to obtain the results. Spread sheet analysis was carried out for existing TGSB of 3m, 6m and 9 m height as found to be in existence in Goa and also for 12 m height just to see if it safer for higher embankments too.

5.2.1 Summary of Results obtained for each type of force acting on the TGSB

Before calculating the FoS the forces and moments acting on the TGSB due to different actions were found out. The following forces were found out: Wave pressure force, Wind

pressure horizontal force, Vehicular pressure force, Wind pressure vertical force, Earth pressure force, Max Vehicular Weight, Seismic horizontal force, Seismic vertical force, Uplift force, Hydrostatic force, Hydrodynamic force, Tree force and Self-weight force.

The following Moments were also found out: Base moment, Wave pressure moment, Wind pressure moment, Earth pressure moment, Vehicular pressure moment, Seismic moment, Uplift moment, Hydrostatic moment, Hydrodynamic moment, Tree moment and Self-weight moment.

Table 5.1 Summary of forces for various heights of bunds

Force (kN)				
Moment(kN.m)				
TGSB Height (m)	3	6	9	12
Wave pressure force	21.72	52.66	108.88	185.77
Wind pressure horizontal force	566.55	1133.1	1699.65	2266.2
Vehicular pressure force	0.09	0.36	0.8	1.43
Wind pressure vertical force	-20.4	-40.79	-61.19	-81.58
Earth pressure force	10.99	40.1	98.31	185.63
Max Vehicular Weight	50	50	50	50
Seismic horizontal force	16.67	66.69	150.04	266.74
Seismic vertical force	8.34	33.34	75.02	133.37
Uplift force	45	225	525	945
Hydrostatic force	11.25	101.25	281.25	551.25
Hydrodynamic force	11.43	45.74	102.91	182.95
Tree force	20	40	60	80
Self-weight force	163.35	668.25	1410.75	2390.85
Base moment	5665.51	11331.02	16996.53	22662.04
Wave pressure moment	154.23	1438.5	9903.24	36951.52
Wind pressure moment	1699.62	6090.31	14871.68	26769.02

Earth pressure moment	22.03	102.41	313.76	743.41
Vehicular pressure moment	0.18	1.43	4.81	11.4
Seismic moment	33.34	266.74	900.26	2133.95
Uplift moment	90	750	2450	5670
Hydrostatic moment	5.63	151.88	703.13	1929.38
Hydrodynamic moment	5.72	68.61	257.28	640.33
Tree moment	31.5	185	338.5	492
Self-weight moment	490.05	3341.25	9875.25	21517.65

The summary of the forces and moments acting on the TGSBs using calculated as per equations given in the previous chapter are shown in Table 5.1. They were grouped into respective categories to find out their combined Factors of Safety (FoS) for different conditions both Static and Dynamic.

5.2.2 Results of Static factor of safety

As TGSB are used different purposes including for infrastructure (on landside for transportation, slope stabilization, habitation etc.) and for water retaining (on waterfront for rainwater harvesting, river training etc.).

Consequently the static factor of safety of the bunds for sliding and overturning are found out for two conditions: -water-retaining TGSB and plain TGSB with no water retained or plain (Table 5.2). The factor of safety was found out for sliding and overturning at toe.

The following factors of safety were found out FoS_{SS-w} (Static Sliding-water retaining), FoS_{SO-w} (Static Overturning -water retaining), FoS_{SS} (Static Sliding-plain), FoS_{SO} (Static Overturning -plain), FoS_{SG} (Static Global-plain),

Table 5.2 Static Factor of Safety for different bund heights

		TGSB Height (m)	3	6	9	12
Water	FOS _{SS-W}		196	18	6.9	4.
Retained	FOS _{SO-W}		4.6	2.4	1.95	1.75
No Water	FOS _{SS}		186	52	22	14
Retained	FOS _{SO}		54	49	41	35
	FOS _{SG}		8.9	2.49	2.3	1.98

All Static factor of safety were found out to be well above 1.5 for both sliding and overturning (Table 5.2).

5.2.3 Results of Dynamic factor of safety

Different dynamic loads can act on TGSB. Some act independently and some act in combination with others. Normal sea-breeze is 15 kmph in Goa. Recent cyclones to hit Goa in 2019 and 2021 had winds of 150 to 180 kmph. Maximum earthquake acceleration for the zone in which Goa falls is 0.11. All these were factored into the resulting values.

The values of the dynamic factor of safety were found out using for the following conditions:

1. Dynamic Full– vehicular, earthquake, wind, hydro-dynamic (Table 5.3).
2. Dynamic earthquake forces only (Table 5.4).
3. Dynamic normal wind forces only – wind velocity 4.4m/s or 15kmph (Table 5.5).
4. Dynamic cyclonic wind forces only – wind velocity 44m/s or 158 kmph (Table 5.6).

The following factors of safety were found out FoS_{DS} (Dynamic Sliding-All Loads), FoS_{DO} (Dynamic Overturning -All Loads), FoS_{DS-E} (Dynamic Sliding-Earthquake only), FoS_{DO-E} (Dynamic Overturning - Earthquake only), FoS_{DG-E} (Dynamic Global- Earthquake only), FoS_{DS-W1} (Dynamic Sliding- Normal Wind only), FoS_{DO-W1} (Dynamic Overturning - Normal Wind only), FoS_{DS-WC} (Dynamic Sliding- Cyclonic Wind only), FoS_{DO-WC} (Dynamic Overturning - Cyclonic Wind only),

Table 5.3 Dynamic Factor of Safety for different bundheights if all loads act simultaneously

TGSB Height (m)	3	6	9	12
FOS _{DS}	2.576	1.878	1.568	1.529
FOS _{DO}	1.449	1.016	0.724	0.587

When all dynamic forces act the Dynamic factor of safety varied from 2.576 to 1.529 in sliding and from 1.449 to 0.587 for overturning (Table 5.3).

Table 5.4 Dynamic Factor of Safety for different bundheights when only maximum earthquake acts

TGSB Height (m)	3	6	9	12
FOS _{DS-E}	32.409	8.446	3.844	2.613
FOS _{DO-E}	8.859	5.128	3.968	3.418
FOS _{DG-E}	4.500	1.981	0.956	0.830

When only earthquake force acts the Dynamic factor of safety varied from 32.409 to 2.613 in sliding, from 8.859 to 3.418 for overturning and from 4.500 to 0.830 for general slope failure (Table 5.4).

Table 5.5 Dynamic Factor of Safety for different bund heights if normal wind only acts

TGSB Height (m)	3	6	9	12
FOS _{DS-WI}	31.403	14.237	8.455	6.715
FOS _{DO-WI}	2.186	4.277	6.657	8.979

When normal wind force acts the Dynamic factor of safety varied from 31.403 to 6.715 in sliding and from 2.186 to 8.979 for overturning. The increase in the FoS with height is due to aerodynamic effect of the tree canopy causing damping (Table 5.5).

Table 5.6 Dynamic Factor of Safety for different bund heights if Cyclonic wind only acts

TGSB Height (m)	3	6	9	12
FOS _{DS-WC}	3.701	1.880	1.279	1.147
FOS _{DO-WC}	0.227	0.464	0.778	1.163

When cyclonic winds act the Dynamic factor of safety varied from 3.701 to 1.147 in sliding and from 0.227 to 1.163 for overturning (Table 5.7).

5.2.4 Results of Pseudo Static Safety of TGSB

The pseudo static factor of safety was found out using IS code method as described in the analysis chapter and taking the earth quake acceleration as 0.11. The pseudo-static FoS is found out for two conditions first for plain TGSB without roots and next for TGSB considering improved cohesion and friction due to roots. Pseudo static factor of safety was found out for existing TGSB of 3m, 6m and 9 m height as found to be in existence in Goa.

Table 5.7 Pseudo static Factor of Safety of TGSB as per IS Code

TGSB Height (m)	3	6	9	12
FoS No roots	2.002	1.654	1.263	1.104
With roots	3.741	3.096	2.380	2.208

The IS code method shows the improvement in pseudo-static factor of safety with presence of roots in TGSB (Table 5.7). When only earthquake force acts the pseudo-static factor of safety varied from 2.002 to 1.104 for general slope failure when roots are absent and from

3.741 to 2.208 when roots are present. It is seen that there is almost doubling of safety with presence of roots in TGSB.

5.2.5 Results of the Simplified Spectral Force Based Pseudo-Dynamic-Analysis

Spectral force is the force calculated from response spectrum given in the IS code 1893 for earthquakes as described in analysis chapter. It gives a rough estimate of Dynamic FoS. Spectral Pseudo Dynamic FoS was found out for existing TGSB of 3m, 6m and 9 m height as found to be in existence in Goa.

Table 5.8 Simplified Spectral Force Based Factor of Safety

TGSB Height (m)	3	6	9
Damping Ratio	2.98	3.77	4.32
Vs	130	158	182
Ts	0.092	0.152	0.198
Spectral Force	0.11	1.35	4.53
Dynamic Force	1.08	13.24	44.44
Static Force	26.73	106.92	240.57
Sliding force	27.80	120.164	285.009
Resisting force	186.94	436.212	747.792
Factor of Safety	6.72	3.63	2.62

The pseudo dynamic factor of safety by Simplified-Spectral-Force Pseudo-Dynamic Method varies from 6.72 to 2.62 and is well above 1.5 for 3m 6 m and 9mTGSB (Table 5.8).

5.2.6 Results of Simplified Pseudo Dynamic Safety of TGSB

Pseudo dynamic force method considers the effect of man factors influencing earthquake as described in the analysis chapter. It is rather broad based though many empirical simplifications made by past researchers have been incorporated and hence will tend to

give a more accurate result. Simplified Pseudo Dynamic FoS was found out for existing TGSB of 3m, 6m and 9 m height as found to be in existence in Goa.

Table 5.9 Factor of Safety from Simplified Pseudo-Dynamic Analysis

	TGSB Height (m)		
	3	6	9
W_a	3.605	12.224	26.182
W_p	14.54	19.945	16.182
Q_a	11.268	25.827	41.660
Q_p	0.931	0.866	0.531
Factor of Safety	2.762	2.032	1.077

The pseudo dynamic factor of safety by simplified Pseudo-Dynamic method is above 1.0. The simplified pseudo dynamic factor of safety varies from 2.762 to 1.007 for TGSB (Table 5.9).

5.2.7 Results of Liquefaction Safety of TGSB

One major disaster in sandy soils is Liquefaction. The susceptibility for liquefaction is quantified using the LPI (Liquefaction Potential Index) as described in the analysis chapter. The liquefaction potential was found out using data from borehole logs for seven locations covering Goa.

Table 5.10 Liquefaction Potential Index for soil profiles at Goa

location	Mapusa	Panjim	Vasco	Margao	Ponda	Canacona	Bicholim
LPI	0.405	0.389	0.376	0.389	0.374	0.386	0.394

The LPI varies from 0.374 to 0.405 for TGSB in Goa (Table 5.9).As it is between 0 and 2 the incidence is extremely low. Liquefaction also results in settlement due to densification

and compaction of soils by violent shaking of wet saturated soil and realignment of particles.

Table 5.11 Liquefaction Settlement mm of soil profile at Goa

location	Mapusa	Panjim	Vasco	Margao	Ponda	Canacona	Bicholim
Settlement	1.0	0.5	0.25	0.2	0.04	0.25	0.1

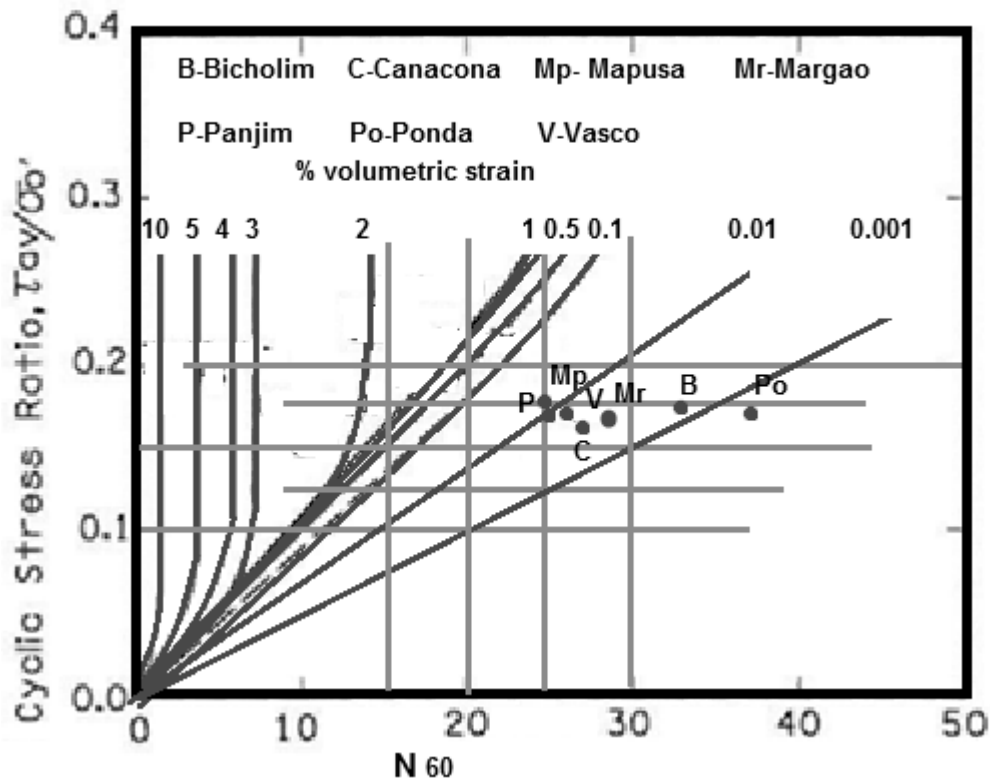


Figure 5.1 Plot of Liquefaction settlement strains in Goa

The displacement caused due to cyclic loading during earthquake of M 5.5 magnitude were calculated (Table 8.20 to 8.25). The displacement from the Tokimatsu and Seed 1987 criteria for strains in sand-like soils is less than 2.5 mm in all TGSBs (Figure 4.89).

5.2.8 Results of Tsunami Safety of TGSB

Tsunamis cause increase in velocity and quantity of water discharged into the land. A hydraulic jump can reduce the discharge. Effect of tsunami with different height TGSB without trees and 3m TGSB with tree were studied after the hydraulic jump.

Table 5.12 Tsunami Velocity and Quantity change by using TGSB

Initial Values		y ₁	0.5	1	2	3	4	5	10	%
		Q	5000	10000	20000	30000	40000	50000	100000	
V₄	no tree on	3	4.5	9.2	13.1	15.2	16.6	17.8	21.2	
m/s	top	6	-	-	7.5	11.1	13.3	14.8	19.3	
		9	-	-	-	4.1	8.7	11.2	17.1	
	tree on	3								
	top		-	-	-	-	-	-	7.5	
Qf	no tree on	3	1251	2068	2684	3036	3294	3500	4202	0.042
m³/s	top	6	-	-	1851	2466	2833	3103	3941	0.039
		9	-	-	-	1261	2136	2566	3639	0.036
	tree on	3								0.021
	top		-	-	-	-	-	-	2097	

The values for different wave heights have been calculated using Microsoft excel. Calculations carried out for 3m with 15 m coconut trees on the top show that it protects up to 8m Tsunami waves (Table 5.12).

Table 5.13 Experimental and calculated Tsunami Wave Height for 3m TGSB without trees

Experimental	h1	m	1	2	3	5
		h2	m	0.75	1.5	1.9
	reduction	%	25	25	36	38
Calculated	h1	m	2.0	4.5	8.2	9.9
	h2	m	1.6	3.3	5.3	6.1
	reduction	%	27	27	35	38

Model experimental setup values were compared with the calculated values. The values for different wave heights have been calculated using Microsoft excel matched with the values found out during the experimental setup.

5.3 Results of Software Analysis of TGSB

Two software GeoStudio2019 and Midas GTX-NX were used in the analysis of the TGSB. In GeoStudio2019 the analysis was split into three components stability analysis by SLOPE/W, seepage analysis by SEEP/W and dynamic analysis by QUAKE/W. In Midas all analysis can be done in single file using Stages. The results are given below.

5.3.1 Results of GeoStudio Analysis of TGSB

Geosudio2019 analysis was systematically performed considering different possibilities.

Table 5.14 Factor of Safety using diverse components for 3 m TGSB

Components	FoS	%
Soil without roots	1.828	Increase
Soil with roots	4.486	245.40
Soil with lateritic facing wall	3.597	196.77
Soil with root pile	4.398	240.59
Soil with all components	3.637	198.96

First the impact of different components, individually and separately were studied. Next the effect of roots as a mat was considered. Then the different soil models were studied. After this the seepage and earthquake analysis was done. Further the effect of real earthquakes in the world was calculated. The results were tabulated and the increase of strength in percentage was compared over the unreinforced soil. There is overall 200% rise in Factor of safety from the complementary parts that the TGSB has. Initially plain soil TGSB was modelled for factor of safety. Then root reinforced soil TGSB was modelled for factor of safety. Soil model was a single layer Mohr-Coulomb material with additional strength parameters to account for root strength.

Table 5.15 Factor of Safety for TGSB compared with and without roots

Bund Height	FoS for landward TGSB		% Increase	FoS for seaward TGSB	
	no roots	with roots		seaward	leeward
3 m	1.828	4.486	245.40	1.734	1.848
6 m	1.340	2.784	207.76	1.489	1.259
9 m	1.126	2.284	202.84	1.234	0.904

The comparative results were tabulated for percentage increase of FoS of reinforced soil as to unreinforced soil (Table 5.15).

The next analysis dealt with impact of water retaining TGSB. Here the bund only was modelled. Initially TGSB was modelled for factor of safety on the seaward side. Then TGSB was modelled on the leeward side for factor of safety. The FoS on either demonstrated a general decrease in safety on the leeward side when compared to the seaward side. However for a 3m TGSB the opposite case occurred as the soil was unsaturated in the slip circle above the piezometric line. The Factor of safety versus height plotted on a graph of showed linear reduction in safety on leeward and seaward side, more so, on the leeward side.

Bishop’s method was selected for analysis and compared with different other methods for TGSB analysis. 3 m high TGSB with plain soil was modelled for factor of safety using the different methods found in GEOSTUDIO 2019 SLOPE/W. The comparison of tabulated values (Table 5.16) showed that the error margin in any other method is extremely small and the average FoS of all methods is almost 100% matching with Bishops’ method.

Table 5.16 FoS from Different soil models.

Soil Model	FoS	Difference	
Ordinary Bishop’s	1.828	amount	%
Ordinary method of slices	1.788	-0.400	97.81
Janbu	1.850	0.022	101.20
Morgenstern-Price	1.826	0.002	99.89
Spencer	1.889	0.061	103.33
Average	1.836	0.008	100.43

Next TGSB were examined in GeoStudio2019 SEEP/W for seepage at the toe.

Table 5.17 Results of seepage from SWEEP/W

	Bund Height			
	m	3	6	9
Total head	m	1.5	4.5	7.5
Flux at toe	(m³/s)/m²	2e-7	5e-7	6e-7

The leakage from a TGSB is 0.0000006 (m³/s) per m² face area, which indicates that even a 9 m high bund leaks a very small quantity of 0.05 m³ or 51 liters of water per day at highest fill level (Table 5.17) and is taken care of by root absorption of the tree.

Coconut roots act as natural geotextiles to reinforce soils. Studies of Coir fibre reinforced soil have shown such soil have more elasticity and less plasticity with a significant damping.

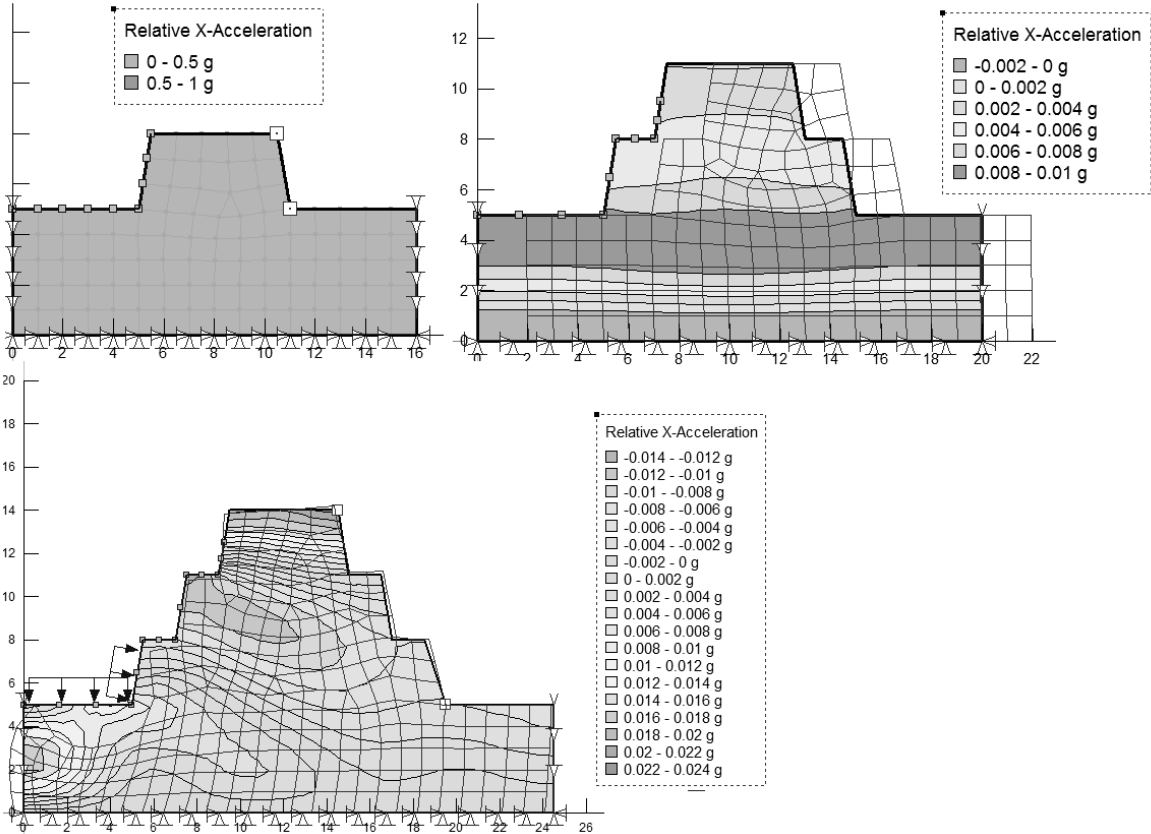


Figure. 5.2 Horizontal acceleration and deformation of TGSB caused by earthquake

Coconut roots similar in structure to a bundle of coir fibres give comparable damping. They act as elastic springs. The 3m, 6m and 9 m TGSB were analysed in GeoStudio2019 QUAKE/W to find displacements, accelerations, horizontal and vertical stresses, (Table 5.18). Stresses increased with height of TGSB. Because vibration mode varies with height, Displacements and Accelerations decreased with height of TGSB (Figure 5.2).

Table 5.18 Results of QUAKE/W analysis

Bund height	Horizontal Stress		Vertical stress		Displacements		Accelerations	
	Toe	Top	Toe	Top	x	y	Toe	Top
m	kPa	kPa	kPa	kPa	kPa	kPa	g	g
3	5	40	15	20	0.05	0.05	0.05	0.05
6	5	60	5	20	0.001	0.001	0.003	0.008
9	5	60	5	20	0.0005	0.0005	0.008	0.022

Table 5.19 Dynamic Factor of safety of TGSB

Bund Height	Dynamic FoS	
	toe	top
3 m	2.0	2.0
6 m	33.3	12.5
9 m	12.5	4.5

Dynamic Factor of safety is estimated from ratio of input to output acceleration (table 5.19).

5.3.2 Seismic Effect Results of Different Real Earthquakes on TGSB in QUAKE/W

In order to estimate the viability of TGSB technology for regions other than Goa the TGSBs were analysed for selected real earthquakes (Figure 5.3).

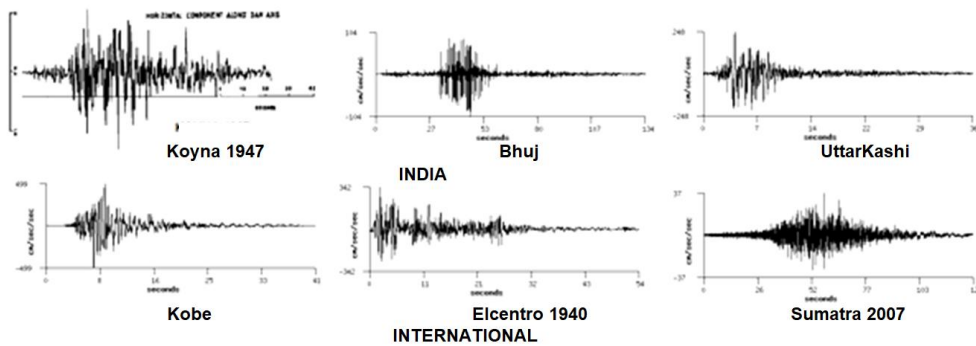


Figure. 5.3 Accelerograms of selected earthquakes (COSMOS strongmotion.org)

Three earthquakes in India (Bhuj, Utarkashi and Koyna) and three in world (El-Centro, Sumatra, and Kobe) were chosen. The default Software (SW) earthquake was compared to them. Only 9m TGSB was analysed since it has the least factor of safety.

Table 5.20 Comparison for QUAKE/W for earthquakes at 9m-TGSB Top

	India			International			
	SW	Koyna	Bhuj	Uttar Kashi	Kobe	El Centro	Sumatra
X-Total Stress	6.10	19.37	5.24	-5.28	25.49	118	13
Y-Total Stress	14.52	4.99	5.73	-1.10	-13.4	-179	20.89
Z-Total Stress	6.19	7.31	3.29	-1.92	3.62	-18.13	10.17
Mean- Effective Stress (p')	8.93	10.56	4.75	-2.77	5.24	-26.18	14.69
Max Shear stress	4.48	15.26	0.88	6.80	32.12	223	4.76
Deviatronicstress (q)	8.53	26.82	2.19	11.39	55.69	387	10.20
X-Strain	1.02	122	21.3	31	220	1368	30
Y-Strain	-1.89	-108	-61	77	-255	1694	21
Z-Strain	0	0	0	0	0	0	0
Cyclic Stress Ratio	0.014	0	0	0	0	0	0

All Stresses (kPa) All Strains (1e-05)

Table 5.21 Comparison for QUAKE/W for earthquakes at 9m-TGSB Toe

	India			International			
	SW	Koyna	Bhuj	Uttar Kashi	Kobe	El Centro	Sumatra
X-Total Stress	57.89	-679	96.47	1541	-840	-5302	-912
Y-Total Stress	72.39	-576	93.40	1190	-791	-5098	-658
Z-Total Stress	39.08	-376	56.96	819	-	-3120	-471
Mean- Effective Stress (p')	56.43	-544	82.28	1184	-707	-4506	-680
XY-Shear Stress	-	372	-	-892	456	2896	547
	35.83		39.01				
Max Shear stress	36.55	375	39.04	909	456	2892	562
Deviatronic stress (q)	69.00	699	79.46	1662	860	5463	1016
X-Strain	12	-32011	21.9	7045	-3687	21999	4585
Y-Strain	8.3	-2331	32.2	3376	-3347	20111	2204
Z-Strain	0	0	0	0	0	0	0
Cyclic Stress Ratio	0.036	0	0	0	0	0	0

All Stresses (kPa) All Strains (1e-05)

5.3.3 Results of Midas Analysis of TGSB

The static Factors of Safety for TGSBs of various heights with and without root reinforcement were analysed (Table 5.22).

Table 5.22 Static Factor of Safety of Slope

Bund Height	Factor Of Safety		
	3	6	9
Without roots	2.98	1.78	1.46
With roots	4.533	2.46	1.98
Increase	1.55	0.67	0.52
% Increase	34.2	27.3	26.2

The effect of pendulum damping due to the row of uniformly spaced coconut trees on top (the leaf mass is arbitrarily considered as a ball 1.5m diameter and 25kN in weight on top of a weightless rod 10 m high) was not considered and the additional factor of safety provided by the rubble facing that act as a flexible skin was also not considered.

The dynamic stability was also analysed. It was seen that there was a significant improvement in the dynamic stability of the slope on addition of roots alone. The displacements in X (horizontal) and Z (vertical) directions and the principal stresses were found out for bunds of various heights with and without root reinforcement the results for TGSB reinforced by root piles and root mat displayed nearly zero displacements and stress throughout the earthquake.

Table 5.23 Horizontal and vertical displacements

Distance from bottom		Horizontal displacements Tx for bunds of heights			Vertical displacements Tz for bunds of heights		
		9m	6m	3m	9m	6m	3m
		9	Level 3	-0.0368			-0.004
6	Level 2	-0.0351	-0.039		-0.0017	-0.00038	
3	Level 1	-0.0344	-0.037	-0.0024	-0.0025	-0.0027	-0.0054
0	Toe	-0.0309	-0.026	-0.012	-0.0002	-0.0023	-0.0039

Table 5.24 Major and Minor Principal Stress

Distance from bottom	from	Major principal stress			Minor Principal Stress		
		9m	6m	3m	9m	6m	3m
9	Level 3	-1.54			-38		
6	Level 2	3.25	-1.45		-26	-41	
3	Level 1	4.02	5.19	23	-17	-22	-37
0	Toe	16.23	16	21	-31	-41	-34

5.4 Discussions on Results of Computerized Analysis

Today there is readymade software available to geotechnically analyse any structure. However, for basic computer users such calculations can also be done using spreadsheets. Both have been done in this thesis and the results are discussed below.

5.4.1 Discussion on Results of Spreadsheet based approach

There is overdependence on readymade software to analyse the seismic stability of embankments. Such software gives good results for standard structures but encounter some difficulty when unusual problem like TGSBs (vegetated earthen embankments) are to be analysed. In such circumstances Microsoft-excel spreadsheets are indispensable as they can give tailor made results. TGSBs are embankments. In Goa mostly TGSBS are 1 to 3 m high with rare 9m high. TGSBs of 12 m are not in existence in Goa but have been also analysed to find out if the TGSB height can be extended. These embankments are sustainable carbon negative and have withstood devastation floods and cyclones while performing their functions.

The static FoS is extremely high for normal TGSB < 3m high as the size is very small. For dynamic loads the factor of safety reduces to below 1 for TGSB > 9m height which implies failure in those particular conditions only, so proper caution has to be used when using this technology in earthquake prone zones. Factor of safety is highest for dry static and it

decreases with height. Factor of safety is lowest for dynamic overturning. All other conditions have lower factor of safety.

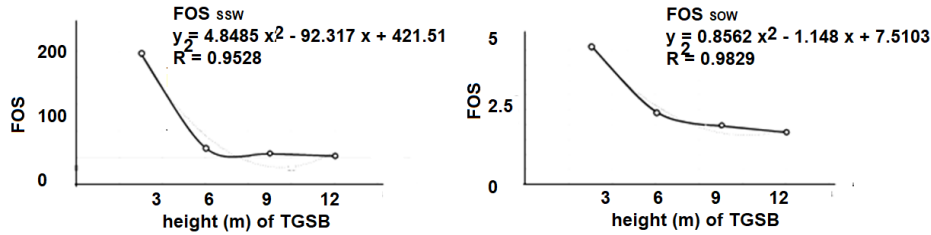


Figure. 5.4 Factor of safety for sliding and overturning for water retaining TGSB for static load

There is a sharp drop in Factor of safety for water retaining for static loading TGSB as the height increases from 3 to 6m (Figure 5.4). The Factor of safety levels off from 6 to 12 m almost becoming level after 12m. The critical height therefore is 6m.

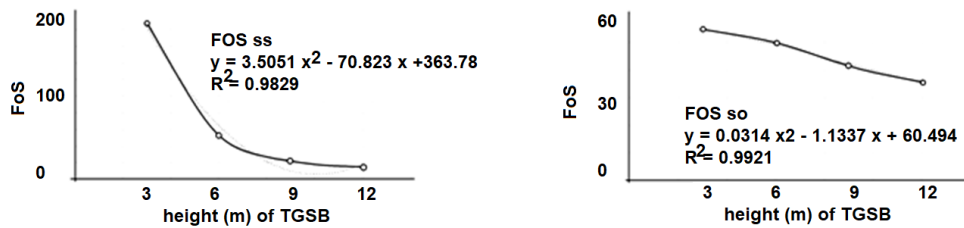


Figure. 5.5 Factor of safety for sliding and overturning for normal TGSB embankment for static load

There is a sharp drop in Factor of safety for normal for static loading TGSB as the height increases from 3 to 6m (Figure 5.5). The Factor of safety levels off from 6 to 12 m almost becoming level after 12m. The critical height therefore is 6m.

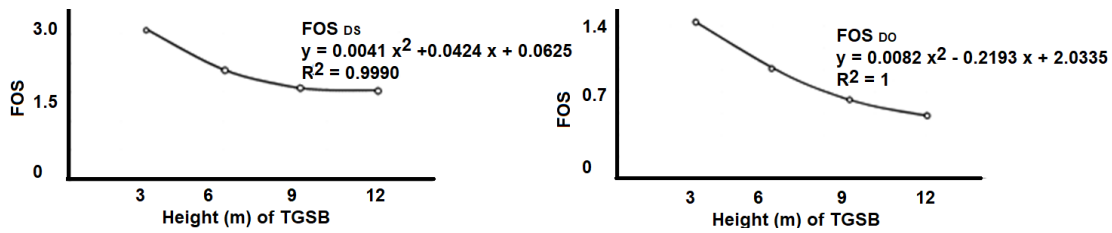


Figure. 5.6 Factor of safety for sliding and overturning for dynamic load

There is a sharp drop in Factor of safety for dynamic loading on TGSB as the height increases from 3 to 12 m (Figure 5.6). The Factor of safety levels off after 12 m. The critical height therefore is 12 m.

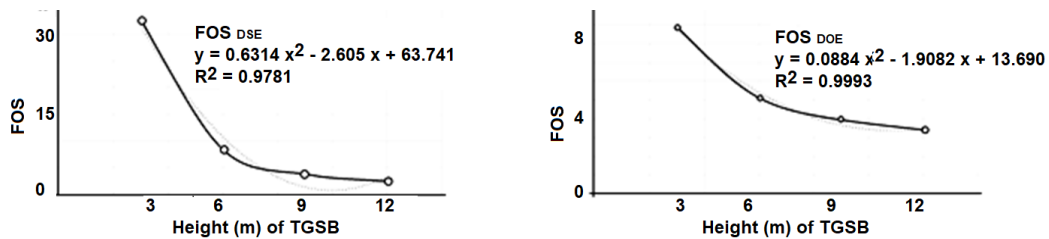


Figure. 5.7 Factor of safety for sliding and overturning for earthquake load

There is a sharp drop in Factor of safety for earthquake loading on TGSB as the height increases from 3 to 12 m (Figure 5.7). The Factor of safety levels off after 12 m. The critical height therefore is 12 m.

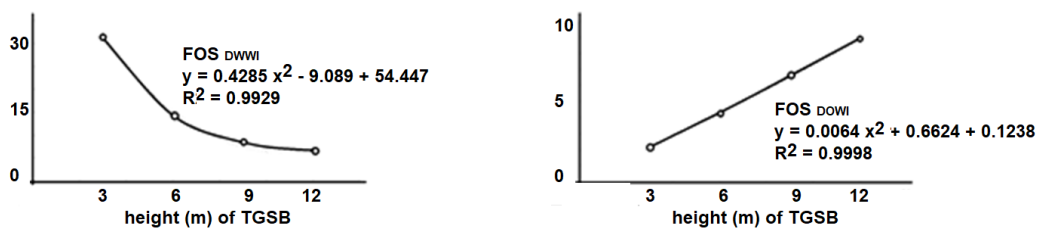


Figure. 5.8 Factor of safety for sliding and overturning for wind load

There is a sharp drop in Factor of safety of sliding for wind loading on TGSB as the height increases from 3 to 12 m (Figure 5.8). The Factor of safety levels off after 12 m. The

critical height therefore is 12 m. The overturning safety shows increase with increase in height as the weight of the embankment resists the overturning.

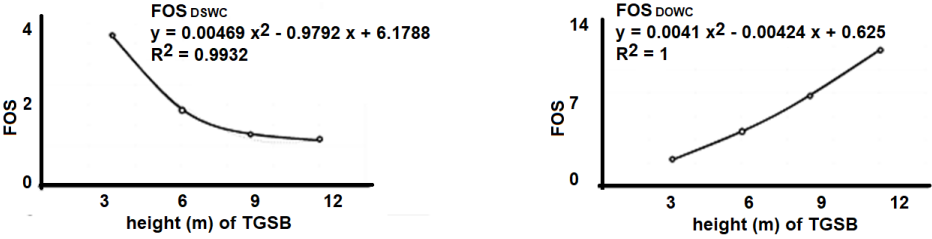


Figure. 5.9 Factor of safety for sliding and overturning for cyclonic load

There is a sharp drop in Factor of safety for cyclonic loading on TGSB as the height increases from 3 to 12 m (Figure 5.9). The Factor of safety levels off after 12 m. The critical height therefore is 12 m. The overturning safety shows increase with increase in height as the weight of the embankment resists the overturning.

5.4.2 Equations for factor of safety of TGSB based on Spreadsheet based approach

In order for applicability of results they should be applicable to All TGSBs of different heights. As all bunds are not of same height the Factors of safety can be estimated by using equations based on the data generated. Equation for trend line for factor of safety were generated using Microsoft excel. The Factor of Safety is given by (Y) and the height of the TGSB is given by (x) for different conditions (Table 5.25).

Most of the bunds are safe up to 6m height for all conditions except wind, because the enhanced factor of safety in overturning from anchorage of the TGSB to the ground was not considered in the analysis. However as stated in practice the bunds have survived the storms so in future analysis this must be considered.

Spread sheet analysis has shown that Factor of safety for less than 3 m TGSB is greatly high. The FoS approaches 1.5 as height rises to 12 m in worst case scenario for static conditions. In overall dynamic condition when all loads act the recommended height is less than 6m. In all other dynamic condition, the embankment is safe for sliding but in overturning the safety is showing opposite effect that needs further investigation as this is

not corresponding with the facts seen on the ground in the past several millennia of their existence.

Table 5.25 Equations for factor of safety of TGSB

Condition		Equation for factor of safety	R²	Max height
Sliding	Static-no water	$3.5051 x^2 - 70.823 x + 363.78$	0.9829	12
	Static-water	$4.8485 x^2 - 92.317 x + 421.51$	0.9528	12
Overturning	Static-no water	$0.0314 x^2 - 1.7337 x + 60.494$	0.9921	12
	Static-water	$0.0562 x^2 - 1.148 x + 7.5103$	0.9829	12
Sliding	Dynamic-general	$0.0041 x^2 + 0.0424 x + 0.0625$	0.9990	12
	Dynamic-earthquake	$0.6314 x^2 - 12.605 x + 63.741$	0.9781	12
	Dynamic-wind	$0.4285 x^2 - 0.9.089 x + 54.447$	0.9929	12
	Dynamic-cyclonic	$0.0469 x^2 - 0.9792 x + 6.1788$	0.9932	12
Overturning	Dynamic-general	$0.0082 x^2 - 0.2193 x + 2.0335$	1	6
	Dynamic-earthquake	$0.0884 x^2 - 1.9082 x + 13.690$	0.9893	12
	Dynamic-wind	$0.0064 x^2 + 0.6642 x + 0.1238$	0.9998	--
	Dynamic-cyclonic	$0.0041 x^2 + 0.0424 x + 0.0625$	1	--

They have survived multiple cyclones as well as one this year. Today modern embankments have been known to consistently fail. Such reliable and stable structures need to be recommended in similar tropical zones around the world.

5.4.3 Discussion on Results of Pseudo Static Approach

Pseudo-static approach relies on horizontal component of earthquake acceleration on a slope to estimate the factor of safety. It gives a rough overall picture of stability of slopes. It

is an easy method and part of many codes including IS code. For Goa region where the threat of earthquake is minimal this method can be used safely.



Figure. 5.10 Factor of safety for pseudo-static approach as per IS code

Results of pseudo-static analysis carried out for two conditions with roots and without roots show a sharp rise in Factor of safety when the TGSB is reinforced with coconut tree roots. The FoS is very high for lower height embankments and flattens out for higher embankments. The safety of TGSB with coconut tree roots is almost double that of TGSB without roots (Figure 5.10). Depending on pseudo-static factor of safety has its own inherent risk.

Representation the complex, dynamic and transient shaking effects of earthquake by a single unidirectional constant pseudo-static acceleration is noticeably inadequate. Terzaghi (1950), the father of soil mechanics, commented that “the concept it conveys of earthquake effects on slopes is very inaccurate, to say the least,” and that a slope may be unstable even when the pseudo-static factor of safety computed was bigger than 1. Practically the pseudo-static analyses are unreliable for soils that can accumulate large pore pressures or demonstrate above 15% strength degradation during earthquake shaking. This method does not predict deformation. It only delivers a relative slope stability index. Nowadays it is considered as outdated hence only used rarely. More complex techniques are generally needed which are easier to do in modern software. The earthquake induced forces are time varying so the FoS varies all through the duration of the earthquake. However, the maximum value is often taken even in other methods.

5.4.4 Discussion on Results of the Spectral Force Based Pseudo-Dynamic-Analysis

The response spectrum overcomes major shortcomings of Pseudo-static method i.e., the time and maximum intensity relationship distributed over the period of the earthquake in relationship to the type of soil. Spectral Force based factor of safety is more reliable than purely pseudo-static factor of safety because the spectrum is based on reliable actual spectrum of the acceleration of the earthquake not just one maximum value. The Spectral force is calculated from spectral acceleration and gives a better depiction of the seismic slope stability. The Spectral force-based Factor of safety was estimated considering the coconut tree root reinforcement only. As this approach indirectly considers the time-acceleration relationship it is a basic pseudo dynamic approach.

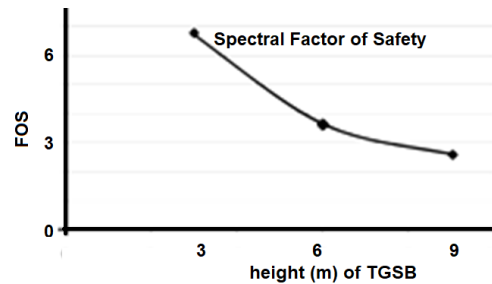


Figure. 5.11 Factor of safety for spectral acceleration-based approach

This approach to slope stability gave a higher value for lower height TGSB and a lower value for higher TGSB as compared to pseudo-static approach. In all cases the factor of safety was greater than 1 and hence the TGSB embankment carrying coconut tree roots is very safe (Figure 5.11). The difference in values in these two approaches is due to the difference in finding the impact of seismic acceleration.

This approach though pseudo dynamic has many limitations as it does not consider the other parameters of an earthquake like distance from epicentre, primary and secondary seismic wave velocities, frequency of the shock wave and other similar parameters.

A better pseudo-dynamic approach is therefore needed.

5.4.5 Discussion on Results of Simplified Pseudo Dynamic Safety of TGSB

A purely pseudo-dynamic approach is large, cumbersome and needs specialized mathematical software like Matlab. However, it is possible to use empirical relationships as demonstrated in the analysis chapter to get reasonably accurate pseudo-dynamic analysis while at the same time factoring in all the various parameters associated with earthquakes that are not possible in purely pseudo-static or spectral based methods. In this thesis the different parameters were inputted considering active and passive wedges and the interaction between them for 3m, 6m and 9m TGSBs.

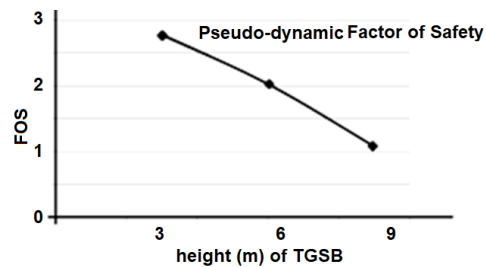


Figure. 5.12 Factor of safety for simplified pseudo-dynamic approach

The results of simplified pseudo-static method showed a better though lower Factor of Safety appraisal of TGSB (Figure 5.12) as compared to pseudo-static and spectrum-based method.

This result is much more reliable as different factors like period, spectral acceleration, distance of earthquake, Primary and secondary wave velocities, natural frequencies and sub soil conditions are all considered in the approach.

Even with lower factor of safety the value still remains above 1 for the existing 3m, 6m and 9m TGSBs found in Goa. This demonstrates that the TGSB will not fail by slope failure though they have a sub-vertical profile of angle more than 80° in practice. This can be attributed solely due to the improvement of the properties of soil by the addition of coconut roots as reinforcing element.

5.4.6 Discussion on Results of Liquefaction Safety of TGSB

Liquefaction usually occurs in shallow sandy soil deposits underlain by hard igneous rock like the Katmandu earthquake of 2015 and Peru earthquake of 2021, where severity of damage was primarily due to liquefaction of shallow (20 to 30 m deep) sandy-gravelly soil layers. In TGSB as the roots as spring-reinforcing element much of the earthquake vibrations are absorbed. In Goa the soil is lateritic in nature and has a high sand and gravel content with some fines. Furthermore, the igneous rock lies 25 to 40 m below the surface which is geo-technically quite shallow. The Liquefaction Potential Index or LPI is an indicator of the impending probability of the soil below the structure to liquefy in case a devastating earthquake strikes.

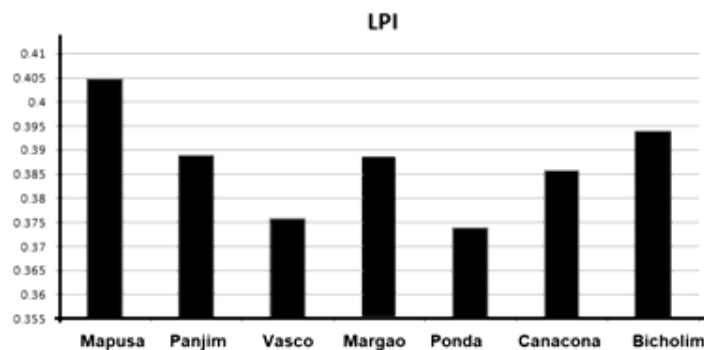


Figure. 5.13 Liquefaction Potential Index of TGSB

The LPI of first 20m of soil below TGSB in 7 different areas of Goa: Mapusa, Panjim, Vasco, Margao, Ponda, Canacona and Bicholim, were investigated (Figure 5.13). The areas chosen represented the spread of Goa as well as the different uses to which TGSB are used like transportation (land based), slope stabilization, and water retaining. All the TGSB showed a LPI score between 0.37 to 0.45 which is close to 0. This shows that the soil below TGSB has almost no possibility of liquefaction. From the above it can be concluded that TGSB can be used safely in Goa for all intended purposes without the danger of liquefaction.

5.4.7 Discussion on Results of Liquefaction Settlement of TGSB

A main significant consequence of liquefaction is settlement. Entire buildings are known to sink into the ground and bridges have toppled as it happened in Nigata Japan. The amount of possible settlement needs to be studied to study the effect of possible liquefaction in Goa. The same seven sites as above were studied for liquefaction settlement.

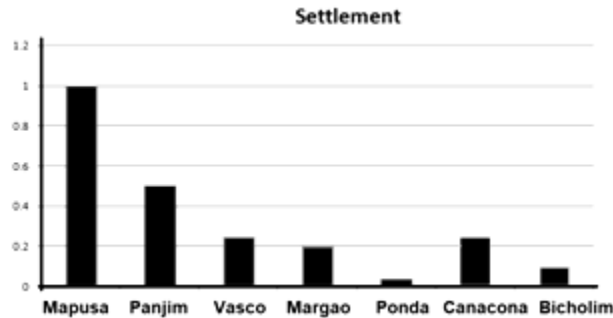


Figure. 5.14 Liquefaction Settlement of TGSB in millimeters

The displacement caused due to cyclic loading during earthquake of M 5.5 magnitude calculated and the displacement from the Tokimatsu and Seed 1987 criteria for strains in sand-like soils is less than 1 mm in all TGSBs tested. This is less than the permissible value of 100 mm for long non-building structures as required by various codes IS 8009-1976 and IS1904-1986. Liquefaction settlement is more in the wet alluvial regions than in the hilly regions but it still very minimal. This again reinforces the fact that there will be almost no liquefaction failure of TGSB.

5.4.8 Discussion on Results of Tsunami Safety of TGSB

The bund (TGSB) or seaward mangrove forest (MF) acts as a discharge weir. This causes a jump upstream with loss of energy. Limited experimental studies and model studies carried out in this thesis shows a substantial reduction in wave height by TGSB and is similar to the reduction theoretically found out. Extended and repeat experimental studies and model studies need to be done to find coefficient of discharge of TGSB. Further experimental studies and model studies need to be done to find coefficient of discharge over other

embankments and coastal forests. Under normal coastal sandbars even a small tsunami of 0.5m will have a jump of 3.5m. This can be absorbed by mangrove forests and TGSB very easily. Hydraulic jump head loss is there only for small tsunamis. Bigger tsunamis will show negative head loss which means there is a gain in head and gain in velocities though there is a decrease in the discharge.

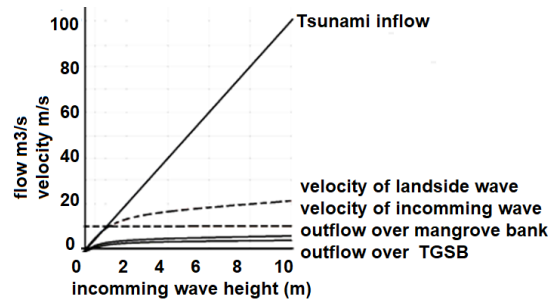


Figure 5.15 Incoming wave height and outgoing wave parameters for Tsunami

This diagram shows how the final wave velocity increases as incoming wave height increases beyond 1 m for Tsunami (Figure 5.15). The outflow over mangroves is higher than the outflow over TGSBs. The calculations were done for 3 m TGSB and 3 m Mangrove forest. Calculations carried out for 6m show that TGSB better protects up to 1m Tsunami waves. Calculations carried out for 9m show that TGSB better protects up to 2m Tsunami waves. Calculations carried out for 3m with 15 m coconut trees on the top show that TGSB give better protection up to 8m Tsunami waves. This shows the enormous disruptive impact on the Tsunami force of coconut trees thus that of fully functional TGSBs.

As per Institute of Seismological Research Gujarat the tsunami produced only a 1 m extra height in waves in Goa. The TGSBs provide more than adequate protection for this type of wave in Goa. As this was the biggest earthquake in the Indian Ocean in history it can be safely assumed that 3 m TGSBs can deal with any tsunami that will come up in Goa. Thus it is evident that the best coastal protection method for earthquake generated Tsunamis are TGSBs of 3m height topped with zigzag coconut trees in double row.

5.4.9 Discussion on Results of GeoStudio2019 Analysis of TGSB

Today tedious calculation for evaluating the Factor of safety of Embankments like TGSB can be avoided by using free and proprietary Software. Software analysis uses either finite element or finite difference techniques. Full earthquake dynamics can be modelled depending on the software used. Deformation can be easily estimated using soil specific elasto-plastic and other constitutive models. This approach however required advanced training and basic coding experience. There exists several exceptional software for static and seismic stability analysis of geotechnical structures, such as embankments, like GeoStudio2019. The present SLOPE/W analysis has demonstrated immensely high Factor of safety for sub-3 m TGSB. For static conditions the FoS reduces with increased height. The SEEP/W analysis demonstrates insignificant seepage in the TGSB at full reservoir level. The QUAKE/W analysis has revealed a elevated factor of safety and reduced cyclic stress meaning TGSB don't liquefy easily. TGSB have survived multiple cyclones with minimal self and surrounding damage when compared to other similar world events.

The first study in GeoStudio2019 was using SLOPE/W to analyse the different components and their impact on safety 3m TGSB. The safety of TGSB without roots and facing was first found out. The safety of TGSB without roots and facing was then compared to each component individually and all together. The horizontal root mat and the vertical root pile were analysed separately to see the impact on slope stability if each acted separately.

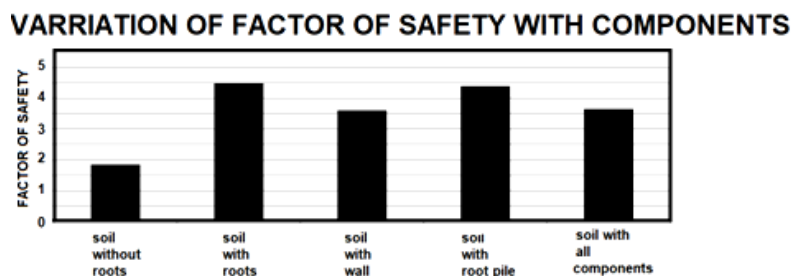


Figure. 5.16 Increase in FoS due to TGSB Components.

The above component-based study (Figure 5.16) shows that the existence of roots tremendously increases stability and factor of safety of TGSB. The increase in safety

provided by Coconut Tree Root reinforcement has proved the wisdom and discernment of the very old TGSB know-how.

The next analysis considered 4 options:

- TGSB without roots for bund on land, not retaining water.
- TGSB with Roots for bund on land, not retaining water.
- TGSB with Roots for bund retaining water on water side.
- TGSB with Roots for bund retaining water on other side.

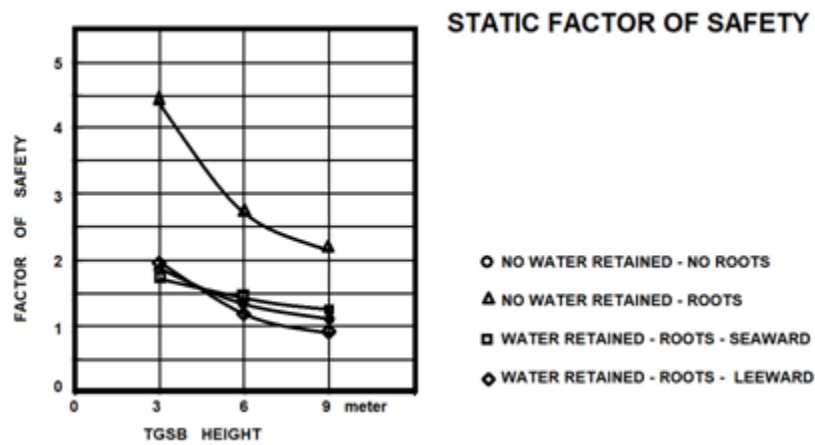


Figure. 5.17 FoS Trend in static stability of TGSB.

The change in FoS versus the TGSB height was plotted (Figure 5.17) to find out its trend. It was seen that the static FoS slightly decline with height levelling off at 9m. The plot shows that the presence of the coconut tree fibrous roots doubles the strength compared to unreinforced bund for no water retained category.

Though there are different methods of evaluating slope stability and as bishops' method was chosen, since it was also used in spread sheet analysis, the TGSB were analysed using different methods to see their impact on slope stability.

FACTOR OF SAFETY USING DIFFRENT METHODS FOR 3M TGSB

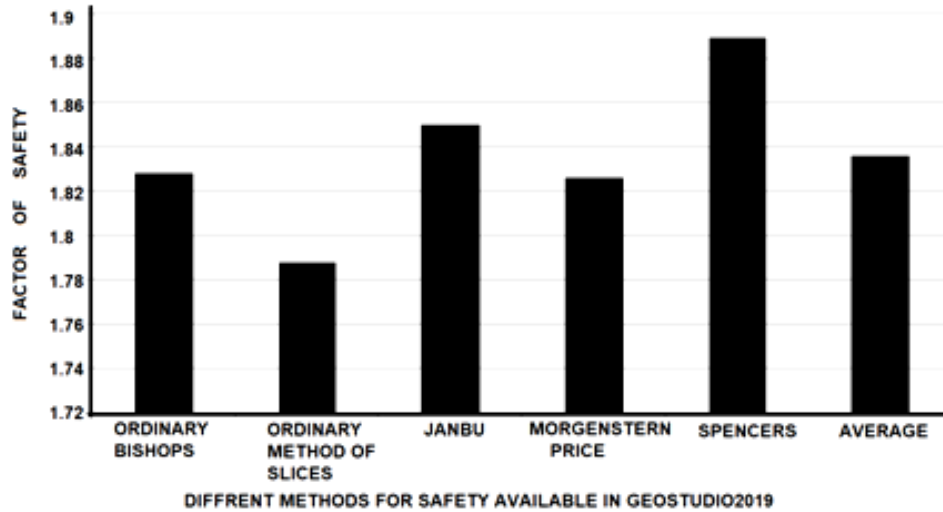


Figure. 5.18 FoS by different methods in static stability of TGSB.

Most standard methods gave equal if not higher factors of safety for the TGSB analysed (Figure 5.18). The average value of all the Factors of Safety also is almost the same as Bishop’s method. This shows that selecting Bishop’s method for analysis of TGSBs to be a rational choice as the dissimilarity in results is negligible.

Since TGSB are also used to retain water, they were analysed for potential leakages using SEEP/W feature of GeoStudio2019.

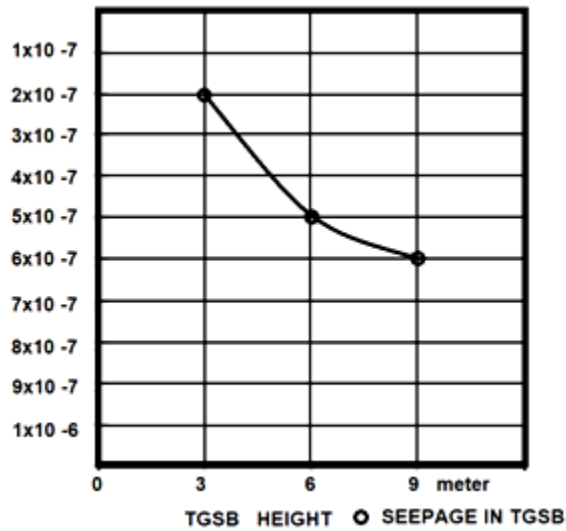


Figure 5.19 Seepage in TGSB

The 51 litres of water per day leakage from a 9 m high TGSB is a very small quantity (Fig 5.19). Although minimal leakage is shown in software, in actual practice none is there. This is due to matric suction from root water uptake, which makes the seepage actually reduce to zero. A coconut tree needs 35 to 55 litres of water per day in irrigation. A 9 m water retaining TGSB carries 4 coconut trees which makes the total water demand 140 to 220 liters per day which is far more than the leakage of a non-rooted TGSB so effectively seepage is negated.

In order to gauge the impact of the seismic acceleration on the TGSB the standard default acceleration was used by suitably modifying the period and duration of the earthquake and the maximum acceleration. TGSB of 3m, 6m and 9m were analysed and the resulting acceleration at the top and at the toe was found out. The ratio of input to output acceleration gave the factor of safety.

As the size, shape and configuration of the structure influence the mode and intensity of vibration the factor of safety showed an increase with height from 3m to 6m before decreasing at height of 9m.

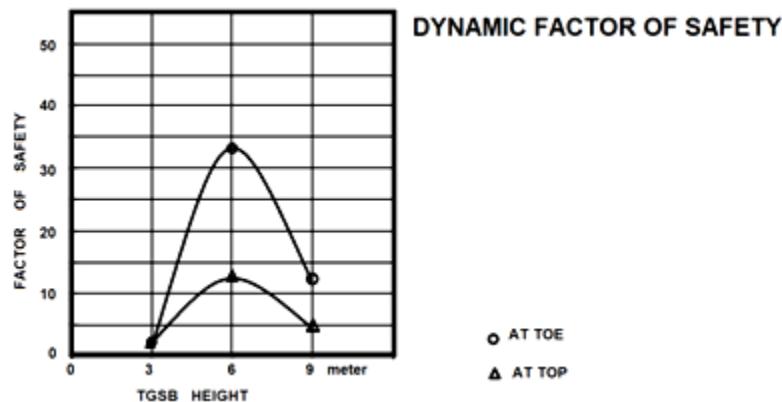


Figure. 5.20 Dynamic factor of safety at top and at toe of TGSB

The dynamic analysis reveals that the 6m TGSB is best suited for earthquakes in Goa (Figure 5.20). We observe that 9 m high bunds performed better than 3m bunds due to

vibration modes. In all cases the FoS was above 2 making TGSB safe in earthquake prone zones having maximum horizontal earthquake acceleration below 0.11g.

The El-Centro earthquake gave the most unfavourable response when the TGSBs were tested for different real earthquakes: Bhuj, Koyna, Utarkashi, Sumatra, Kobe and El-Centro. This is because the chosen earthquakes had dissimilar periods, dissimilar maximum acceleration and 3m dissimilar accelerograms causing the values of stresses and strains generated in the TGSB to vary consequently. It is observed that the earthquakes in India produce smaller effect in TGSB to those outside India. It was also observed that earthquakes along coast like the one in Bhuj had less effects on TGSB than earthquake sin mountains like the one in Uttarkashi. This demonstrates that the TGSB are ideal for tropical coastal areas. Different earthquakes showed cyclic stress ratio is zero which implies that the TGSB will not liquefy. This is correlated in the spreadsheet-based analysis for LPI (Liquefaction Potential Index) where the possibility is extremely low and settlement is less than 1mm.

5.4.10 Discussion on Results of Midas Analysis of TGSB

Midas GTX-NX analysis was carried out for TGSB to calculate the static and dynamic Factors of safety. The static factor of safety was found out for rooted and non-rooted TGSB and the increase in factor of safety was calculated.

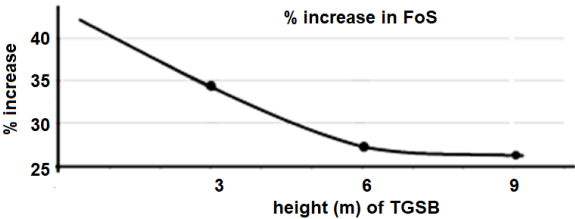


Figure 5.21 Variation of Factor of safety with height

The percentage of Factor of Safety of rooted TGSB over non rooted TGSB showed an increase of 25 to 35 % (Figure 5.21). This result demonstrated that aTGSB reinforced with root mat showed a marked improvement in safety. The increase in safety trends to levels out after 6.5 m height.

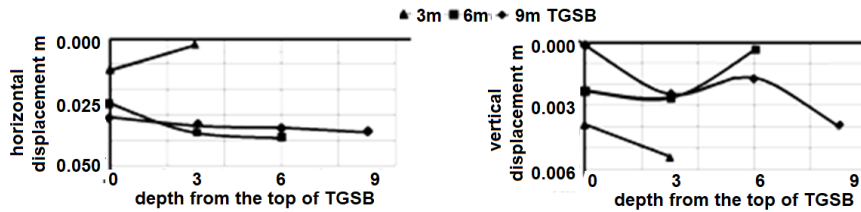


Figure 5.22 Horizontal and Vertical displacements by Midas analysis

For unreinforced TGSB the horizontal displacements increased with height of Bund. The Vertical displacements increased and decreased with height of Bund per bund (Figure 5.22). Topmost displacement was much more than bottom displacement. The horizontal displacement showed a decrease from top to bottom of TGSB same as the case of vertical displacement. This shows that the top of the embankment moves more than the bottom of the embankment as is normal in an earthquake however the difference in movement is very small and will not cause significant damage to the structure during the shaking.

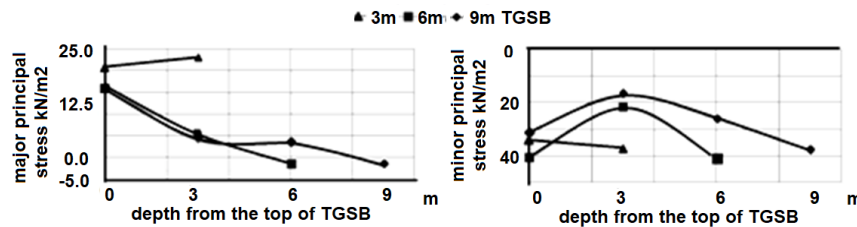


Figure 5.23 Major Principal Stress by Midas analysis

For unreinforced TGSB the Major Principal Stress decreased with height of Bund. The Minor Principal Stress increased with height of Bund (Figure 5.23).

The results for TGSB reinforced with root piles and root mat demonstrated nearly zero stress and displacements during earthquake. This resulted from the damping provided by the roots. The Midas software analysis again demonstrates the importance and role played by the coconut tree root acting as geo-reinforcement in strengthening the soil and providing damping thus reducing the seismic damage to negligible.

5.5 Comparison of FoS by various methods for Computerized analysis of TGSB

All the stability and seismic studied have shown the tremendous increase in the factor of safety both static and dynamic by different methods using spread sheets and software. Each method depending on its limitations and approach has given a different set of values although all are in concordance to the fact that the coconut tree reinforced TGSB is much more stable, strong and safe.

Therefore, there is a need to compare all the methods with each other to get an overall idea of the factor of safety of TGSB and the trend of the results.

Table 5.26 Comparison of Static and Dynamic Factor of Safety Obtained for TGSB Considering Root Reinforcement by Different Approaches

Approach to finding Factor of Safety		3	6	9
spreadsheet	Static	8.624	2.492	2.308
	Dynamic	4.500	1.984	0.956
	Pseudo-Static	3.741	3.096	2.380
	Spectral Based	6.27	3.63	2.62
	Pseudo-Dynamic	2.762	2.032	1.007
software	Geo-Studio (LEM)	4.486	2.784	2.284
	Midas (FEM)	2.98	1.78	1.46

The comparison of static and dynamic factor of safety obtained for TGSB considering root reinforcement by different approaches has been done (Table 5.26) and their values plotted on a graph (Figure 5.24). As expected, the comparison shows that the static factor of safety is far greater than the dynamic/seismic factor of Safety for all cases. The Factors of safety obtained by software used: Geostudio2019 SLOPE/W and Midas GTX-NX, also have a similar range of values and similar trend of results.

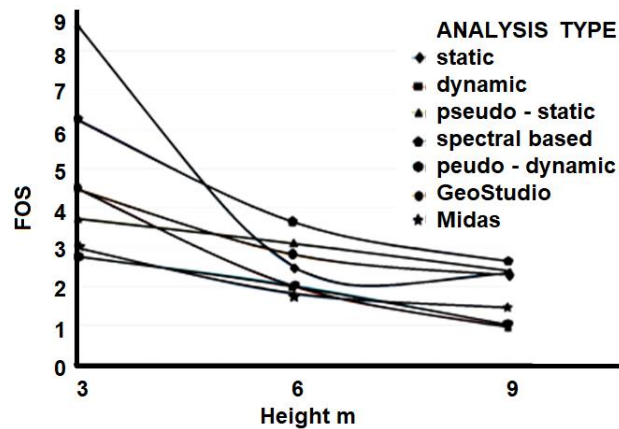


Figure 5.24 Plots of static and dynamic factor of safety obtained for TGSB considering root reinforcement by different approaches for 3, 6 and 9 m TGSB

The curves obtained by various methods are almost parallel too tech other and thus can be expressed by a trend line (Figure 5.25).

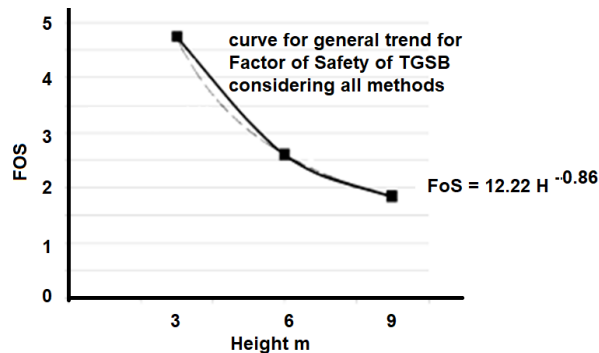


Figure 5.25 Trend of Factor of safety obtained for TGSB

The trend of the average factor of safety of all methods considered together can be expressed by the equation

$$FoS = 12.22 H^{-0.86}$$

This equation with an R^2 value of 1 can be used to assess the Factor of Safety for any TGSB less than 9 m in height. Using this equation, the factor of safety for TGSB of any height is easy to determine. As TGSBs exist already in Goa and they come in various sizes

and since only the maximum size for a particular configuration was considered in this study this equation is useful for finding the safety of any existing TGSB

Table 5.27 Trend of Factor of safety obtained for TGSB

Height Of TGSB	3	6	9
FoS	4.75	2.61	1.85

Although this (Table 5.27) is just an approximation it will give fairly compatible results with the values given in the analysis and results discussed in the above sections (Table 5.26).

5.6 Summary

Results of the analysis of TGSB were tabulated and discussed in this chapter. The results were tabulated and discussed in the same manner as they were analyzed. The spread sheet based slope stability results were split into the following areas: Static Slope Stability Analysis, Dynamic Slope Stability Analysis, Pseudo Static Slope Stability Analysis, Spectral Pseudo Dynamic Analysis, Simplified Pseudo Dynamic Analysis. The spread sheet based liquefaction results were for Liquefaction potential analysis and Liquefaction settlement analysis. The spread sheet-based tsunami results were for Hydraulic Jump Analysis and Experimental Verification of Analysis. The software-based results were divided into the following categories: Geostudio-2019 Analysis, Midas GTX-NX Analysis. The different approaches and the procedures showed a great similarity in range and trend of values. All the analysis showed that the TGSB has high static and seismic factors of safety. On an average the Factor of safety is around 4.75 for 3m TGSB, 2.61 for 6m TGSB and 1.85 for 9m TGSB. The factor of safety for dynamic condition is almost half that for static condition. The presence of roots doubles the factor of safety both static and dynamic due to overall increase in shear properties and damping properties by addition of roots in the soil. They not only are safe in liquefaction but also provide protection against Tsunamis.

It is found that the construction and design of the TGSB structure by the ancient Rishis (Engineers) of the Saraswat civilization is very safe. This is proved by the high safety obtained by extensive geotechnical analysis. Though developed using thumb rules by ancient scientifically minded thinkers, the empirical background and improvements over centuries to the technique ensure the sustainability and success of this infrastructure. The TGSB can also better resist seismic loads. Thus we can definitely say that there is a vast increase in safety on analysis of coconut root reinforced traditional embankment (TGSB) found in Goa. The similarity of results by different approaches validate the existence of the structure in Geotechnical terms. More studies are definitely needed for better understanding and further validation of this sustainable and carbon negative technology. Software considering the root reinforcement can be developed in the future for better analysis of rooted embankments.

CHAPTER 6

CONCLUSIONS

6.1 Introduction

For thousands of years Goa has unique embankments that carry two rows of coconut trees on the top. They were built by ancient Saraswat Engineers called Rishis using empirical methods and thumb rules incorporating technologies that are being discovered today like soil-stabilization and geo-fabrics. Today pressures of modern technology threaten their existence. In thesis an effort was undertaken to study the seismic stability of TGSB considering coconut root reinforcement. As there are no prior studies on TGSB many additional studies had to be carried out to support the analysis. Although this limited the scope of the thesis a vast as possible evaluation was done within the temporal and financial limitations of the thesis. Both static and dynamic analysis was carried out for comparison purposes. Safety of TGSB was evaluated with both roots and no roots. In total seven different stability analyses were carried out and also the liquefaction and tsunami protection were carried also out as these are also the effects of earthquake on coastal structures.

6.2 Work Progression and Summary of Thesis Contributions

In the first two semesters the Background topic review and detailed literature survey was carried out. The thesis hypothesis was finalized. Critical review was conducted and additional literature survey was conducted to fill in the gaps.

During the third semester detailed soil testing and Soil Classification of lateritic soil was carried out. Testing of properties roots of plants trees from bunds was done. Identification of soil Root parameters was done based on the Interpretation of test results. Predicting earthquakes parameters for Goa needed for seismic analysis of bunds was completed.

During the fourth semester additional studies were carried out in soil-root-matric suction and soil stabilization. Additional soil testing was done to evaluate soil variation properties with depth and to collect data for liquefaction analysis. Supplementary soil

testing was executed to find the anisotropy in soil. Dynamic analysis of bunds was carried out using MS Excel. Liquefaction analysis of soils of Goa was carried out using MS Excel. During the fifth semester a number of case studies were carried out in TGSB technology for origins, destruction, replacement and usage. Also, the static and dynamic analysis was done using commercially available software: MIDAS-GTX-NX, and GEOSTUDIO2019. Site specific seismographs, Liquefaction settlement and tsunami dynamics study was carried out. Limited computational method using python programming language was done using the formulae developed for spread sheet analysis.

During the sixth semester geo-synthetic action of root-reinforcement was studied and additional simplified pseudo-dynamic studies were carried out and the finalizing of the first draft of the thesis was completed.

6.3 Major contributions from the present study

The present research fills the research-gap by study of the coconut tree root as a natural geo-reinforcement in embankments. It is validated by the existence of these structures for past 5000 years. The objectives of the present research were achieved as follows:

1. Studies shows that the existing TGSBs are built as per thumb-rules and have sound scientific basis. They are surveyed, evaluated and quantified in this thesis.
 - a. Existing TGSBs must be repaired and maintained using same technology only, but modern machinery may be used
 - b. TGSBs technology can be used in combination with modern technology like mechanically stabilized earth walls
 - c. The sides of the TGSB must have a rubble facing that extends to a parapet 50cm above it for overtopping protection.
2. On performing the laboratory studies to evaluate geotechnical properties of soils used in the embankments/bunds in Goa it was found that
 - a. The soil used in the TGSBs was alluvial sandy-loam (with < 10% silt) nature.

- b. The soils (Kaloi) used must be stabilized using of 1.7 – 2.5 % Lime and 4.3 - 5.8 % Coconut Leaf Ash(CLA) and balance amount (%) soil with molasses if possible.
 - c. Soils in TGSB must be compacted to OMC using rice-straw-hay as initial geofabric.
3. After testing the coconut tree roots, root reinforced soil and their geosynthetic reinforcing actions in bunds it was found that roots doubled the factor of safety as compared to plain soil due to their geosynthetic action.
 4. Upon studying the seismic ground motion parameters affecting the seismic behavior of bunds it was established that the maximum seismic acceleration for Goa is 0.1g and the maximum earthquake magnitude was $M_w=1$.
 5. After completing static and seismic analysis of bunds considering coconut tree root reinforcements it was seen that
 - a. The maximum seepage at maximum flood level without considering root suction (as software can't model it) gave flux for TGSB is 17 liters per day for 3 m bund, 42 liters per day for 6 m bund, and 51 liters per day for 9 m bund at full supply level which is absorbed by root suction so is effectively zero.
 - b. The static Factor of Safety for TGSB is 5 to 25 for 3 m bund, 4 to 34 for 6 m bund, and 3 to 30 for 9 m bund,
 - c. The pseudo-dynamic Factor of safety for TGSB is 2 to 6 for 3 m bund, 1.6 to 3.2 for 6 m bund, and 1.2 to 2.3 for 9 m bund,
 - d. The maximum earthquake acceleration that can topple TGSB is 0.97g for 3 m bund, 0.66g for 6 m bund, and 0.47g for 9 m bund (maximum earthquake to strike Goa gives 0.11g) so they are very safe.
 - e. The Liquefaction Potential Index for TGSB is almost zero and as the minimum is 2 for liquefaction so there is no possibility of liquefaction.
 - f. The Liquefaction settlement for TGSB is less than 0.02% of height.
 - g. The reduction in flood flow in Tsunami for TGSB is 75 to 80 % for 1 m wave, 85 to 90 % for 5 m wave, and 90 to 95 % for 10 m wave,

The TGSB is shows small displacements when tested with different earthquakes in India and in the world, which means it can be used in other places too,

6.3 Conclusions based on work

Based on the extensive research and experimental work of soils and roots the spreadsheet based and software-based analysis was carried out. The results were tabulated and discussed in detail. The work was done phase wise and reasonable conclusions were drawn. The conclusions that can be safely drawn based on the work done during this thesis are as stated below:

6. Existing TGSBs built as per thumb-rules have sound scientific basis which are surveyed, evaluated and quantified in this thesis.
7. Existing TGSBs must be repaired and maintained using same technology only, but modern machinery can be used
8. TGSBs technology can be used in combination with modern technology like Mechanically Stabilized Earth Walls
9. The soil used in the TGSBs was alluvial sandy-loam (with < 10% silt) nature.
10. The soils (Kaloi) used must be stabilized using of 1.7 – 2.5 % Lime and 4.3 - 5.8 % Coconut Leaf Ash (CLA) and balance amount (%) soil with molasses if possible.
11. Soils in TGSB must be compacted to OMC using rice-straw-hay as initial geofabric.
12. The sides of the TGSB must have a rubble facing that extends to a parapet 50cm above it for overtopping protection.
13. The maximum seepage at maximum flood level without considering root suction (as software can't model it) gave flux for TGSB is 17 liters per day for 3 m bund, 42 liters per day for 6 m bund, and 51 liters per day for 9 m bund at full supply level which is very little.
14. The static Factor of Safety for TGSB is 5 to 25 for 3 m TGSB, 4 to 34 for 6 m TGSB, and 3 to 30 for 9 m TGSB,
15. The pseudo-dynamic Factor of safety for TGSB is 2 to 6 for 3 m TGSB, 1.6 to 3.2 for 6 m TGSB, and 1.2 to 2.3 for 9 m TGSB,

16. The maximum earthquake acceleration that can topple TGSB is 0.97g for 3 m TGSB, 0.66g for 6 m TGSB, and 0.47g for 9 m TGSB(maximum earthquake to strike Goa gives 0.11g) so they are very safe.
17. The Liquefaction Potential Index for TGSB is almost zero and as the minimum is 2 for liquefaction so there is no possibility of liquefaction.
18. The Liquefaction settlement for TGSB is less than 0.02% of height.
19. The reduction in flood flow in Tsunami for TGSB is 75 to 80 % for 1 m wave, 85 to 90 % for 5 m wave, and 90 to 95 % for 10 m wave,
20. The TGSB is shows small displacements when tested with different earthquakes in India and in the World which means it can be used in other places too,

Based on the work conducted in this thesis along with the experimental results, we draw the following specific conclusion, and are listed as follow:

21. Existing TGSBs are statically safe
22. Existing TGSBs are seismically safe
23. TGSB technology can be extended for higher bunds than those in existence.
24. TGSB technology is suitable in any other region of the world.

However, even the approaches that are utilized in this thesis raise many research questions.

6.4 Limitation of Present Study

Natural Geosynthetic reinforcement specially root-reinforcement is a relatively new research field, although it has been practiced on thumb rule basis for thousands of years so there are very few research publications available in this area. Seismic evaluation of root reinforced slopes is almost non-existent so it has to be studied in details. Although many pressing research challenges that need to be addressed were looked into there are a number of further research avenues available for post-doctoral work and further research. The major ones include

1. Although, the advantages of TGSB are promising, it requires socio-political will to increase in their use owing to lack of evaluation, Sustainability analysis and green rating for TGSBs

2. Present study of some of the existing revealed that more Soil-studies of lateritic soils in Goa are needed
3. Detailed root modeling of fibrous roots is needed.
4. Possibility of exploring and developing software for coconut tree roots is needed.
5. Another possibility on the basis of understanding of earthquakes is Site specific Seismic studies for Goa
6. Additional examination of Tsunami dynamics and analysis for Goa.
7. It is also important to note that further research is necessary to investigate the Liquefaction analysis including microzonation for Goa etc.
8. Development of better Site Specific Seimographs and their resultant stresses in TGSB for site specific response.

This needs to be carried out as a consequence of this work. A fair and reliable seismic examination platform for root reinforced slopes needs to be built on the pillars of strong research.

6.5 Scope for Future Work

Further research is needed to clarify the impact of unique, existing, multi-use TGSB build using ancient technologies, with reasonable scientific information. Much research also remains to be done on:

1. Further surveys and studies and compilation of information on TGSBs for Goa
2. Further surveys and studies and compilation of information on destruction of TGSBs and their impact for Goa
3. Sustainability and Green Rating studies for TGSBs
4. Further Soil-Stabilization studies using locally available Secondary Cementitious Materials (SCM) for Lateritic soils
5. Further classification studies for Lateritic soils in Goa
6. Further coconut root and other root Soil shear improvement studies
7. Further rice hay Soil shear improvement studies
8. Further rubble facing Soil property improvement studies
9. Further Site-specific Seismic studies including micro-zonation for Goa

10. Further Site-specific seismograms for Goa and India
11. Further Liquefaction Potential studies including micro-zonation for Goa
12. Further Liquefaction Settlement studies including micro-zonation for Goa
13. Further Tsunami Dynamics studies for Goa
14. Further Python Programming studies including GUI platform generation for Geotechnical Seismic Pseudo-dynamic analysis.

The emerging TGSB technology can also be used for low height embankments all over the world.

6.6 Closing Remarks

Thus, it is evident that the use of ancient technology provides promising ways of solving many of the lacunae associated with current embankment failures. The methods outlined in this thesis provide possible ways of seismically evaluating root reinforced embankment. Traditional Goan Saraswat Bunds is a potential tool for meeting challenges associated with earthquake and flood related damages to infrastructure embankments the world over.

// Value the past, it holds the key to the future //

ANNEXURE I

ADDITIONAL INFORMATION ON TGSB

Survey of TGSBs for the Thesis

For the purpose of arriving at the sizes of bunds a small sample survey of a total of 390 bunds from 30 villages and towns in Goa was conducted. The bunds were measured by tape measure. They were found to be of varying heights (H) and widths (B). They were hence classified as per a range of sizes linked to heights: <1x3 <3x5, <6x6.5, <9x9. (Table A1.1)

Table A1.1 Typical Cross-sections of Various TGSBs Sampled in Goa

Sr. No.	Village Name	Number per Average -height(H) , top-width(B) meter							
		In Fields		Near canals		Near seasonal Lakes			
		H 1-2	B 1-3	H 2-3	B 3-5	H 3-6	B 5-7	H 6-9	B 5-9
1	Agasaim	23		2					
2	Baga	5							
3	Batim	24					1		
4	Benaulim	8		3					
5	Betul	13							
6	Bicholim	3		2					
7	Boma	12							
8	Borim	7		3					
9	Curtorim	17		2			1		1
10	Dewadi	12							
11	Dhargal	5							
12	Galgibaga	25		10					
13	Karmali	5							
14	Kumarzuva	4							
15	Loliem	14		8					
16	Loutolim	15							
17	Macazana	5					1		
18	Mapusa	5		2					
19	Netravali	4							
20	Nuven	18		2					

21	Panjim	10	1		
22	Pillar	14			
23	Ponda	8			
24	Raia	9			
25	Raibandar	12			
26	Saligao	22			
27	Shiridao	15	2		
28	Siolim	25			
29	San Estevao	2			
30	Verna	20	4	1	
	Total	344	41	4	1
	% of total	88.2	10.5	1	0.3

The maximum numbers of TGSBs lie in the first and second category. Only those used for river-training, canals and lakes lie in the third and fourth category. Some of these have by now disappeared under the sewage treatment plant/National Highways bypass infrastructure in Mapusa, Margao, Ponda, Agasaim and Cortalim and Mercedes etc. while others have been swallowed up in various housing and infrastructure projects in areas including Mercedes, Caranzalem and Talegao on the outskirts of Smart City-Panjim.

Functions of TGSB

TGSBs are primarily used for lining, shaping and protecting the low-lying called Agricultural Lands, Irrigation Canals and rain water harvesting Seasonal Lakes.

Table A1.2 Functions of Traditional GoanSaraswat Bunds

Sr. No.	Primary Function	Percentage	Classification
1	Agriculture	60	Non-Engineering
2	Coastal protection/River Training/Flood Control	5	Transportation Eng.
3	Salt Panning	3	Non-Engineering
4	Rain Water Harvesting/ Pisciculture	2	Irrigation Eng.
5	Habitation and Infrastructure	10	Construction Eng.
6	Hill slope stabilization and landslide prevention	20	Geotechnical Eng.

They had many engineering and non-engineering functions given (Figure A1.1 and Table A1.2). While the primary function was land reclamation for agriculture and secondary function was flood protection, they also served various other purposes.

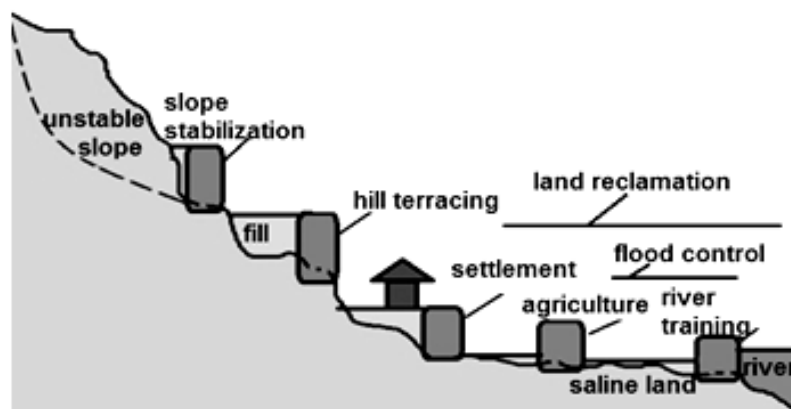


Figure A1.1 Multiple Functions of TGSB

Economic Value of TGSB

TGSBs were an ancient fix-it for multiple purposes. They have tremendous employment based economic value. They serve as direct and indirect job providers to the population of Goa (Table A1.3). Their products and by-products (Coconuts and coconut products) have tremendous sale value. The reclaimed land increases in value. Many small and medium scale industries have a potential of being developed by these marvellous geotechnical structures. These activities have a potential to generate about Rs 150 to 250 million a year.

Table A1.3 Jobs provided by Traditional Goan Saraswat Bund

Sr. No	Job Description	Local Name	Number	Industries
1	Farmers	Xethkar	40,000	Agriculture
2	Horticulturists	Kullagarti	15,000	Florist
3	Toddy-Tappers	Rendher	20,000	Vinegar and liquor
4	Fisher folk	Raponkar	10,000	Fisheries
5	Salt Farmers	Mittkar	5,000	Salt manufacturing
6	Indirect	Vavraddi	30,000	Others
7	Maintenance	Kamdar	50,000	Construction
8	Coir workers		10,000	Coir products
9	Coconut processing		10,000	Oil, copra,
10	Sweet makers	Khajekar	10,000	coconut based sweets

Spatial Requirements for TGSBs

The TGSBs have a great spatial advantage over normal embankments. They offer savings in space and materials and hence cost. As the materials are usually renewable and locally sourced their Environmental Impact Assessment is very favourable. The spatial requirements of TGSB are more than that of Panel walls but the costs are much less (Table A1.4).

Table A1.4 Capital requirements of 3x5 m embankments

Sr No	Requirements	Normal Earth Embankments	Panelled walls MSERW	TGSB
1	Side slope	2.5H:1V	1H:1V	1H:3V
2	interior angle	20°-30°	90°	70°-80°
3	Extra width per m height	2 - 5	0	0.3
4	% Extra land area per m height	300-350	100	130
5	% Earth per m height	200	100	120
6	Approximate Pitching	58000	-	31000
	cost Earthwork	30000	15000	18000
	Reinforcement	-	100000	-
	Labour	20000	20000	10000
	Total	1,08,000	1,35,000	59,000
	%	180	230	100

MSERW-Mechanically Stabilized Earth Retaining Walls

ANNEXURE II

SOIL AND ROCK PROPERTIES

Table A2.1 Particle Size Analysis of Bunds at Curtorim

sieve	0.002	0.075	0.40	2.00	4.50	20.0	80.0
soil	C	M	FS	MS	CS	FG	CG
A	7	15	20	26	29	2	1
B	4	20	22	35	15	2	2
C	10	16	28	18	20	5	3
D	12	20	26	25	14	1	2

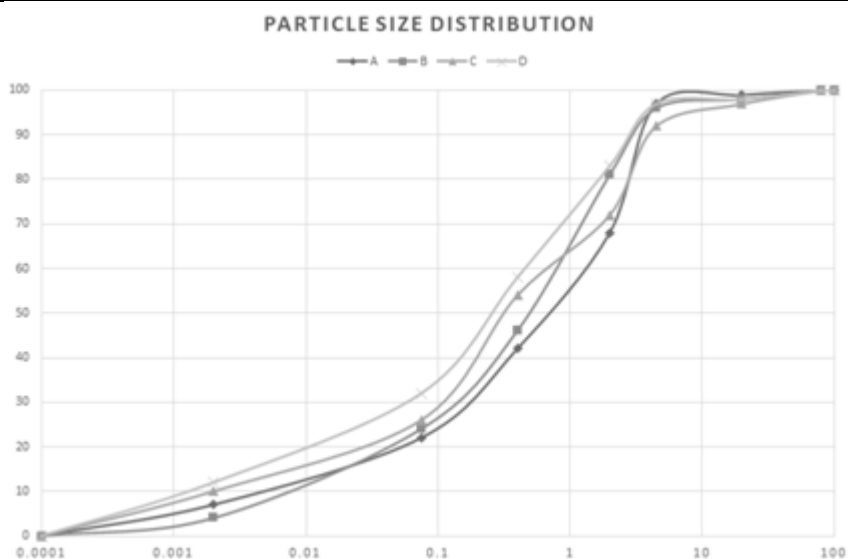


Figure A2.1 Particle Size Analysis of Bunds at Curtorim

Table A2.2 Typical values inputted for software

Component	E	v	γ_d	γ_{sat}	c	ϕ	$k_{pv}=k_{ph}$
	N/mm ²		kN/mm ³	kN/mm ³	kN/mm ²	°	m/day
Bund Soil	5	0.33	16.1	18.3	20	30	2.0e-5
Root Soil	10	0.30	15.3	17.1	30	40	0.2e-5
Bottom soil	2	0.25	18.2	20.0	15	30	0.3e-5
Rubble	100	0.30	24.4	25.3	200	45	2.0e-5

Table A2.3 UCS for soils 50x100 cylinder

Area=1965

L=100

xxvi

Stress N/mm ²	Strain		
	Bottom soil	Bund soil	Root soil
0.0125	0.01150	0.01550	0.01500
0.0250	0.03215	0.02050	0.03010
0.0375	0.03630	0.02575	0.03555
0.0500	0.04250	0.03120	0.04005
0.0625	0.04750	0.03255	0.04115
0.0750	0.05450	0.03550	0.04250
0.0875	0.05940	0.03750	0.04375
0.1000	0.06430	0.04015	0.04500
0.1125	0.07200	0.04350	0.04625
0.1250	0.09020	0.04550	0.04750
0.1375	-	0.04655	0.04875
0.1500	-	0.05025	0.05100
0.1625	-	0.06030	0.05250
0.1750	-	0.07040	0.05505
0.1875	-	-	0.05650
0.2000	-	-	0.05755
0.2125	-	-	0.06000
0.2250	-	-	0.06725
Lateral strain	0.02215	0.02315	0.02010

Tangent Youngs modulus from UCS at 50% stress E_{50}

$$E_{50\text{-bottom}} = 0.02/0.01 = 2$$

$$E_{50\text{-bund}} = 0.05/0.01 = 5$$

$$E_{50\text{-root}} = 0.10/0.01 = 10$$

Poissons ratio = ν = lateral strain/linear strain



Figure A2.2 Disturbed samples in bags and cores of different colour lateritic soils from Goa

Table A2.4 Typical Geotechnical Properties for Lateritic Soils at Verna

colour	Grain-Size						G_s	γ	w	WL	WP	e	c	ϕ	OMC	MDD	k e-5
	G	CS	MS	FS	M	C											
Red	38	24	12	9	6	11	2.44	1.76	15	50	25	55	12	38	13	1.94	3.1
Brown	28	29	22	12	4	5	2.41	1.87	19	40	18	56	11	43	12	2.04	2.8
Yellow	14	9	12	23	22	20	1.95	1.32	21	45	13	45	17	29	9	1.55	2.7
Pink	12	10	28	15	30	15	2.01	1.38	24	48	13	48	17	33	8	1.60	2.7
White	2	10	9	21	30	28	1.60	1.17	25	40	11	42	21	23	7	1.30	5.0
Black	10	5	7	18	35	25	1.78	1.19	23	42	12	44	20	24	7	1.35	5.0

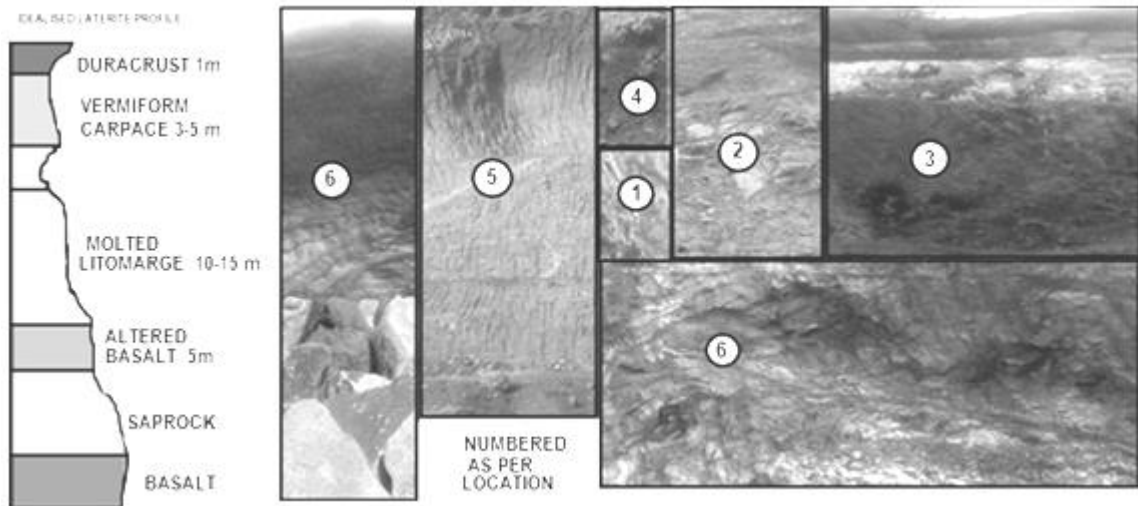


Figure A2.3 lateritic profile and collage of different colour lateritic soils in Goa at approximate depth of position -numbers correspond to location in Goa (1-Borim, 2-Bambolim, 3-Raia, 4-Kadamba Plateau, 5-Farmagudi, 6-Verna),

Table A2.5 Typical Geotechnical Properties for Bund Soils

Site	Grain-Size						G _s	γ	w	WL	WP	WS	c	φ	OMC	MDD	CBR	k e-5
	G	CS	MS	FS	M	C												
Curtori m A	8	29	26	20	15	7	2.51	1.67	19	26	17	7.7	15	29				
Curtori m B	4	15	35	22	20	4	2.54	1.62	21	28	17	7.2	17	30				
Curtori m C	8	20	18	28	16	10	2.53	1.68	20	25	15	7.4	16	30				
Curtori m D	3	14	25	26	20	12	2.50	1.67	20	24	16	7.0	18	28				
Mapusa A	11	26	11	16	16	20	2.52	1.56	17	26	16	7.6	20	30	9.6	1.78	30	2.5
Mapusa B	10	24	29	26	8	3	2.61	1.61	19	27	15	7.8	15	32	13.5	1.85	32	2.8
Panaji A	7	12	21	25	20	15	2.57	1.57	18	26	20	9.2	16	35	15.4	1.83	29	2.4
Panaji B	9	17	18	18	22	16	2.55	1.58	16	38	27	9.2	22	34	17.4	1.9	26	2.3
Margao A	10	17	15	21	25	12	2.54	1.55	17	39	24	10.7	19	30	15.8	1.78	36	2.7
Margao B	8	12	19	19	22	20	2.59	1.58	18	31	22	10.5	24	27	17.0	1.75	32	2.8
Bicholi m	15	28	18	20	10	9	2.54	1.57	19	27	18	9.2	22	30	10.1	1.91	31	2.5
Vasco	14	29	20	14	12	9	2.53	1.56	18	29	19	9.8	25	31	12.2	1.93	28	2.4
Canacon a	12	27	28	12	8	13	2.55	1.59	16	28	17	8.9	20	32	10.1	1.79	29	2.6
Ponda A	2	10	22	22	25	19	2.58	1.68	22	27	16	6	10	25				
Ponda B	11	25	12	16	14	22	2.53	1.58	18	25	15	9	18	29	15	1.78	28	2.9

Classification SC to SM as per USCS-ASTM d2478-11 and IS1498-1970

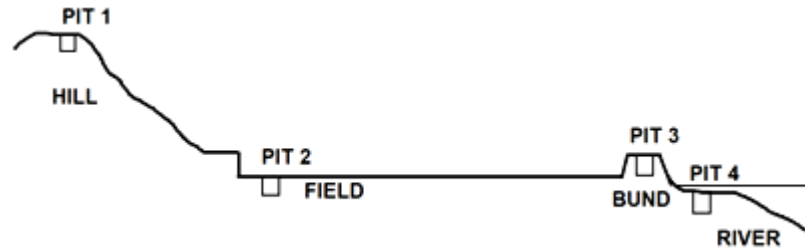


Figure A2.4 Schematic cross section showing notional location of shallow pits for Lateritic Soils at Curtorim

Table A2.6 Variation in properties in shallow pits for Lateritic Soils at Curtorim

		z	G+CS	MS+FS	M+C	G_s	γ	e	c	ϕ	w
Pit 1	Red -Hill	0.3	57	14	29	2.75	2.25	35	16	25	38
		0.6	37	28	35	2.65	2.15	37	15	24	35
		1.0	32	36	32	2.66	2.22	38	13	28	35
Pit 2	Alluvial-Field	0.3	39	21	40	2.63	1.85	52	5	16	38
		0.6	38	25	37	2.65	1.92	5.5	8	17	22
		1.0	42	27	31	2.68	1.98	53	10	12	25
Pit 3	Bund	0.3	33	24	43	2.69	1.63	49	26	31	30
		0.6	40	28	32	2.78	1.65	48	25	29	32
		1.0	44	30	26	2.72	1.68	49	23	32	35
Pit 4	River-Sand	0.3	45	40	15	2.81	2.11	55	5	38	39
		0.6	47	35	18	2.75	2.05	57	3	39	37
		1.0	58	37	5	2.89	2.14	60	2	42	37

Table A2.7 Variation in Geotechnical Properties indepth for Lateritic Soils for a borehole at Ponda

colour	Description	z	coarse	finer	G _s	γ	w	WL	WP	c	φ
Red	Silty Sand	0.0	56	44	2.50	1.68	22	27	16	10	25
Red	Gravelly Silty Sand	0.45	51	49	2.54	1.65	47	35	21	7	35
Yellow	With Fines	4.5	56	44	2.56	1.66	49	32	23	15	32
White											
Yellow	Medium	7.5	45	55	2.56	1.67	52	31	24	5	36
Pink	Silty Sand										
Pink	With Fines	15	43	57	2.58	1.68	55	30	23	6.5	37
Pink	Gravelly Coarse Sand	21	72	28	2.71	1.94	58	33	22	2.2	40

Properties of Lateritic stones

The lateritic stones in quarries are softer but harden on exposure to air. The upper strata which is harder than the underlain stratum is used for rubble while the lower is quarried for buildings and architectures. The lateritic rubble used in TGSB is darker, harder, heavier and more resistant to moisture in the region. The physical, geotechnical and geochemical properties of lateritic rubble at different depths for Mapusa (Mp), Panjim (Pj), Ponda (Pd) and Margao (Mg) in Goa is presented below

Table A2.8 properties of lateritic stone at different depth

z	SiO ₂ %			
	Pj	Mp	Mg	Pd
0	24.0	23.0	23.5	27.0
1	25.9	24.9	25.2	28.2
2	27.2	27.0	27.4	29.5
3	28.1	28.2	28.4	29.5
4	28.8	28.8	29.0	x
5	29.4	29.2	30.1	x
6	30.0	29.5	x	x

Table A2.9 properties of lateritic stone at different depth

Fe₂O₃ %				
z	Pj	Mp	Mg	Pd
0	35.0	34.8	27.0	34
1	34.8	34.2	28.2	34.5
2	34.5	34.6	29.1	33
3	33.0	33.0	28.1	25
4	30.0	30.2	27.0	x
5	26.0	26.4	25.0	x
6	22.0	23.5	x	x

Table A2.10 properties of lateritic stone at different depth

Al₂O₃ %				
z	Pj	Mp	Mg	Pd
0	21.8	21.1	22.3	23.5
1	22.2	22.0	22.8	25.5
2	23.4	23.2	23.4	26.8
3	24.2	24.2	23.7	27.8
4	25.1	25.0	24.3	x
5	26.0	26.0	25.7	x
6	28.0	27.4	x	x

Table A2.11 properties of lateritic stone at different depth

UCS N/mm²				
z	Pj	Mp	Mg	Pd
0	5.8	6.0	5.5	6.1
1	6.4	6.2	6.2	6.2
2	6.2	5.8	6.8	5.8
3	5.9	5.5	6.2	4.2
4	5.5	5.2	5.5	x
5	4.6	4.5	4.0	x
6	2.8	3.0	x	x

Table A2.12 properties of lateritic stone at different depth

Split tensile strength N/mm²				
z	Pj	Mp	Mg	Pd
0	1.55	1.60	1.58	1.50
1	1.71	1.65	1.69	1.35
2	1.65	1.62	1.68	1.20
3	1.60	1.58	1.60	0.90
4	1.51	1.52	1.50	x
5	1.36	1.30	1.20	x
6	0.92	1.00	x	x

Table A2.13 properties of lateritic stone at different depth

Mhos Hardness no				
z	Pj	Mp	Mg	Pd
0	4	4	3	44
1	4	4	4	4
2	4	4	4	3
3	3	3	4	2
4	3	3	3	x
5	3	3	2	x
6	2	2	x	x

Table A2.14 properties of lateritic stone at different depth

Specific Gravity				
z	Pj	Mp	Mg	Pd
0	2.7	2.70	2.66	2.68
1	2.69	2.68	2.68	2.66
2	2.67	2.65	2.65	2.58
3	2.64	2.64	2.55	2.50
4	2.59	2.58	2.50	x
5	2.53	2.50	2.45	x
6	2.40	2.42	x	x

Table A2.15 properties of lateritic stone at different depth

Density g/cc				
z	Pj	Mp	Mg	Pd
0	2.40	2.40	2.32	2.30
1	2.42	2.38	2.36	2.25
2	2.35	2.35	2.32	2.10
3	2.33	2.32	2.25	1.90
4	2.25	2.24	2.10	x
5	2.19	2.10	1.80	x
6	1.80	1.82	x	x

Table A2.16 properties of lateritic stone at different depth

Moisture Content %				
z	Pj	Mp	Mg	Pd
0	19.0	20.0	19.5	19.2
1	20.3	20.7	19.9	20.1
2	21.0	21.2	20.5	21.0
3	21.6	21.4	21.4	21.5
4	22.1	21.6	22.6	x
5	22.5	22.0	23.2	x
6	23.0	22.5	x	x

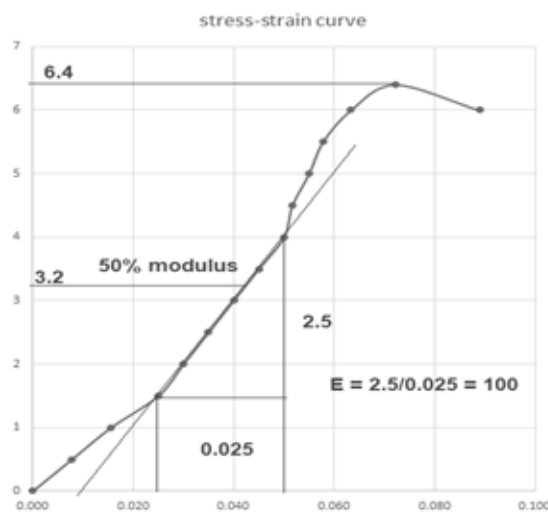


Figure A2.5 Stress Strain curve for Lateritic stone

Table A2.17 properties of lateritic stone at different depth

Load N	Deflection mm	stress	strain
0	0	0	0.000
800	7	0.5	0.008
1600	14	1	0.016
2400	22.5	1.5	0.025
3200	27	2	0.030
4000	31.5	2.5	0.035
4800	36	3	0.040
5600	40.5	3.5	0.045
6400	45	4	0.050
7200	46.5	4.5	0.052
8000	49.5	5	0.055
8800	52	5.5	0.058
9600	57	6	0.063
10240	65	6.4	0.072
9600	80	6	0.089

Area of sample = 1600mm², length of sample = 900mm

Geochemical Properties of Lateritic Stones

Lateritic stones in Goa contain oxides of iron; goethite (HFeO₂); lepidocrocite; FeO(OH); hematite, (Fe₂O₃); in addition to gibbsite, Al₂O₃.3H₂O and titanium oxides (TiO₂). They contain exceptionally poor amount of lime, magnesia, phosphorus, potassium, and sodium. The chemical analysis of the powdered lateritic stones samples was done with the help of X-Ray spectrometer by using the Adaptive Sample Characterization. The TiO₂ ranges between 3 to 4 %. CaO₂ is 0.01 % and Mn was 0.4 %. The pH of the soil was 8.4 to 7.2

ANNEXURE III

SOIL STABILIZATION STUDIES

Table A3.1 Geotechnical Properties of CLA and FA

	Grain Size			Index				Consistency	
	S	M	C	G	γ	γ_d	w_n	w_L	w_P
CLA	30	65	5	1.599	0.282	0.281	22.7	68	55
FA	17	80	3	1.896	0.761	0.759	52.8	35	33

Table A3.2 Chemical properties of CLA and FA

	pH	alkalinity	hardness	SiO ₂	Al ₂ O ₃	Fe ₂ O ₃	CaO	C
CLA	9.9	1000	480	50	18	5	6	10
FA	10.3	3400	5400	60	22	6	1	0

Table A3.3 UCS values for Lime:Ash Ratio for of CLA and FA

curing	Ash	1:9	2:8	3:7	4:6	5:5
3	CLA	5.8	8.3	10.1	11.6	9
	FA	4.0	6.5	3.9	3.8	3.5
7	CLA	7.2	18.4	21.5	25.9	22.9
	FA	7.0	17.1	12.8	12.2	12.0
14	CLA	120.6	250.3	262.7	297.5	232.2
	FA	105.4	204.4	140.6	135.4	131.2

Table A3.4 properties of LS

%Lime	0	3	6	9	12	15	18	20	25	30
γ	1.73	1.54	1.85	1.97	1.91	1.83	1.77	1.66	1.54	1.51
γ_d	1.51	1.41	1.67	1.73	1.67	1.66	1.65	1.63	1.58	1.51
c	20	45	60	87	84	62	58	50	45	40
ϕ	30	36	40	44	42	39	36	34	33	32
WL	49	35	24	21	25	34	38	45	49	54
WP	18	21	16	15	14	17	18	19	21	24
OMC	18.0	11.8	8.0	6.2	6.1	7.5	9.9	13.1	16.8	21.7
MDD	1.94	2.01	2.05	2.08	2.10	2.09	2.07	2.02	1.96	1.86
CBR	30	38	48	50	49	44	39	37	35	30

Table A3.5 UCS values forLS N/mm2

%Lime	0	3	6	9	12	15	18	20	25
UCS	554	920	1100	1467	980	770	670	540	552

Table A3.6 properties of LCS and LFS

		Soil %							
		Ash	98	96	94	92	90	85	80
WL	LCS	22	24	24.5	25.5	27	29	27.5	
	LFS	14.5	20.5	22.0	24	25.0	26.0	25.8	
WP	LCS	11.1	11.0	10.1	11.5	12.1	12.6	12.4	
	LFS	12	19.3	20.6	22.0	22.8	24.6	23.7	
c	LCS	41	62	51	48	43	40	41	
	LFS	35	34	32	33	35	36	36	
φ	LCS	35	34	32	33	36	42	34	
	LFS	30	28	27	28	29	29	28	
γ	LCS	1.57	1.55	1.52	1.50	1.47	1.41	1.34	
	LFS	1.58	1.57	1.55	1.54	1.52	1.48	1.44	

For 2Lime:8FA and 4Lime:6CLA after 7 days

Table A3.7 UCS values forLime:Ash:Soil Ratio of CLA and FA

		Soil %						
curing	Ash	98	96	94	92	90	85	80
3	LCS	5.8	8.3	9.8	11.6	15.5	29.2	25.0
	LFS	4.0	5.6	6.2	7.2	9.8	19.3	12.5
7	LCS	7.2	15.8	20	26.1	32	51.4	45.2
	LFS	7.0	8.1	8.8	9.8	14.7	49.4	35.4
14	LCS	120.4	250.3	310.2	352.3	398.6	426.3	415.0
	LFS	102.0	212.7	263.5	293.9	338.9	390.5	380.8

For 2Lime:8FA and 4Lime:6CLA15% stabilizer 85% soil = (6 L: 9 CLA: 85 S), (3 L: 12 FA: 85 S)

Table A3.8 soaked CBR test of LCS and LFS

	soil	LCS	LFS
1 day	12	14.7	12.89
7 day	10	79.6	50.7

ANNEXURE IV

COCONUT ROOT PROPERTIES



Figure A4.1 Roots in Fine Sand-Silt, Bund, Lateritic Soil, coarse sand on Sea-Shore



Figure A4.2 Roots pulled out and Roots emerge as they wrap around TGSB Stones

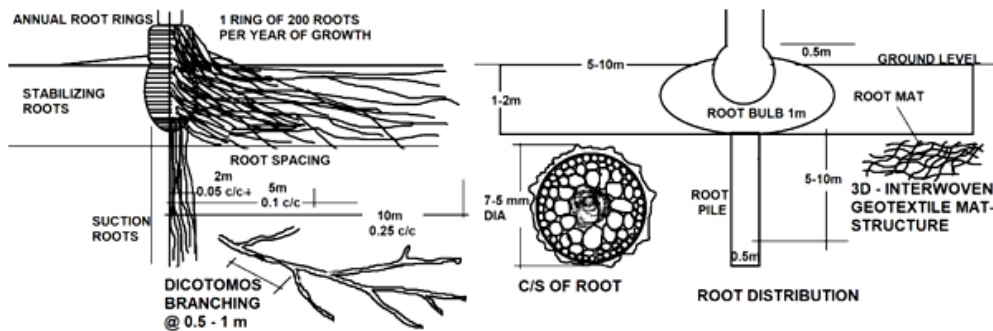


Figure A4.3 Roots distribution in soil and root cross section

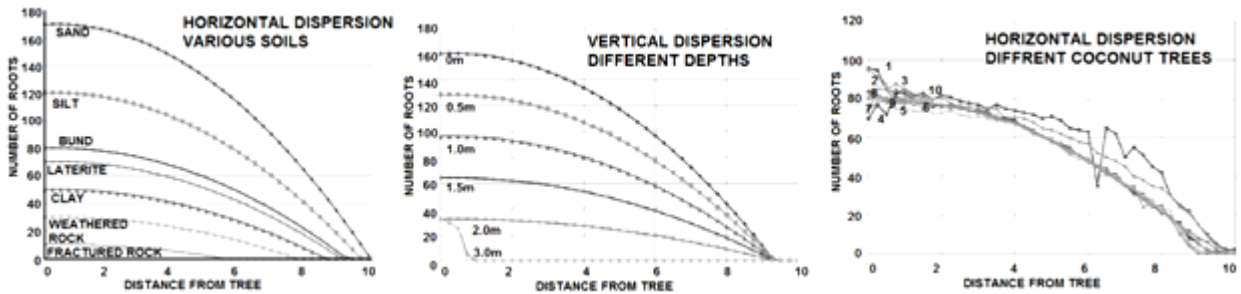


Figure A4.4 Average coconut tree root dispersion for various soils in Goa

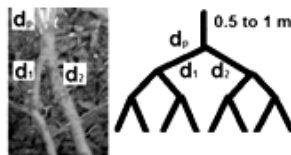


Figure A4.5 coconut tree root branching pattern

Table A4.1 Properties of Coconut Tree Roots

Property		1	2	3	4	5
dr	mm	8	5	10	7	6
γ	kN/m³	2.0	1.24	1.4	1.15	1.30
E	kN/m²	6000	4800	5000	4500	5300
Max elongation	mm	5.0	3.5	4.0	3.0	4.2
Fibre length	mm	200	125	150	160	185
Tenacity	N in 5 sec	5000	4000	4500	3500	4700
Tensile strength	kN/m²	48	35	42	30	45
Damping factor		0.13	0.11	0.12	0.11	0.12
Water absorption	%	15	20	10	18	17

Table A4.2 tensile test of coconut tree roots

	Stress N/mm ²											
	1.5	3.0	4.5	6.0	7.5	9.0	10.5	12.0	13.5	15.0	16.5	18.0
A	.003	.005	.009	.01	.011	.016	.022	.026	.036	.040	.048	.055
B	.002	.004	.008	0.09	0.01	0.02	.250	.027	.035	.040	.045	.050
C	.005		.010		.015		.020		.035	.044	.052	

Table A4.3 increase in UCS v/s RAR of coconut tree roots

RAR	0	0.05	0.1	0.15	0.2	0.3	0.4	0.5	0.6	0.7
UCS	700	710	720	745	770	790	810	825	850	800
Change	0	10	20	45	70	90	110	125	150	100

Table A4.4 shear stress vs deformation of soil and soil-root

deformation	1	2.5	5	7.5	9	10	11	12	15	20
soil	3	6	10	14	15	15.4	16	15.8	14.8	14
Soil-root	9	18	32	43	45	44	42	41.5	41	40

Table A4.5 CBR values (Light and Heavy) of soil and soil-root(RAR 0.4)

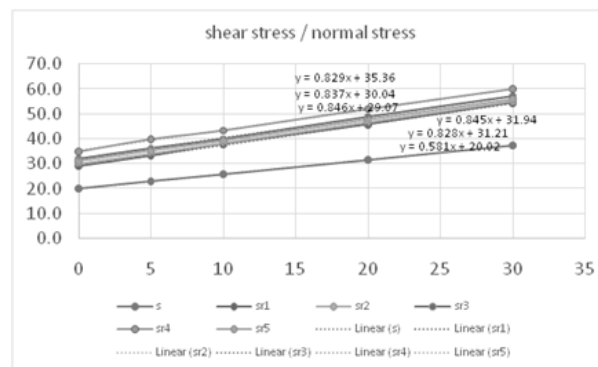
type	Dry set 1		Dry set 2		Dry set 3		Wet set 1	
	L	H	L	H	L	H	L	H
soil	18.3	25.6	17.5	32.0	22.0	31.0	13.8	21.3
Soil-root	28.8	35.6	27.9	41.0	31.1	40.5	20.5	30.7

Table A4.6 Rupture Tensile Strength v/s Diameter of coconut tree roots

diameter	1	2	3	4	5	7	9	10
stress N/mm ²	50	30	15	10	6.5	4.0	3.2	2.0

Table A4.7 box shear stress shear vs normal stress of soil and soil-root at different depth

	Normal stress kPa					Shear parameters		
	0	5	10	20	30	c	tan φ	φ
soil	20.0	23.0	25.8	31.6	37.5	20.02	0.582	30.2
Soil-root	0.1	29.0	33.2	37.9	45.8	29.08	0.846	41.9
at	0.5	30.1	34.2	38.4	46.8	30.05	0.838	40.0
different	1.0	32.0	36.3	40.1	49.0	31.95	0.846	40.2
depth	2.0	35.0	40.0	43.5	52.1	35.36	0.829	39.6
	3.0	31.2	35.4	39.4	47.9	31.25	0.837	39.5



FigureA4.6 box shear stress shear vs normal stress of soil and soil-root at different depth

Table A4.8 Coconut tree stem properties

property	symbol	value
Shape		Cylinder
Youngs modulus	E	5000
Spring constant	K	10000
Damping ratio		0.1
Projected area		0.3/m height
Drag Coefficient	C _D	0.082
Density	γ	1.2
Water absorption		15

ANNEXURE V

EARTHQUAKE MAGNITUDE STUDIES

Table A5.1 Magnitude of earthquake at Mapusa-1, Panjim-2 and Margao-3 due to possible rupture of different faults around Goa

fault	length	B	Mo	Mw1	D1	D2	D3	M1	M2	M3
1	250	83333	1.25E+21	7.46	150	165	180	-0.11	-0.20	-0.29
2	152	50667	7.6E+20	7.32	175	190	195	-0.27	-0.36	-0.38
3	185	61667	9.25E+20	7.38	85	200	210	0.43	-0.41	-0.46
4	310	103333	1.55E+21	7.53	170	180	150	-0.23	-0.29	-0.11
5	350	116667	1.75E+21	7.56	215	205	180	-0.47	-0.42	-0.29
6	240	80000	1.2E+21	7.45	205	220	210	-0.43	-0.50	-0.45
7	200	66667	1E+21	7.40	200	190	170	-0.41	-0.35	-0.24
8	210	70000	1.05E+21	7.41	250	235	205	-0.65	-0.58	-0.43
9	80	26667	4E+20	7.13	310	290	270	-0.90	-0.83	-0.75
10	30	10000	1.5E+20	6.85	350	335	305	-1.06	-1.01	-0.90
11	80	26667	4E+20	7.13	380	315	340	-1.15	-0.92	-1.01
12	80	26667	4E+20	7.13	260	275	200	-0.70	-0.77	-0.42
13	155	51667	7.75E+20	7.33	215	225	260	-0.49	-0.54	-0.69
14	220	73333	1.1E+21	7.43	205	225	250	-0.43	-0.53	-0.64
15	215	71667	1.08E+21	7.42	200	220	245	-0.41	-0.51	-0.62
16	190	63333	9.5E+20	7.39	80	100	120	0.49	0.28	0.10
17	70	23333	3.5E+20	7.10	70	80	100	0.59	0.47	0.26
18	50	16667	2.5E+20	7.00	50	50	70	0.89	0.89	0.59
19	300	100000	1.5E+21	7.52	100	100	120	0.28	0.28	0.11
20	135	45000	6.75E+20	7.29	70	50	70	0.60	0.90	0.60
21	180	60000	9E+20	7.37	150	125	125	-0.11	0.06	0.06
22	40	13333	2E+20	6.93	200	180	170	-0.43	-0.32	-0.26
23	200	66667	1E+21	7.40	125	100	100	0.07	0.28	0.28
24	30	10000	1.5E+20	6.85	200	190	200	-0.43	-0.38	-0.43
25	20	6667	1E+20	6.73	205	195	205	-0.47	-0.41	-0.47
26	30	10000	1.5E+20	6.85	185	175	185	-0.35	-0.30	-0.35
27	155	51667	7.75E+20	7.33	125	110	115	0.06	0.19	0.14
28	115	38333	5.75E+20	7.24	225	245	265	-0.54	-0.63	-0.72

ANNEXURE VI

BOREHOLE LOGS FOR LIQUEFACTION STUDIES

Figure A6.1 BOREHOLE LOG 1, 2

z	Bicholim						Canacona					
		SPT	soil	γ	G	e_0		SPT	soil	γ	G	e_0
0	red granular	8		1.66	2.32	0.52	granular red pink	14		1.52	2.22	0.50
2		8						14				
3		10						12				
4	pink white sandy	12						14				
5		12		1.65	2.38	0.52	15	1.58	2.36	0.53		
6		1					yellow lithomarge	16				
7	14				18							
8	12				19							
9	yellow lithomarge	17						18				
10		15		16.8	2.4	0.51		18		1.75	2.40	0.55
11		17					21					
12		19					24					
13		22				pink lithomarge	28					
14	pink lithomarge	26							26			
15		25		1.76	2.45		0.52		28	18.3	2.53	0.54
16		26							29			
17		28							28			
18		29							27			
19		32							26			
20		34		1.79	2.50	0.55	26	18.6	2.54	0.58		

Figure A6.2 BOREHOLE LOG 3, 4

		Mapusa					Margao							
z		SPT	soil	γ	G	e_0		SPT	soil	γ	G	e_0		
1	yellow river silt	3		1.52	2.25	0.54	red granular	10		1.75	2.36	0.52		
2		3						15						
3		5						18						
4		7						12						
5	10				15									
6	brown silt sand	10		1.56	2.30	0.53	yellow lithomarge	18		1.69	2.41	0.53		
7		12						21						
8		14						20						
9		18						18						
10		15		1.63	2.48	0.60		21		1.70	2.42	0.56		
11		16						20						
12	white pink lithomarge	20						pink lithomarge		21				
13		21								24				
14		23					22							
15		25		1.75	2.50	0.56	25		1.76	2.45		0.55		
16		25					25							
17		24					28							
18		25					34							
19		25					32							
20		25		1.73	2.49	0.55	28		1.80	2.43		0.57		

Figure A6.3 BOREHOLE LOG 5,6

z	Panjim						Ponda					
	SPT	soil	γ	G	e_0	SPT	soil	γ	G	e_0		
1	7		1.65	2.40	0.52	8		1.65	2.40	0.52		
2	8					10						
3	10	yellow river silt				10	red granular					
4	12					12						
5	15		1.67	2.40	0.53	15		1.68	2.40	0.50		
6	17					15	pink white sandy					
7	19					16						
8	18	brown silt sand				20						
9	22					24						
10	21		1.72	2.50	0.55	21	yellow lithomarge	1.72	2.45	0.48		
11	24					22						
12	21	yellow lithomarge				28						
13	24					29						
14	25					32						
15	30		1.76	2.40	0.58	35		1.88	2.51	0.49		
16	30					36	pink lithomarge					
17	29	red pink lithomarge				35						
18	32					36						
19	31					38						
20	25		1.74	2.43	0.55	37		1.92	2.55	0.53		

Figure A6.4 BOREHOLE LOG 7

		Vasco					
	z		SPT	soil	γ	G	e_0
actual first SPT at 0.45 m	1	brown silt sand	6		1.65	2.33	0.48
	2		5				
water table	3		8				
	4		10				
	5	red pink granular	18		1.70	2.35	0.50
	6		20				
	7		21				
	8		24				
	9		22				
	10		21		1.77	2.42	0.55
	11	yellow	25				
	12	lithomarge	26				
	13	pink lithomarge	29				
	14		31				
	15		30		1.84	2.40	0.50
	16		31				
	17		32				
	18		28				
	19		22				
	20		25		1.86	2.45	0.55

ANNEXURE VII

LIQUEFACTION POTENTIAL INDEX OF SOIL IN

GOA (FOR BOREHOLES GIVEN IN ANNEXURE VI)

Table A7.1 Liquefaction Potential Index of soil profile at Mapusa

z	0.45	5	10	15	20
zw	0	0	5	10	15
Y	15.2	15.6	16.8	17.5	17.3
Gs	2.25	2.3	2.48	2.5	2.49
e0	0.54	0.53	0.6	0.56	0.55
STP-N60	3	10	15	25	25
CPT-qu	2430	2450	2470	2490	2485
Vs	70	90	105	135	135
Fc	0.2	0.22	0.17	0.1	0.12
CSR-7.5	0.076	0.070	0.089	0.092	0.088
CSR	0.150	0.138	0.177	0.182	0.174
CRR-N60	0.108	0.135	0.218	0.187	0.047
CRR-qu	0.429	0.088	0.077	0.069	0.064
CRR-Vs	0.234	0.107	0.104	0.137	0.119
LPI-N60	-32.212	<1=0			
LPI-qu	-39.685	<1=0			
LPI-Vs	-34.319	<1=0			
LPI-e	-32.636	<1=0			
rd	1.165	1.071	0.967	0.864	0.760
σ_v	6.84	84.84	168.84	256.34	342.84
$\sigma'v$	6.84	84.84	118.84	156.34	192.84
es	0.425	0.397	0.518	0.511	0.489
ecr	0.25	0.3	0.48	0.5	0.49
N-60c	11.127	10.531	13.347	19.394	17.463
quc	168.9477	63.51199	54.14323	47.21382	41.89572
Vsc	134.923	93.776	92.113	106.691	99.211
FoS-N60	1.585	2.154	2.707	2.255	0.595

FoS-qu	6.291	1.408	0.953	0.833	0.806
Fos-Vs	3.430	1.707	1.289	1.650	1.500
FoS-e	1.294	1.661	2.038	2.152	2.206
FL-N60	-0.585	-1.154	-1.707	-1.255	0.405
FL-qu	-5.29087	-0.4076	0.046994	0.16654	0.193617
FL-Vs	-2.430	-0.707	-0.289	-0.650	-0.500
FL-e	-0.294	-0.661	-1.038	-1.152	-1.206

Table A7.2 Liquefaction Potential Index of soil profile at Panjim

z	0.45	5	10	15	20
zw	0	0	5	10	15
Y	16.5	16.7	17.2	17.6	17.4
Gs	2.4	2.4	2.5	2.4	2.43
e0	0.52	0.53	0.55	0.58	0.55
STP-N60	7	15	21	30	25
CPT-qu	2660	2650	2690	2700	2750
Vs	80	105	120	145	130
Fc	0.24	0.23	0.26	0.22	0.25
CSR-7.5	0.076	0.070	0.088	0.090	0.086
CSR	0.150	0.138	0.173	0.179	0.170
CRR-N60	0.157	0.196	0.282	0.181	0.047
CRR-qu	0.499	0.093	0.081	0.073	0.067
CRR-Vs	0.330	0.133	0.130	0.157	0.111
LPI-N60	-51.307	<1=0			
LPI-qu	-49.422	<1=0			
LPI-Vs	-52.407	<1=0			
LPI-e	-50.444	<1=0			
rd	1.165	1.071	0.967	0.864	0.760
σ_v	7.425	90.925	176.925	264.925	351.925
$\sigma'v$	7.425	90.925	126.925	164.925	201.925
es	0.368	0.390	0.392	0.462	0.400
ecr	0.4	0.4	0.5	0.4	0.43
N-60c	24.918	15.259	18.081	22.659	17.065
quc	179.0573	67.34846	57.56741	50.4943	44.9721

Vsc	153.160	105.223	103.918	114.047	95.827
FoS-N60	2.303	3.131	3.570	2.230	0.607
FoS-qu	7.321	1.491	1.023	0.894	0.861
Fos-Vs	4.850	2.122	1.644	1.937	1.435
FoS-e	2.389	2.259	2.807	1.907	2.365
FL-N60	-1.303	-2.131	-2.570	-1.230	0.393
FL-qu	-6.32097	-0.49098	-0.02252	0.106355	0.138577
FL-Vs	-3.850	-1.122	-0.644	-0.937	-0.435
FL-e	-1.389	-1.259	-1.807	-0.907	-1.365

Table A7.3 Liquefaction Potential Index of soil profile at Vasco

z	0.45	5	10	15	20
zw	0	0	5	10	15
Y	16.5	17	17.7	18.4	18.6
Gs	2.33	2.35	2.42	2.4	2.45
e0	0.48	0.5	0.55	0.5	0.55
STP-N60	6	18	21	25	27
CPT-qu	2650	2680	2680	2690	2700
Vs	75	110	120	130	135
Fc	0.24	0.23	0.26	0.22	0.25
CSR-7.5	0.076	0.070	0.087	0.089	0.084
CSR	0.150	0.138	0.172	0.175	0.166
CRR-N60	0.197	0.192	0.202	0.192	0.047
CRR-qu	0.497	0.093	0.080	0.071	0.065
CRR-Vs	0.298	0.156	0.128	0.125	0.118
LPI-N60	-49.302	<1=0			
LPI-qu	-49.147	<1=0			
LPI-Vs	-49.767	<1=0			
LPI-e	-50.844	<1=0			
rd	1.165	1.071	0.967	0.864	0.760
σ_v	7.425	92.425	180.925	272.925	365.925
σ'_v	7.425	92.425	130.925	172.925	215.925
es	0.316	0.351	0.392	0.359	0.400
ecr	0.33	0.35	0.42	0.4	0.45

N-60c	21.359	18.161	17.802	18.441	17.823
quc	178.7531	67.0302	56.80026	49.31806	43.61867
Vsc	147.700	113.514	103.339	102.115	99.018
FoS-N60	2.896	3.063	2.581	2.410	0.624
FoS-qu	7.288	1.484	1.020	0.894	0.868
Fos-Vs	4.372	2.484	1.640	1.571	1.568
FoS-e	2.299	2.196	2.358	2.451	2.475
FL-N60	-1.896	-2.063	-1.581	-1.410	0.376
FL-qu	-6.28764	-0.48388	-0.01963	0.106379	0.131898
FL-Vs	-3.372	-1.484	-0.640	-0.571	-0.568
FL-e	-1.299	-1.196	-1.358	-1.451	-1.475

Table A7.4 Liquefaction Potential Index of soil profile at Margao

z	0.45	5	10	15	20
zw	0	0	5	10	15
Y	17.5	16.9	17	17.6	18
Gs	2.36	2.41	2.42	2.45	2.43
e0	0.52	0.53	0.56	0.55	0.57
STP-N60	10	15	21	25	28
CPT-qu	2670	2680	2690	2690	2700
Vs	85	95	110	120	125
Fc	0.24	0.22	0.25	0.23	0.25
CSR-7.5	0.076	0.070	0.088	0.090	0.085
CSR	0.150	0.138	0.173	0.178	0.169
CRR-N60	0.155	0.196	0.208	0.210	0.047
CRR-qu	0.475	0.093	0.081	0.072	0.066
CRR-Vs	0.365	0.115	0.110	0.107	0.104
LPI-N60	-46.898	<1=0			
LPI-qu	-46.694	<1=0			
LPI-Vs	-47.060	<1=0			
LPI-e	-46.906	<1=0			
rd	1.165	1.071	0.967	0.864	0.760
σ_v	7.875	92.375	177.375	265.375	355.375
σ'_v	7.875	92.375	127.375	165.375	205.375

es	0.368	0.397	0.413	0.416	0.427
ecr	0.36	0.41	0.42	0.45	0.43
N-60c	34.566	15.139	18.049	18.857	18.952
quc	175.7483	66.9062	57.47953	50.32052	44.68104
Vsc	158.380	97.770	95.481	93.823	92.440
FoS-N60	2.281	3.123	2.647	2.591	0.611
FoS-qu	6.966	1.481	1.022	0.892	0.864
Fos-Vs	5.355	1.842	1.402	1.320	1.355
FoS-e	2.150	2.270	2.235	2.382	2.217
FL-N60	-1.281	-2.123	-1.647	-1.591	0.389
FL-qu	-5.96647	-0.48112	-0.0222	0.107765	0.136145
FL-Vs	-4.355	-0.842	-0.402	-0.320	-0.355
FL-e	-1.150	-1.270	-1.235	-1.382	-1.217

Table A7.5 Liquefaction Potential Index of soil profile at Ponda

z	0.45	5	10	15	20
zw	0	0	5	10	15
Y	16.5	16.8	17.2	18.8	19.2
Gs	2.4	2.4	2.45	2.51	2.55
e0	0.52	0.5	0.48	0.49	0.53
STP-N60	8	15	21	35	37
CPT-qu	2950	2970	2990	3005	3010
Vs	84	105	123	165	171
Fc	0.22	0.21	0.25	0.26	0.23
CSR-7.5	0.076	0.070	0.088	0.089	0.083
CSR	0.150	0.138	0.173	0.176	0.165
CRR-N60	0.156	0.196	0.365	0.322	0.047
CRR-qu	0.677	0.105	0.089	0.079	0.071
CRR-Vs	0.383	0.138	0.136	0.207	0.188
LPI-N60	-72.680	<1=0			
LPI-qu	-72.487	<1=0			
LPI-Vs	-72.408	<1=0			
LPI-e	-72.218	<1=0			
rd	1.165	1.071	0.967	0.864	0.760

σ_v	7.425	91.425	177.425	271.425	367.425
σ'_v	7.425	91.425	127.425	171.425	217.425
es	0.385	0.367	0.307	0.311	0.390
ecr	0.4	0.4	0.45	0.51	0.55
N-60c	28.478	15.217	18.045	25.930	24.340
quc	199.3785	74.95457	64.3328	55.88102	49.2844
Vsc	160.918	107.380	106.574	128.550	123.511
FoS-N60	2.295	3.122	4.628	4.020	0.626
FoS-qu	9.930	1.671	1.133	0.983	0.948
Fos-Vs	5.620	2.211	1.731	2.588	2.504
FoS-e	2.288	2.397	3.228	3.610	3.106
FL-N60	-1.295	-2.122	-3.628	-3.020	0.374
FL-qu	-8.93	-0.67117	-0.13299	0.017082	0.052216
FL-Vs	-4.620	-1.211	-0.731	-1.588	-1.504
FL-e	-1.288	-1.397	-2.228	-2.610	-2.106

Table A7.6 Liquefaction Potential Index of soil profile at Canacona

z	0.45	5	10	15	20
zw	0	0	5	10	15
Y	15.2	15.8	17.5	18.3	18.6
Gs	2.22	2.36	2.4	2.53	2.54
e0	0.5	0.53	0.55	0.54	0.58
STP-N60	14	15	18	28	26
CPT-qu	2530	2530	2540	2550	2550
Vs	85	90	95	105	105
Fc	0.27	0.24	0.2	0.23	0.22
CSR-7.5	0.076	0.070	0.088	0.090	0.085
CSR	0.150	0.138	0.175	0.179	0.168
CRR-N60	0.163	0.163	0.250	0.187	0.047
CRR-qu	0.478	0.090	0.077	0.069	0.063
CRR-Vs	0.427	0.100	0.083	0.093	0.079
LPI-N60	-45.364	<1=0			
LPI-qu	-45.806	<1=0			
LPI-Vs	-45.628	<1=0			

LPI-e	-45.700	<1=0			
rd	1.165	1.071	0.967	0.864	0.760
σ_v	6.84	85.84	173.34	264.84	357.84
σ'_v	6.84	85.84	123.34	164.84	207.84
es	0.315	0.382	0.438	0.403	0.462
ecr	0.22	0.36	0.4	0.53	0.54
N-60c	51.924	15.704	15.721	21.154	17.494
quc	176.1511	65.13967	54.82792	47.45036	41.63362
Vsc	166.600	90.385	80.528	86.541	77.651
FoS-N60	2.385	2.599	3.144	2.306	0.614
FoS-qu	7.009	1.442	0.973	0.854	0.829
FoS-Vs	6.261	1.601	1.046	1.148	1.028
FoS-e	1.536	2.076	2.011	2.896	2.574
FL-N60	-1.385	-1.599	-2.144	-1.306	0.386
FL-qu	-6.00868	-0.44239	0.02664	0.146406	0.170591
FL-Vs	-5.261	-0.601	-0.046	-0.148	-0.028
FL-e	-0.536	-1.076	-1.011	-1.896	-1.574

Table A7.7 Liquefaction Potential Index of soil profile at Bicholim

z	0.45	5	10	15	20
zw	0	0	5	10	15
Y	16.6	16.5	16.8	17.6	17.9
Gs	2.32	2.38	2.4	2.45	2.5
e0	0.52	0.49	0.51	0.52	0.55
STP-N60	8	12	15	25	34
CPT-qu	2570	2580	2585	2600	2610
Vs	80	90	100	120	145
Fc	0.11	0.15	0.14	0.22	0.21
CSR-7.5	0.076	0.070	0.088	0.091	0.086
CSR	0.150	0.138	0.175	0.180	0.171
CRR-N60	0.124	0.132	0.212	0.295	0.047
CRR-qu	0.453	0.090	0.078	0.071	0.065
CRR-Vs	0.333	0.105	0.091	0.114	0.137
LPI-N60	-43.541	<1=0			

LPI-qu	-43.428	<1=0			
LPI-Vs	-44.133	<1=0			
LPI-e	-43.451	<1=0			
rd	1.165	1.071	0.967	0.864	0.760
σv	7.47	89.97	173.97	261.97	351.47
σ'v	7.47	89.97	123.97	161.97	201.47
es	0.461	0.400	0.430	0.385	0.430
ecr	0.32	0.38	0.4	0.45	0.5
N-60c	28.392	12.272	13.068	19.054	23.235
que	172.6956	65.0563	55.78067	48.8445	43.39664
Vsc	153.636	92.903	85.418	97.074	106.893
FoS-N60	1.819	2.107	2.667	3.606	0.606
FoS-qu	6.655	1.441	0.989	0.866	0.840
Fos-Vs	4.894	1.679	1.149	1.393	1.769
FoS-e	1.528	2.090	2.045	2.574	2.556
FL-N60	-0.819	-1.107	-1.667	-2.606	0.394
FL-qu	-5.65465	-0.44059	0.01118	0.134161	0.159504
FL-Vs	-3.894	-0.679	-0.149	-0.393	-0.769
FL-e	-0.528	-1.090	-1.045	-1.574	-1.556

ANNEXURE VIII

LIQUEFACTION SETTLEMENT FOR SOIL IN

GOA (FOR BOREHOLES GIVEN IN ANNEXURE VI)

Table A8.1 Liquefaction Settlement of soil profile at Mapusa

z	0.45	5	10	15	20
zw	0	0	5	10	15
N60	3	10	15	25	25
CSR-7.5	0.076	0.070	0.089	0.092	0.088
CSR	0.150	0.138	0.177	0.182	0.174
CRR-N60	0.108	0.135	0.218	0.187	0.047
FoS-N60	1.585	2.154	2.707	2.255	0.595
Strain %	-	-	-	-	0.02
Settlement mm	-	-	-	-	1.0
Total					1.0

Table A8.2 Liquefaction Settlement of soil profile at Panjim

z	0.45	5	10	15	20
zw	0	0	5	10	15
N60	7	15	21	30	25
CSR-7.5	0.076	0.070	0.088	0.090	0.086
CSR	0.150	0.138	0.173	0.179	0.170
CRR-N60	0.157	0.196	0.282	0.181	0.047
FoS-N60	2.303	3.131	3.570	2.230	0.607
Strain %	-	-	-	-	0.01
Settlement mm	-	-	-	-	0.5
Total					0.5

Table A8.3 Liquefaction Settlement of soil profile at Vasco

z	0.45	5	10	15	20
zw	0	0	5	10	15
N60	6	18	21	25	27
CSR-7.5	0.076	0.070	0.087	0.089	0.084

CSR	0.150	0.138	0.172	0.175	0.166
CRR-N60	0.197	0.192	0.202	0.192	0.047
FoS-N60	2.896	3.063	2.581	2.410	0.624
Strain %	-	-	-	-	0.005
Settlement mm	-	-	-	-	0.25
Total					0.25

Table A8.4 Liquefaction Settlement of soil profile at Margao

z	0.45	5	10	15	20
zw	0	0	5	10	15
N60	10	15	21	25	28
CSR-7.5	0.076	0.070	0.088	0.090	0.085
CSR	0.150	0.138	0.173	0.178	0.169
CRR-N60	0.155	0.196	0.208	0.210	0.047
FoS-N60	2.281	3.123	2.647	2.591	0.611
Strain %	-	-	-	-	0.004
Settlement mm	-	-	-	-	0.2
Total					0.2

Table A8.5 Liquefaction Settlement of soil profile at Ponda

z	0.45	5	10	15	20
zw	0	0	5	10	15
N60	8	15	21	35	37
CSR-7.5	0.076	0.070	0.088	0.089	0.083
CSR	0.150	0.138	0.173	0.176	0.165
CRR-N60	0.156	0.196	0.365	0.322	0.047
FoS-N60	2.295	3.122	4.628	4.020	0.626
Strain %	-	-	-	-	0.0008
Settlement mm	-	-	-	-	0.04
Total					0.04

Table A8.6 Liquefaction Settlement of soil profile at Canacona

z	0.45	5	10	15	20
zw	0	0	5	10	15

N60	14	15	18	28	26
CSR-7.5	0.076	0.070	0.088	0.090	0.085
CSR	0.150	0.138	0.175	0.179	0.168
CRR-N60	0.163	0.163	0.250	0.187	0.047
FoS-N60	2.385	2.599	3.144	2.306	0.614
Strain %	-	-	-	-	0.005
Settlement mm	-	-	-	-	0.25
Total					0.25

Table A8.7 Liquefaction Settlement of soil profile at Bicholim

z	0.45	5	10	15	20
zw	0	0	5	10	15
N60	8	12	15	25	34
CSR-7.5	0.076	0.070	0.088	0.091	0.086
CSR	0.150	0.138	0.175	0.180	0.171
CRR-N60	0.124	0.132	0.212	0.295	0.047
FoS-N60	1.819	2.107	2.667	3.606	0.606
Strain %	-	-	-	-	0.002
Settlement mm	-	-	-	-	0.1
Total					0.1

ANNEXURE IX

TSUNAMI PROTECTION FOR GOA

Table A9.1 Tsunami Velocity and Wave Height for 3m TGSB

TGSB(bund), MF(mangrove forest)

Height of obstruction 3m, $V_1=10$ m/s, $b = 1000$ m, $g=9.81$ m/s²

y_1	m	0.5	1	2	3	4	5	10	
Q	m³/s	5000	10000	20000	30000	40000	50000	100000	
V₂	m/s	1.4	2.0	2.7	3.2	3.6	3.9	5.0	
y₂	m	3.5	5.0	7.5	9.5	11.2	12.9	20.1	
L	m	20.7	30.3	44.8	56.8	67.5	77.4	120.8	
ΔH	m	2.0	0.9	-0.7	-1.9	-2.8	-3.6	-6.3	
h₁	m	0.5	2.0	4.5	6.5	8.2	9.9	17.1	
V₃	m/s	2.8	6.0	8.9	10.7	12.1	13.2	17.4	
h₂	m	0.4	1.6	3.3	4.4	5.3	6.1	8.6	
L₂	m	1.5	6.6	13.1	17.7	21.3	24.3	34.5	
V₄	MF	m	6.3	13.0	18.4	21.4	23.5	25.1	29.9
	TGSB	m	4.5	9.2	13.1	15.2	16.6	17.8	21.2
Qf	MF	m³/s	1766	2918	3787	4284	4647	4939	5929
	TGSB	m³/s	1251	2068	2684	3036	3294	3500	4202

Table A9.2 Tsunami Velocity and Wave Height for 6 m TGSB

Height of obstruction 6m, $V_1=10$ m/s, $b = 1000$ m, $g=9.81$ m/s²

y_1	m	0.5	1	2	3	4	5	10
h₁	m	Below bund		1.5	3.5	5.2	6.9	14.1
V₃	m/s	-	-	5.1	7.8	9.6	11.1	15.8
h₂	m	-	-	1.1	2.4	3.4	4.2	7.1
L₂	m	-	-	4.3	9.5	13.5	16.9	28.4
V₄	m	-	-	7.5	11.1	13.3	14.8	19.3
Qf	m³/s	-	-	1851	2466	2833	3103	3941

Table A9.3 Tsunami Velocity and Wave Height for 9 m TGSB

Height of obstruction 9m, $V_1=10$ m/s, $b = 1000$ m, $g=9.81$ m/s²

y_1	m	0.5	1	2	3	4	5	10
-------	----------	------------	----------	----------	----------	----------	----------	-----------

h₁	m	Below bund			0.5	2.2	3.9	11.1
V₃	m/s	-	-	-	2.9	6.3	8.3	14.0
h₂	m	-	-	-	0.3	1.4	2.4	5.6
L₂	m	-	-	-	1.3	5.8	9.6	22.4
V₄	m	-	-	-	4.1	8.7	11.2	17.1
Qf	m³/s	-	-	-	1261	2136	2566	3639

Table A9.4 Tsunami Velocity and Wave Height for 3 m TGSB with trees

Height of obstruction 18m, $V_1=10$ m/s, $b = 1000$ m, $g=9.81$ m/s²

y₁	m	0.5	7	8	9	10
h₁	m	Below bund			0.8	2.1
V₃	m/s	-	-	-	3.7	6.1
h₂	m	-	-	-	0.4	1.1
L₂	m	-	-	-	1.6	4.3
V₄	m	-	-	-	4.6	7.5
Qf	m³/s	-	-	-	1496	2097

ANNEXURE X

RECENT NATURAL DISASTERS IN GOA

Recent Cyclones to strike Goa

In the past there have been many super-cyclones to hit India. They were mostly in the Bay of Bengal but in recent years there have been major super cyclones affecting Goa. Two of these have been super cyclones. With sustained gusts of wind exceeding 200kmph and rotating rain bands hundreds of kilometres wide.

Table A10.1 Recent Cyclones in Arabian Sea near Goa

year	name	max wind speeds (sustained 1 min)	category of storm (scale 1 to 5)
2009	PHYAN	95	2
2011	ARB 01	45	1
2014	NANUK	85	2
2015	ARB02	55	2
2017	OCKHI	155	3
2018	GAJA	130	3
2019	VAYU	185	3-4
2019	MAHA	185	3-4
2019	KYARR	240	4-5
2020	FANI	110	2
2020	NISARGA	140	3
2021	TAUTAKE	220	4-5

Due to global warming and El-Nino syndrome there has been a surge in cyclones in the Arabian Sea off the coast of Goa. TGSBs have survived all recent super cyclones. Super events have increased in intensity in past 10 years.

Tropical Cyclone Kyarr was seen on October 27, 2019, by NASA's Aqua satellite. At the time, Kyarr was the second strongest tropical cyclone ever observed in the Arabian Sea, with 150 mph winds and a 928 mb central pressure. This true-color image was captured by the VIIRS sensor on board the NOAA-20 satellite, which provides daily, high-resolution visible and infrared images of Earth's atmosphere from across the globe. Satellite picture shows the eye and the spin-wheel

clouds as Super cyclone Kyarr approaches Goa (green spot). You can see the wave front and storm surge approaching the shore.

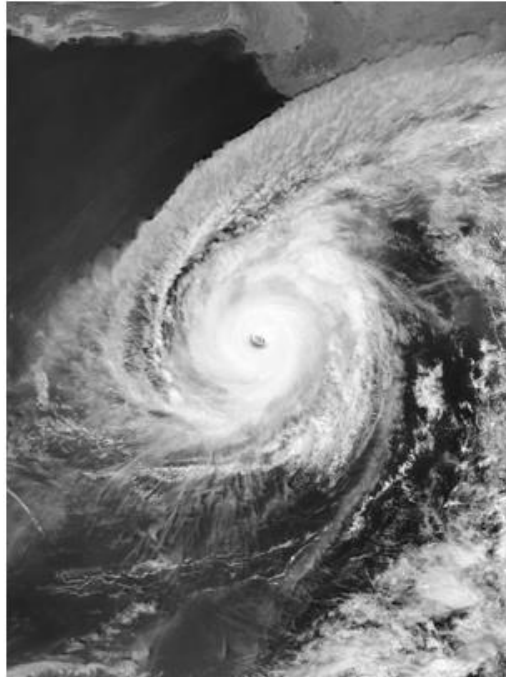


Figure A10.1 Super cyclone Kyarr approaches Goa: NASA.



Figure A10.2 Roof of residences damaged by wind. The shovel was used to clear the fallen trees)



Figure A10.3 (a) Government and Public buildings damaged by 75 year old gulmohar tree fall by uprooting (ToI).

(b) Roads damaged at Panjim by 200 year old banyan tree fall by uprooting (ToI).

(c) Roads flooded and areas cut-off below kadamba plateau near Panjim (Times of India)



Figure A10.4 (a) Donna Paula jetty inundated by huge waves as cyclone approaches (ToI) as a 2 m storm surge makes the water touch the top of the jetty.

(b) Jetty during normal times a hub of tourist activity and fishing.

Even with this massive storm surge there was no much flooding in Goa due to TGSBs

Cyclone Tauktae:

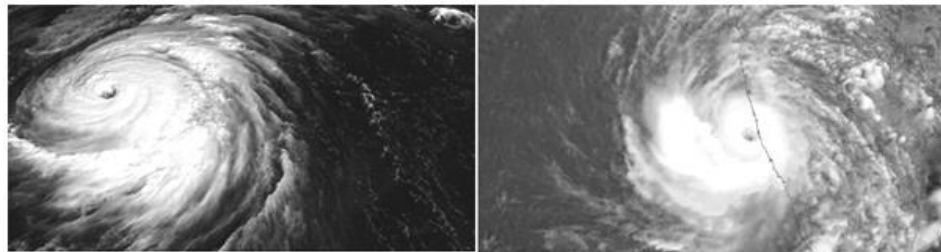


Figure A10.5 Cyclone Tauktae-Skymet weather

Tauktae intensified to a Very Severe Cyclonic Storm located Northwest of Goa which received very heavy rainfall of over 100mm yesterday with high-velocity winds gusting to 100kmh. The cyclone kept on intensifying further, adding wind speed to the order of 160kmh. It had the potential to even strengthen further to an Extremely Severe Cyclonic Storm, albeit remaining on the borderline. The winds exceeded 170 kmph gusting to 190kmph before reaching the coastline of Saurashtra on 18th May early morning. The huge storm after making landfall remained a significant cyclone obliterating and flooding even in Rajasthan and Madhya Pradesh. Tauktae spent more than 12 hours as a storm traveling across India before weakening to a depression.



Figure A10.6 Cyclone Tauktae Damage (News 18, India Today)

There were huge waves and some tree falls of tall tap-root trees but the flooding was quickly dispersed within 24 to 48 hours. Electricity was almost immediately restored. The coastal photo above shows how the rear row of trees are protected by the front row trees which act as aerodynamic wind break negating the wind within a space of few meters.

July 21 floods

From 23 to 25 July there were devastating floods in Goa caused by release of dam waters at late night due to filling of dam by cloud burst that occurred in the preceding five days. 600 mm rain fell in 5 days which was like a month's rain.



Figure A10.7 July floods in Goa due to cloud break



Figure A10.8 July floods in Goa due to cloud break

While rest of Goa was able to deal reasonably well due to TGSB network this floods were caused as the waters of Tilar Dam in Maharashtra which has FSL 93 m reached 91.5m at 3pm at night. A panic opening of dam's gates resulted in a flash flood downstream in Goa. However due to the excellent TGSB network the water cleared within 24 hours, although there was considerable loss to property due to the excess flow of water that the TGSBs had to handle.

ANNEXURE XI

GENERAL EARTHQUAKE DATA

Table A11.1 Comparative Earthquake Scale (USGS)

Richter	Mercali	Scale	MSK-64	Description
1-3	Not Felt	I	Not perceivable	Not felt except by few under favourable circumstances
3-4	Weak	II	Hardly Perceivable	Felt by few in upper floor of building
	Weak	III	Weak	Felt noticeably indoors. Standing cars rock slightly.
4-5	Light	IV	Largely Observed	Felt indoors by many, outdoors by few. Heavy trucks rock.
	Moderate	V	Fairly strong	Felt indoors by all. Windows break. Objects overturned
5-6	Strong	VI	Strong	Heavy furniture move. Slight damage to buildings
	Very Strong	VII	Very Strong	Moderate damage in poor designed buildings. Chimney break.
6-7	Severe	VIII	Damaging	Considerable building damage. Chimney fall.
	Violent	IX	Destructive	Framed structures damaged. Partial collapse of buildings
> 7	Extreme	X	Devastating	Masonry structures destroyed. Rails bent
	Extreme	XI	Catastrophic	Underground lines Bridges and buildings destroyed.
	Extreme	XII		Total damage. Waves seen on ground structures.

Table A11.2 Magnitude Energy and damage by Earthquakes

Magnitude	Energy in joules	Notes
1.0	2.0×10^6	
2.0	6.3×10^7	Only felt nearby
3.0	2.0×10^9	Energy from 50 liters of petrol
4.0	6.3×10^{10}	Often felt up to 10's of miles away
5.0	2.0×10^{12}	Energy from 50 000 liters of petrol
6.0	6.3×10^{13}	3.3 Hiroshima-size A bombs

7.0	2.0×10^{15}	
8.0	6.3×10^{16}	1–2 earthquakes this size each year
9.0	2.0×10^{18}	Total annual energy use of UK

Earthquake data For TGSBs.

As Goa is a non-seismic region, we need to study earthquakes from neighboring and similar regions for seismic analysis of TGSBs. Earthquake data used is mainly seismograms. However additional data is needed for more understanding of earthquakes. Many earthquakes were studied but only few were finally chosen for the software analysis

In case TGSB ha to be universally applicable the different earthquakes of different regions need studies. The earthquakes considered from India were

1. Koyna, (Closest to Goa)
2. Bhuj, (Most powerful closest to goa - For TGSB in North-West India region)
3. Uttarkashi, (Himalayan quakes - For TGSB in Ganga-Bramaputra region)

The earthquakes considered from outside India were

1. Sumatra – Indonesia (Caused tsunami in India - For TGSB in Indo-China region)
2. El Centro –USA (Most studied earthquake in the world - standard for comparison- For TGSB in American region)
3. Kobe – Japan, (pominent earthquake in the Japan-For TGSB in Japan-Korea region)

Time is given in UCT (Universal Corrected Time) or GMT (Greenwich Mean time). Acceleration is measured in cm/s/s velocity in cm/s and displacement in cm. (: Acceleration x 0.0102 = g, velocity x 0.01 = m/s and displacement x 0.01 = m).

Table A11.3 Magnitude and Effect of Real Earthquakes

	Magnitude	Duration (s)	PGA (g)	Effective stress	XY Strain
Koyna	5.6	40	0.16	10.56	302
Bhuj	7.0	134	0.10	4.75	50.3
Uttarkashi	7.0	36	0.24	-2.77	96
Sumatra	8.4	125	0.04	14.69	86
El Centro	6.9	54	0.34	-26.18	3373
Kobe	6.9	45	0.49	5.24	544

Table A11.4 Data set For Koyna1967 Earthquake

Location	Koyna	
Date	1967/12/10	
Time	22:51	GMT
Region	India	
Latitude	17.50	
Longitude	73.73	
Depth	3 km	
Mechanism	Fault-Slip	
Mw	5.6	Moment Magnitude
Ms		Surface Wave Magnitude
Mb		Body wave magnitude
ML		Richter magnitude

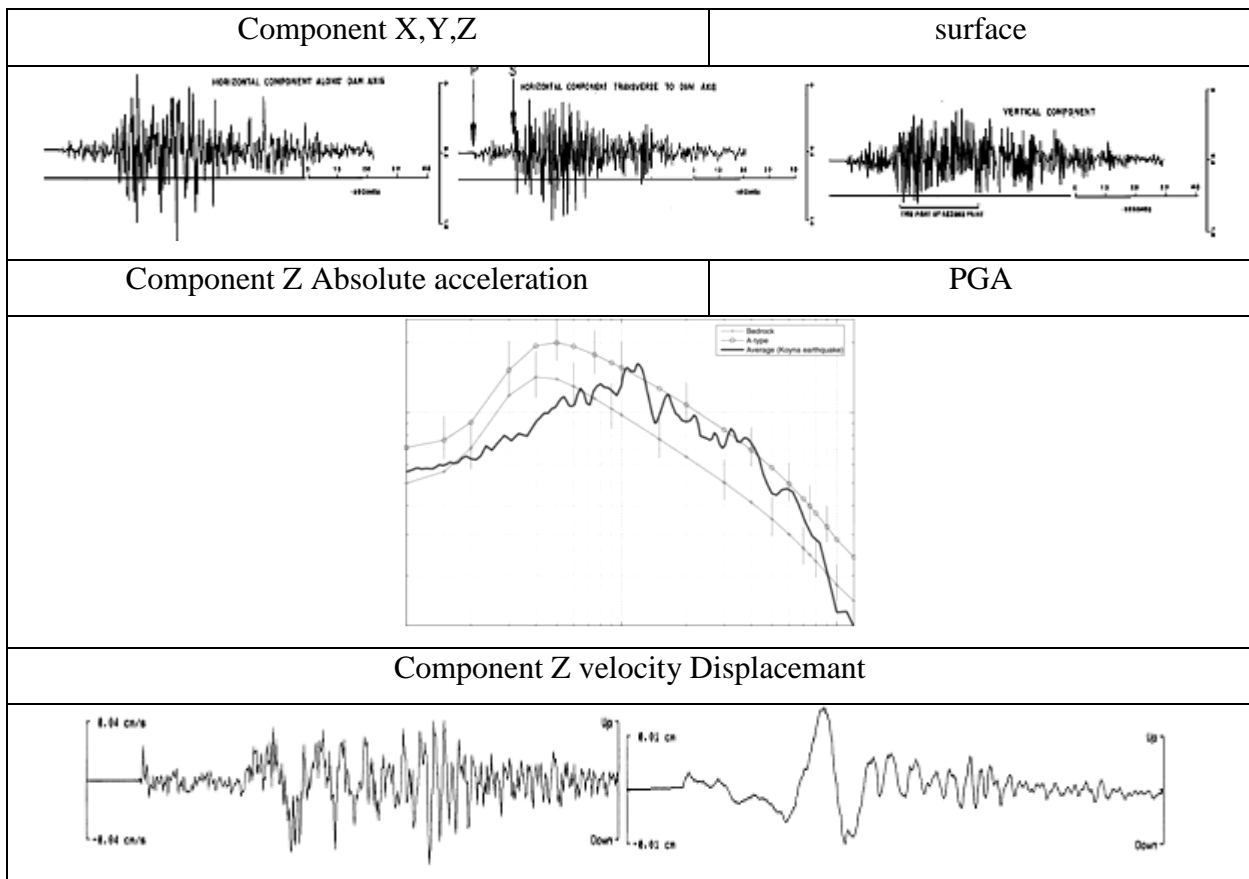


Figure A11.1 Accelerogram and Spectra for Koyna1967 Earthquake

Table A11.5 Filtered Accelerogram readings for Koyna1967 Earthquake
(Period 0.075 s),(Acceleration g)

0.075	0.102		3.075	2.346		6.075	-2.04
0.15	-0.051		3.15	1.02		6.15	0.51
0.225	-0.204		3.225	-1.428		6.225	-0.51
0.3	-0.51		3.3	4.08		6.3	3.57
0.375	0.153		3.375	-2.55		6.375	2.55
0.45	0.51		3.45	2.04		6.45	-4.08
0.525	0.357		3.525	-2.346		6.525	1.02
0.6	0.204		3.6	1.53		6.6	-1.53
0.675	-0.051		3.675	-0.51		6.675	3.06
0.75	0.612		3.75	2.55		6.75	-1.53
0.825	-0.714		3.825	-0.408		6.825	1.632
0.9	1.122		3.9	0.051		6.9	-0.51
0.975	-0.408		3.975	-1.224		6.975	1.632
1.05	0.204		4.05	1.734		7.05	-0.816
1.125	0.51		4.125	-0.816		7.125	1.02
1.2	-0.408		4.2	1.02		7.2	-2.04
1.275	0.765		4.275	-3.06		7.275	1.53
1.35	-0.4284		4.35	1.02		7.35	-1.734
1.425	0.102		4.425	-2.55		7.425	1.734
1.5	0.612		4.5	-2.04		7.5	1.53
1.575	-0.102		4.575	0.51		7.575	-0.51
1.65	0.102		4.65	-2.55		7.65	2.04
1.725	-0.255		4.725	0.51		7.725	-0.612
1.8	0.765		4.8	-2.04		7.8	0.51
1.875	-0.306		4.875	1.53		7.875	-2.04
1.95	0.255		4.95	-1.53		7.95	2.04
2.025	0.153		5.025	2.55		8.025	-0.714
2.1	-0.102		5.1	-1.53		8.1	1.734
2.175	0.765		5.175	-2.04		8.175	-0.51
2.25	-0.714		5.25	-1.53		8.25	0.51

2.325	0.51	5.325	3.264	8.325	-0.51
2.4	-0.0204	5.4	-1.428	8.4	1.02
2.475	2.04	5.475	1.428	8.475	-0.51
2.55	-2.55	5.55	-2.55	8.55	1.53
2.625	1.836	5.625	2.55	8.625	-0.51
2.7	-0.51	5.7	-4.08	8.7	1.53
2.775	0.051	5.775	1.02	8.775	-0.102
2.85	-1.326	5.85	3.57	8.85	1.53
2.925	0.51	5.925	-2.04	8.925	-0.204
3	-1.53	6	3.06	9	1.02

Figure A11.2 Filtered Accelerogram for Koyna1967 Earthquake in Microsoft Excel

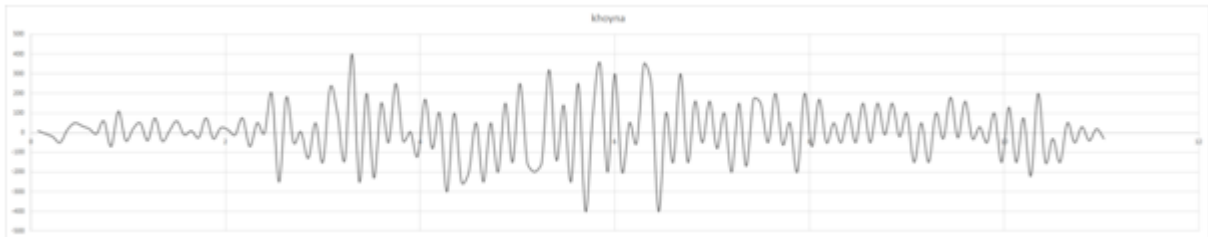


Table A11.6 Data set For Bhuj 2001 Earthquake

Location	Bhuj/Kachchh	
Date	2001-01-26	
Time	03:16:40	GMT
Region	India	
Latitude		
Longitude		
Mw		Moment Magnitude
Ms		Surface Wave Magnitude
Mb		Body wave magnitude
ML	7.0	Richter magnitude

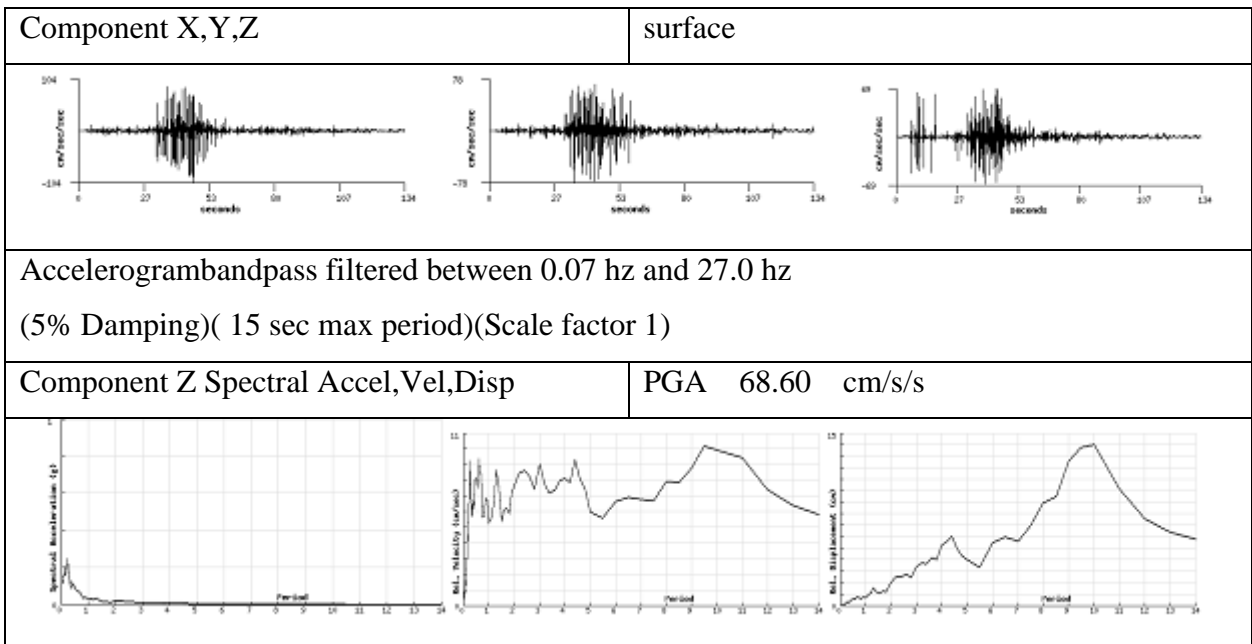
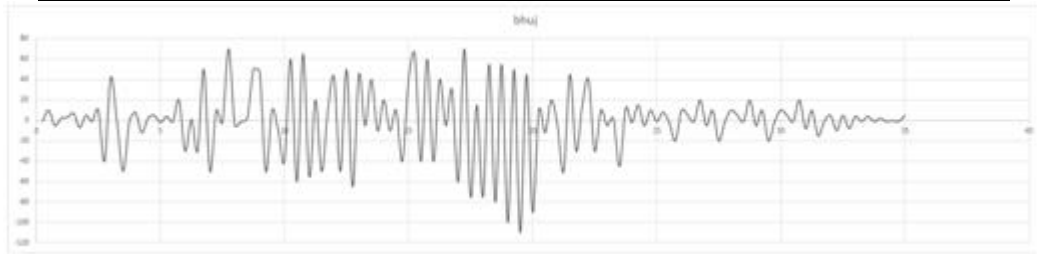


Figure A11.3 Accelerogram and Spectra for Bhuj 2001 Earthquake

Table A11.7 Filtered Accelerogram readings for Bhuj 2001 Earthquake
 (Period 0.25 s),(Acceleration g)

0.25	-0.0102		7.25	0.102		14.25	-0.102
0.5	0.102		7.5	-0.0204		14.5	0.102
0.75	-0.051		7.75	0.714		14.75	-0.408
1	0.0204		8	-0.051		15	0.408
1.25	0.0306		8.25	-0.0102		15.25	0.663
1.5	0.0714		8.5	0.0204		15.5	-0.408
1.75	-0.0714		8.75	0.51		15.75	0.612
2	0.051		9	0.4896		16	-0.408
2.25	-0.0102		9.25	-0.51		16.25	0.408
2.5	0.102		9.5	0.102		16.5	-0.051
2.75	-0.408		9.75	-0.102		16.75	0.306
3	0.4284		10	-0.408		17	-0.612
3.25	-0.0102		10.25	0.612		17.25	0.714
3.5	-0.51		10.5	-0.612		17.5	-0.765
3.75	-0.0102		10.75	0.663		17.75	0.153
4	0.0816		11	-0.561		18	-0.765
4.25	-0.1224		11.25	0.204		18.25	0.561

4.5	0.0204	11.5	-0.51	18.5	-0.816
4.75	0.051	11.75	0.102	18.75	0.561
5	-0.0204	12	0.4284	19	-1.02
5.25	0.0408	12.25	-0.51	19.25	0.51
5.5	-0.0102	12.5	0.51	19.5	-1.122
5.75	0.204	12.75	-0.663	19.75	0.459
6	-0.306	13	0.459	20	-0.918
6.25	0.0102	13.25	-0.051	20.25	0.102
6.5	-0.306	13.5	0.408	20.5	-0.1224
6.75	0.51	13.75	-0.102	20.75	0.204
7	-0.51	14	0.204	21	-0.051



FigureA11.4FilteredAccelerogram for Bhuj 2001 Earthquake in Microsoft Excel

Table A11.8 Data set For Uttarkashi 1991 Earthquake

Location	Uttarkashi	
Date	1991-10-19	
Time	21:23:15	GMT
Region	India	
Latitude	30.7800	
Longitude	78.7740	
Depth	10.0 km	
Mechanism	Unknown	
Mw		Moment Magnitude
Ms	7.0	Surface Wave Magnitude
Mb		Body wave magnitude
ML		Richter magnitude

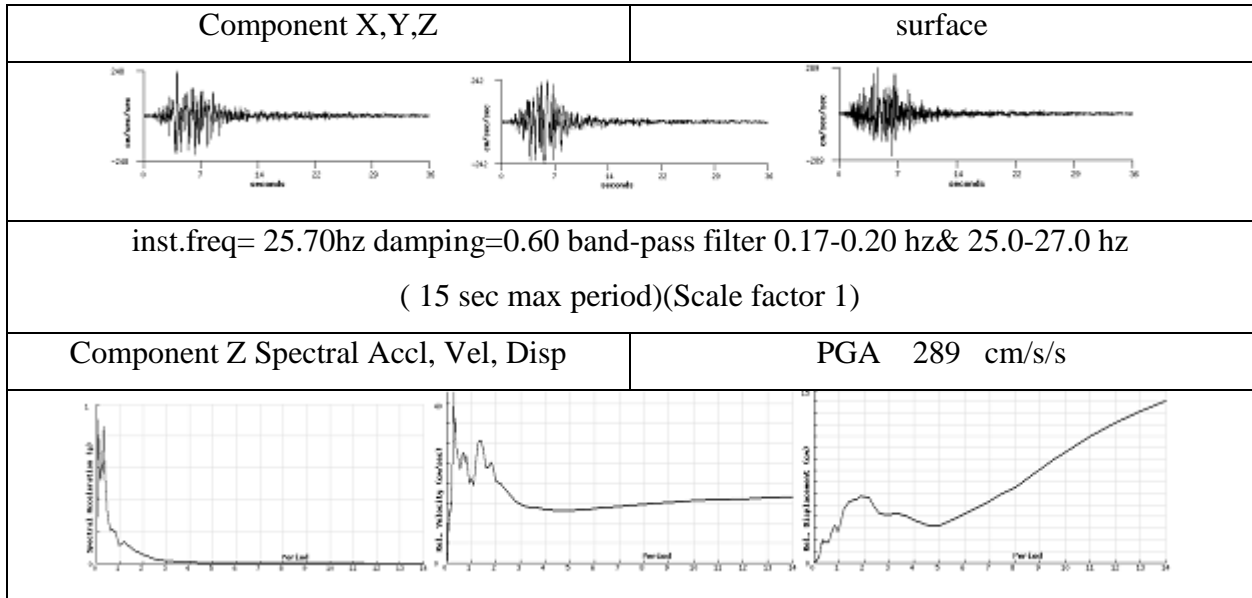


Figure A11.5 Accelerogram and Spectra for Uttarkashi 1991 Earthquake

Table A11.9 Filtered Accelerogram readings for Uttarkashi 1991 Earthquake

(Period 0.25 s),(Acceleration g)

0.25	-0.051		5.25	-2.244		10.25	0.612
0.5	0.051		5.5	0.612		10.5	-0.714
0.75	-0.0612		5.75	2.04		10.75	0.51
1	0.0408		6	-1.224		11	-0.51
1.25	-0.102		6.25	0.51		11.25	0.306
1.5	0.102		6.5	-2.448		11.5	-0.51
1.75	0.051		6.75	0.612		11.75	0.408
2	-0.204		7	2.55		12	-0.306
2.25	0.51		7.25	-0.918		12.25	0.51
2.5	-0.51		7.5	0.102		12.5	-0.255
2.75	-0.612		7.75	-0.714		12.75	0.357
3	0.714		8	1.02		13	0.051
3.25	-0.918		8.25	-0.51		13.25	-0.102
3.5	0.612		8.5	1.53		13.5	0.459
3.75	1.224		8.75	-1.53		13.75	-0.255
4	-0.204		9	2.04		14	0.204

4.25	-2.244	9.25	-0.51	14.25	-0.102
4.5	0.612	9.5	-1.53	14.5	0.051
4.75	-1.53	9.75	1.53	14.75	-0.051
5	0.918	10	-0.612	15	0.0816
				15.25	-0.051
				15.5	0.0408

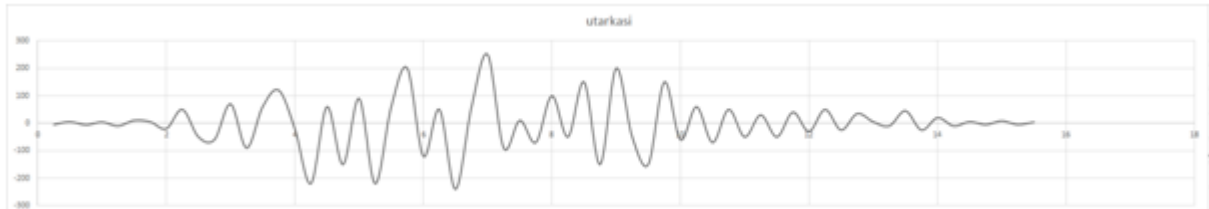
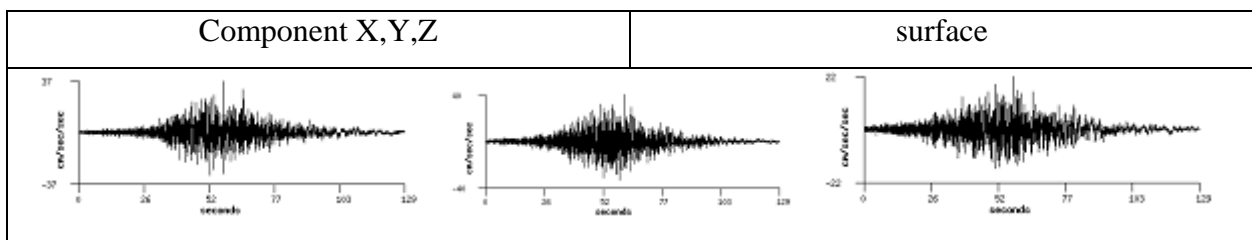


Figure A11.6 Filtered Accelerogram for Uttarkashi 1991 Earthquake in Microsoft Excel

Table A11.10 Data set For Southern Sumatra 2007 Earthquake

Location	Southern Sumatra,	
Date	2007-09-12	
Time	11:10:00	GMT
Region	Indonesia	
Latitude	-4.5200	
Longitude	101.3740	
Depth	34.0 km	
Mechanism		
Mw	8.4	Moment Magnitude
Ms		Surface Wave Magnitude
Mb		Body wave magnitude
ML		Richter magnitude



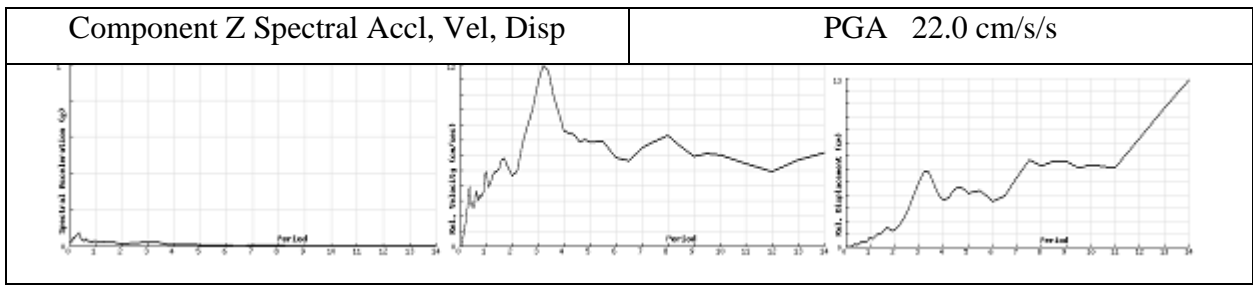


Figure A11.7 Accelerogram and Spectra for Southern Sumatra 2007 Earthquake

Table A11.11 Filtered Accelerogram readings for Southern Sumatra 2007 Earthquake

(Period s),(Acceleration g)

1	0.2448		31	2.2032		61	1.836
2	-0.2448		32	-2.8152		62	-1.4688
3	0.4896		33	2.5704		63	0.612
4	-0.4896		34	-1.836		64	0.9792
5	0.612		35	3.06		65	1.836
6	-0.612		36	-2.448		66	-1.836
7	0.3672		37	3.672		67	-0.612
8	-0.612		38	-3.06		68	0.612
9	0.612		39	1.836		69	1.224
10	-0.3672		40	3.672		70	-1.4688
11	0.612		41	-3.672		71	1.836
12	-0.612		42	4.5288		72	-1.224
13	1.224		43	-3.06		73	1.4688
14	-0.612		44	1.836		74	-0.9792
15	0.9792		45	-2.448		75	1.1016
16	-0.612		46	2.2032		76	-0.8568
17	1.224		47	-0.612		77	0.612
18	-1.224		48	2.2032		78	-0.612
19	1.4688		49	-1.224		79	0.4896
20	-1.224		50	1.224		80	-0.2448
21	1.4688		51	-1.836		81	0.3672
22	-1.4688		52	3.672		82	-0.1224
23	-2.448		53	-1.836			
24	1.224		54	3.06			

25	-0.8568		55	-1.836		
26	1.4688		56	1.836		
27	-0.8568		57	-1.9584		
28	-2.6928		58	1.7136		
29	1.9584		59	-1.224		
30	-1.224		60	-0.9792		

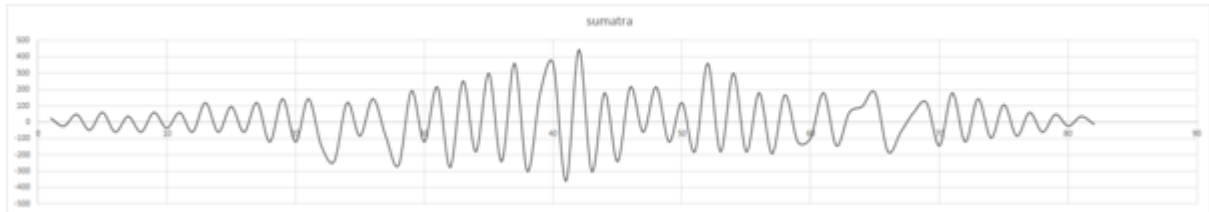


Figure A11.8 Filtered Accelerogram for Southern Sumatra 2007 Earthquake in Microsoft Excel

Table A11.12 Data set For El Centro 1940 Earthquake

Location	El Centro,	
Date	1940-05-19	
Time	04:36:41	GMT
Region	California,USA	
Latitude	32.7601	
Longitude	-115.4162	
Depth	8.8 km	
Mechanism	Strike-slip	
Strike	323	
Dip	80	
Rake	180	
Mw	6.9	Moment Magnitude
Ms	6.7	Surface Wave Magnitude
Mb		Body wave magnitude
ML	6.9	Richter magnitude

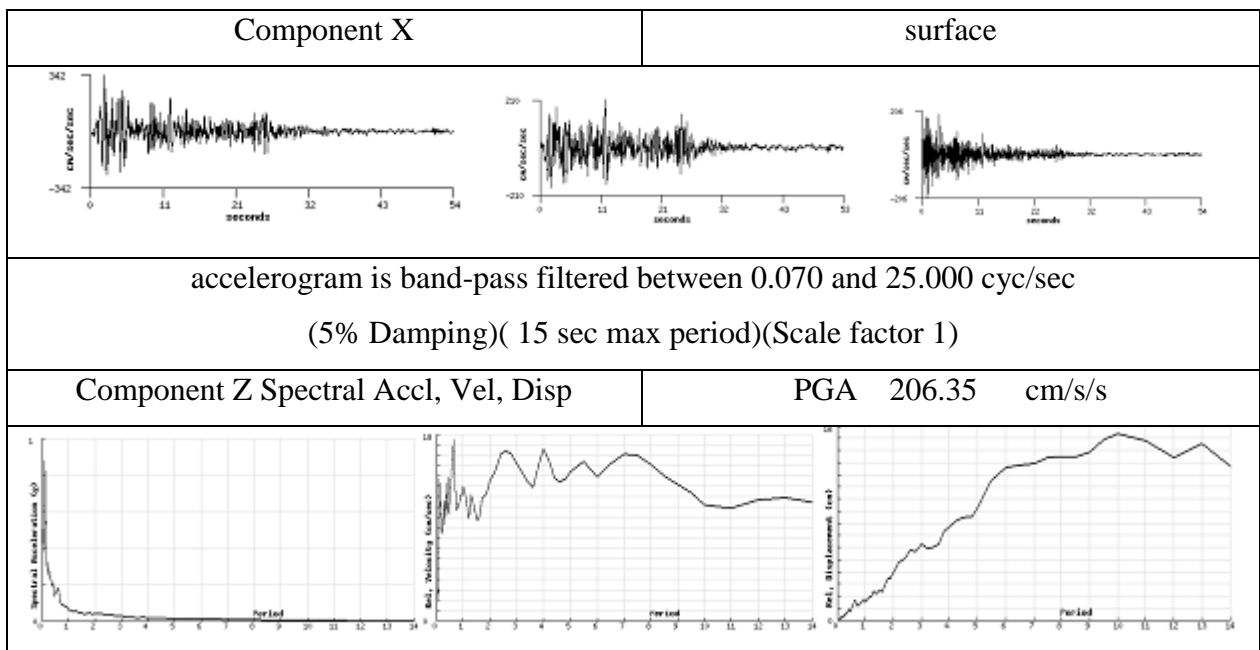


Figure A11.9 Accelerogram and Spectra for El Centro 1940 Earthquake

Table A11.13 Filtered Accelerogram readings for El Centro 1940 Earthquake

(Period s),(Acceleration g)

0.25	-0.204		7.25	-0.816		14.25	1.224
0.5	0.408		7.5	0.816		14.5	-0.816
0.75	-0.51		7.75	-0.51		14.75	0.51
1	0.612		8	0.408		15	-0.408
1.25	-0.816		8.25	-1.224		15.25	1.224
1.5	0.816		8.5	0.51		15.5	-0.051
1.75	2.04		8.75	-1.53		15.75	0.306
2	-2.04		9	1.734		16	-0.306
2.25	3.468		9.25	-1.224		16.25	-0.0816
2.5	-2.55		9.5	1.632		16.5	0.051
2.75	2.04		9.75	-1.53		16.75	0.204
3	1.53		10	1.53		17	-0.204
3.25	-2.55		10.25	0.408		17.25	0.408
3.5	0.51		10.5	-0.51		17.5	-0.816
3.75	-0.408		10.75	0.51		17.75	0.612
4	0.408		11	-0.612		18	-0.714
4.25	-0.51		11.25	-0.102		18.25	0.408

4.5	1.53	11.5	-1.02	18.5	-0.204
4.75	-1.224	11.75	2.04	18.75	0.714
5	1.53	12	-1.02	19	-0.765
5.25	-3.06	12.25	0.816	19.25	0.816
5.5	2.04	12.5	-0.0102	19.5	-0.918
5.75	-1.53	12.75	1.632	19.75	1.02
6	2.04	13	-0.204	20	-0.51
6.25	-2.55	13.25	1.02	20.25	0.918
6.5	2.55	13.5	-0.51	20.5	-0.714
6.75	-0.408	13.75	0.816	20.75	1.02
7	0.816	14	-0.612	21	-0.816

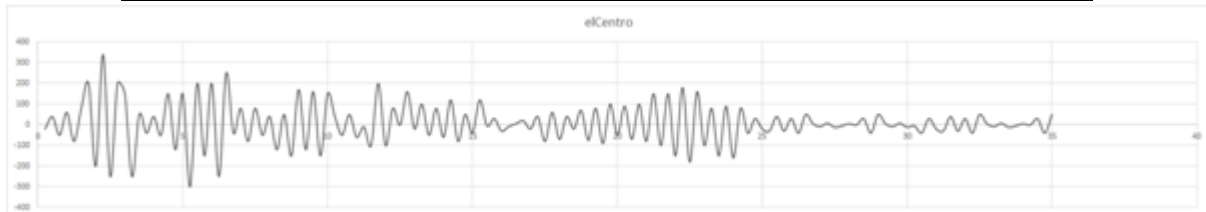


Figure A11.10 Filtered Accelerogram for El Centro 1940 Earthquake in Microsoft Excel

Table A11.14 Data set For Kobe 1995 Earthquake

Location	Kobe,	
Date	1995-01-16	
Time	20:46:52	GMT
Region	Japan	
Latitude	34.5948	
Longitude	135.0121	
Depth	17.9 km	
Mechanism	Strike-slip	
Strike	230	
Dip	85	
Rake	180	
Mw	6.9	Moment Magnitude

Ms		Surface Wave Magnitude
Mb		Body wave magnitude
ML		Richter magnitude

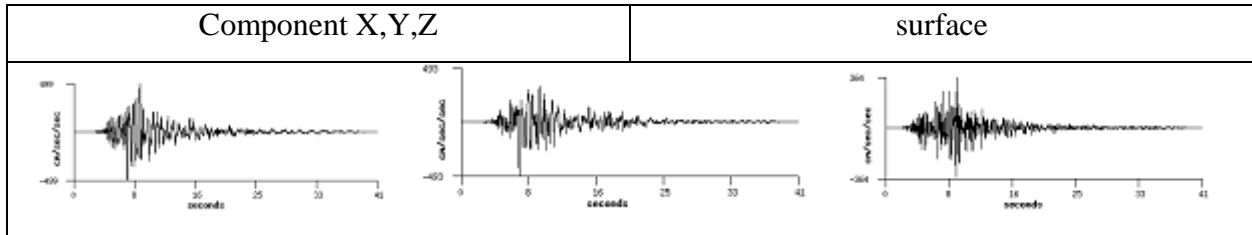


Figure A11.11 Accelerogram for Kobe 1995 Earthquake

Table A11.15 Filtered Accelerogram readings for Kobe 1995 Earthquake
(Period s),(Acceleration g)

0.25	0.102	7	-0.51	13.75	0.918
0.5	0.0816	7.25	1.53	14	1.53
0.75	0.051	7.5	-1.53	14.25	-1.224
1	-0.0714	7.75	1.224	14.5	1.836
1.25	-0.153	8	-1.53	14.75	-0.612
1.5	0.153	8.25	2.04	15	-0.102
1.75	0.204	8.5	-5.1	15.25	0.765
2	-0.204	8.75	2.55	15.5	-0.51
2.25	0.408	9	-4.59	15.75	0.51
2.5	-0.102	9.25	2.55	16	-0.204
2.75	0.459	9.5	-3.06	16.25	1.53
3	-0.1224	9.75	3.06	16.5	-0.204
3.25	1.02	10	-0.3264	16.75	1.53
3.5	-0.765	10.25	3.57	17	-1.224
3.75	1.122	10.5	-3.06	17.25	-0.102
4	-1.02	10.75	4.08	17.5	0.102
4.25	1.53	11	-3.06	17.75	-0.816
4.5	-0.051	11.25	4.59	18	0.816
4.75	0.408	11.5	-3.06	18.25	0.51

5	-0.0408		11.75	5.1		18.5	-0.51
5.25	-1.53		12	-2.754		18.75	0.51
5.5	-1.02		12.25	2.55		19	-0.357
5.75	1.53		12.5	-0.816		19.25	0.408
6	-1.02		12.75	0.918		19.5	-0.408
6.25	2.04		13	-1.53		19.75	0.306
6.5	-0.102		13.25	1.53		20	-0.153
6.75	2.244		13.5	-1.224			

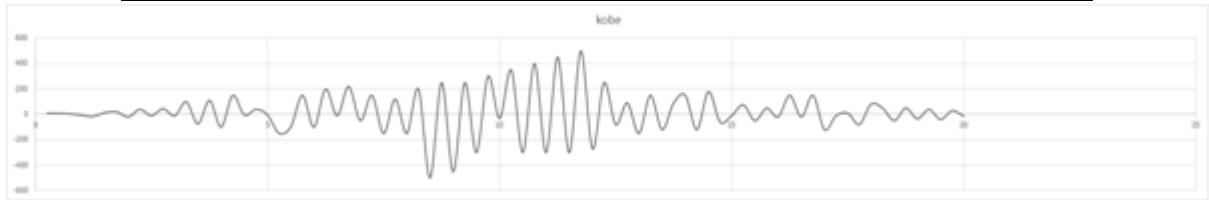


Figure A11.12 Filtered Accelerogram for Kobe 1995 Earthquake in Microsoft Excel

ANNEXURE XII

SPECTRAL FORCE

Spectral force acting on a structure

Using spectral diagrams we can then come up with a generalized set of diagrams that give the force acting on a structure for any natural period in terms of spectral acceleration. Spectral force hence can be denoted in terms of acceleration due to gravity.

Spectral force

$$F_{sa} = P_a / g \tag{A12.1}$$

We can then plot the spectral force for different damping ratios.

Table A121. Spectral force (Pa/g) acting on bund 3 m heights for different damping

Damping%	0	2	5	10	20	30	40
Natural Period(s)							
0.00	0.1	0.1	0.1	0.1	0.1	0.1	0.1
0.25	1.14	0.51	0.37	0.29	0.22	0.19	0.16
0.75	1.14	0.51	0.37	0.29	0.22	0.19	0.16
1.00	0.78	0.39	0.28	0.20	0.17	0.14	0.10
2.00	0.30	0.19	0.16	0.12	0.10	0.08	0.06
3.00	0.16	0.11	0.09	0.07	0.04	0.03	0.03
4.00	0.06	0.05	0.04	0.04	0.03	0.03	0.02

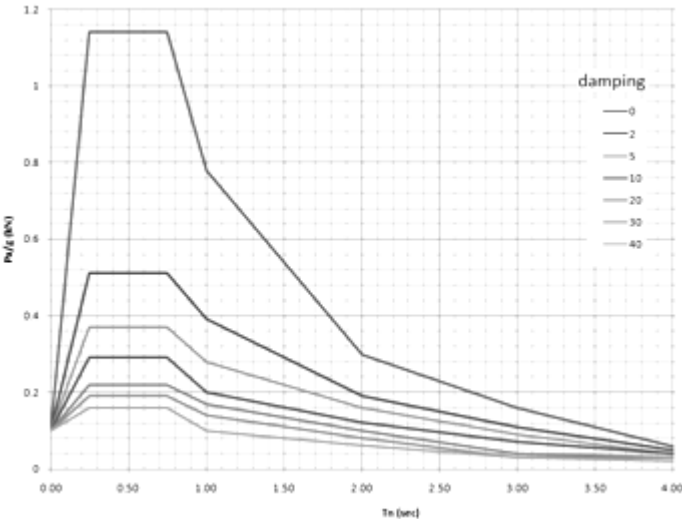


Figure A2.1 Spectral force (Pa/g) acting on bund 3 m heights for different damping

Table A12.2 Spectral force (Pa/g) acting on bund 6 m heights for different damping

Damping% Natural Period(s)	0	2	5	10	20	30	40
0.00	0.50	0.50	0.50	0.50	0.50	0.50	0.50
0.25	4.58	2.04	1.47	1.16	0.89	0.76	0.62
0.75	4.58	2.04	1.47	1.16	0.89	0.76	0.62
1.00	3.11	1.56	1.11	0.80	0.67	0.58	0.40
2.00	1.20	0.76	0.62	0.49	0.40	0.31	0.24
3.00	0.62	0.44	0.36	0.27	0.18	0.13	0.11
4.00	0.22	0.20	0.18	0.16	0.13	0.11	0.09

Table A12.3 Spectral force (Pa/g) acting on bund 9 m heights for different damping

Damping% Natural Period(s)	0	2	5	10	20	30	40
0.00	1.00	1.00	1.00	1.00	1.00	1.00	1.00
0.25	10.30	4.60	3.30	2.60	2.00	1.70	1.40
0.75	10.30	4.60	3.30	2.60	2.00	1.70	1.40
1.00	7.00	3.50	2.50	1.80	1.50	1.30	0.90
2.00	2.70	1.70	1.40	1.10	0.90	0.70	0.55
3.00	1.40	1.00	0.80	0.60	0.40	0.30	0.25
4.00	0.50	0.45	0.40	0.35	0.30	0.25	0.20

Knowing the natural period and damping of the soil the spectral force (F_{sa}) is read from the plots given below, then the horizontal force (F_h) acting on the TGSB can then be calculated from the Tables or Charts provided below and using the seismic acceleration ($k_h = a_{max}/g$).

$$F_h = F_{sa} \cdot k_h \cdot g \quad (A12.2)$$

ANNEXURE XIII

ARTIFICIAL SEISMOGRAPH FROM SPT/CPT

Table A13.1 Shear Velocity from SPT

Soil type		Cohesionless soils		Cohesive soils		
Soil sub type		Loose	Dense	Soft	Stiff	
SPT		0 - 20	20 - 50	0 - 6	6 - 30	
Vs	m/s	130 - 280	200 - 400	40 - 90	65 - 90	
From	SPT	Goa	130 + 7.5N	60 + 7N	40 + 8.38N	46.25 + 125N
		rest	100.3 N ^{0.338}		94.4 N ^{0.379}	
	CPT		227 q _t ^{0.132} σ _{vo} ^{0.27}		0.1 q _c	
	Density		ρ = 0.352 V _s ^{0.283}		ρ = 0.724 V _s ^{0.166}	

Table A13.2 Sonic Velocity generated for 6 sites in Goa

		Depth	0	5	10	15	20	25	30
Standard penetration	Beach		7	9	24	36	40	58	100
	Bridge		0	6	5	10	26	35	26
P	Test	TGSB	4	18	10	21	26	-	-
A	Shear	Beach	182.5	197.5	310	400	430	466	760
	velocity	Bridge	130	175	167.5	205	325	392.5	325
J	Normalized	TGSB	160	265	205	287.5	325	-	-
	for 30m							Normalized	
M			116.3	192.7	149.0	209.0	236.3	for depth	
	Normalized	Beach	24.0	26.0	40.8	52.6	56.6	61.3	100.0
N	shear	Bridge	33.1	44.6	42.7	52.2	82.8	100.0	82.8
	velocity	TGSB	49.2	81.5	63.1	88.5	100.0	100.0	100.0
R	Standard	TGSB 1	3	5	8	11	65	-	-
	penetration	TGSB 2	1	23	25	11	35	31	67
E	Test	TGSB 3	3	8	4	11	45	50	-
S	Shear	TGSB 1	81	95	116	137	515	-	-
	velocity		175	205	251	296	1113	-	
T	Normalized	TGSB 2	67	221	235	137	305	277	529
	for 30m		150	495	526	307	683	620	1185
Of		TGSB 3	81	116	88	137	375	410	-

G			146	208	158	246	674	737	-
O	Normalized	TGSB 1	16	18	23	27	100	100	100
A	shear	TGSB 2	13	42	44	26	58	52	100
	velocity	TGSB 3	20	28	21	33	91	100	100

Table A13.3 acceleration for Caranzalem-Miramar Beach Panjim synthesized from Artificial Shear Wave Velocity

t	a	t	a	t	a	t	a	t	a	t	a
0.25	-2.4	6.25	-27.6	12.25	-42.1	18.25	-7.8	24.25	-25.0	30.25	-5.6
0.5	2.4	6.5	27.6	12.5	42.1	18.5	7.8	24.5	25.0	30.5	5.6
0.75	-2.6	6.75	-45.0	12.75	-44.8	18.75	-12.0	24.75	-4.8	30.75	-6.1
1	2.6	7	45.0	13	44.8	19	12.0	25	4.8	31	6.1
1.25	-4.0	7.25	-24.0	13.25	-49.0	19.25	-15.8	25.25	-5.2	31.25	-10.0
1.5	4.0	7.5	24.0	13.5	49.0	19.5	15.8	25.5	5.2	31.5	10.0
1.75	-5.3	7.75	-26.0	13.75	-80.0	19.75	-16.8	25.75	-8.0	31.75	-1.2
2	5.3	8	26.0	14	80.0	20	16.8	26	8.0	32	1.2
2.25	-5.6	8.25	-40.0	14.25	-10.8	20.25	-18.4	26.25	-10.5	32.25	-1.3
2.5	5.6	8.5	40.0	14.5	10.8	20.5	18.4	26.5	10.5	32.5	1.3
2.75	-6.1	8.75	-52.6	14.75	-11.7	20.75	-30.0	26.75	-11.2	32.75	-2.0
3	6.1	9	52.6	15	11.7	21	30.0	27	11.2	33	2.0
3.25	-10.0	9.25	-56.0	15.25	-18.0	21.25	-6.0	27.25	-12.3	33.25	-2.6
3.5	10.0	9.5	56.0	15.5	18.0	21.5	6.0	27.5	12.3	33.5	2.6
3.75	-10.8	9.75	-61.3	15.75	-23.7	21.75	-6.5	27.75	-20.0	33.75	-2.8
4	10.8	10	61.3	16	23.7	22	6.5	28	20.0	34	2.8
4.25	-11.7	10.25	-100.0	16.25	-25.2	22.25	-10.0	28.25	-2.4	34.25	-3.1
4.5	11.7	10.5	100.0	16.5	25.2	22.5	10.0	28.5	2.4	34.5	3.1
4.75	-18.0	10.75	-19.2	16.75	-27.6	22.75	-13.2	28.75	-2.6	34.75	-5.0
5	18.0	11	19.2	17	27.6	23	13.2	29	2.6	35	5.0
5.25	-23.7	11.25	-20.8	17.25	-45.0	23.25	-14.0	29.25	-4.0	35.25	-1.2
5.5	23.7	11.5	20.8	17.5	45.0	23.5	14.0	29.5	4.0	35.5	1.2
5.75	-25.2	11.75	-32.0	17.75	-7.2	23.75	-15.3	29.75	-5.3	35.75	-1.3
6	25.2	12	32.0	18	7.2	24	15.3	30	5.3	36	1.3

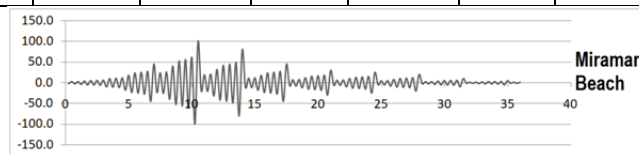


Figure A13.1 Artificial Seismograph for Caranzalem-Miramar Beach

Table A13.4 acceleration for AtalSetu (Mandovi) Bridge Panjim synthesized from Artificial Shear Wave Velocity

t	a	t	a	t	a	t	a	t	a	t	a
0.25	-3.3	6.25	-45.0	12.25	-41.8	18.25	-13.4	24.25	-20.7	30.25	-8.3
0.5	3.3	6.5	45.0	12.5	41.8	18.5	13.4	24.5	20.7	30.5	8.3
0.75	-4.5	6.75	-37.3	12.75	-66.2	18.75	-12.8	24.75	-6.6	30.75	-10.0
1	4.5	7	37.3	13	66.2	19	12.8	25	6.6	31	10.0
1.25	-4.3	7.25	-33.1	13.25	-80.0	19.25	-15.7	25.25	-8.9	31.25	-8.3
1.5	4.3	7.5	33.1	13.5	80.0	19.5	15.7	25.5	8.9	31.5	8.3
1.75	-5.2	7.75	-44.6	13.75	-66.2	19.75	-24.8	25.75	-8.5	31.75	-1.7
2	5.2	8	44.6	14	66.2	20	24.8	26	8.5	32	1.7
2.25	-8.3	8.25	-42.7	14.25	-14.9	20.25	-30.0	26.25	-10.4	32.25	-2.2
2.5	8.3	8.5	42.7	14.5	14.9	20.5	30.0	26.5	10.4	32.5	2.2
2.75	-10.0	8.75	-52.2	14.75	-20.1	20.75	-24.8	26.75	-16.6	32.75	-2.1
3	10.0	9	52.2	15	20.1	21	24.8	27	16.6	33	2.1
3.25	-8.3	9.25	-82.8	15.25	-19.2	21.25	-8.3	27.25	-20.0	33.25	-2.6
3.5	8.3	9.5	82.8	15.5	19.2	21.5	8.3	27.5	20.0	33.5	2.6
3.75	-14.9	9.75	-100.0	15.75	-23.5	21.75	-11.2	27.75	-16.6	33.75	-4.1
4	14.9	10	100.0	16	23.5	22	11.2	28	16.6	34	4.1
4.25	-20.1	10.25	-82.8	16.25	-37.3	22.25	-10.7	28.25	-3.3	34.25	-5.0
4.5	20.1	10.5	82.8	16.5	37.3	22.5	10.7	28.5	3.3	34.5	5.0
4.75	-19.2	10.75	-26.5	16.75	-45.0	22.75	-13.1	28.75	-4.5	34.75	-4.1
5	19.2	11	26.5	17	45.0	23	13.1	29	4.5	35	4.1
5.25	-23.5	11.25	-35.7	17.25	-37.3	23.25	-20.7	29.25	-4.3	35.25	-1.7
5.5	23.5	11.5	35.7	17.5	37.3	23.5	20.7	29.5	4.3	35.5	1.7
5.75	-37.3	11.75	-34.2	17.75	-9.9	23.75	-25.0	29.75	-5.2	35.75	-2.2
6	37.3	12	34.2	18	9.9	24	25.0	30	5.2	36	2.2

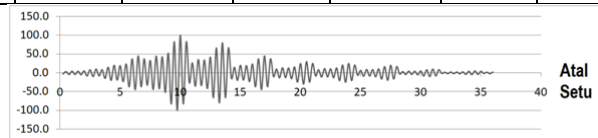


Figure A13.2 Artificial Seismograph for AtalSetu Bridge

Table A13.5 acceleration for TGSB embankment Panjim synthesized from Artificial Shear Wave Velocity

t	a	t	a	t	a	t	a	t	a	t	a
0.25	-4.9	6.25	-45.0	12.25	-70.8	18.25	-24.5	24.25	-25.0	30.25	-10.0
0.5	4.9	6.5	45.0	12.5	70.8	18.5	24.5	24.5	25.0	30.5	10.0

0.75	-8.2	6.75	-45.0	12.75	-80.0	18.75	-18.9	24.75	-9.8	30.75	-10.0
1	8.2	7	45.0	13	80.0	19	18.9	25	9.8	31	10.0
1.25	-6.3	7.25	-49.2	13.25	-80.0	19.25	-26.6	25.25	-16.3	31.25	-10.0
1.5	6.3	7.5	49.2	13.5	80.0	19.5	26.6	25.5	16.3	31.5	10.0
1.75	-8.9	7.75	-81.5	13.75	-80.0	19.75	-30.0	25.75	-12.6	31.75	-2.5
2	8.9	8	81.5	14	80.0	20	30.0	26	12.6	32	2.5
2.25	-10.0	8.25	-63.1	14.25	-22.1	20.25	-30.0	26.25	-17.7	32.25	-4.1
2.5	10.0	8.5	63.1	14.5	22.1	20.5	30.0	26.5	17.7	32.5	4.1
2.75	-10.0	8.75	-88.5	14.75	-36.7	20.75	-30.0	26.75	-20.0	32.75	-3.2
3	10.0	9	88.5	15	36.7	21	30.0	27	20.0	33	3.2
3.25	-10.0	9.25	-100.0	15.25	-28.4	21.25	-12.3	27.25	-20.0	33.25	-4.4
3.5	10.0	9.5	100.0	15.5	28.4	21.5	12.3	27.5	20.0	33.5	4.4
3.75	-22.1	9.75	-100.0	15.75	-39.8	21.75	-20.4	27.75	-20.0	33.75	-5.0
4	22.1	10	100.0	16	39.8	22	20.4	28	20.0	34	5.0
4.25	-36.7	10.25	-100.0	16.25	-45.0	22.25	-15.8	28.25	-4.9	34.25	-5.0
4.5	36.7	10.5	100.0	16.5	45.0	22.5	15.8	28.5	4.9	34.5	5.0
4.75	-28.4	10.75	-39.4	16.75	-45.0	22.75	-22.1	28.75	-8.2	34.75	-5.0
5	28.4	11	39.4	17	45.0	23	22.1	29	8.2	35	5.0
5.25	-39.8	11.25	-65.2	17.25	-45.0	23.25	-25.0	29.25	-6.3	35.25	-2.5
5.5	39.8	11.5	65.2	17.5	45.0	23.5	25.0	29.5	6.3	35.5	2.5
5.75	-45.0	11.75	-50.5	17.75	-14.8	23.75	-25.0	29.75	-8.9	35.75	-4.1
6	45.0	12	50.5	18	14.8	24	25.0	30	8.9	36	4.1

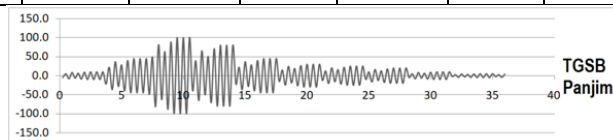


Figure A13.3 Artificial Seismograph for TGSB - Santa Cruz

Table A13.6 acceleration for TGSB embankment Mapusa synthesized from Artificial Shear Wave

Velocity

t	a	t	a	t	a	t	a	t	a	t	a
0.25	-1.6	6.25	-45.0	12.25	-21.6	18.25	-5.4	24.25	-25.0	30.25	-10.0
0.5	1.6	6.5	45.0	12.5	21.6	18.5	5.4	24.5	25.0	30.5	10.0
0.75	-1.8	6.75	-45.0	12.75	-80.0	18.75	-6.9	24.75	-3.2	30.75	-10.0
1	1.8	7	45.0	13	80.0	19	6.9	25	3.2	31	10.0
1.25	-2.3	7.25	-16.0	13.25	-80.0	19.25	-8.1	25.25	-3.6	31.25	-10.0
1.5	2.3	7.5	16.0	13.5	80.0	19.5	8.1	25.5	3.6	31.5	10.0
1.75	-2.7	7.75	-18.0	13.75	-80.0	19.75	-30.0	25.75	-4.6	31.75	-0.8

2	2.7	8	18.0	14	80.0	20	30.0	26	4.6	32	0.8
2.25	-10.0	8.25	-23.0	14.25	-7.2	20.25	-30.0	26.25	-5.4	32.25	-0.9
2.5	10.0	8.5	23.0	14.5	7.2	20.5	30.0	26.5	5.4	32.5	0.9
2.75	-10.0	8.75	-27.0	14.75	-8.1	20.75	-30.0	26.75	-20.0	32.75	-1.2
3	10.0	9	27.0	15	8.1	21	30.0	27	20.0	33	1.2
3.25	-10.0	9.25	-100.0	15.25	-10.4	21.25	-4.0	27.25	-20.0	33.25	-1.4
3.5	10.0	9.5	100.0	15.5	10.4	21.5	4.0	27.5	20.0	33.5	1.4
3.75	-7.2	9.75	-100.0	15.75	-12.2	21.75	-4.5	27.75	-20.0	33.75	-5.0
4	7.2	10	100.0	16	12.2	22	4.5	28	20.0	34	5.0
4.25	-8.1	10.25	-100.0	16.25	-45.0	22.25	-5.8	28.25	-1.6	34.25	-5.0
4.5	8.1	10.5	100.0	16.5	45.0	22.5	5.8	28.5	1.6	34.5	5.0
4.75	-10.4	10.75	-12.8	16.75	-45.0	22.75	-6.8	28.75	-1.8	34.75	-5.0
5	10.4	11	12.8	17	45.0	23	6.8	29	1.8	35	5.0
5.25	-12.2	11.25	-14.4	17.25	-45.0	23.25	-25.0	29.25	-2.3	35.25	-0.8
5.5	12.2	11.5	14.4	17.5	45.0	23.5	25.0	29.5	2.3	35.5	0.8
5.75	-45.0	11.75	-18.4	17.75	-4.8	23.75	-25.0	29.75	-2.7	35.75	-0.9
6	45.0	12	18.4	18	4.8	24	25.0	30	2.7	36	0.9

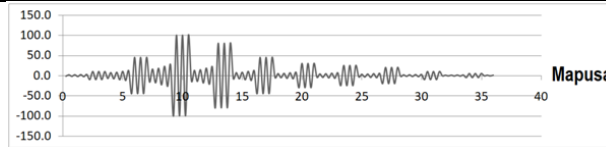


Figure A13.4 Artificial Seismograph for TGSB - Mapusa

Table A13.7 acceleration for TGSB embankment Vasco synthesized from Artificial Shear Wave Velocity

t	a	t	a	t	a	t	a	t	a	t	a
0.25	-1.3	6.25	-23.4	12.25	-20.8	18.25	-12.6	24.25	-25.0	30.25	-5.8
0.5	1.3	6.5	23.4	12.5	20.8	18.5	12.6	24.5	25.0	30.5	5.8
0.75	-4.2	6.75	-45.0	12.75	-46.4	18.75	-13.2	24.75	-2.6	30.75	-5.2
1	4.2	7	45.0	13	46.4	19	13.2	25	2.6	31	5.2
1.25	-4.4	7.25	-13.0	13.25	-41.6	19.25	-7.8	25.25	-8.4	31.25	-10.0
1.5	4.4	7.5	13.0	13.5	41.6	19.5	7.8	25.5	8.4	31.5	10.0
1.75	-2.6	7.75	-42.0	13.75	-80.0	19.75	-17.4	25.75	-8.8	31.75	-0.7
2	2.6	8	42.0	14	80.0	20	17.4	26	8.8	32	0.7
2.25	-5.8	8.25	-44.0	14.25	-5.9	20.25	-15.6	26.25	-5.2	32.25	-2.1
2.5	5.8	8.5	44.0	14.5	5.9	20.5	15.6	26.5	5.2	32.5	2.1
2.75	-5.2	8.75	-26.0	14.75	-18.9	20.75	-30.0	26.75	-11.6	32.75	-2.2
3	5.2	9	26.0	15	18.9	21	30.0	27	11.6	33	2.2

3.25	-10.0	9.25	-58.0	15.25	-19.8	21.25	-3.3	27.25	-10.4	33.25	-1.3
3.5	10.0	9.5	58.0	15.5	19.8	21.5	3.3	27.5	10.4	33.5	1.3
3.75	-5.9	9.75	-52.0	15.75	-11.7	21.75	-10.5	27.75	-20.0	33.75	-2.9
4	5.9	10	52.0	16	11.7	22	10.5	28	20.0	34	2.9
4.25	-18.9	10.25	-100.0	16.25	-26.1	22.25	-11.0	28.25	-1.3	34.25	-2.6
4.5	18.9	10.5	100.0	16.5	26.1	22.5	11.0	28.5	1.3	34.5	2.6
4.75	-19.8	10.75	-10.4	16.75	-23.4	22.75	-6.5	28.75	-4.2	34.75	-5.0
5	19.8	11	10.4	17	23.4	23	6.5	29	4.2	35	5.0
5.25	-11.7	11.25	-33.6	17.25	-45.0	23.25	-14.5	29.25	-4.4	35.25	-0.7
5.5	11.7	11.5	33.6	17.5	45.0	23.5	14.5	29.5	4.4	35.5	0.7
5.75	-26.1	11.75	-35.2	17.75	-3.9	23.75	-13.0	29.75	-2.6	35.75	-2.1
6	26.1	12	35.2	18	3.9	24	13.0	30	2.6	36	2.1

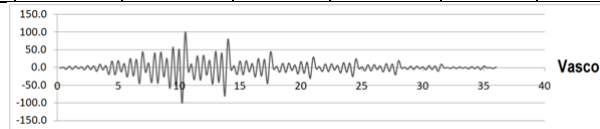


Figure A13.5 Artificial Seismograph for TGSB – Vasco

Table A13.8 acceleration for TGSB embankment Margao synthesized from Artificial Shear Wave Velocity

t	a	t	a	t	a	t	a	t	a	t	a
0.25	-2.0	6.25	-41.0	12.25	-26.4	18.25	-8.4	24.25	-25.0	30.25	-9.1
0.5	2.0	6.5	45.0	12.5	26.4	18.5	8.4	24.5	25.0	30.5	9.1
0.75	-2.8	6.75	-45.0	12.75	-72.8	18.75	-6.3	24.75	-4.0	30.75	-9.1
1	2.8	7	45.0	13	72.8	19	6.3	25	4.0	31	10.0
1.25	-2.1	7.25	-20.0	13.25	-72.8	19.25	-9.9	25.25	-5.6	31.25	-10.0
1.5	2.1	7.5	20.0	13.5	80.0	19.5	9.9	25.5	5.6	31.5	10.0
1.75	-3.3	7.75	-28.0	13.75	-80.0	19.75	-27.3	25.75	-4.2	31.75	-1.0
2	3.3	8	28.0	14	80.0	20	27.3	26	4.2	32	1.0
2.25	-9.1	8.25	-21.0	14.25	-9.0	20.25	-27.3	26.25	-6.6	32.25	-1.4
2.5	9.1	8.5	21.0	14.5	9.0	20.5	30.0	26.5	6.6	32.5	1.4
2.75	-9.1	8.75	-33.0	14.75	-12.6	20.75	-30.0	26.75	-18.2	32.75	-1.1
3	10.0	9	33.0	15	12.6	21	30.0	27	18.2	33	1.1
3.25	-10.0	9.25	-91.0	15.25	-9.5	21.25	-5.0	27.25	-18.2	33.25	-1.7
3.5	10.0	9.5	91.0	15.5	9.5	21.5	5.0	27.5	20.0	33.5	1.7
3.75	-9.0	9.75	-91.0	15.75	-14.9	21.75	-7.0	27.75	-20.0	33.75	-4.6
4	9.0	10	100.0	16	14.9	22	7.0	28	20.0	34	4.6
4.25	-12.6	10.25	-100.0	16.25	-41.0	22.25	-5.3	28.25	-2.0	34.25	-4.6

4.5	12.6	10.5	100.0	16.5	41.0	22.5	5.3	28.5	2.0	34.5	5.0
4.75	-9.5	10.75	-16.0	16.75	-41.0	22.75	-8.3	28.75	-2.8	34.75	-5.0
5	9.5	11	16.0	17	45.0	23	8.3	29	2.8	35	5.0
5.25	-14.9	11.25	-22.4	17.25	-45.0	23.25	-22.8	29.25	-2.1	35.25	-1.0
5.5	14.9	11.5	22.4	17.5	45.0	23.5	22.8	29.5	2.1	35.5	1.0
5.75	-41.0	11.75	-16.8	17.75	-6.0	23.75	-22.8	29.75	-3.3	35.75	-1.4
6	41.0	12	16.8	18	6.0	24	25.0	30	3.3	36	1.4

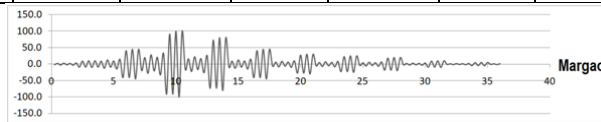


Figure A13.6 Artificial Seismographs for TGSB – Margao

ANNEXURE XIV

COMPUTATIONAL MODELLING FOR TGSB

Many of the analysis needed for design and analysis of TGSBs are not available in conventional software. Computer programming is useful in such matters. Powerful maths-based software like MATHLAB and PYTHON can suitably model and analyse these structures.

Python Programming Language

Python is general-purpose programming language. It is an interpreted high-level programming platform first created and released by Guido van Rossum in 1991. Python's design philosophy and focus emphasizes on productivity and code readability. Its syntax allows programmers to express concepts in fewer lines of code. Below is given samples of the code generated for using the equations used in spreadsheet analysis of TGSB. Further such programs can be integrated using GUI interface for developing separate software in this area of research as such software for considering the root reinforcement are not available in the market.

Python Program for Pseudostatic Factor of Safety of TGSB.

```
import math
print 'Enter the height of bund'
H = input()
print 'Enter angle of shear resistance'
phi = input()
print 'Enter cohesion of soil(in kN/m2)'
c = input()
print 'Enter unit weight of soil(in kN/m3)'
gama = input()
C= 2.5*gama* c*H
W= 2.5*H*gama
N= 0.877*W
U=10*H
W1= 2.5*H*(gama+10)
FOS=((C+(N-U)*math.tan(math.radians(phi)))-
W1*math.sin(10)*math.tan(math.radians(phi))*0.11)/(W*math.sin(10)+0.11*W1*math.cos(10))
```

print 'Pseudo Static Factor of Safety for slope Stability for',H,'m TGSB is ',FOS

Python Program for Pseudo-dynamic factor of safety of bund.

```
import math
print 'Enter the height of TGSB bund'
d = input()
print 'Enter the height of water retained by the bund'
h = input()
print ' Enter angle of shear resistance'
phi = input()
sp=math.sin(phi)
print ' Enter cohesion of soil(in kN/m2)'
c = input()
print ' Enter unit weight of soil(in kN/m3)'
gama = input()
gamasub = (gama-1)
Ka =(1+sp)/(1-sp)
Kh= 0.11
Kv=Kh/2
Kae = 0.2
gamawater=10
Pa1=0.5*Ka*gama*(d-h)**2
Pa2=0.5*Ka*gamasub*h**2
Ps=Pa1+Pa2
Ms=Pa1*(h+0.5)+Pa2*(h/2)+Pa2*(h/3)
print 'Static Earth pressure',Ps
print 'Static Earth pressure Moment', Ms
Paeh=0.5*Kae*gama*(1-Kv)*d**2
Paev=0.5*gama*Kv*d**2
Mae=Paeh*(2*d/3)+Paev*(2.5+0.2*d)
print 'Horizontal Seismic Force',Paeh
print 'Vertical Seismic Force',Paev
```

```

print 'Seismic Moment' ,Mae
Phw=0.5*gamawater*h**2
Mhw=Phw*(h/3)
print 'Hydrostaticpressure' ,Phw
print 'HydrostaticMoment' ,Mhw
Pew=(7.0*Kh*gama*d**2)/12
Mew=Pew*(d/3)
print 'Hydrodynamic pressure' ,Pew
print 'HydrodynamicMoment' ,Mew
Psw=(0.5+0.2*d)*gama*d
Msw=Psw*(2.5+0.2*d)
print 'Self-weight pressure' ,Psw
print 'Self-weight Moment' ,Msw
SR=(Ps+ (Psw-Paev)*tan(phi))*1.2*1.4
SF=Paeh+Phw+Pew
OR=Ms+Msw
OM=Mae+Mhw+Pew
FOSS=SR/SF
FOSO=OR/OM
print 'Pseudo-dynamic Factor of SafetyagainstSlidingfor ',d,'m bund is ',FOSS
print 'Pseudo-dynamic Factor of SafetyagainstOverturningfor ',d,'m bund is ',FOSO

```

Python Program to plot the above data as a graph.

```

import pylab
import numpy as N
x = N.arange ( 0 , 2 , 1)
y1 = FOSS
y2 = FOSO
plot (x, y1, 'bo ',label = 'sliding')
plot (x, y2, 'go ',label = 'overturning')
pylab .figure ( figsize =(2 , 2))
pylab .ylabel ('FoS')

```

```
pylab .title ('PseudoDynamic Factor of safety')  
pylab .show () # necessary to display graph  
#size of figure is 2x2 inches.
```

ANNEXURE XV

CASE STUDIES OF TGSB

To exemplify and authenticate the findings, in this thesis, a few case studies were undertaken to encompass the past, present and future. More studies are definitely needed but are beyond the primary, temporal and budgetary scope of the present thesis. For purpose of these studies seven sites Aggasaim, (Diwar) Dewadi, Loutolim, Galgibaga, Curtorim 1, Curtorim 2 and Gurimonly were chosen.

Case studies of TGSB Aggasaim,

To demonstrate the antiquity of TGSB this case study was undertaken. To trace the ancientness of TGSB it is necessary to study the oldest specimen in existence: the Ancient Prehistoric Port Bund of Govapuri (Cattle-city) the City that gave the territory Goa its name.



Figure A15.1 Typical Ancient Bull and Temple in Goa



Figure A15.2 The famous ancient Port-Wall at Agasaim



Figure A15.3 Location and village of Agasaim

When the River Saraswati broke banks and flooded the region the river shifted its path and moved to Sind (present day Pakistan). The area once fertile was reduced to a desert without irrigation (Thar Desert Rajasthan). This forced a mass exodus of Saraswats. The fleeing of

Saraswats were in search of a holy land where they needed a new sangam (meeting of holy Rivers Ganga Jamuna and Saraswati). They found such a spot in Goa. Where a miniature version of the sangam existed the meeting of the Mapusa-River, the Zuari-River and the Mandovi-River. They settled on threetracts of lands. The three lands were separated by perennial rivers fed by the mighty Shayadri Mountains. On the banks of the River Mapusa were the Brahmin settlement. It was called bardez or bara-desh i.e.12 countries. On the banks of the River Mandovi were the Shatriya settlement. It was called Tiswadi or Tis-Wadi i.e. thirty cities. On the banks of the River Zuari were the settlements of the other cast and subsidiary bhramin and shatrya. It was called SalcetteorSha-shastii.e. Sixty six principalities. They built their new capital here in Tiswadi and called it Govapuri (after the Sacred Bull) and the great port to continue their trade route to the rest of the world. The port and city is a little away from the new-sangam (Donna-Paula) today occupied by the Indian Governor of Goa. So they used lateritic stones from the plateau behind to build their new Port city and Port bund.



Figure A15.4 The Quay Wall with the start of the breakwater and the destroyed TGSB



Figure A15.5 Stone anchors found on the beach

The line of stones of the Port bund is still visible in Agasaim today.



Figure A15.6 Excavations carried out by NIO near steps

Case studies of TGSB (Diwar) Dewadi,

To demonstrate the destruction in name of modern repairs this case study was undertaken. The whole island of Dewadi (also called Diwar or Deewar or Diwadi) is reclaimed from the river

Mandovi by bunds. The name Dewadi derives from the ancient name from Dee(vli)-Wadi or land of lamps. The island is shaped like a hand held lamp (Deevli).

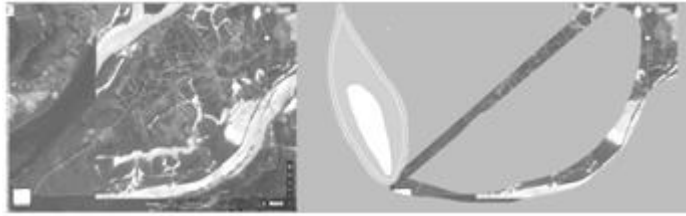


Figure A15.7 Location plan for Dewadi bund (Google maps)–Lamp shape.



Figure A15.8 Dewadi bund showing extensive barren and mangrove invaded areas.



Figure A15.9 Bunds on the Mandovi River overrun by mangroves

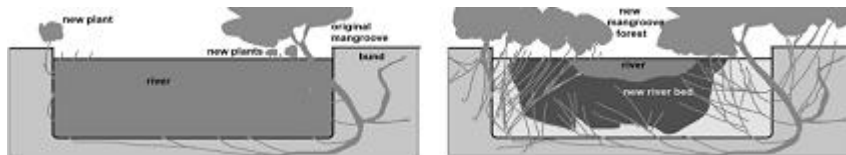


Figure A15.10 Mangrove incursion and gradual riverbed shrinking

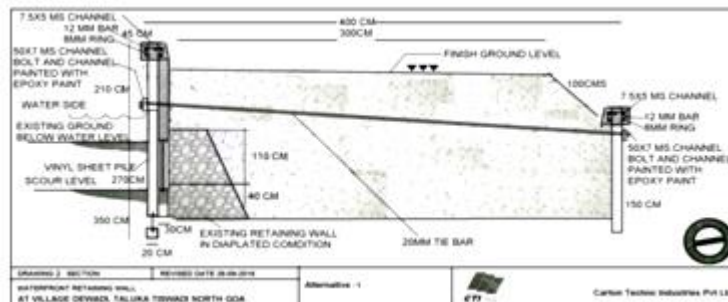


Figure A15.11 snapshot of alternative 1 by the contractors Carlton Techno Pvt Ltd

The above photos show the destruction of TGSB and retained Khazans by mangroves and the new construction proposed in name of repairs which totally substitute the traditional sustainable structure at Diwar.

Case studies of TGSB Loutolim,

To demonstrate the destruction in name of access roads this case study was undertaken.



Figure A15.12 Location Map of Loutolim-Village on Zuari River —Red Circle Shows The Location of Tembi River Site—Source Google Maps



Figure A15.13 Old Lateritic Stone Arch Bridge Culvert and (b) ancient sluice gate on Tembi Rivulet.



Figure A15.14 Untrained labour(no masons) and equipment used for construction



Figure A15.15 Bad embankment repairs-Rubble, PCC and masonry all above the riverbed.



Figure A15.16 Damage and flooding immediately during construction itself

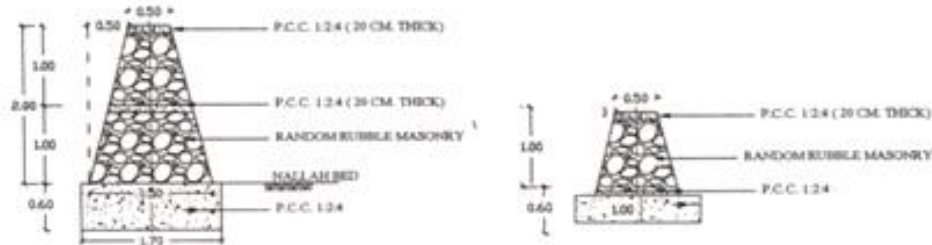


Figure A15.17 Comparison of proposed and constructed embankment.

The above photos show the destruction of TGSB and retained Khazans by mangroves and the new construction of a road for mining trucks proposed in name of repairs which totally substitute the traditional sustainable structure at Loutolim.

Case studies of TGSB Galgibaga,

To demonstrate the storm control capacity of original TGSB and their present destroyed state leading to floods this case study was undertaken.



Figure A15.18 Satellite Imagery of Galgibaga River (Google maps)

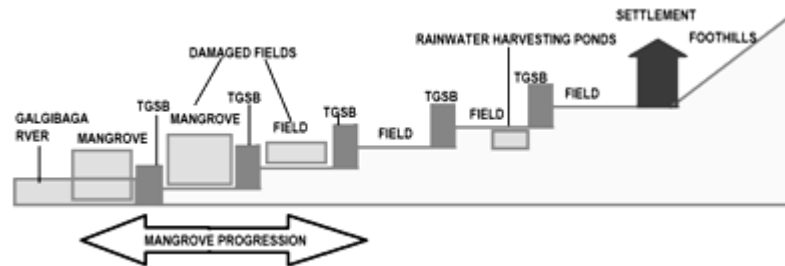


Figure A15.19 Schematic representation of the Series of TGSBs at Galgibaga River

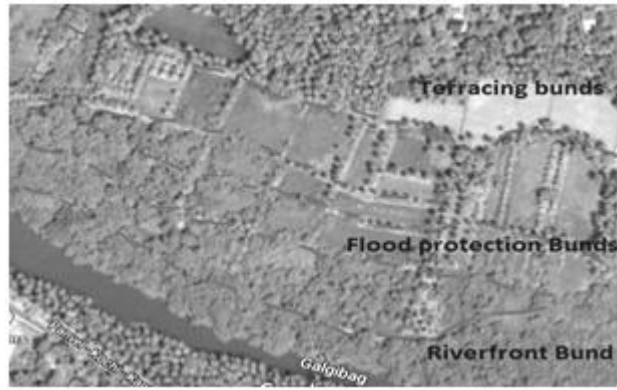


Figure A15.20 Satellite Image of Series of TGSBs at Galgibaga River

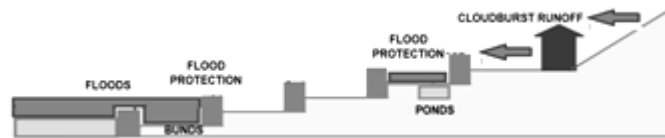


Figure A15.21 Flood protection function of TGSBs at Galgibaga River



Figure A15.22 Traditional Rubble facing and pitching for TGSB.



Figure A15.23 Site inspection and aerial view of sluice gate at Kolya Khazan



Salinity and mangroves have destroyed fields, bunds and coconut trees.



Figure A15.24 Reduced River Waterway

The once navigable 30 m wide River Galgibaga is today reduced to shallow 5 m water body. The TGSB behind the mangroves is hardly visible. The destruction has been hastened by the holes causing piping made by burrowing crabs and lobsters and other animals that infest a mangrove ecosystem.

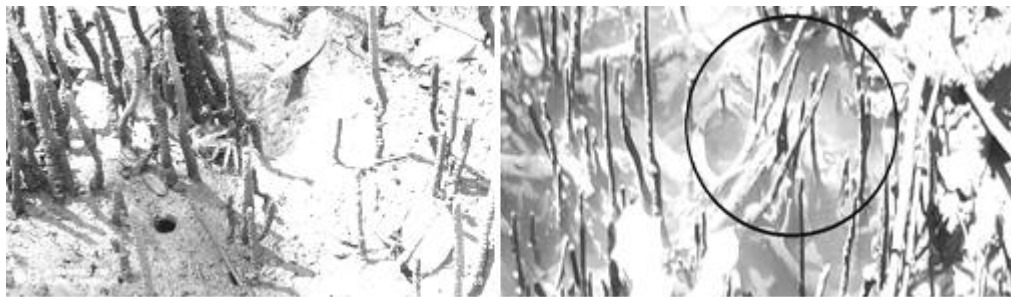


Figure A15.25 Burrowing crabs and lobster amongst mangrove roots.

Case studies of TGSB Curtorim 1,

To demonstrate the rainwater harvesting, flood-control and Environmental impact assessment this case study was undertaken.

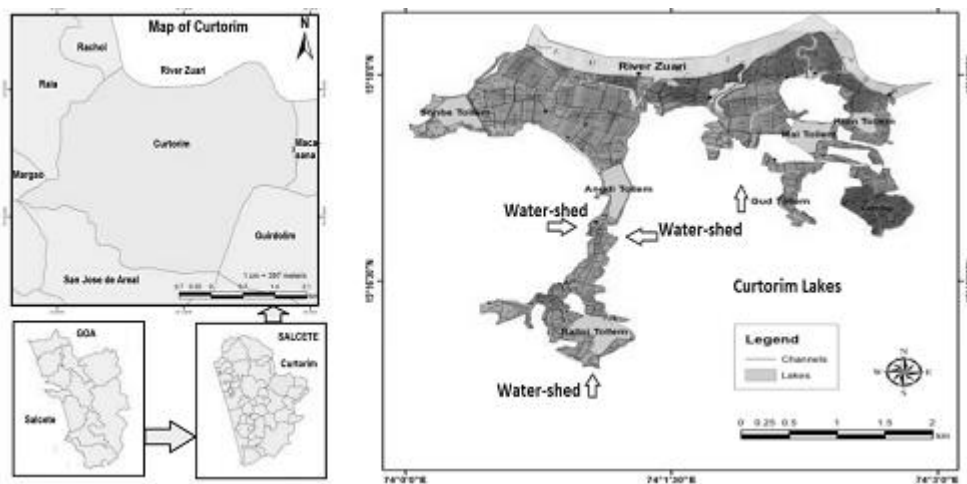


Figure A15.26 Location, Watershed and connected lakes of Curtorim village

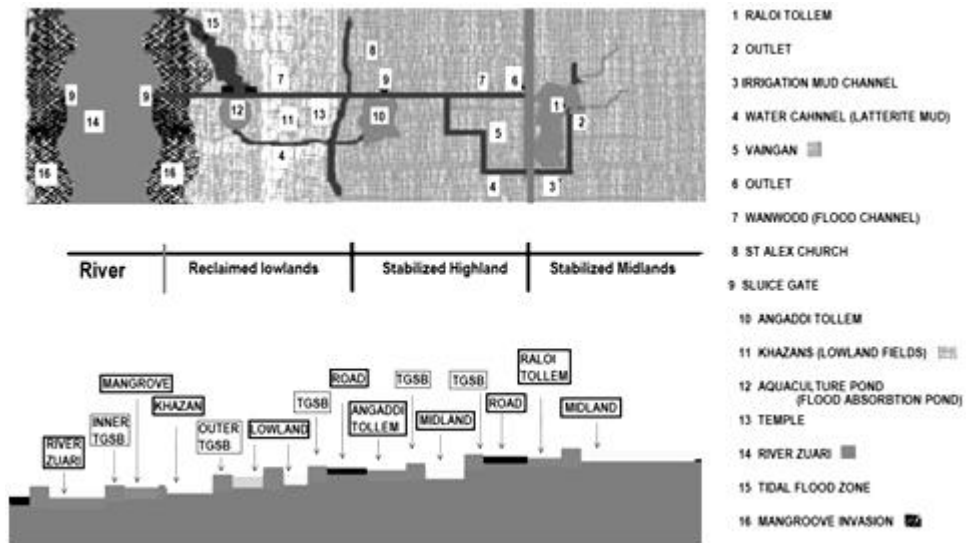


Figure A15.27 Rainwater harvesting scheme in Curtorim

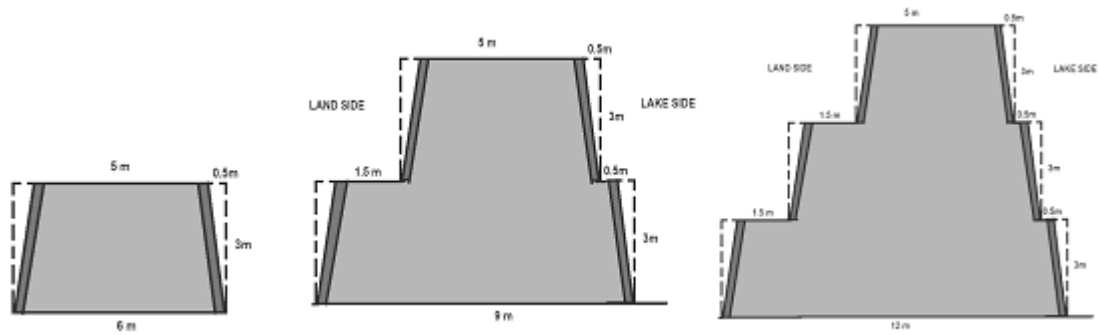


Figure A15.28 Typical maximum size of a TGSB found at Curtorim

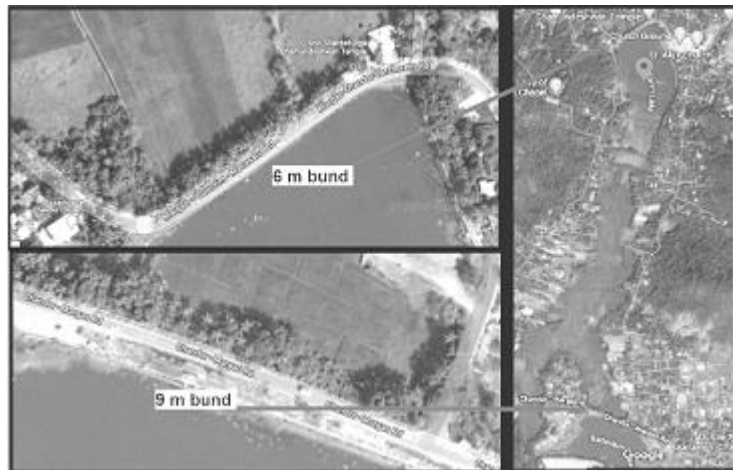


Figure A15.29 Google-map location of 6m and 9 m TGSB at Curtorim

There are: lake ecosystems, river ecosystems, pond ecosystems, wetland ecosystems, plain ecosystems forest ecosystems and plateau ecosystems. 250 Local, Rare and Migratory Birds live here. The area is teeming with life: 15 wild mammal species, 12 domesticated species, 21

amphibians, reptiles and snakes. 200 plus plant species including cultivated and wild, trees shrubs, creepers and weeds are found here. These include a huge cache of medicinal plants.

There is severe damage caused to the bunds of Curtorim due to loss of lining material and growth of trees other than coconut trees by the locals on the bunds.



Figure A15.30 The damage to the 3 m bund protecting the wanvodd



Figure A15.31 The River Zuari originally flanked by coconut tree laden bunds used for transportation of iron ore now flanked by destroyed bunds and mangrove forests used for sand mining and fishing.

The above photos show the destruction of TGSB and retained Khazans by negligence and malpractices combined with ignorance has posed a grave danger to the environment at Curtorim.

Case studies of TGSB Curtorim 2

To demonstrate applicability of traditional technology this case study was undertaken. A 3m high compound wall built of coursed cement-mortar lateritic masonry which repeatedly collapsed every rainy season was repaired using TGSB technology. It has since survived three monsoons, 2 cloud bursts which caused floods in India's west coast and two super cyclones.



Figure A15.32 Collapsed masonry portion and proximity of completed wall to the Borges house and neighbours' house



Figure A15.33 Google satellite image showing the location of the house of Dr Vijay Borges uphill of the Curtorim Church Cemetery



Figure A15.34 pressure bulb of the structure on the retaining wall and the different options explored by the owner



Figure A15.35 Two layers of dry rubble masonry per course and gap filled with smaller stones to pack them.



Figure A15.36 Backfill, stabilized with 10% ash and 4% lime then raked to mix in



Figure A15.37 Reinforce with rice straw, and compact with 25 blows of 10 kg hand-rammer

Table A15.1 Steps in laying TGSB

Step	TGSB construction/repair Process/Methodology
1	Lay two layer of rubble and fill gap with smaller stones to pack them.
2	back fill with lateritic soil
3	Add approximately 10% ash and 4% lime by volume
4	Use the hand rake and mix the stabilizers in the mud
5	lay a thin layer of rice straw
6	ram uniformly with 25 blows of 10 kg hand-rammer

This enabled a fast repair without compromising the safety of both the houses.



Figure A15.38 Two views of the completed wall built using TGSB technology.

After an exceptionally long and delayed monsoon season of 2019 to 2021 with heavy rains falling every month of the year, and the super cyclones Kyarr in 2019 and Tautake in 2021 the wall showed little damage when inspected.

A1.7.7 Case studies of TGSBGuirim

To demonstrate modern applicability this case study was undertaken.



Figure A15.39 Location of Guirim overpass

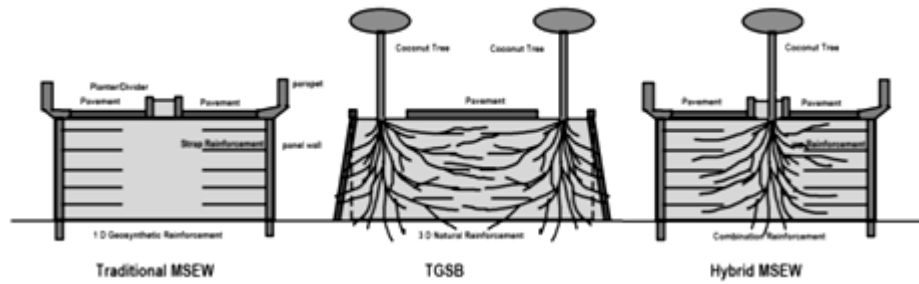


Figure A15.40 Comparison of cross-sections of MSEW and TGSB








Figure A15.41 Coconut trees planted at the centre of MSEW at Guirim




This unique experiment hopes to combine the benefits of both these Structures: the MSEW and TGSB into a working Hybrid of modern and traditional technologies. It also is a working mix of natural and synthetic reinforcement.




ANNEXURE XVI




Additional Photographs of TGSBs in various Villages in Goa




		
Field TGSB	Road crossing a TGSB	Riverside TGSB
AGASAIM		

		
Road TGSB	Road TGSB	Riverside TGSB
BATIM-PILAR		

		
TGSB on overrun river	Beachside TGSB	Road TGSB
BENAULIM		




		
Riverside TGSB	Riverside TGSB	Casuarinas trees replacing coconut trees
BETUL		




		
Field TGSB showing pilfered facing	Sluice-gate TGSB	Riverside TGSB
BORIM		




		
Riverside TGSB	Terracing TGSB	Riverside TGSB
COLA BEACH		




		
Traditional Coconut Dam – sluice gate on TGSB	6m Lakeside TGSB with modern concrete wall	Road on and electric poles on Lakeside TGSB
MACAZANA		




		
Field TGSB	No trees on TGSB	Dying trees on TGSB
NUVEM		



		
Buildings onfield TGSB at Caranzalem	Hotels on TGSB at Dona Paula	Flooding due to destroyed TGSB at Talegaon
PANJIM		

		
Riverside TGSB with concrete wall	Field TGSB with missing Coconut Trees	Riverside TGSB with concrete wall
PONDA		

		
Field TGSB	RCC wall built for TGSB facing	Riverside TGSB near ferryboat Jetty
RAIA		

		
Road TGSB	Field TGSB	Road, parapet on TGSB
SALIGAO		

		
Field TGSB	Hill Terracing TGSB	Riverside TGSB
SAVOI		

		
Riverside TGSB view from hilltop fort	Modern Jetty on TGSB	Riverside TGSB old Jetty
SIOLIM		

		
Canal-bank TGSB	Riverside TGSB	Road TGSB
VERNA		

These photographs are just a small indicative sample of the range of TGSB in Goa. They also show the possible causes of destruction due to non-maintenance, pilferage of facing materials and recent growth of Tap root trees by the new private owners of the ancient community owned property.

ANNEXURE XVII

DESTRUCTION OF TGSB

(REASONS AND PRESENT-DAY CONDITION)



Figure A17.1 Destruction of coconut tree, over growth at Mapusa River and depilated TGSB at Borim-Ponda



Figure A17.2 Disappearance of TGSB by nil maintenance at River Sal Verna and animal damage and invasion of mangroves at River Sal Nuvem



Figure A17.3 Pilferage of facing material and overgrowth of other trees and collapsed new cemented stone masonry wall at Curtorim



Figure A17.4 TGSB getting cut and damaged by the new Highway construction at Agasaim



Figure A17.5 Fallen & dead mangrove, damaged & missing pitching, disappeared TGSB and bluish grey marine soil at Diwar



Figure A17.6 Aerial view of destructive inland march of mangrove at Canacona.

Aerial view showing the gradual progression of mangrove forest in intensity from riverfront to land, the destruction of bunds with disappearance of coconut trees and the gradual disappearance of farm land. Obliteration and devastation are seen everywhere (Figure):

- The mangrove has completely engulfed the river – top side
- Coconut trees have died on the bund – right side
- Coconut trees have disappeared from bund – center
- Fields lie fallow and uncultivable – center of photograph
- Saline water incursion – top left of photograph
- A few hardy chilly plants only can be grown 100 m away from river front – bottom left
- A few trees that exist, can exist on a hill intrusion into the lowland – bottom center
- Lateritic Iron pan soils have leached into the field from the hill – center

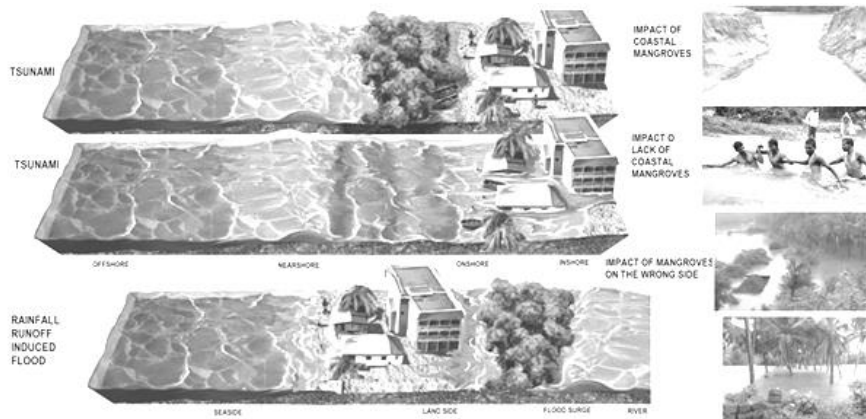


Figure A17.7 Cause of floods by destruction of TGSB at Canacona.

Flood and devastation are seen everywhere due to reasons mentioned in previous section due to wrong placement of Mangroves as explained in above Figure:

- The mangrove on sea coast protect from Tsunami and cyclonic surges – top
- No mangrove allows flooding during extreme weather events – middle
- The mangrove on inland side blocks flood from reaching the river causing inland flooding disasters as seen worldwide today– bottom

Due to overtopping during the Canacona floods the TGSGot damaged and burst worsening the flood damage.

REFERENCES

- Abdissa G., (2016), Evaluation Of Embankment Dam Stability Analysis: The Case Of Arjo Dhidhessa Embankment Dam, *Thesis*, Ababa Science and Technology University
- Aboobacker V. M., (2010), Wave transformation at select locations along the Indian coast through measurements, modelling and remote sensing, *PhD thesis*, Goa University
- Abrahamson N., Silva W., Kamai R., (2014), Summary of the ASK14 Ground-Motion Relation for Active Crustal Regions, *Earthquake Spectra*, August 2014
- Aginam C. H., Chidolue C. A., Nwakaire C., (2014), Geotechnical Properties of Lateritic Soils from, Nigeria, *International Journal of Engineering Research and Development-ISSN: 2278-067X, p-ISSN: 2278-800X, www.ijerd.com* Volume 10, Issue 12 (December 2014), PP.23-29
- Al-Chaar G. K., Alkadi M., Asteris P. G., (2013), Natural Pozzolan as a Partial Substitute for Cement in Concrete, *The Open Construction and Building Technology Journal*,7, 33-42
- Ali M., (2011), Coconut Fibre – A Versatile Material and its Applications in Engineering, *Journal of Civil Engineering and Construction Technology* Vol. 2(9), pp. 189-197,
- Ali N., Farshchi I., Mu'azu M. A., Rees S. W., (2012), Soil-Root Interaction and Effects on Slope Stability Analysis *EJGE* Vol. 17 -2012, Bund. C Pg 319-328
- Amadi A., (2010), Evaluation of Changes in Index Properties of Lateritic Soil Stabilized with Fly Ash, *Leonardo Electronic Journal of Practices and Technologies* ISSN 1583-1078
- Amiralian S., Chegenizadeh A., Nikraz H., (2012), Laboratory Investigation on the Compaction Properties of Lime and Fly Ash Composite, *International Conference on Civil and Architectural applications* (ICCAA'2012), Phuket (Thailand)
- Anaswara S., Shivashankar R., (2015,) Effect Of Vegetation On Stability of slopes,50th *Indian Geotechnical Conference*, Pune, Maharashtra, India

Andreea C., (2016), Unsaturated Slope Stability and Seepage Analysis of a Dam, Sustainable Solutions for Energy and Environment, Sustainable Solutions for Energy and Environment, EENVIRO – YRC 2015, 18 - 20 November 2015, Bucharest, Romania, *Energy Procedia* 85 93 – 98

Anggraini V., (2016), Potential of Coir Fibres as Soil Reinforcement, PJSRR (2016) 2(1):95-106 eISSN: 2462-2028 Universiti Putra Malaysia Press 95 Pertanika *Journal of Scholarly Research Reviews* <http://www.pjsrr.upm.edu.my/>

ASCE 7-05, (2006), Minimum design loads for buildings and other structures (*ASCE Standard ASCE/SEI 7-05*). American Society of Civil Engineers, Virginia

ASCE/SEI 7-10, (IBC U.S. standard) Minimum Design Loads for Buildings and Other Structures, International Building Code (IBC)

ASTM d2487-11, *USCS unified soil classification system (USCS)*

Badarnah L., Farchi Y.N., Knaack U., (2010), Solutions from nature for building envelope thermoregulation Design and Nature V 251, WIT *Transactions on Ecology and the Environment*, Volume 138, WIT Press

Baoliang Z., Dahua L., Xianfeng S., (2017), Mountain Area Based on MIDAS/GTS Model Earthwork Excavation Slope Stability Analysis, 2nd International Conference on Advances in Materials, Mechatronics and Civil Engineering (ICAMMCE 2017), *Advances in Engineering Research*, volume 121

Becker C., (2014), Sustainability and Longevity: Two Sides of the Same Quality? *research-gate, Conference Paper*, August, DOI: 10.13140/2.1.2214.0800

Bellezza I., (2014), A New Pseudo-Dynamic Approach for Seismic Active Soil Thrust. *Geotechnical and Geological Engineering* 32 (2): 561–576.

Bessonov N., Volpert V., (2000), Dynamical Models of Plant Growth, Mathematics and Mathematical Modelling, Mathematics Subject Classification, *Primary 92C80; Secondary 92C15, 35Q80*

Bessonov N., Volpert V., (2006), Dynamic models of plant growth, *Book*, Publibook

Bin-Shafique M. S., Benson C. H., Edil T. B., (2003), Leaching of heavy metals from fly ash stabilized soils used in highway pavements , Final Report To *Combustion By-products Recycling Consortium*, West Virginia University February

Biodiversity Management Committee - Curtorim, (2018), Curtorim Biodiversity Heritage Site, Report and Proposal for Curtorim, *BHS*, Curtorim2018 *Proposal for Biodiversity Heritage Site* <http://gsbb.goa.gov.in/wp-content/uploads/2018/02/Curtorim-BHS-Draft-Report.pdf>

Bishop A. W., (1955), The Use of the Slip Circle in the Stability Analysis of Earth Slopes. *Geotechnique*, 5 (1), 7-17.

BMTPC, (2021), Vulnerability Atlas of India, <https://bmtpc.org/topics.aspx?mid=56&Mid1=180>

Boore D. M., (2003), Simulation of Ground Motion Using the Stochastic Method, *Pure applied geophysics*. 160 (2003) 635–676,0033 – 4553/03/040635 – 42

Boore D. M., Atkinson G. M., (2006), Earthquake Ground-Motion Prediction Equations for Eastern North America - *Bulletin of Seismology of America* Vol 96, No 6 pp 2181-2205

Boore D. M, Atkinson G. M., (2008), Ground-Motion Prediction Equations for the Average Horizontal Component of PGA, PGV, and 5% Damped PSA at Spectral Periods between 0.01 s and 10.0 s - *Earthquake Spectra* Vol. 24 No 1 pp 99-138

Boore D. M., Joyner. , (1997), Site Amplification of Generic Rock Sites- *Bulletin of Seismology of America* Vol 87, No 2

Bore D. M., (2003), Simulation of Ground Motion Using the Stochastic Method, *Pure applied geophysics* 160 (2003) 635–676,0033 – 4553/03/040635 – 42

Boyle S., (2013), Geo-synthetics for Erosion Control and Reinforcement, https://botanicgardens.uw.edu/wp-content/uploads/sites/7/2013/12/Boyle_Geosynthetics_Botanic_Gardens_Dec2013.pdf

Bray J. D., Macedo J., (2017a) 6th Ishihara Lecture: Simplified Procedure for Estimating Liquefaction-Induced Building Settlement, *Soil Dynamics and Earthquake Engineering J.*, V 102, 215-231, <https://doi.org/10.1016/j.soildyn.2017.08.026>.

Bray J. D., Macedo J., (2017b), Simplified procedure for estimating liquefaction-induced building settlement, Proceedings of the 19th *International Conference on Soil Mechanics and Geotechnical Engineering*, Seoul

Bray J. D., Macedo J., (2019), Procedure for Estimating Shear-Induced Seismic Slope Displacement for Shallow Crustal Earthquakes, *Journal of Geotechnical and Geoenvironmental Engineering*, ASCE, Volume 145(12), doi: 10.1061/(ASCE)GT.1943-5606.0002143.

Bray J. D., Macedo J., Travasarou T., (2018), Simplified Procedure for Estimating Seismic Slope Displacements for Subduction Zone Earthquakes, *Journal of Geotechnical and Geoenvironmental Engineering*, ASCE, V. 144(3): 04017124, DOI: 10.1061/(ASCE)GT.1943-5606.0001833.

Bray J. D., Travasarou T., (2007), Simplified Procedure for Estimating Earthquake-Induced Deviatoric Slope Displacements, *Journal of Geotechnical and Geoenvironmental Engineering*, ASCE, Vol. 133(4), 381-392.

Bray J. D., Travasarou T., (2009), Pseudostatic Coefficient for Use in Simplified Seismic Slope Stability Evaluation, *Journal of Geotechnical and Geoenvironmental Engineering*, ASCE, 135(9), 1336-1340.

Bretas E. M., Batista A. L., Lemos J. V., Léger P., (2014), Seismic analysis of gravity dams: a comparative study using a progressive methodology, Proceedings of the 9th *International Conference on Structural Dynamics*, EURO DYN 2014 Porto, Portugal, 30 June - 2 July 2014A. Cunha, E. Caetano, P. Ribeiro, G. Müller (eds.) ISSN: 2311-9020; ISBN: 978-972-752-165-4

- Bretas E. M., Lemos J. V., Lourenço P. B., (2015), Seismic analysis of masonry gravity dams using the Discrete Element Method: Implementation and application, *Journal of Earthquake Engineering* September 20(2):150901094713002, DOI: 10.1080/13632469.2015.1085463
- Bryant E., (2008), Tsunami dynamics. In: Tsunami. *Springer Praxis Books*. Springer, Berlin, Heidelberg. https://doi.org/10.1007/978-3-540-74274-6_2
- Burrall M., DeJong J. T., Martinez A., Wilson D.W., (2020) Bio-Inspiration through Tree Root Pullout Tests for Innovative Anchorage Design, *Geo-Congress 2020*
- Capilleria P. P., Motta E., Raciti E., (2016), Experimental study on native plant root tensile strength for slope stabilization, VI Italian Conference of *Researchers In Geotechnical Engineering – Geotechnical Engineering in Multidisciplinary Research: from Microscale to Regional Scale*, CNRIG2016
- Castanga J. P., Batzle M. L., Eastwood R. L., (1985), Relationship between compressional wave velocity and shear wave velocity in elastic silicate rocks, *Geophysics*, 50(4)143,147
- Cazzuffi D., Cardile G., Giofrè D., (2014), Geo-synthetic Engineering and Vegetation Growth in Soil Reinforcement Applications Transportation Infrastructure *Geotechnology* volume 1, pp 262–300
- Chakraborty R., Dey A., (2016a), Effect Of Toe Cutting On Hillslope Stability, *Indian Geotechnical Conference*, IIT Madras, Chennai, India
- Chakraborty R., Dey A., (2016b), Numerical Investigation of Slope Instability Induced by Hydraulic and Seismic Forces, *North East Students Geo-Congress On Advances In Geotechnical Engineering*, NIT Agartala.
- Chakraborty R., Dey A., (2016c), Stability of a Hill Slope using LE and FE Analyses, National Level Conference on *Engineering Problems and Application of mathematics*: Agartala, India,
- Chandra U., (1992), Seismotectonics of Himalayas, *Current Science* V-62, pp 40-72

Cho D., Couloumbe C., Margave G. F., (2012), On Extraction Of Angle Dependent Wavelets From Synthetic Shear Wave Sonic Logs , Recorder Journal Article, *Canadian Society of Exploratory Geophysists*.

Chock G., Robertson I., Kriebel D., Francis M., Nistor I., (2013), Tohoku Japan Tsunami of March 11, 2011 – Performance of Structures under Tsunami Loads, American Society of Civil Engineers, *Structural Engineering Institute*, pp. 350.

Chock G., (2016), Design for Tsunami Loads and Effects in the ASCE 7-16 Standard May 2016 *Journal of Structural Engineering* 142(11) :04016093, 10.1061/(ASCE) ST.1943-541X.0001565

Chok Y. H., (2008), Modelling the effects of soil variability and natural vegetation on the stability of natural slopes, *The University of Adelaide School of Civil, Environmental and Mining Engineering*

Chou C. W., (2007), Bioimprovement of geotechnical properties of sandy soils, *Thesis- Master of Science*, Graduate School of the University of Maryland, College Park

Choudhury D., Nimbalkar S. S., Mandal J. N., (2006), Comparison of Pseudo-Static and Pseudo-Dynamic Methods for Seismic Earth Pressure on Retaining Wall, *Journal of Ind. Geophysics. Union*, Volume-10, No.4, pp.263-27

Choudhury D., Savoikar P. P., (2009), Simplified method to characterize municipal solid waste properties under seismic conditions, *Waste Management*, (ISSN 0956-053X, Impact Factor: 2.208/2008) Elsevier, U.K., Volume 29, No. 2, pp. 924-933.

Christy C. T., (2000), Engineering with the Spreadsheet: Structural Engineering Templates Using Excel, *Book*, ASCE Press, ISBN (print): 9780784408278 ISBN (PDF): 9780784471388

Clough R. W., Penzien J., (1993), Dynamics Of Structures *Computers & Structures*, Inc.1995 University Ave. Berkeley, CA 94704 USA

Cordero P., (2013), Carbon footprint estimation for a sustainable improvement of supply chains: state of the art, *Journal of Industrial Engineering and Management*, JIEM, 2013 – 6(3): 805-813 – Online ISSN: 2013-0953 – Print ISSN: 2013-8423, <http://dx.doi.org/10.3926/jiem.570>

COSMOS, (2021), <https://www.strongmotion.org>, 2443 Fillmore St #380-6131 San Francisco, CA 94115 (415) 766-0665 www.strongmotion.org cosmos@strongmotion.org

Coulomb C. A., (1776). Essaisurune Application Des Regles Des Maximisetminimis A Quellquells Problems Destatiquerelatifs, A La Architecture. *Mem. Acad. Roy. Div. Sav.*, volume 7, pp. 343–387. Acad. des Science Paris.

Dani A. H., Thappar B. K., (1992), The Indus Civilization, en.unesco.org, ISBN 978-92-102719-12

Das D., Kaundinya D., Sarkar R., Deb B., (2016), Shear Strength Improvement Of Sandy Soil Using Coconut Fibre, *International Journal of Civil Engineering and Technology* (IJCIET) Volume 7, Issue 3, pp. 297–305,

DeJong J. T., Martinez B. C., Mortensen B. M., Nelson D. C., Waller J. T., Weil M. H., Ginn T. R., Weathers T., Barkouki T., Fujita Y., Redden G., Hunt C., Major D., Tanyu B., (2009), Upscaling of bio-mediated soil improvement, Proceedings of the 17th International Conference on *Soil Mechanics and Geotechnical Engineering*, M. Hamza et al. (Eds.) IOS Press. doi:10.3233/978-1-60750-031-5-2300

DeJong T. J., Mortensen B. M., Martinez B. C., Nelson D. C., (2010), Bio-mediated soil improvement, *Ecological Engineering* 36 197–210

DeSousa S. N., (2007), The Khazana Of Goa, www.niobioinformatics.in / [indianestuaries](http://indianestuaries.org) / Dsouza

Dessai A., (2018), Geology and Mineral Resources of Goa, *Book*, jainbookdepot.com ISBN: 9789386453105

Dias F., Dutykh D., (2007), Dynamics Of Tsunami Waves, *Extreme Man-Made and Natural Hazards in Dynamics of Structures* pp 201-224, conference paper

Dobry R., Abdoun T., Stokoe K. H., Moss R. E. S., Hatton M., El Ganainy H., (2015), Liquefaction Potential of Recent Fills versus Natural Sands Located in High-Seismicity Regions Using Shear-Wave Velocity, *Journal of Geotechnical and Geoenvironmental Engineering* , Volume 141 Issue 3 - March 2015 10.1061/(ASCE)GT.1943-5606.0001239, 141, 3, (04014112),

Doshi D. P., Desai A. K., Solanki C. H., (2015), Micro pile for embankment foundation-An innovative technique, *International Journal of Science, Engineering and Technology*, 2015, Volume 3 Issue 6 ISSN (Online): 2348-4098 , ISSN (Print): 2395-4752,

Drucker D. C., Prager W., (1952), Soil mechanics and plastic analysis for limit design. *Quarterly of Applied Mathematics*, vol. 10, no. 2, pp. 157–165

D'Silva R., Barreto E., (2012), Goa Government's Dilemma. [http://www.iosrjournals.org / iosr-jbm / pages / ies-mcsc-volume-2.html](http://www.iosrjournals.org/iosr-jbm/pages/ies-mcsc-volume-2.html)

Dupuy L., Gregory P. G., Bengough A. G.,(2010), Root growth models: towards a new generation of continuous approaches, *Journal of Experimental Botany*, Vol. 61, No. 8, pp. 2131–2143, 2010 doi:10.1093/jxb/erp389 Advance Access publication 27 January, 2010

Earthquake Track, (2020), Recent Earthquakes Near Goa, India, https://earthquaketrack.com/p/india/goa/recent?mag_filter=6

Elia G., Rouainia M., (2013), Seismic Performance of Earth Embankment Using Simple and Advanced Numerical Approaches, *Journal of Geotechnical and Geoenvironmental Engineering* / Volume 139 Issue 7 - July 2013 139(7):1115-1129, DOI: 10.1061/ (ASCE)GT.1943-5606.0000840

El-Kadi, (2016), Finite Elements Analysis for Geo-Technical Engineering, *Book*

EM 1110-1-1906 Engineering And Design , Soil Testing, Department of the Army, *US corps of Engineers*, Washington DC 20314-1000

EM 1110-2-1902, (1902), Engineering And Design, Static Slope Stability, *Department of the Army, US corps of Engineers*, Washington DC 20314-1000

EM 1110-2-1913, (1913), Engineering And Design ,Construction Of Levees, *Department of the Army, US corps of Engineers*, Washington DC 20314-1000

EN 1998-1, (2004), Eurocode 8 (2004) Design of structures for earthquake resistance part 1: general rules, seismic actions and rules for buildings. *European Committee for Normalization (CEN)*, Belgium

ENCE 361, (2001), Soil Mechanics Soil Classification <https://vulcanhammernet.files.wordpress.com/>.

Encyclopedia Britanica, (2012), Soil Liquefaction, [https:// www.encyclopediabritanica.com](https://www.encyclopediabritanica.com)

Estabragh A. R., Javadi A. A., (2012), Effect of suction on volume change and shear behaviour of an overconsolidated unsaturated silty soil, *Geomechanics and Engineering*, Vol. 4, No. 1 (2012) 55-65

Fatahi B., Indraratna B., Khabaz H., (2007a) Soft Soil Improvement by tree root suction, *Australian Geomechanics Journal*, Australian Geomechanics Society, Sydney, Vol 42, No 4, pp13-18:ISSN:0818 9110

Fatahi B., Indraratna B., Khabbaz H., (2007b) Analysing Soft Ground Improvement Caused by Tree Root Suction, *Geo-Denver 2007*, Advances in Measurement and Modeling of Soil Behavior

Fatahi B., Khabbaz H., Indraratna B., (2008) Analysis Of Matric Suction Effects Induced By Tree Roots On Rail Track Subgrade, *Conference: CORE2008*

Fathi L., (2014) Structural and mechanical properties of wood from coconut palms, oil palms and date palms. Ph.D. *Thesis*, University of Hamburg, Hamburg, Germany. 172 p

Fay L., Akin M., Shi X., (2012) Cost-Effective and Sustainable Road Slope Stabilization and Erosion Control, *Transportation Research Board*, Washington, D.C.

Fellenius B. H., (2006), Basics of Foundation Design , *electronic book*, www.Fellenius.net,

Fellenius W., (1936), Calculation of the Stability of Earth Dams. Trans. 2nd *Int. Cong. Large Dams*, Washington, 445-459.

FEMA 356 (2000), Prestandard and commentary for the seismic rehabilitation of buildings. *Federal Emergency Management Agency*, Washington, DC

FEMA 440 (2005), Improvement of nonlinear static seismic analysis procedures. Applied Technical Council, Redwood City *Federal Emergency Management Agency*, Washington, DC

FEMA 450, (2003), NEHRP recommended provisions for seismic regulations for new buildings and other structures part 1: provisions. Building Seismic Safety Council BSSC, *Federal Emergency Management Agency*, Washington, DC

FEMA 534, (2005), Technical Manual for Dam Owners: Impacts of Plants on Earthen Dams- *Federal Emergency Management Agency*, Washington, DC

FEMA 1263, (2005), Dam Owner's Guide To Plant Impact on Earthen Dams - FEMA www.fema.gov, *Federal Emergency Management Agency*, Washington, DC

Foster A. S. J., Rossetto T., Allsop W., (2017), An experimentally validated approach for evaluating tsunami inundation forces on rectangular buildings, *Coastal Engineering* 128 (2017) 44–57

Fourcaud T., Blaise F., Lac P., Castera P., DeReffye P., (2003), Numerical modelling of shape regulation and growth stresses in trees. II. Implementation in the AMAP para software and simulation of tree growth. *Trees – Structure and Function*. 2003;17:31–39. [Google Scholar]

Fourcaud T., Ji J. N., Zhang Z. Q. , Stokes A., (2008,) Understanding the Impact of Root Morphology on Overturning Mechanisms: A Modelling Approach, PMID: PMC2710277, *Annals of Botany* 2008 May; 101(8): 1267–1280

Fredlund D. G., Morgenstern N. R., Widger R. A., (1978), The Shear Strength of Unsaturated Soil. *Canadian Geotechnical Journal*, 15: 313-321

Fredlund D. G., Xing A., Fredlund M. D., Barbour S. L., (1996), The Relationship of the Unsaturated Shear Strength to the Soil-Water Characteristic Curve. *Canadian Geotechnical Journal*, 33(3): 440-448

FWHA-NHI-05-039-Dec (2005), micropile design and construction-*USDoT-No-132078-*

Gao X., Cheng B., Tian W., Zhang Z., Li J., Qi H., (2020a), Simulation Parameter Selection and Steady Seepage Analysis of Binary Structure Slope , *Water* 2020, 12, 2747; doi:10.3390/w12102747, www.mdpi.com/journal/water

Gao X., Tian W. P., Zhang Z., (2020b), Analysis of Deformation Characteristics of Foundation-Pit Excavation and Circular Wall, *Sustainability* 2020, 12, 3164; doi:10.3390/su12083164, www.mdpi.com/journal/sustainability

GCCI, (2007), Brief History of Goa- www.goachamber.org > item > brief-history-of-go

Gentile F., Elia G., Elia R., (2016), Analysis of the stability of slopes reinforced by roots, *Design and Nature* V189

GeoStudio2019 (2019), *Manuals* www.geostudio.com

Getachew H., (2018), Evaluation Of Dynamic Stability Of Embankment Dam, *Thesis* , Addis Ababa Science And Technology University

Ghobrial F., Karray M., (2015), Development of spectral pseudo-static method for dynamic clayey slope stability analysis, *GeoQubec conference*,

Gobinath R., Ganapathy G. P., Akinwumi I. I., (2015), Evaluating the use of lemon grass roots for the reinforcement of a landslide affected soil from Nilgris district, Tamil Nadu, India, *Journal of Materials Environmental Science* 6 (10) 2681-2687,ISSN : 2028-2508,CODEN: JMESCN

Goda Y., (1985), Random seas and design of maritime structures. *University of Tokyo Press*

Goswami R. K., (2004), Geotechnical And Environmental Performance Of Residual Lateritic Soil Stabilised With Fly Ash And Lime, *Thesis*, Civil Engineering Department Indian Institute Of Technology Guwahati

Gray D. H., Ohashi O., (1983), Mechanics Of Fibre Reinforcement In Sand, *Journal of Geotechnical Engineering*, Volume 109 Issue 3 - March 1983, ascelibrary.org / (ASCE) 0733-9410(1983)109:3(335)

Gustafsson J., Lindstrom M., (2014), Applicability of Optimised Slip Surfaces, Department of Civil and Environmental Engineering Division of Geoengineering *Chalmers University Of Technology Gothenburg*, Sweden 2014 Master's Thesis 2014:76

Handbook for Geo-synthetics (2013), Handbook for Geo-synthetics www.gmanow.com.

Harappa.Com, (2021), <https://www.harappa.com/har/indus-saraswati.html>

Heil N. C., Belkadi N. H., (2017), Towards a Platform of Investigative Tools for Biomimicry as a New Approach for Energy - Efficient Building Design, *Buildings*, 7, 19; doi:10.3390/buildings7010019 www.mdpi.com/journal/buildings

Hengchaovanich D., (2003), Vetiver System for Slope Stabilization, *APT Consult Co., Ltd*, Bangkok, Thailand, diti@samart.co.th

Holzer T. L., Bennett M. J., Noce T. E., Padovani A. C., Tinsley J. C., (2006), Liquefaction hazard mapping with LPI in the Greater Oakland, California, area, *Earthquake Spectra*, volume 22, pp 693–708,

Horslev M. J., (1960), Physical components of shear stress of saturated clays, *Proc Res Conf on shear stress of Glacial soils* ASCE, University of Colorado, Boulder Colorado

Horslev M. J., (1937,) *Uber die Pestigkeit Seigen Schaftengest Orterbindigerjboden Ingenijz frvidenskhbelige Skrifter* A.No.45,Copenhagen,1937-

Iai S., (2001), Recent Studies on Seismic Analysis and Design of Retaining Structures, International Conferences on *Recent Advances in Geotechnical Earthquake Engineering and Soil Dynamics*. 4.

IMD (2019), Meteorological Centre, Goa , <http://www.imdgoa.gov.in/>

IMD (2021,) Indian Met Department https://mausam.imd.gov.in /imd_latest/contents/cyclone.php

IMD (2021), Indian Metrological Department, website <http://www.imdgoa.gov.in/>

Indraratna B, Fatahi B., Khabbaz H., (2006), Numerical Analysis of Matric Suction Effects Induced by Tree Roots, *Geotechnical Engineering*, 159(2), 77-90

Indraratna B., Nimbalkar S., Rujikiatkamjorn C., Heitor A., (2014), Ground Improvement in Transport Geotechnics - from Theory to Practice ,*14th IACMAG*, Kyoto, Japan

Indraratna B., Rujikiatkamjorn C., Nimbalkar S., Zhong R. , McIntosh G. W., (2015), Ground Improvement for enhancing the Performance of Road, Rail, and Port Infrastructure , *ICGE Colombo*

IPCC, (2021), The Sixth Assessment Report (AR6) 'Climate Change 2021: <https://www.ipcc.ch/report/ar6/wg1/>,

IS 1498, (1970) Classification and identification of soils *Bureau of Indian Standards* BIS, New Delhi

IS 1893, (2001), Criteria For Earthquake Resistant Design Of Structures, *Bureau Of Indian Standards* Manak Bhavan,9 Bahadur Shah ZafarMargNewDelhI110002

IS 1904, (1986), Indian Standard Code Of Practice For Design And Construction Of Foundations In Soils :General Requirements, *Bureau of Indian Standards* BIS, New Delhi

IS 7894, (1975), Code of practice for stability analysis of earth dams, *Bureau Of Indian Standards* Manak Bhavan, 9 Bahadur Shah Zafar Marg New DelhI110002

IS 8009 Part I, (1976), Code of Practice (Reaffirmed 1993) Standard For Calculation Of Settlements Of Foundations. *Bureau of Indian Standards BIS*, New Delhi

IS SP 36, (1987), part 1, Compendium Of Soil Testing , *Indian Bureau of Standards* New Delhi

IS SP 36, (1988), *part 2*, Compendium Of Soil Testing , *Indian Bureau of Standards* New Delhi

Isah B. W., (2014), Effect of Coconut Shell Ash on Properties of Fired Clay Brick, *Journal of Civil Engineering and Environmental Technology*, ISSN: 2349-8404

Ishihara K., (1985), Stability of natural deposits during earthquakes, Proceedings of the 11th *International Conference on Soil Mechanics and Foundation Engineering*, San Francisco, 12-16

Ishihara K., (1996), Soil Behaviour in Earthquake Geotechnics, *Calderon Press* Oxford University Press, New-York ISBN 0-19-856224-1.

Iwasaki T, Arakawa T, Tokida K (1982), Simplified procedures for assessing soil liquefaction during earthquakes, In Proceedings of *Conference on Soil Dynamics & EQ Engineering*, Southampton, 925-939

Iwasaki T., Tatuoka D., Tokuda K., Yashuda S., (1978), Practical Method For Finding The Soil Liquefaction Potential Based On Case Studies In Japan- Proceedings of 2nd *International Conference on Microzonation*, San Francisco-pp 885-896

Iyengar R. N., Raghukanth S. T. G., (2004), Attenuation of Strong Ground Motion in Peninsular India, 530 *Seismological Research Letters* Volume 75, Number4 July/August2004

Iyer H., (2014), The lost Khazans of Goa - *India Water Portal*-www.indiawaterportal.org , articles , khazans-goa

Izverciana M., Ivascua L., (2015), Waste management in the context of sustainable development: Case study in Romania, *Procedia Economics and Finance*, 26 717–721, 4th World Conference on Business, Economics and Management, WCBEM

Jain S. K., (2013), Strong Ground Motion and Concept of Response Spectrum, *IITG lecture notes*

James J., Saraswathy R., (2020), Performance Of Fly Ash - Lime Stabilized Lateritic Soil Blocks Subjected To Alternate Cycles Of Wetting And Drying, *Scincedo Civil and Environmental Engineering* Vol. 16, Issue 1, 30-38, DOI: 10.2478/cee-2020-0004

Jansen M., (1985), Mohenjo Dhara City of Indus valley Civilization, *Endeavor New Series*, 9:4:161- 69

JSCE, (2007), Guidelines for concrete no. 15: standard specifications for concrete structures. *Japan Society of Civil Engineers JSCE*, Tokyo

Kalita., (2016), Comparative study of soil reinforced with natural fiber, synthetic fiber and waste material, *IJLTET*, ISSN 2278-621X, Vol 6

Kamat N., (2004), History of Khazan land management in Goa: ecological, economic and political perspective, Conference: *Seminar on History of agriculture in Goa*, Department of history, Goa University, Goa, India Goa University

Kamat N., (2013), The Neglected Natural Resources of Goa , *Book-Reconstruction Of Bygone Microbiospheres*

Kanamori H., Jennings P. C., Singh S. K., Astiz L., (1993a), Estimation Of Strong Ground Motions In Mexico City Expected For Large Earthquakes In The Guerrero Seismic Gap - *Bulletin of the Seismological Society of America*, Vol. 83, No. 3, pp. 811-829, June 1993

Kanamori H., Mori J., Hauksson E., Heaton T., Hutton K., Jones L., (1993b), Determination of earthquakes energy release and ML using TERRAScope, *Bulletin of the Seismological Society of America*.,83,330±346.

Karthik S., Ashok K. E., Gowtham P., Elango G., Gokul D., Thangaraj S., (2014), Soil Stabilization By Using Fly Ash, *IOSR Journal of Mechanical and Civil Engineering (IOSR-JMCE)*,e-ISSN: 2278-1684,p-ISSN: 2320-334X, Volume 10, Issue 6 (Jan.), PP 20-26, www.iosrjournals.org

Keni C., (1998), The Saraswats In Goa And Behyond – *Murgaon Mutt Sankul Samiti Vasco-da-Gama*, Goa Van Pelt Library DS432.S35 K46 1998,

Keni C., (2019), The Saraswats –*Sahyadri Books*, online book store, Merven Technologies

Ko H. T. S., Cox D. T., Riggs H. R., Naito C. J., (2015), Hydraulic Experiments on Impact Forces from Tsunami-Driven Debris, 10.1061/(ASCE)WW.1943-5460.0000286 *J. Waterway, Port, Coastal, Ocean Engineering*. 2015.141

Koda E., Pasik T., Osinski P., Miskowska A., Bursa B., (2017), Landfill slopes reinforcements for adapting the structure into a new development plan: Radiowo landfill case study, Proceedings of the 19th International *Conference on Soil Mechanics and Geotechnical Engineering*, Seoul 2017

Kramer S. L., (1996) - *Geotechnical Earthquake Engineering – Book*, Prentice Hall, New Jersey

Kundu S. K., (2013), Indus valley Civilization, *Book -Sword Diagnostics* Doi: 10.13140/2.1.216.3202

Kuriakose L., van-Beek L. P. H., van-Westen C. J., (2009), Root strength of tropical plants - An investigation in the Western Ghats of Kerala, India, *Geophysical Research Abstracts*, Vol. 11, EGU2009-2896-2, 2009EGU General Assembly 2009.

Lade P. V., Duncan J. M., (1975) Elasto-plastic Stress strain theory for Cohesionless soils, *ASCE Journal Geotechnical Engineering Div* 101 1037

Le V. D., Dao D. H., (2015), Modeling An Geofoam Embankment Behind Bridge Abutment Using Midas Soilworks, *Conference on Numerical Analysis in Geotechnics*, Ha Noi, Vietnam August 2015

Ling H. I., Yue D., Kaliakin V. N., Themelis N. J., (2002), Anisotropic Elasto-plastic Bounding Surface Model for Cohesive Soils , *Journal Of Engineering Mechanics*, July 2002

Liptack R. J., (2013), Motion Based Seismic Design and Loss Estimation of Diagrid Structures, Department of Civil and Environmental Engineering, Masters *Thesis*, the Massachusetts Institute of Technology

Liu C., Huang Y., Stout M.G., (1997), On the asymmetric yield surface of plastically orthotropic materials: A phenomenological study. *Acta Materialia*, vol. 45, no. 6, pp. 2397–2406

Liu K. S., Tsai Y. B., (2005), Attenuation Relationships of Peak Ground Acceleration and Velocity for Crustal Earthquakes in Taiwan, *Bulletin of the Seismological Society of America*, Vol. 95, No. 3, pp. 1045–1058, June 2005, doi: 10.1785/0120040162

Liu Z., Zhang J., Chen W., Wu D., (2020), Influence of Anisotropy and Nonhomogeneity on Stability Analysis of Fissured Slopes Subjected to Seismic Action, *Mathematical Problems in Engineering*, Volume 2020, Article ID 6582787, <https://doi.org/10.1155/2020/6582787>

Løkke A., Chopra A. K., (2013), Response Spectrum Analysis of Concrete Gravity Dams Including Dam-Water-Foundation Interaction, *PEER Report 2013/17*

Lv Y. (2020), Numerical Simulation and Model of Deformation Features of Destabilized Mining Slope Under Fault-Controlled Conditions. *Earth Sciences Research Journal*, 24(1), 61-69. DOI: <https://doi.org/10.15446/esrj.v24n1.85290>

Lv Z., (2013), The Seismic Analysis of an Exhibition in Shanxi, *Applied Mechanics and Materials*, Volumes 275-277, pp 1540-1543

Madun A., Tajuddin S. A. A., Abdullah M. E., Abidin M. H. Z., Sani S. A., Siang J. L. M., Yusof M. F., (2015), Conversion Shear Wave Velocity to Standard Penetration Resistance, IOP Conference Series: *Materials Science and Engineering* 136 012009 Soft Soil Engineering International Conference 2015 (SEIC2015)

Maglic M. J., (2012), Biomimicry: Using Nature as a Model for Design, Masters, *Theses* University of Massachusetts Amherst

Marcuson W. .F, (1978), Definition of Terms Related to Liquefaction, *Journal of the Geotechnical Engineering Division*, 1978, Vol. 104, Issue 9, Pg. 1197-1200

Marshal J., (1931), Mohenjo Dharo and the Indus Civilization, *Archived Book*

Mascarenhas A, Kalavampara G (2009), Natural Resources of Goa:A Geological Perspective, *Book*, Geological Society of Goa

Maula B. H., Zhang L., (2011), Assessment of Embankment Factor Safety Using Two Commercially Available Programs in Slope Stability Analysis, *Procedia Engineering* 14 559–566, doi: 10.1016/j.proeng.2011.07.070

Maurer B. M., Green R. A., Cubrinovski M., Bradley B. A., (2014), Evaluation of the Liquefaction Potential Index for Assessing Liquefaction Hazard in Christchurch, New Zealand, *Journal of Geotechnical and Geoenvironmental Engineering* ,Volume 140 Issue 7 - July 2014

Mavko G., (1990), Conceptual Overview of Rock and Fluid Factors that Impact Seismic Velocity and Impedance, *Stanford Rock Physics Laboratory*

Medvedev S., Sponheuer W., Karník V., (1964), Neueseismische Skala Intensity scale of earthquakes,.7. *Tagung der Europäischen Seismologischen Kommission* vom 24.9. bis 30.9.1962. In: Jena, Veröff. Institut für Bodendynamik und Erdbebenforschung in Jena, Deutsche Akademie der Wissenschaften zu Berlin, 77, 69-76.

Meheroff G. G., Adams J. J., (1968), the ultimate uplift capacity of foundations-*Canadian Geotech Journal* s4

Mehra P., Prabhudesai R. G., Joseph A., Vijaykumar, Agarvadekar Y., Luis R., Damodaran S., Viegas B., (2009), A One Year Comparison of Radar and Pressure Tide Gauge at Goa, West Coast of India, *Proceedings of the International Symposium on Ocean Electronics (SYMPOL-2009)*, 18-20 November 2009. eds. by: Pillai, P.R.S.; Supriya, M.H.; 173-183.

Melo C., Sharma S., (2004), Seismic Coefficients For Pseudostatic Slope Analysis, 13th World Conference on Earthquake Engineering, Vancouver, B.C., Canada August 1-6, 2004 Paper No. 369

Menikpura S. N. M., Gheewala S. H., Bonnet S., Chiemchaisri C., (2013), Evaluation of the Effect of Recycling on Sustainability of Municipal Solid Waste Management in Thailand, *Waste Biomass Valor* 4:237–257, DOI 10.1007/s12649-012-9119-5

MIDAS (2015.), GTX NX *release notes*, Midas International, Korea

MidasGTS NX(2015), *Manuals* www.midas.com

Mitogawa T., Nishimura T., (2020). Coulomb stress change on inland faults during megathrust earthquake cycle in southwest Japan, *Earth, Planets and Space*, 72, Article number: 66, springer: 13 May

Mohr O., (1900). Die Elastizitätsgrenze und der Bruch von Materialien, *Zeitsch.d.Ver.Deutsch.Ing.* (1900) p, 15X

Moldovan D. V., (2010). Contributions Regarding the Use of Geo-synthetic Material in Ground Massifs, *Technical University of Cluj-Napoca*;

Mononobe N., Matsuo H., (1929), On the determination of earth pressures during earthquakes, in Proceedings of the *World Engineering Congress*, p. 9, Tokyo, Japan,. View at: Google Scholar

Morgenstern N. R., Price V. E., (1965), The Analysis of the Stability of General Slip Surfaces. *Geotechnique*, 15(1), 70-93

Mörner N. A., (2016) Coastal Morphology and Sea-Level Changes in Goa, India during the Last 500 Years, *Journal of Coastal Research* (2017) 33 (2): 421–434.

NASA, (2021), IPCC AR6 Sea Level Projection Tool https://sealevel.nasa.gov/data_tools/17

Nasrin S., (2013), Erosion Control And Slope Stabilization Of Embankments Using Vetiver System, *thesis*, Department of Civil Engineering Bangladesh University Of Engineering And Technology

Nayak J. G., (2017), Study on Culture of Goud Saraswat Brahmins-Special Reference on Uttar Kannada District, *International Journal of History and Cultural Studies (IJHCS)* Volume3, Issue 1, 2017, PP 32-38 ISSN2454-7646 (Print) & ISSN2454-7654 (Online) DOI: <http://dx.doi.org/10.20431/2454-7654.0301004> www.arcjournals.org ARC

NCS-MoES (2021), National Center of Seismology, *Seismological Research Wing*, Ministry of Earth Sciences, Government of India

NDMA (2008), Development Of Probabilistic Seismic Hazard Map of India, *The National Disaster Management Authority*, Govt. Of India, New Delhi

New York Times. (2021), New Orleans without power Aug. 29, Updated Sept. 1, 2021, 5:17 a.m. ET <https://www.nytimes.com/live/2021/08/29/us/hurricane-ida-live-updates-new-orleans-louisiana>

Nimbalkar S. S., Choudhury D., Mandal J. N., (2006,) Seismic stability of reinforced soil-wall by pseudo-dynamic method, *Geosynthetics International*, ISSN: 1072-6349, Impact Factor: 0.89/2004, London, U.K., Vol. 13, No. 6: pp. 277-278.

NOAA (2021), National Center for Environmental Information-National Oceanic And Atmospheric Administration, www.ngdc.noaa.gov

Okabe S., (1926), General theory of earth pressures, *Journal of the Japan Society of Civil Engineering*, vol. 12, no. 1, 1926. View at: Google Scholar

Okafor F. O., Okonkwo U. N., (2009), Effects of Rice Husk Ash on Some Geotechnical Properties of Lateritic Soil, *Leonardo Electronic Journal of Practices and Technologies*, ISSN 1583-1078, Issue 15, July-December, p. 67-74

Olugbenga O. A., Akinwale A. A., (2010), Characteristics of Bamboo Leaf Ash Stabilization on Lateritic Soil in Highway Construction, *International Journal of Engineering and Technology* Vol.2(4), 2010, 212-219

Padalkar P. A., Kulkarni T. A., Joshi C. G., (2013), Study On Properties Of Lateritic Soil Using Fly Ash And Coir Fibers, *IJARSE* vol 6, no 03 march, ISSN (o)2319-8354

Pages L, (2014) Branching patterns of root systems: quantitative analysis of the diversity among dicotyledonous species, *Annals of Botany* Volume 114, Issue 3, September 2014, Pages 591–598, doi:10.1093/aob/mcu145, www.aob.oxfordjournals.org

Palmeira E. M., Tatsuoka F., Bathurst R. B., Stevenson P. E., Zornberg J. G.,(2008), Advances in Geosynthetic Materials and Applications for Soil Reinforcement and Environmental Protection Works, *Electronic Journal of Geotechnical Engineering*, EJGE BOQUET 08Vol. 13, Special Issue State of the Art in Geotechnical Engineering, December, pp. 1-38.

Pasha G. A., Tanaka N., (2020), Characteristics of a Hydraulic Jump Formed on Upstream Vegetation of Varying Density and Thickness, *Journal of Earthquake and Tsunami*, Vol. 14, No. 03, 2050012

Pelecanos L., (2013), Seismic Response And Analysis Of Earth Dams, *Thesis*, Department of Civil & Environmental Engineering Imperial College of Science, Technology & Medicine London, United Kingdom,

Pilecka E., Białek M., Manterys T., (2016), The Influence Of Geotechnical Conditions On The Instability Of Road Embankments And Methods Of Protecting Them , Carcow Poland, 3-B/2016 *Transactions Civil Engineering*, DOI 10.4467/2353737XCT.16.218.5967

Possel G. L., (1990), Revolution in Urban Revolution – emergence of Indus Urbanization, *Annual Review of Anthropology* 19:261-82

Presti D. L., Marchetti D., Fontana T., (2010), Pseudo-static vs. pseudo-dynamic slope stability analysis in seismic areas of the northern Apennines, *Rivista Italiana Di Geotecnica* 2/2010

Preti F., Giadrossich F., (2009), Root reinforcement and slope bioengineering stabilization by Spanish Broom (*Spartiumjunceum*L.). *Hydrol Earth Syst. Sci.*, 13, 1713–1726,

RaghuKanth SGT, Iyengar RN, (2007), Estimation of seismic spectral acceleration in Peninsular India, *Journal of Earth System Science* volume 116, pp 199–214 - Attenuation relationships for peninsular India

Raghunandan M. E., Juneja A., (2009), Site Specific Ground Response Analysis: An Example of Test Area in Mumbai, 6th *International Congress on Environmental Geotechnics*,2010, New Delhi, India

Raji S. A., Ogbaje S. A., Fatolu A. S., (2016), Computer Aided Analysis Of A Gravity Dam Using MIDAS GTS NX, *International Journal of Technical Research and Applications* e-ISSN: 2320-8163, www.ijtra.com Volume 4, Issue 2 (March-April, 2016), PP. 298-301

Rankine W., (1857), On the stability of loose earth. *Philosophical Transactions of the Royal Society of London*, Vol. 147.

Rao R., Seshamma C. V., Mandal P., (1998), Estimation of Coda Qc and spectral characteristics of some moderate earthquakes of southern Indian peninsula. *Unpublished Report*.

Raychaudhuri S. P., (1980), The Occurrence, Distribution, Classification And Management Of Laterite And Lateritic Soils, *Journée Georges Aubert - Gah. O.R.S.T.O.kl.*, sér. Pédol., vol. XVIII, nO' 3-4, 1980-1981 : 249-252.

Sadeeq J. A., Ochepo J., ,Salahudeen A. B., Tijjani S. T., (2015), Effect of Bagasse Ash on Lime Stabilized Lateritic Soil, *Jordan Journal of Civil Engineering*, Volume 9, No. 2,

Saikia S., Chopra S., Baruah S., Baidya P. R., Singh U. K., (2016), Crustal imaging of the Northwest Himalaya and its fore deep region from teleseismic events, *Geomatics, Natural Hazards and Risk*, 7:4, 1265-1286, DOI: 10.1080 / 19475705.2015.1063095

Saini S., Goyal T., (2019), Analysis Of Piled Raft Foundation Using MIDAS GTS NX, *International Research Journal of Engineering and Technology (IRJET)* e-ISSN: 2395-0056 Volume: 06 Issue: 05 , www.irjet.net p-ISSN: 2395-007

Sasaki Y., Kano S., Matsuo O., (2004), Research And Practices On Remedial Measures For River Dikes Against Soil Liquefaction, January 2004 *Journal of Japan Association for Earthquake Engineering* 4(3):312-335, DOI: 10.5610/jaee.4.3_312

Sasaki Y., Towhata I., Tokida K., Yamada K., Matsumoto H., Tamari Y., Saya S., (1992), Mechanisms of permanent displacements of ground caused by seismic liquefaction. *Soils and Foundations*, V-32-3 pp79-96,

Sastry N., (2007) Tracing the Effects of Hurricane Katrina on the Population of New Orleans, WR-483, *University of Michigan* and RAND Corporation

Satyanarayana K. G., Pillai C. K. S., Sukumaran K., Pillai S. G. K., Rohatgi P. K., Vijayan K., (1982), Structure property studies of fibers from various parts of the coconut tree -*Journal Of Materials Science* 17 2453- 2462

Savoikar P. P., Choudhury D., (2009), Equivalent-Linear Seismic analysis of MSW landfills using Flac3d, 6th *International Congress on Environmental Geotechnics*, 2010, New Delhi, India

Savoikar P. P., Choudhury D., (2010a,) Computation of pseudo-static yield accelerations of landfills, *International Journal of Geotechnical Engineering*,(ISSN: 1938-6362)J. Ross Publishing Co., USA, Vol. 4, No. 3, pp. 305-317

Savoikar P. P., Choudhury D., (2010b), Effect of cohesion and fill amplification on seismic stability of MSW landfills using limit equilibrium method, *Waste Management & Research*, (ISSN: 0734-242X, Impact Factor: 1.308/2009) Sage Publications Ltd., London, U.K., Vol. 28, No. 12, pp. 1096-1113.

Savoikar P. P., Choudhury D., (2012), Translational seismic failure analysis of MSW landfills using pseudo-dynamic approach, *International Journal of Geomechanics*, ASCE, (ISSN: 1532-3641) USA, Vol. 12, No. 2, pp. 136-146. doi:10.1061/(ASCE)GM.1943-5622.0000127

Seed H. B., Idriss I. M., (1971), Simplified procedure for evaluating soil liquefaction potential, *Journal of Soil Mech. Foundation Division*, 97,1249–1273, 1971

Seed H. B., Idriss I. M., (1982) Ground motions and soil liquefaction during earthquakes, *Monograph*, Earthquake Engineering Research Institute, Berkeley, CA

Seed H. B., Tokimatsu K., Harder L. F., Chung R., (1985), Influence of SPT procedures in soil liquefaction resistance evaluations, *J. Geotech. Eng. Division*, 111, 1425–1445

Seed R. B., Cetin K. O., Moss R. E. S., Kammerer A. M., Wu J., Pestana J. M., Reimer M. F., (2001), Recent Advances in Soil Liquefaction Engineering and Seismic Site Response Evaluation, Proceedings fourth *International Conference on Recent Advances In Geotechnical Earthquake Engineering And Soil Dynamics*, and symposium San Diego, California, March

Seed R. B., Cetin K. O., Moss R. E. S., Kammerer A. M., Wu J., Pestana J. M., Riemer M. F., Sancio R. B., Bray R. B., Kayen R. E., Faris A., (2003), Recent advances in soil liquefaction engineering: a unified and consistent framework. Report No. EERC 2003–06, *Earthquake Engineering Research Center*, University of California, Berkeley

Shahien M. M., (2007) New Procedure To Estimate Liquefaction Resistance From Penetration Resistance Using Field Records, 4th *International Conference on Earthquake Geotechnical Engineering*, June 25-28, 2007 Paper No. 1542

Sharma B., Teotia S. S., Kumar D., (2007), Attenuation of P, S, and coda waves in Koyna region, India, *Journal of Seismology*, 11:327–344.

Sonak S., Sonak M., Kazi S., Abraham M., (2006), Determinants of successful environmental regimes in the context of the coastal wetlands of Goa -Conference: IDGEC conference, Bali, Indonesia

Sonak S. M., (2014), Khazan Ecosystems of Goa, Building on Indigenous Solutions to Cope with Global Environmental Change, *Advances in Asian Human-Environmental Research* Springer book series (AAHER) ISBN978-94-007-7201-4

Souza L., Naik A., Chanekar T, P., Savoikar P., (2016), Stability Of Traditional ‘Bundhs’ - Earthen Levees -From Goa, *Indian Geotechnical Conference IGC2016-15-17 December*, IIT Madras, Chennai, India

Souza L., Savoikar P., (2019a), Dynamic Soil–Foundation–Structure Interaction for Bunds in Goa, *Advances in Computer Methods and Geomechanics IACMAG Symposium 2019*

Souza L., Savoikar P., (2019b), Design of Traditional Goan Saraswat Bunds, *Indian Geotechnical Conference IGC 2019-Surat proceedings*

Souza L., Savoikar P., (2019c), Characterization of Lateritic soils used for bunds in Goa, 16th ARC, *Asian Regional Conference on Soil Mechanics and Geotechnical Engineering*, Taipei

Souza L., Savoikar P., (2017), Ground Improvement Using Coconut Leaf Ash, *Indian Geotechnical Conference IGC – Indian Institute of Technology ,Guwahati,Assam*

Spencer E., (1967), A Method of Analysis of the Stability of Embankments Assuming Parallel Inter-Slice Forces. *Geotechnique*, 17(1), 11-26

Srbulov M., (1999), Geotechnical Earthquake Engineering-Simplified Analyses with Case Studies and Examples-*Geotechnical, Geological, and Earthquake Engineering* Springer book series

Steedman R. S., Zeng X., (1990), The Influence of Phase on the Calculation of Pseudo-Static Earth Pressure on a Retaining Wall. *Géotechnique* 40 (1): 103–112.

Su J. B., Yu Z. Y., Lv Y. R., Zhu Y. H., Wang H. Q., (2018), Differential Settlement of Intersecting Buildings in an Offshore Reclamation Project, *Advances in Civil Engineering*, Hindawi, Volume 2019, Article ID 9453620, 11 pages, <https://doi.org/10.1155/2019/9453620>

Subeesh M. P., Unnikrishnan A. S., Fernando V., Agarwadekar Y., Khalap S. T., Satelkar N. P., Sheno S. S. C., (2013), Observed tidal currents on the continental shelf off the west coast of India, *Cont. Shelf Res.*, vol.69; 2013; 123-140

Sundar D., Shetye S. R., (2005), Tides in the Mandovi and Zuari estuaries, Goa, west coast of India, *J. Earth Syst. Sci.* 114, No. 5, October 2005, pp. 493–503

Taylor D. W., (1948), *Fundamentals of Soil Mechanics. Book*, John Wiley, New York

Teerawattanasuk C., Maneecharoen J., Bergado D. T., Voottipruex P., Lam L. G., (2014), Root Strength Measurements Of Vetiver And Ruzi Grasses, *Lowland Technology International* Vol. 16, No. 2, 71-80, December International Association of Lowland Technology (IALT), ISSN 1344-9656

Terzaghi K., (1950) Mechanisms of landslides, *Engineering Geology* (Berkey) Volume, Geological Society of America.

Terzhagi K., Peck R. B., Mesri G., (1950), *Soil Mechanics Engineering Practice, Book*, 3rd edition, 1996, John Wiley and sons inc New-york

TNAU (2014), Coconut Research Station, *webnotes*, Tamil Nadu Agricultural University, Aliyar Nagar – 642 101, Tamil Nadu, , <http://tnau.ac.in>

Tobin B., Erma J. C., Chiatante D., Danjon F., Di-Iorio A., Dupuy L., Eshel A., Jourdan C., Kalliokoski T., Laiho R., Nadezhdina N., Nicoll B., Pages L., Silva J., Spanos I., (2007), Towards developmental modelling of tree root systems ISSN 1126-3504 print/ISSN 1724-5575 online- Societa Botanica Italiana DOI: 10.1080/11263500701626283, *Plant Biosystems*, Vol. 141, No. 3, pp. 481 – 501

Tokimatsu K., Seed H. B., (1987), simplified procedures for the evaluation of settlements in clean sand. *Earthquake Engineering Research Centre* RNo UBC/EERC-84/16, university of California, Berkeley

Toprak S., Holzer T. L., (2003), Liquefaction Potential Index: Field Assessment, *Journal of Geotechnical and Geoenvironmental Engineering* / Volume 129 Issue 4 - April 2003

Tresca H., (1875), Technische Mechanik für Ingenieure, *the International Bureau of Weights and Measures*

Truong P., (2013), Review on the Application Of Vetiver System For Infrastructure Protection, TVNI *Veticon Consulting*. www.veticon.com.au

Turner J. S. , Soar R. C., (2008), Beyond biomimicry: What termites can tell us about realizing the living building. *First International Conference on Industrialized, Intelligent Construction (I3CON)* Loughborough University, 14-16 May 2008

Unified Soil Classification System (2020), USCS unified soil classification system (USCS) (ASTM d2487-11)

USGS (2020), *Vs30 Models and Data* <https://earthquake.usgs.gov/data/vs30/>

USGS (2021), *United States Geographical Society*, Website <https://earthquake.usgs.gov>

Valdiya K.S., (2001), Reactivation of terrain-defining boundary thrusts in central sector of the Himalaya: *Implications. Current Science*,81(11), 1418-1431.

Von-Mises R., (1913,) *Mechanik der festen Körperimplastisch-deformablen Zustand*. Nachrichten von der Gesellschaft der Wissenschaftenzu Göttingen. *Mathematisch-Physikalische Klasse*. (1): 582–592.

Wadhwa R. S., Ghosh N., Subba-Rao C. H., (2010), Empirical relation for estimating shear wave velocity from compressional wave velocity of rocks, *J. Ind. Geophys. Union*, January, Vol.14, No.1, pp.21-30

Wandana L. S., Wadanambi R. T., Preethika D. D. P., Dassanayake N. P., Chathumini K. K. G. L. , Arachchige U. S. P. R., (2021), Carbon Footprint Analysis: Promoting Sustainable Development, *Journal Of Research Technology And Engineering*, Vol 2, Issue 1, January 2021 ISSN 2714-1837

Westergaard H. M., (1938), A problem of elasticity suggested by a problem in soil mechanics – *Contributions To Soil Mechanics*, 60th anniversary volume, Macmillan, N.Y.

Widdowson M, (2009), Evolution of Laterite in Goa, [https:// www.researchgate.net /publication /42800308](https://www.researchgate.net/publication/42800308), ISBN 978-81-908737-0-3.

Wiebe D. M., Park H., Cox D. T., (2014), Application of the Goda pressure formulae for horizontal wave loads on elevated structures. *KSCE Journal of Civil Engineering*, 18(6), 1573-1579. doi:10.1007/s12205-014-0175-1

Wikipedia (2021a), Goud Saraswat Bhramins, [https:// en.wikipedia.org/wiki/Goud_Saraswat_Bhramins](https://en.wikipedia.org/wiki/Goud_Saraswat_Bhramins)

Wikipedia (2021b), Pore water pressure [https:// en.wikipedia.org](https://en.wikipedia.org)

Wikipedia (2021c), Soil_liquefaction [https:// en.wikipedia.org](https://en.wikipedia.org)

Wilson S. J., Sujitha S. B., Shruti V. C., Ahmed S. Z., Kumar S. P., Chandrasekar N., (2015), Seasonal variability of beach characteristics between Candoliam and Colva coast, Goa, India, *Journal of Coastal Sciences* hoisted by Centre for Geotechnology, MSU.

Wolf J. P., (1985), Dynamic Soil-Structure Interaction, *Book*, prentice-Hall International, Eglewoods Cliffs N.J,

Wu T. H., (1976), Investigation of Landslides on Prince of Wales Island, Alaska, *Geotechnical Engineering Report* No. 5 Dept. of Civil Engineering, Ohio State University Columbus, Ohio

Wu T. H., (2013), Root reinforcement of soil: review of analytical models, test results, and applications to design, March 2013 *Canadian Geotechnical Journal* 50(3), DOI: 10.1139/cgj-2012-0160

Wu T. H., McKinnell W. P., Swanston D. N., (1979), Strength of tree roots and landslides on Prince of Wales Island, Alaska, *Canadian Geotechnical Journal*, 1 February, <https://doi.org/10.1139/t79-003>

Yang Y., Irish J. L., Weiss R., (2017). Impact of Patchy Vegetation on Tsunami Dynamics, *Journal of Waterway, Port, Coastal, and Ocean Engineering* ,V-143 Issue 4

Yanina O., Yanin A., Chigarev A., (2019), Influence of modern technogenic conditions on historical urban territories, *E3S Web of Conferences* 135, 01028, ITESE-2019,<https://doi.org/10.1051/e3sconf/201913501028>

Youd T. L., Idriss I. M., Andrus R. D., Arango I., Castro G., Christian J. T., Dobry R., Finn W. D. L., Harder-Jr, L. F., Hynes M. E., Ishihara K., Koester J. P., Liao S. S. C., Marcuson-III W. F., Martin G. R., Mitchell J. K., Moriwaki Y., Power M. S., Robertson P. K., Seed R. B., Stokoe-II K. H., (2001) Liquefaction resistance of soils summary report from 1996 NCEER and 1998 NCEER/NSF workshops on Evaluation of Liquefaction Resistance of Soil, *J. Geotech. Geoenviron. Eng.*, 127, 817–833,2001.· October 2001, DOI: 10.1061 / (ASCE) 1090-0241, 127:10(817)

Zanetti C., Vennetier M., Mériaux P., (2014), Plasticity of tree root system structure in contrasting soil materials and environmental conditions *Plant Soil*: doi:10.1007/s11104-014-2253

Zanetti C., Vennetier M., Mériaux P., Royet P., Provansal M., Blanc G., (2011), Managing woody vegetation on earth dikes: risks assessment and maintenance solutions *Procedia Environmental Sciences* 9:196-200,

Zari M. P., (2007), Biomimetic Approaches to Architectural Design For Increased Sustainability, SB07 New Zealand *Paper*: 033

Zhang K., Zang Z., Okine L., Torres J. L. C., (2018), Microstudy of the Anisotropy of Sandy Material, *Advances in Civil Engineering* Volume 2018, Article ID 3971643, 13 pages <https://doi.org/10.1155/2018/3971643> Article ID 3971643, <https://doi.org/10.1155/2018/3971643>

Zornberg J. G., (2011), Advances in the use of Geosynthetic in Pavement Design. Invited Keynote Paper, Proceedings of the *Second National Conference on Geosynthetics*, Geosynthetics India, India Institute of Technology Madras, Chennai, India, September 23-24, Vol. 1, pp. 3-21

LIST OF RESEARCH RELATED COMMUNICATED PAPERS

From the research work carried out in the current PhD programme and reported in the chapters 3, 4, 5 and 6 of this thesis the following technical papers have been published / accepted / communicated for publication.

Published / Accepted Papers

In Referred International journals

Souza L., Savoikar P., (2021) Case History of TGSB at Curtorim with static and seismic analysis, *Indian Geotechnical Journal* Vol. 52, pp. 542–555, Springer Publishers, New Delhi.

In proceedings of International Conferences

Souza L., Savoikar P. P., (2019), Characterization of Lateritic soils used for bunds in Goa, *16th ARC, Asian Regional Conference on Soil Mechanics and Geotechnical Engineering*, Taipei. 14-18 Oct 2019.

Souza L., Savoikar P. P., (2018), Innovative Construction as a criterion for Sustainability, *International Conference on Sustainable Construction and Building Materials (SCBM 2018) at National Institute of Technology Karnataka, Surathkal*. June 18-22, 2018.

Souza L., Savoikar P. P., (2019), Dynamic soil foundation structure interaction for bunds in Goa, *IACMAG Symposium, IIT Gandinagar*. 5-7 Mar 2019.

Souza L., Savoikar P. P., (2019), Biomechanics of coconut tree root reinforcement in soils for Traditional Goan Saraswat Bunds, *ICCMS2019, international conference on Computational mechanics and Simulation, IIT Mandi*. 11-13 Dec 2019.

Souza L., Savoikar P. P., (2020), Case study successful Repairs of retaining wall of Dr. Borges House at Curtorim using sustainable TGSB technology, *International Conference on Recent Development in Sustainable Infrastructures, Orissa*. 2020.

Souza L., Savoikar P. P., (2021), Liquefaction Potential Index for Lateritic soils in Goa , *7th International Conference on Recent Advances in Geotechnical Earthquake Engineering and Soil Dynamics (ICRAGEE)* , Indian Institute of Science, Bangalore July 14-16,

In proceedings of National Conferences

Souza L., Savoikar P. P., (2017), Comparison of Ground Improvement Using Coconut-Leaf Ash and Lime with Fly Ash and Lime , *Geotechnics for Natural and Engineered Sustainable Technologies (GeoNEst)*, Indian Institute of Technology Guwahati (IIT Guwahati) .14-16 Dec 2017.

Souza L., Savoikar P. P., (2017), Forensic Case Study Of Retaining Wall Failure In Goa , *Geotechnics for Natural and Engineered Sustainable Technologies (GeoNEst)*, Indian Institute of Technology Guwahati (IIT Guwahati) .14-16 Dec 2017.

Souza L., Savoikar P. P., (2018), Coconut tree root reinforcement in embankments as geoenvironmental engineering, *Advances in Concrete and Structural and Geotechnical Engineering_2018*, BITS Pilani.26-28 Feb 2018.

Souza L., Savoikar P. P., (2018), L.E.G.S. a new approach to evaluation of sustainability of structures , *Advances in Concrete and Structural and Geotechnical Engineering_2018*, BITS Pilani .26-28 Feb 2018.

Souza L., Savoikar P. P., (2018), Advanced Geotechnical Testing of Bunds , *National Conference of Challenges in Geotechnical Investigations, Analysis, Design and Construction of Foundations*, ISBN: 978-93-86724-76-2 .April 2018.

Souza L., Savoikar P. P., (2018), Testing of Root Reinforcement in Soil of Trees Found on Bunds in Goa , *National Conference of Challenges in Geotechnical Investigations, Analysis, Design and Construction of Foundations*, ISBN: 978-93-86724-76-2 .April 2018.

Souza L., Savoikar P. P., (2018), Dynamic Design of Riverfront Bunds, *National Conference of Challenges in Geotechnical Investigations, Analysis, Design and Construction of Foundations*, ISBN: 978-93-86724-76-2 .April 2018.

Souza L., Savoikar P. P., (2018), Biomimicry as a sustainable Geotechnical Practice, *Next frontiers in Civil Engineering : Sustainable and Resilient Infrastructure, IIT Mumbai*.30 Nov 2018.

Souza L., Savoikar P. P., (2018), Bunds for flood and river and coastal defense, *Next frontiers in Civil Engineering : Sustainable and Resilient Infrastructure, IIT Mumbai*.30 Nov 2018.

Souza L., Savoikar P. P., (2018),Review Of Historic Forensic Geotechnical Engineering, *IGC-2018, IISc Bangalore* .13-15 dec 2018.

Souza L., Savoikar P. P., (2019),Coconut leaf ash as futuristic green material, *VISWACON – 3rd National Conference On Recent Trends In Engineering And Technology*.8-9 feb 2019.

Souza L., Savoikar P. P., (2019), Traditional Goan Saraswat Bunds – Ancient Technology For Modern Times, *Trending Moments and Steer Forces – Civil Engineering 2019* , *Don Bosco College of Engineering, Fatorda Goa* .31 Oct 1 Nov 2019.

Souza L., Savoikar P. P., (2019), Effect Of Root Suction Of Coconut Tree Roots On Soil Shear Strength, *Trending Moments and Steer Forces – Civil Engineering 2019* ,*Don Bosco College of Engineering, Fatorda Goa* .31 Oct 1 Nov 2019.

Souza L., Savoikar P. P., (2019), Design of Traditional Goan Saraswat Bunds, *IGC 2019 GEOINDUS, SVNIT Surat* .19-21 Dec 2019.

Souza L., Savoikar P. P. (2021), Geotechnical Characterization of Laterite Stones used for Bunds in Goa , *EGCON2021Indian Society of Engineering Geology (ISEG)* 9-11 Dec,

Souza L., Savoikar P. P. (2021), Coconut_Tree_Roots_As_Natural_Geosynthetics , *IGC-2018, NIT* December 16-18, 2021, NIT Tiruchirappalli